

VAPOUR-LIQUID EQUILIBRIA STUDIES FOR BINARY SYSTEMS CONTAINING 1-HEXENE AND n-HEXANE

PREBANTHA MOODLEY

University of KwaZulu-Natal

January 2009

Submitted in fulfillment of the academic requirements for the degree Master of Science in Chemical Engineering. All the work presented in this dissertation is original unless otherwise stated and has not (in whole or part) been submitted previously to any tertiary institute as part of a degree.

As the candidate's supervisor, I approve this dissertation for submission

Prof. D Ramjugernath

As the candidate's co-supervisor, I approve this dissertation for submission

Dr. P. Naidoo

The financial assistance of the National Research Foundation (NRF) towards this research is hereby acknowledged. Opinions expressed and conclusions arrived at, are those of the author and not necessarily to be attributed to the NRF.

DECLARATION

I, Prebantha Moodley declare that

- (i) The research reported in this thesis, except where otherwise indicated, is my original work.
- (ii) This thesis has not been submitted for any degree or examination at any other university.
- (iii) This thesis does not contain other persons' data, pictures, graphs or other information, unless specifically acknowledged as being sourced from other persons.
- (iv) This thesis does not contain other persons' writing, unless specifically acknowledged as being sourced from other researchers. Where other written sources have been quoted, then:
 - a) their words have been re-written but the general information attributed to them has been referenced;
 - b) where their exact words have been used, their writing has been placed inside quotation marks, and referenced.
- (v) Where I have reproduced a publication of which I am an author, co-author or editor, I have indicated in detail which part of the publication was actually written by myself alone and have fully referenced such publications.
- (vi) This thesis does not contain text, graphics or tables copied and pasted from the Internet, unless specifically acknowledged, and the source being detailed in the thesis and in the References sections.

Signed: _____

Date: _____

ABSTRACT

Experimental vapour-liquid equilibria (VLE) data is required for the design of separation processes such as distillation which accounts for a large percentage of energy usage in a chemical plant and separation process in industry. Thus, the experimental acquisition of highly accurate VLE data is invaluable for the design of such unit operations as it allows for efficiency, profit margins and energy savings to be maximized during operation.

In this study VLE data was obtained for the systems given below. All systems investigated except for the test system are currently unavailable in literature.

- a. 1-hexene with n-hexane at 55 °C, 80 °C and 105 °C,
- b. 2-methyl-2-pentene with n-hexane at 55 °C, 80 °C and 105 °C
- c. n-methyl-2-pyrrolidone with 1-hexene at 45 kPa, 80 kPa and 100 kPa

The stainless steel VLE recirculating still of Reddy (2006) was used in the acquisition of the experimental data. The still is based on the low pressure recirculating still of Raal (Joseph et al. 2000) but its use extends to both high pressure and high temperature. The reliability of the method and calibrations were confirmed by the test system of 1-hexene with n-hexane at 55 °C in comparison to literature data.

The isothermal data were reduced using the direct approach to VLE where the fugacity coefficient is used to describe both liquid and vapour phase non-idealities. Fugacity coefficients were calculated using the Peng-Robinson-Stryjek-Vera cubic equation of state with Wong and Sandler mixing rules and excess Gibbs energy models of Van Laar, Wilson and NRTL.

The isobaric data were reduced using the combined approach to VLE where the fugacity coefficient accounts for the vapour phase non-ideality and the activity coefficient accounts for the liquid phase non-ideality. The fugacity coefficient was calculated using the Pitzer virial equation of state together with Prausnitz mixing rules. The activity coefficient was calculated using the Gibbs excess energy models of Van Laar, Wilson and NRTL. Aspen simulation was also used to regress the isobaric data. The fugacity coefficient was calculated using the Redlich-Kwong cubic equation of state together with mixing rules defined in Aspen. The activity coefficient was calculated using the UNIQUAC Gibbs excess energy model.

Best fit models were chosen based on objective function residuals. The best fit model for 1-hexene with n-hexane at 55 °C was Wilson and at 80 °C and 105 °C was NRTL. The best fit model for 2-methyl-2-pentene with n-hexane at 55 °C and 105 °C was Wilson and at 80 °C was NRTL. For the system of n-methyl-2-pyrrolidone the best fit model was Van Laar at 45kPa and Wilson at 80 kPa and 100 kPa.

Infinite dilution activity coefficients were also calculated for the systems of 1-hexene with n-hexane and 2-methyl-2-pentene with n-hexane using the method of Maher and Smith (1979) as well as temperature dependency of the model parameters.

The VLE data were subjected to consistency tests and according to the Point test, were of high consistency as the average absolute deviations between experimental and calculated vapour mole fractions were below 0.01.

ACKNOWLEDGMENTS

I would like to express my sincerest gratitude to my supervisors, Professor Deresh Ramjugernath for his guidance throughout my studies and for affording me the opportunities to realise my potential. His support and belief in me has allowed the once impossible to become possible. Dr. Prathieka Naidoo for her willingness to help; her encouragement in difficult times and for taking the time to listen. Their professional advice and the knowledge they shared with me has spurred on my interest in research, and as well as their patience, will always be appreciated.

To my parents, Santha and Maga, for their unconditional love and support, without which these studies and much more in my life would not be possible. My brothers Keagan and Navern for their words of encouragement, their support, motivation and technical advice, and to my grandmother for always being there.

I would also like to extend my gratitude to the following people Professor J. D Raal for his expertise. The School of Chemical Engineering Workshop staff in particular Les Henwood and Kelly Robertson for making the time to assist me and understanding when times were dire.

To the pleasant secretarial staff and the lab technicians at the School of Chemical Engineering in particular Loveena Kissoon, Niri Naidu and Rekha Maharajh for her assistance whenever needed.

To the ICT department Dudley Naidoo and Collin Mandri, in particular Preyothan Nayager for his much needed assistance and patience. Thermodynamic Research Group laboratory assistant, Ayanda Khanyile for his willingness to help. Stanley Sandler for the use of the regression programs and Dr Prashant Reddy for assisting in the operation of the equipment and for his technical expertise.

To my friends and colleagues at the School of Chemical Engineering for the much needed tea breaks, advice and ideas. I am honoured to have met and conversed with such great minds. To Minal Soni, for taking the time and being so accommodating; your efforts to help me understand will always be appreciated.

I acknowledge the National Research foundation (NRF) for financial assistance.

I am grateful to God for this experience; for all that I have achieved and more.

CONTENTS

ABSTRACT.....	iii
ACKNOWLEDGMENTS.....	v
LIST OF FIGURES.....	x
LIST OF TABLES.....	xv
NOMENCLATURE	xviii
CHAPTER ONE	
INTRODUCTION.....	1
CHAPTER TWO	
VAPOUR LIQUID EQUILIBRIA DATA REDUCTION AND ANALYSIS.....	4
2.1 Fugacity and fugacity coefficient.....	5
2.1.1 Fugacity coefficients from the Virial equation of state.....	9
2.1.2 Fugacity Coefficients from Cubic Equations of State.....	11
2.2 Activity coefficient and Excess Gibbs Energy Models.....	16
2.2.1 Evaluating activity coefficients.....	18
a) The Van Laar Model (Prausnitz <i>et al.</i> , 1986).....	18
b) The Wilson Model (Wilson, 1964).....	19
c) The Non-Random Two Liquid Model (NRTL) (Renon and Prausnitz, 1968).....	20
d) The UNIQUAC (Universal Quasi-chemical) Model (Abrams and Prausnitz, 1975)	21
2.2.2 Evaluating Limiting Activity Coefficients.....	24
2.3 The Gamma-Phi Approach.....	25
2.4 Equation of State Approach.....	30
2.5 Thermodynamic consistency tests for binary VLE.....	33
2.5.1 Area test.....	33
2.5.2 Point test.....	35

CHAPTER THREE**EQUIPMENT REVIEW.....36**

3.1	High Pressure Vapour-Liquid Equilibria (HPVLE)	36
3.1.1	Classification of HPVLE Equipment	36
3.1.2	HPVLE Two Phase Recirculation Method.....	38
3.1.3	Features of HPVLE Equipment.....	39
3.1.4	Experimental Challenges in the Acquisition of HPVLE Data	40
3.2	Low Pressure Vapour-Liquid Equilibria (LPVLE)	44
3.2.1	Classification of low pressure vapour-liquid equilibria (LPVLE) equipment	44
3.2.4	LPVLE Recirculating Stills.....	46
3.2.2	Features of LPVLE Recirculating Equipment.....	47
3.2.3	Challenges of LPVLE Recirculating Equipment	48
3.3	Development of LPVLE Still for Operation at High Pressures and High Temperatures	48
3.3.1	Difference between HPVLE equipment and LPVLE equipment modified for high temperatures and pressures.....	51

CHAPTER FOUR**EXPERIMENTAL EQUIPMENT.....52**

4.1	Description of experimental apparatus.....	54
4.2	Features of experimental apparatus.....	61
4.3	Modifications to VLE still.....	64

CHAPTER FIVE**EXPERIMENTAL PROCEDURE.....67**

5.1	Leak test	67
5.2	Sensor and detector calibration	68
5.2.1	Pressure calibration	68
5.2.2	Temperature calibration	68
5.2.3	Gas chromatograph detector calibration.....	68
5.3	Start up procedure	70
5.4	Procedure for the measurement of isobaric VLE (attaining equilibrium).....	72
5.5	Shut down Procedure	73

5.6	Procedure for measurement of isothermal VLE	73
5.7	Cleaning the still.....	74

CHAPTER SIX

EXPERIMENTAL RESULTS.....75

6.1	Calibrations	76
6.1.1	Temperature calibration	76
6.1.2	Pressure calibration	77
6.1.3	Gas Chromatograph calibrations	78
6.2	Vapour Pressures.....	81
6.2	VLE measurements for 1-hexene (1) + n-hexane (2) systems	86
6.3	VLE measurements for 2-methyl-2-pentene (1) + n-hexane (2) systems	90
6.4	VLE measurements for n-methyl-2-pyrrolidone (1) + 1-hexene (2) systems	94

CHAPTER SEVEN

DISCUSSION.....98

7.1	Chemicals used in this investigation	98
7.2	VLE Systems Investigated	100
7.2.1	1-Hexene (1) + n-Hexane (2) System.....	101
7.2.2	2-Methyl-2-pentene (1) + n-Hexane (2) System	103
7.2.3	n-Methyl-2-pyrrolidone (1) + 1-Hexene (2) System	105
7.3	Data Reduction.....	108
7.3.1	1-Hexene (1) + n-Hexane (2) System.....	112
7.3.2	2-Methyl-2-pentene (1) + n-Hexane (2) System	119
7.3.3	n-Methyl-2-pyrrolidone (1) + 1-Hexene (2) System	126
7.4	Consistency Tests.....	134
7.4.1	Area Test	134
7.4.1.1	1-Hexene (1) + n-Hexane (2) System.....	135
7.4.1.2	2-Methyl-2-pentene (1) + n-Hexane (2) System.....	137
7.4.1.3	n-Methyl-2-pyrrolidone (1) + 1-Hexene (2) System	139
7.4.2	Point Test.....	140
7.4.2.1	1-Hexene (1) + n-Hexane (2) System	142
7.4.2.2	2-methyl-2-pentene (1) + n-hexane (2) Systems	143
7.4.2.3	n-Methyl-2-pyrrolidone (1) + 1-Hexene (2) System.....	145

CHAPTER EIGHT	
CONCLUSION.....	147
CHAPTER NINE	
RECOMMENDATIONS	149
CHAPTER TEN	
REFERENCES.....	150
APPENDIX A	
SUMMARIES OF LPVLE AND HPVLE EQUIPMENT.....	155
APPENDIX B	
CHEMICAL PROPERTIES AND CONSTANTS.....	158
APPENDIX C	
LIMITING ACTIVITY COEFFICIENTS.....	159
APPENDIX D	
CONSISTENCY POINT TEST	164
D1. 1-Hexene (1) + n-Hexane (2) System.....	165
D2. 2-Methyl-2-pentene (1) + n-Hexane (2) System	167
D3. n-Methyl-2-pyrrolidone (1) + n-Hexane (2) System.....	168

LIST OF FIGURES

CHAPTER TWO

Figure 2-1: Block diagram of basic overview of solution thermodynamics adapted from Soni (2003).....	4
Figure 2-2: Algorithm for the bubble point temperature iteration for the combined method (Smith <i>et al.</i> , 2001).....	28
Figure 2-3: Algorithm for the bubble point pressure iteration for the direct method (Smith <i>et al.</i> , 2001).	32

CHAPTER THREE

Figure 3-1: Classification of HPVLE (adapted from Raal and Mülhbauer, 1998).....	37
Figure 3-2: Schematic of common HPVLE two phase recirculating apparatus, adapted from Harris (2004).	38
Figure 3-3: Classification of LPVLE equipment (adapted from Reddy, 2006).	44
Figure 3-4: Low-pressure recirculating still of Raal and Mülhbauer (1998).	46
Figure 3-5: Schematic of apparatus of Harris (Harris, 2004).....	49

CHAPTER FOUR

Figure 4-1: Schematic of VLE apparatus (Reddy, 2006).....	53
Figure 4-2: Schematic to illustrate pressure control system.....	57
Figure 4-3: Schematic to illustrate pressure control.....	58
Figure 4-4: Isobaric control flow sheet (Harris, 2004).....	60
Figure 4-5: Schematic of position of transducers.....	65

CHAPTER FIVE

Figure 5-1: Auxiliary equipment and layout of experimental apparatus (Reddy, 2006).....	70
---	----

CHAPTER SIX

Figure 6-1: Plot of actual temperature versus resistance of Pt-100 sensor.....	76
--	----

Figure 6-2: Plot of actual pressure versus pressure readings from transducers.	77
Figure 6-3: Calibration of GC detector response for 1-hexene (1) with n-hexane (2).....	78

CHAPTER SEVEN

Figure 7-1: Plot of liquid molar volume and second virial coefficients against temperature..	113
Figure 7-2: NRTL, Wilson and Van Laar model fits to P-x-y diagram of 1-hexene (1) + n-hexane (2) at 55°C.....	114
Figure 7-3: NRTL, Wilson and Van Laar model fits to x-y diagram of 1-hexene (1) + n-hexane (2) at 55°C.....	114
Figure 7-4: NRTL, Wilson and Van Laar model fits to P-x-y diagram of 1-hexene (1) + n-hexane (2) at 80°C.....	115
Figure 7-5: NRTL, Wilson and Van Laar model fits to x-y diagram of 1-hexene (1) + n-hexane (2) at 80°C.....	115
Figure 7-6: NRTL, Wilson and Van Laar model fits to P-x-y diagram of 1-hexene (1) + n-hexane (2) at 105°C.....	116
Figure 7-7: NRTL, Wilson and Van Laar model fits to x-y diagram of 1-hexene (1) + n-hexane (2) at 105°C.....	116
Figure 7-8: Temperature dependency of NRTL parameters for 1-hexene with n-hexane	118
Figure 7-10: Temperature dependency of Wilson parameters for 1-hexene with n-hexane	119
Figure 7-11: NRTL, Wilson and Van Laar model fits to P-x-y diagram of 2-methyl-2-pentene (1) + n-hexane (2) at 55°C.....	120
Figure 7-12: NRTL, Wilson and Van Laar model fits to x-y diagram of 2-methyl-2-pentene (1) + n-hexane (2) at 55°C	121
Figure 7-14: NRTL, Wilson and Van Laar model fits to x-y diagram of 2-methyl-2-pentene (1) + n-hexane (2) at 80°C	122
Figure 7-15: NRTL, Wilson and Van Laar model fits to P-x-y diagram of 2-methyl-2-pentene (1) + n-hexane (2) at 105°C.....	122
Figure 7-16: NRTL, Wilson and Van Laar model fits to x-y diagram of 2-methyl-2-pentene (1) + n-hexane (2) at 105°C	123
Figure 7-17: Temperature dependency of NRTL parameters for 2-methyl-2-pentene with n-hexane	125
Figure 7-18: Temperature dependency of Van Laar parameters for 2-methyl-2-pentene with n-hexane	125

Figure 7-19: Temperature dependency of Wilson parameters for 2-methyl-2-pentene with n-hexane	126
Figure 7-20: NRTL and Wilson model fits to T-x-y diagram of n-methyl-2-pyrrolidone (1) + 1-hexene (2) at 45 kPa.....	127
Figure 7-21: Van Laar and UNIQUAC model fits to T-x-y diagram of n-methyl-2-pyrrolidone (1) + 1-hexene (2) at 45 kPa.....	127
Figure 7-22: NRTL and Wilson model fits to x-y diagram of n-methyl-2-pyrrolidone (1) + 1-hexene (2) at 45 kPa.....	128
Figure 7-23: Van Laar and UNIQUAC model fits to x-y diagram of n-methyl-2-pyrrolidone (1) + 1-hexene (2) at 45 kPa	128
Figure 7-24: NRTL and Wilson model fits to T-x-y diagram of n-methyl-2-pyrrolidone (1) + 1-hexene (2) at 80 kPa.....	129
Figure 7-25: Van Laar and UNIQUAC model fits to T-x-y diagram of n-methyl-2-pyrrolidone (1) + 1-hexene (2) at 80 kPa.....	129
Figure 7-26: NRTL and Wilson model fits to x-y diagram of n-methyl-2-pyrrolidone (1) + 1-hexene (2) at 80 kPa.....	130
Figure 7-27: Van Laar and UNIQUAC model fits to x-y diagram of n-methyl-2-pyrrolidone (1) + 1-hexene (2) at 80 kPa	130
Figure 7-28: NRTL and Wilson model fits to T-x-y diagram of n-methyl-2-pyrrolidone (1) + 1-hexene (2) at 100 kPa.....	131
Figure 7-29: Van Laar and UNIQUAC model fits to T-x-y diagram of n-methyl-2-pyrrolidone (1) + 1-hexene (2) at 100 kPa.....	131
Figure 7-30: NRTL and Wilson model fits to x-y diagram of n-methyl-2-pyrrolidone (1) + 1-hexene (2) at 100 kPa.....	132
Figure 7-31: Van Laar and UNIQUAC model fits to x-y diagram of n-methyl-2-pyrrolidone (1) + 1-hexene (2) at 100 kPa	132
Figure 7-31: Consistency area test for 1-hexene (1) + n-hexane (2) at 55 °C.....	135
Figure 7-32: Consistency area test for 1-hexene (1) + n-hexane (2) at 80 °C.....	135
Figure 7-33: Consistency area test for 1-hexene (1) + n-hexane (2) at 105 °C.....	136
Figure 7-34: Consistency area test for 2-methyl-2-pentene (1) + n-hexane (2) at 55 °C.....	137
Figure 7-35: Consistency area test for 2-methyl-2-pentene (1) + n-hexane (2) at 80 °C.....	137
Figure 7-36: Consistency area test for 2-methyl-2-pentene (1) + n-hexane (2) at 105 °C.....	138
Figure 7-37: Consistency area test for n-methyl-2-pyrrolidone (1) + 1-hexene (2) at 45 kPa.....	139
Figure 7-38: Consistency area test for n-methyl-2-pyrrolidone (1) + 1-hexene (2) at 80 kPa.....	139

Figure 7-39: Consistency area test for n-methyl-2-pyrrolidone (1) + 1-hexene (2) at 100 kPa.....	140
Figure 7-40: Consistency Point test for 1-hexene (1) + n-hexane (2) at 55 °C.....	142
Figure 7-41: Consistency Point test for 1-hexene (1) + n-hexane (2) at 80 °C.....	142
Figure 7-42: Consistency Point test for 1-hexene (1) + n-hexane (2) at 105 °C.....	143
Figure 7-43: Consistency Point test for 2-methyl-2-pentene (1) + n-hexane (2) at 55 °C.....	143
Figure 7-44: Consistency Point test for 2-methyl-2-pentene (1) + n-hexane (2) at 80 °C.....	144
Figure 7-45: Consistency Point test for 2-methyl-2-pentene (1) + n-hexane (2) at 105 °C.....	144
Figure 7-47: Consistency Point test for n-methyl-2-pyrrolidone (1) + 1-hexene (2) at 80 kPa.....	145
Figure 7-48: Consistency Point test for n-methyl-2-pyrrolidone (1) + 1-hexene (2) at 100 kPa.....	146

APPENDIX C

Figure C-1: Plot of $\left(\frac{x_1x_2}{P_D}\right)$ for 1-hexene (1) + n-hexane (2) system at 55 °C.....	159
Figure C-2: Plot of $\left(\frac{P_D}{x_1x_2}\right)$ for 1-hexene (1) + n-hexane (2) system at 80 °C.....	160
Figure C-3: Plot of $\left(\frac{P_D}{x_1x_2}\right)$ for 1-hexene (1) + n-hexane (2) system at 105 °C.....	160
Figure C-4: Plot of $\left(\frac{P_D}{x_1x_2}\right)$ for 2-methyl-2-pentene (1) + n-hexane (2) system at 55 °C.....	161
Figure C-5: Plot of $\left(\frac{x_1x_2}{P_D}\right)$ for 2-methyl-2-pentene (1) + n-hexane (2) system at 55 °C.....	161
Figure C-6: Plot of $\left(\frac{P_D}{x_1x_2}\right)$ for 2-methyl-2-pentene (1) + n-hexane (2) system at 80 °C.....	162
Figure C-7: Plot of $\left(\frac{P_D}{x_1x_2}\right)$ for 2-methyl-2-pentene (1) + n-hexane (2) system at 105 °C....	162
Figure C-8: Plot of $\left(\frac{x_1x_2}{P_D}\right)$ for 2-methyl-2-pentene (1) + n-hexane (2) system at 105 °C....	163

APPENDIX D

Figure D-1: Consistency Point test for 1-hexene (1) + n-hexane (2) at 55 °C.....	165
Figure D-2: Consistency Point test for 1-hexene (1) + n-hexane (2) at 80 °C.....	165
Figure D-3: Consistency Point test for 1-hexene (1) + n-hexane (2) at 105 °C.....	166
Figure D-4: Consistency Point test for 2-methyl-2-pentene (1) + n-hexane (2) at 55 °C.....	167
Figure D-5: Consistency Point test for 2-methyl-2-pentene (1) + n-hexane (2) at 80 °C.....	167
Figure D-6: Consistency Point test for 2-methyl-2-pentene (1) + n-hexane (2) at 105 °C.....	168
Figure D-7: Consistency Point test for n-methyl-2-pyrrolidone (1) + n-hexane (2) at 45 kPa	168
Figure D-8: Consistency Point test for n-methyl-2-pyrrolidone (1) + n-hexane (2) at 80 kPa	169
Figure D-9: Consistency Point test for n-methyl-2-pyrrolidone (1) + n-hexane (2) at 100 kPa	169

LIST OF TABLES

CHAPTER TWO

Table 2-1: Prausnitz mixing rules for cross coefficient parameters (O' Connell and Prausnitz, 1967).....	11
--	----

CHAPTER THREE

Table 3-3: Differences between traditional HPVLE recirculation equipment and LPVLE recirculation equipment modified for high pressures and high temperatures.	51
--	----

CHAPTER SIX

Table 6-1: Operating conditions of GC used during calibration and analysis of experimental VLE samples	78
Table 6-2: P-T data for 1-hexene	82
Table 6-3: P-T data for n-hexane	83
Table 6-4: P-T data for 2-methyl-2-pentene	84
Table 6-5: P-T data for n-methyl-2-pyrrolidone	85
Table 6-6: Isothermal data for the 1-hexene (1) + n-hexane (2) systems	86
Table 6-7: Isothermal data for 2-methyl-2-pentene (1) + n-hexane (2) systems	90
Table 6-8: Isobaric data for the systems of n-methyl-2-pyrrolidone (1) + 1-hexene (2)	94

CHAPTER SEVEN

Table 7-1: Purities of chemicals used in this study.....	98
Table 7-2: AAD percentage between experimental and calculated temperature.....	99
Table 7-3: Comparison of experimental and literature Antoine constants	100
Table 7-4: AAD percentage of temperature and composition data for the systems of 1-hexene (1) + n-hexane (2).....	101
Table 7-5: Relative volatilities of 1-hexene (1) + n-hexane (2) systems	102
Table 7-6: AAD percentage of temperature and composition data for the systems of 2-methyl-2-pentene (1) + n-hexane (2).....	103
Table 7-7: Relative volatilities of 2-methyl-2-pentene (1) + n-hexane (2) systems	104
Table 7-8: AAD percentage of composition data for the systems of n-methyl-2-pyrrolidone (1) + 1-hexene (2).....	105

Table 7-9:	Relative volatilities of n-methyl-2-pyrrolidone (1) + 1-hexene (2) systems	108
Table 7-10:	Summary of isothermal data regression.....	108
Table 7-11:	Summary of isobaric data regression.....	110
Table 7-12:	Best fit models for the system of 1-hexene (1) + n-hexane (2).....	112
Table 7-13:	Liquid molar volumes (V , $\text{cm}^3 \text{mol}^{-1}$) and second virial coefficients (B , $\text{cm}^3 \text{mol}^{-1}$) of n-hexane at different temperatures (T , $^{\circ}\text{C}$).	113
Table 7-14:	Infinite activity coefficients for the systems of 1-hexene (1) + n-hexane (2)	113
Table 7-15:	Excess Gibbs energy parameters regressed for the system of 1-hexene (1) with n-hexane (2).....	117
Table 7-16:	Best fit models for the system of 2-methyl-2-pentene (1) + n-hexane (2).....	119
Table 7-17:	Infinite dilution activity coefficients for the systems of 2-methyl-2-pentene (1) + n-hexane (2).....	120
Table 7-18:	Excess Gibbs energy parameters regressed for the system of 2-methyl-2-pentene (1) + n-hexane (2).....	124
Table 7-19:	Best fit models for the system of n-methyl-2-pyrrolidone (1) + 1-hexene (2)...	126
Table 7-20:	Excess Gibbs energy parameters regressed for the system of n-methyl-2-pyrrolidone (1) + 1-hexene (2).....	133
Table 7-21:	Results of area test for 1-hexene (1) + n-hexane (2)	136
Table 7-22:	Results of area test for 2-methyl-2-pentene (1) + n-hexane (2)	138
Table 7-23:	Results of area test for n-methyl-2-pyrrolidone (1) + 1-hexene (2)	140
Table 7-24:	The best fit models and percentage bias	141

CHAPTER EIGHT

Table 8-1:	Best fit models for all systems investigated	147
------------	--	-----

APPENDIX A

Table A-1:	Chronological order of HPVLE equipment development.....	155
Table A-2:	Chronological order of LPVLE equipment development	156

APPENDIX B

Table B1: Chemical properties.....	158
Table B2: Antoine constants	158

APPENDIX D

Table D-1: Best models for consistency point test	164
---	-----

NOMENCLATURE

ω	Acentric factor (Equation 2-26)
γ	Activity coefficient of species i (Equation 2-17)
μ_i	Chemical Potential of species i (Equation 2-11)
Φ	Correction factor for vapour phase non-ideality (Equation 2-19)
A^E	Excess Helmholtz energy
$\hat{\phi}_i$	Fugacity coefficient of species i in solution (Equation 2-16)
\hat{f}_i	Fugacity of species i in solution (Equation 2-13)
\bar{G}_i	Partial Molar Gibbs energy of species i (Equation 2-11)
ϕ	Pure component fugacity coefficient (Equation 2-4)
Γ	Temperature dependant integration constant (Section 2.1)
α_{ij}	Empirical parameter of NRTL equation equivalent to α_{ji} related to non-randomness of a mixture (Equation 2-67)
τ_{ji}, τ_{ji}	Adjustable parameters of NRTL model (Equation 2-68)
a	Temperature dependent constant accounts for intermolecular attraction force of molecules in Peng-Robinson Equation of state (Equation 2-35)
B	Second virial coefficient (Equation 2-22)
b	Temperature independent constant accounts for the molecular size of the molecule in the Peng-Robinson Equation of state (Equation 2-35)
B_{ii}	Pure component second Virial coefficient (Equation 2-24)
B_{ij}	Cross second virial coefficient (Equation 2-26)
f	Pure component fugacity of species i . (Equation 2-1)
G	Gibbs Energy (Section 2.1)
H^E	Excess enthalpy (Equation 2-57)
K_I	Peng-Robison Stryjek-Vera adjustable parameter (Equation 2-39)
n	number of moles
P	Pressure
P_D	Deviation pressure (Equation 2-73)
R	Universal Gas constant
T	Temperature
V	Molar Volume
x_i	Liquid mole fraction of component i
y_i	Vapour phase mole fraction of component i

Z	Compressibility factor (Equation 2-6).
δ	Residual defined as difference between calculated and experimental values (Equation 2-82).
S	Objective function equivalent to sum of squares of residuals (Equation 2-82).
a_1, a_2	Defined as area above (a_1) and below (a_2) graph for area test (Equation 2-92)

SUBSCRIPTS

r	Reduced property
c	Critical property
i	Property of species i
1	Component 1
2	Component 2

SUPERSCRIPTS

0	Pitzer correlation parameter (Equation 2-26)
1	Pitzer correlation parameter (Equation 2-26)
∞	Property at infinite dilution concentration (Equation 2-69)
exp	Experimental property values
l	Liquid phase property
v	Vapour phase property
sat	saturated property value
id	Property value for an ideal solution
ig	Property value for an ideal gas
R	Residual property
E	Excess property

ABBREVIATIONS

EOS	Equation of state
NRTL	Non-random two liquid theory
RMS	Root mean square
VLE	Vapour-liquid equilibria
UNIQUAC	Universal Quasi-chemical Model

CHAPTER ONE

INTRODUCTION

It has been evident in the past years that distillation represents a large percentage of separation processes in industry and according to Seader and Henley (1998) separation processes account for a significant percentage of all processes on a typical chemical plant. They also account for more than 50% of total capital costs and 90% of total energy usage (Streicher *et al.*, 1995).

It is necessary then, that the parameters responsible for the design of these processes, obtained from vapour-liquid equilibria (VLE) studies, are accurate and reliable for optimisation purposes. Not only does the acquisition of binary VLE data allow for optimisation of these processes and the ability to assess multi-component systems but it also allows for the feasibility of separating a system to be established. It is obvious that increased energy efficiency and savings are possible, and the product of extensive research and consistent VLE data.

The aim of this study is to obtain VLE data for binary systems involving 1-hexene and n-hexane which will aid in better predicting parameters and contributes to the ongoing research in the Thermodynamics Research Unit, University of KwaZulu-Natal. These systems are of interest and importance in the petrochemical industry.

The system of 1-hexene with n-hexane is separated in industry by extractive distillation and is used to understand the separation of olefins and paraffins respectively. Separation of olefins and paraffins is a very specific problem in the field of hydrocarbon processing. The boiling points of these hydrocarbons fall in a narrow range, with relative volatilities close to one, and as a result are expensive and difficult to separate. It would require more than 100 trays (Seader and Henley, 1998) to separate by conventional distillation. The solution is to employ enhanced distillation, in particular, extractive distillation which is common to the petrochemical- and chemical processing industries (Seader *et al.*, 1998). However this type of separation process requires the use of a third component, an entrainer. Essentially the entrainer alters the relative volatility of the system by changing the activity coefficients of one of the components, allowing separation and reducing the number of trays in the column.

Common entrainers include ionic liquids and polar solvents. Ionic liquids have desirable characteristics, but are significantly more expensive than polar solvents. One of the most common polar solvents used is n-methyl-2-pyrrolidone (NMP), which is investigated with 1-hexene at three different isobars in this study. Other than cost, availability and toxicity, the

choice of an entrainer depends on its selectivity as well as its capacity, which according to Lei *et al.* (2006) should be high. The applications of NMP in industry include absorption of sour gases from natural gas, separation of aromatics from non-aromatics and different dienes from C4 and C5 fractions (Fischer and Gmehling, 1996).

In the publication of Fischer and Gmehling (1996) the selectivity of NMP in the system of 1-hexene with n-hexane is proven to be greater towards 1-hexene than n-hexane. This can be explained by the mobility of the carbon double bond which is based on the use of ionic liquids as entrainers discussed in Lei *et al.* (2006). Therefore in a distillation column 1-hexene and NMP can be removed together in a single stream and can be separated with the help of thermodynamic data, in particular VLE. The separation of this stream will allow for the recovery and recycling of NMP for further use as an entrainer.

The combination of accurate VLE data and suitable solvent choice is a recipe for effective and economical design of extractive distillation (Lei *et al.*, 2007)

The system of 2-methyl-2-pentene with n-hexane is similar to the system of 1-hexene and n-hexane with relative volatilities approaching unity and requiring unconventional distillation to achieve separation. This binary system represents just one of interactions occurring in exit streams in the petrochemical industry which could contain as many as 29 different components (Wentik *et al.*, 2007). 2-Methyl-2-pentene's most noteworthy use is in the synthesis of ethers, which until recently (\pm ten years) has experienced rapid growth due to the use of ethers as octane enhancers in gasoline. This was mainly due to the environmental safety benefits offered by ethers, in particular reduced CO and unburned hydrocarbon emissions.

The systems described above are part of a growing data base of experimental VLE data upon which predictive models are based. Numerous models exist in literature for the prediction of binary VLE data, however they are still in the development stage and their reliability, in the case of non-ideal systems is questionable (Joseph, 2001). There is certainly a strong need for direct experimentation, since the accuracy of prediction is determined by comparison with experimental VLE data.

The benefits of better fit parameters and consistent VLE data are indispensable to the process industry. In light of the current environmental regulations and given that energy efficiency and optimisation are the focus of the process industry, experimental work and ongoing research in the analysis of data are critical to both the improvement of current processes and the efficient design of future processes.

The recent hype with regard to environmental standards, regulations and the state of our environment has made industry and the general population aware of the consequences of neglect and disregard for the environment. It would be impossible, as attractive as the option is to environmentalists, to stop all industrial processes in the pursuit of healing the environment. The economic, political and social ramifications would be daunting. The solution therefore has to be to the implementation of more stringent regulations and, just as important, to optimise and re-design these processes to a point where their carbon footprint is significantly reduced.

The outline of this dissertation is as follows; Chapter two and three highlight VLE data reductions and analysis required for the interpretation of the VLE data and a review of equipment and method respectively. Chapter four focuses on the experimental equipment used in this investigation and discusses the features as well as some minor, though significant modifications. The experimental procedure including the start up and shut down procedures are presented in Chapter five. Chapter six and seven present the results of this investigation and the discussion thereof. The conclusions drawn from this investigation and recommendations are presented in Chapters eight and nine respectively.

CHAPTER TWO

VAPOUR LIQUID EQUILIBRIA DATA REDUCTION AND ANALYSIS

VLE data reduction and analysis over the years has been discussed in great detail by many authors and the reader is directed to texts such as Van Ness and Abbott (1982) and Smith *et al.* (2001). This section will discuss briefly those aspects of solution thermodynamics applicable to the work presented in this investigation. A basic over view of solution thermodynamics presented in this chapter, is illustrated in the block diagram below, adapted from Soni (2003).

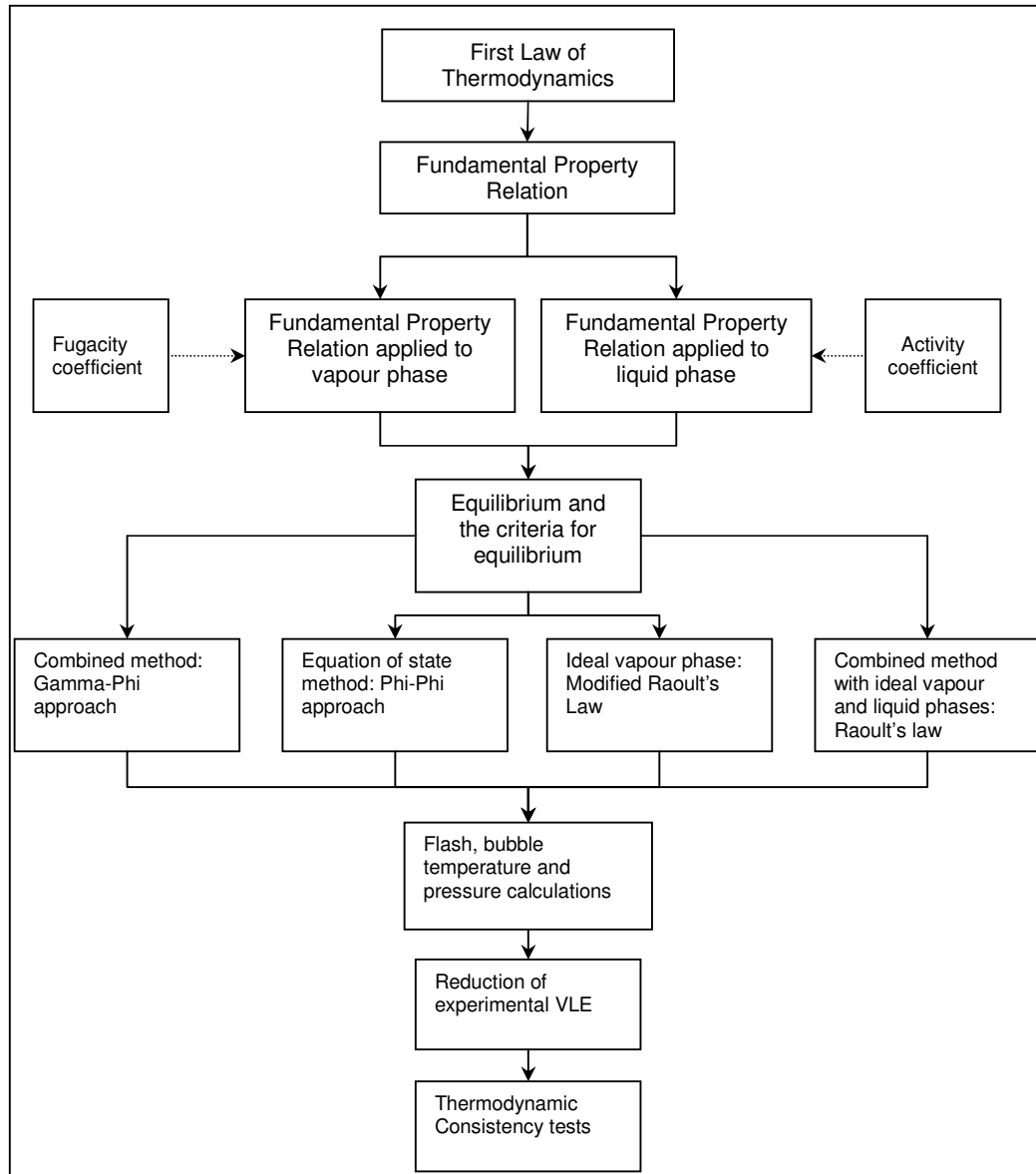


Figure 2-1: Block diagram of basic overview of solution thermodynamics adapted from Soni (2003).

2.1 Fugacity and fugacity coefficient

Equilibrium as defined in Smith *et al.* (2001) is when macroscopic changes in a system do not occur. Chemical potential, μ_i is a criterion for phase equilibria, however it has no physical meaning. Fugacity, f_i was introduced to afford chemical potential an actual physical meaning and has the units of pressure. It is related to the chemical potential at constant temperature by the following equation of Gibbs energy for a real fluid:

$$G_i \equiv \Gamma(T) + RT \ln f_i \quad (2-1)$$

In Equation (2-1) $\Gamma(T)$ is a temperature dependant integration constant.

Gibbs energy for an ideal gas is therefore

$$G_i^{ig} = \Gamma(T) + RT \ln P \quad (2-2)$$

The behaviour of real gases may be compared to the ideal gas model which is used to define residual properties. The residual property is defined as the difference between the real fluid and ideal fluid and in the case of Gibbs energy can be written as:

$$G^R = G_i - G_i^{ig} = RT \ln \frac{f_i}{P} \quad (2-3)$$

The dimensionless ratio $\frac{f_i}{P}$ is the definition of the fugacity coefficient, ϕ_i and can be written as:

$$\phi_i = \frac{f_i}{P} \quad (2-4)$$

Therefore,

$$G^R = RT \ln \phi_i \quad (2-5)$$

For a pure component the fugacity coefficient is related to the compressibility factor, Z by the following equation

$$\ln \phi = \int_0^P (Z - 1) \frac{dP}{P} \quad (2-6)$$

Where $Z = \frac{PV}{RT}$ and P , R , T and V are pressure, Universal gas constant, temperature and molar volume respectively.

Equation 2-2 may be written for species i as a saturated vapour and liquid and by difference gives the following equation

$$G_i^v - G_i^l = RT \ln \frac{f_i^v}{f_i^l} \quad (2-7)$$

As the system is in equilibrium the term on the left side of the above equation is reduced to zero in a two phase system of a pure species (Smith *et al.*, 2001) since Gibbs energy does not change in a phase transition. Therefore, for both the saturated liquid and saturated vapour at the same temperature and saturated pressure, one obtains:

$$f_i^v = f_i^l = f_i^{sat} \quad (2-8)$$

Therefore from Equation 2-4,

$$\phi_i^{sat} = \frac{f_i^{sat}}{P_i^{sat}} \quad (2-9)$$

and,

$$\phi_i^v = \phi_i^l = \phi_i^{sat} \quad (2-10)$$

The above equations are applicable to pure species, similarly for a species i in solution, an expression can be derived for chemical potential that is equivalent to the partial molar Gibbs energy:

$$\bar{G}_i \equiv \mu_i = \left(\frac{\partial(nG)}{\partial n_i} \right)_{T,P,n_j} \quad (2-11)$$

For an ideal gas Equation 2-1 differentiated can be written as

$$\mu_i^{ig} = \Gamma_i(T) + RT \ln y_i P \quad (2-12)$$

where $y_i P$ is the partial pressure.

For a species in solution, the fugacity is represented by:

$$\mu_i = \Gamma_i(T) + RT \ln \hat{f}_i \quad (2-13)$$

where \hat{f}_i is the fugacity of species i in solution and should not be mistaken for a partial molar property.

It follows from Equations 2-8 and 2-10

$$\hat{f}_i^\alpha = \hat{f}_i^\beta = \hat{f}_i^{sat} \quad (2-14)$$

In terms of vapour-liquid equilibria

$$\hat{f}_i^v = \hat{f}_i^l \quad (2-15)$$

The fugacity coefficient of species i in solution is then related to fugacity of species i in solution, by the following equation in the vapour phase

$$\hat{f}_i^v = y_i \hat{\phi}_i P \quad (2-16)$$

And in the liquid phase the fugacity in solution can be written as

$$\hat{f}_i^l = x_i \gamma_i f_i \quad (2-17)$$

where γ_i is the activity coefficient of species i in solution.

Liquid pure component fugacity can be derived from the above equations and is done in two parts as established by Smith *et al.* (2001). The resultant equation is

$$f_i = \phi_i^{sat} P_i^{sat} \exp\left[\frac{V_i^l (P - P_i^{sat})}{RT}\right] \quad (2-18)$$

The exponential term is known as the Poynting correction factor. According to Smith *et al.* (2001) it may be neglected at low pressures as its effect is negligible.

Combining equations 2-16, 2-17 and 2-18 above, Equation 2-19 is obtained and is known as the Gamma-Phi ($\gamma - \Phi$) approach to VLE.

$$y_i \Phi_i P = x_i \gamma_i P_i^{sat} \quad (2-19)$$

where

$$\Phi_i = \left(\frac{\hat{\phi}_i}{\phi_{sat}}\right) \exp\left[-\frac{V_i (P - P_i^{sat})}{RT}\right] \quad (2-20)$$

The liquid molar volume can be calculated from the Rackett equation (Rackett, 1970).

$$V_i^L = V_{c,i} Z_{c,i}^{(1-T_r)^{0.2857}} \quad (2-21)$$

T_r is defined as the reduced temperature and is equivalent to $\frac{T}{T_c}$. The critical properties for the

chemicals used in this study can be found in Table B1, Appendix B.

2.1.1 Fugacity coefficients from the virial equation of state

The fugacity coefficient may be evaluated from the compressibility factor (Z) and can be evaluated in two ways either from PVT data or obtained analytically from equations of state.

The two term virial equation of state is given by

$$Z = 1 + \frac{BP}{RT} \quad (2-22)$$

where B is the second virial coefficient.

The generalised correlation of the compressibility factor given by Pitzer *et al.* (1955) is applicable to all gases and is given below in Equation 2-23

$$Z = Z^0 + \omega Z^1 \quad (2-23)$$

Where Z^0 and Z^1 are both function of T_r and P_r and ω is the acentric factor.

The virial equation of state was used in the determination of the fugacity coefficients for isobaric data presented in this investigation. The details and derivation of this equation of state are presented in Smith *et al.* (2001). Presented below are the final equations and the Pitzer correlation.

The fugacity coefficient for a binary mixture is given by

$$\Phi_i = \exp \left[\frac{(B_{ii} - V_i^l)(P - P_i^{sat}) + Py_j^2 \delta_{ij}}{RT} \right] \quad (2-24)$$

where,

$$\delta_{12} = 2B_{12} - B_{11} - B_{22} \quad (2-25)$$

The fugacity coefficient can also be evaluated for a multi-component mixture. The two term Virial equation of state is applicable to pressures up to 5 bar.

There are various methods to calculate the second virial coefficients in Equation 2-23 including the Pitzer and Curl (1957) correlation, correlation of Tsonopolous (1974) and Hayden and O'Connell method (1975). The method described in this section is the Pitzer-type correlation as it was employed in the calculations of second virial coefficients for isobaric data.

The virial coefficients for the Pitzer-Curl correlation can be obtained from Equations 2-22 and 2-23 together,

$$B_{ij} = \frac{RT_{c,ij}}{P_{c,ij}} (B^0 + \omega_{ij} B^1) \quad (2-26)$$

The values for B^0 and B^1 are

$$B^0 = 0.083 - \frac{0.422}{T_r^{1.6}} \quad (2-27)$$

and

$$B^1 = 0.139 - \frac{0.172}{T_r^{4.2}} \quad (2-28)$$

The mixing rules suggested by Prausnitz for the cross coefficient parameters of temperature, volume, compressibility factor, pressure and acentric factor are provided in Table 2-1.

Table 2-1: Prausnitz mixing rules for cross coefficient parameters (O' Connell and Prausnitz, 1967)

VARIABLE	MIXING RULE	EQUATION
Temperature	$T_{c12} = \sqrt{T_{c1}T_{c2}}$	(2-29)
Volume	$V_{c12} = \left[\frac{(V_{c1})^{\frac{1}{3}} + (V_{c2})^{\frac{1}{3}}}{2} \right]^3$	(2-30)
Compressibility factor	$Z_{c12} = \frac{Z_{c1} + Z_{c2}}{2}$	(2-31)
Pressure	$P_{c12} = \frac{Z_{c12}RT_{c12}}{V_{c12}}$	(2-32)
Acentric factor	$\omega_{c12} = \frac{\omega_1 + \omega_2}{2}$	(2-33)

In the event where the acentric factor is not known for a species the generalised equation for acentric factor (Pitzer *et al.*, 1955) is given by,

$$\omega = -1.0 - \log(P_r^{sat})_{T_r=0.7} \quad (2-34)$$

The acentric factor can therefore be evaluated for any fluid from T_c , P_c and a single vapour pressure measurement made at $T_r = 0.7$

2.1.2 Fugacity Coefficients from Cubic Equations of State

The fugacity coefficient can also be evaluated from a cubic equation of state (CEOS). The equations are in fact the simplest form of representing both liquid and vapour behaviour and also give results of high accuracy (Ghosh and Taraphdar, 1998). It also possesses sufficient flexibility to describe wide ranging phase behaviour and has found substantial application in VLE computations (Mülhbauer and Raal, 1995). The Redlich-Kwong and Peng-Robinson-Stryjek-Vera (PRSV) CEOS were used to calculate fugacity coefficients for the isobaric and isothermal systems, investigated in this study, respectively. These will only be briefly covered in this section. For a more detailed look at the CEOS the reader is referred to the text of Smith *et al.* (2001) and the MSc dissertation of Narasigadu (2007).

All cubic equations of state have the general form (Smith *et al.* 2001)

$$P = \frac{RT}{(V-b)} - \frac{a(V-\eta)}{(V-b)(V^2 + \delta V - \epsilon)} \quad (2-35)$$

Where b , a , δ , η are functions of temperature and composition.

The Redlich-Kwong EOS (Redlich and Kwong, 1949) is written as:

$$P = \frac{RT}{(V-b)} - \frac{a}{T^{1/2}V(V+b)} \quad (2-36)$$

where

$$a = 0.4278 \left(\frac{R^2 T_c^2}{P_c} \right) \quad (2-37)$$

and

$$b = 0.0867 \left(\frac{RT_c}{P_c} \right) \quad (2-38)$$

The coefficients a (the attraction coefficient) and b (the limiting volume coefficient) can be evaluated by the use of mixing rules. The Redlich-Kwong EOS is utilised in the Aspen modelling presented in this investigation. The reader is referred to Redlich and Kwong (1949) for details and derivation on the equation and Aspen help files for details on the modelling method.

The second EOS of state used in this investigation is the PRSV. Stryjek and Vera (1986) modified the Peng-Robinson equation by proposing a new temperature and acentric factor dependence of the attractive term. The modification made the Peng-Robinson equation apply to polar, non-polar, associating and non-associating molecules.

The Peng-Robinson equation of state is given by (Peng and Robinson, 1976):

$$P = \frac{RT}{(V-b)} - \frac{a(T, \omega)}{V(V+b)+b(V-b)} \quad (2-39)$$

where a is a temperature dependent constant that is related to the intermolecular attraction force of molecules and b which is temperature independent accounts for the molecular size of the molecule.

The parameters a and b can be determined from the following equations:

$$a_i(T) = a_i(T_c) \alpha(T_r, \omega) \quad (2-40)$$

where

$$a_i = 0.45724 \left(\frac{R^2 T_{ci}^2}{P_{ci}^2} \right) \quad (2-41)$$

and

$$b_i = 0.07780 \left(\frac{RT_{ci}}{P_{ci}} \right) \quad (2-42)$$

$$\alpha = [1 + K_i (1 - T_r^{0.5})]^2 \quad (2-43)$$

The equations proposed for κ by Stryjek and Vera (1986) were

$$\kappa_i = \kappa_0 + \kappa_1 (1 + \sqrt{T_r}) (0.7 - T_r) \quad (2-44)$$

$$\kappa_0 = 0.378 + 1.489\omega - 0.171\omega^2 - 0.019\omega^3 \quad (2-45)$$

κ_i is an adjustable parameter unique to a species and can be calculated by the regression of vapour pressure data.

The fugacity coefficient for component i in a mixture can be represented by the following equation

$$\ln \hat{\phi}_i = \frac{b_i}{b_m} (Z-1) - \ln(Z-B) - \frac{A}{2\sqrt{2}B} \times \left[\frac{2}{a_m} \sum y_i a_{ji} - \frac{b_i}{b_m} \right] \ln \left[\frac{Z + (1 + \sqrt{2})B}{Z - (1 - \sqrt{2})B} \right] \quad (2-46)$$

where

$$A = \frac{a_m(T)P}{R^2 T^2} \quad (2-47)$$

and

$$B = \frac{b_m P}{RT} \quad (2-48)$$

The values of a_m and b_m are evaluated by the use of mixing rules that extend the equation from pure components to mixtures.

where

$$a = \sum x_i x_j a_{ij} \quad (2-49)$$

and

$$b = \sum x_i b_i \quad (2-50)$$

The equation for the cross parameter a_{ij} employed by Peng and Robinson (1976) is

$$a_{ij} = (1 - k_{ij}) (a_i a_j)^{\frac{1}{2}} \quad (2-51)$$

where k_{ij} is an empirically determined binary interaction parameter that characterises the binary formed by component i and j .

The mixing rule used in the analysis of the VLE data at isothermal conditions, presented in this investigation, are those of the density independent mixing rule for cubic equations of state of Wong and Sandler (1992). It relates excess Helmholtz free energy (A^E) at infinite pressure from an equation of state to that from an activity coefficient model. The use of the excess Helmholtz energy, according to Wong and Sandler (1992), provides quadratic composition dependence of the second virial coefficients as is required by statistical mechanics where most other mixing rules fail. The benefits of employing the use of the excess Helmholtz free energy as opposed to excess Gibbs energy models is that whilst the latter are generally used at low pressures the Helmholtz excess energy is less pressure dependent and can be applied at both high and low pressures (Wong and Sandler, 1992). The Wong-Sandler mixing rule has the ability to predict high pressure and high temperature phase equilibria from low pressure G^E models (Ghosh and Taraphdar, 1998) and provides correct low and high density limits without being density dependent (Wong and Sandler, 1992).

This mixing rule is summarised below for component i in a mixture.

$$\frac{a_m}{RT} = \frac{MN}{1-N} \quad (2-52)$$

and

$$b_m = \frac{M}{1-N} \quad (2-53)$$

M and N are defined as follows:

$$M = \sum \sum x_i x_j \left(b - \frac{a}{RT} \right)_{ij} \quad (2-54)$$

and

$$N = \sum x_i \frac{a_i}{b_i RT} + \frac{A_\infty^E(x_i)}{\Omega RT} \quad (2-55)$$

where the excess Helmholtz energy can be modelled using any of the Gibbs energy models by the following relation (Wong and Sandler, 1992)

$$G^E(T, x, P = low) = A^E(T, x, P = low) = A^E(T, x, P = \infty) \quad (2-55a)$$

and the term Ω , which is an equation of state dependent constant, is defined as follows for the Peng-Robinson equation of state,

$$\Omega = \frac{\ln(\sqrt{2}-1)}{\sqrt{2}} \quad (2-56)$$

The mixing rule of Wong and Sandler, is theoretically correct and is accurate in describing simple and complex phase behaviour of binary and ternary systems.

2.2 Activity coefficient and Excess Gibbs Energy Models

Activity coefficients are used to account for the departure of the liquid phase from ideality. The activity coefficient was introduced in the previous section for the definition of liquid fugacity of species i in solution. The activity coefficient for species i is given by, re-arranging Equation 2-17,

$$\gamma_i = \frac{\hat{f}_i}{x_i f_i} \quad (2-17)$$

The molar Gibbs energy is written as

$$\bar{G}_i = \Gamma_i(T) + RT \ln \hat{f}_i \quad (2-57)$$

For an ideal solution, $\gamma_i = 1$ and Equation 2-17 above can be written as,

$$\hat{f}_i^{id} = x_i f_i \quad (2-58)$$

In the case of gases, the residual property was introduced to compare the ideal gas model to real gas. Similarly for liquids, the excess property is introduced which is defined as the difference between real and ideal solution behaviour.

For an ideal solution Equation 2-13 becomes

$$\bar{G}_i^{id} = \Gamma_i(T) + RT \ln x_i f_i \quad (2-59)$$

Subtracting the Gibbs energy for an ideal solution from real solution and substituting for activity coefficient defined above results in the Gibbs excess energy property

$$\bar{G}_i^E = RT \ln \gamma_i \quad (2-60)$$

The fundamental excess property is given by the following equation

$$d\left(\frac{nG^E}{RT}\right) = \frac{nV^E}{RT} dP + \frac{nH^E}{RT^2} dT + \sum_i \frac{\bar{G}_i^E}{RT} dn_i \quad (2-61)$$

and shows the inter-relation and significance of various thermodynamic excess properties.

By substituting the partial molar Gibbs excess energy in the fundamental property relation and solving $\ln \gamma_i$ at constant temperature, pressure and composition, the following equation is obtained

$$\ln \gamma_i = \left(\frac{\partial \left(\frac{nG^E}{RT} \right)}{\partial n_i} \right)_{T,P,n_j} \quad (2-62)$$

Since $\ln \gamma_i$ is a partial molar property with respect to $\frac{G^E}{RT}$

$$\frac{G^E}{RT} = \sum_i x_i \ln \gamma_i \quad (2-63)$$

The liquid phase activity coefficient is slightly pressure dependent at low to moderate pressures and for practical purposes depends only on temperature and composition. However at high pressures the dependence on pressure must be taken into account (Mülhbauer and Raal, 1995).

2.2.1 Evaluating activity coefficients

Activity coefficients can be obtained by evaluating Equations 2-58 and 2-59 in terms of Gibbs energy. Many models have been proposed however; those that were implemented in this investigation are

- a. Van Laar
- b. Wilson
- c. NRTL
- d. UNIQUAC

Prausnitz *et al.* (1986) details calculation techniques using a computer to calculate multi-component VLE from binary parameters only. Temperature independence of model parameters can only be assumed in the case of athermal mixtures, i.e. components can mix isothermally and isobarically without evolution or absorption of heat (Soni, 2003). For practical purposes, the assumption of temperature independence can also be made for small temperature ranges. The activity coefficients and VLE data can be interpolated and extrapolated from the determined adjustable parameters.

a) The Van Laar Model (Prausnitz *et al.*, 1986)

This model is suitable for constituents in a binary system that are similar chemically and have differing molar volumes. All interaction parameters except a_{12} are ignored. This model has been found to represent some complex systems despite its derivation which suggests that it is suitable for simple, non-polar liquids. The advantage of this model is that it is mathematically simple, yet flexible.

The Gibbs excess expression is as follows:

$$\frac{G^E}{RT} = \frac{2a_{12}x_1x_2q_1q_2}{x_1q_1 + x_2q_2} \quad (2-64)$$

where a is a constant characteristic of interaction between molecule 1 and 2 and q_i , the measure of the size of molecule i .

The activity coefficients for the Van Laar Model (Equation 2-61) are obtained by assessing Equations 2-58 together with Equation 2-60.

$$\ln \gamma_1 = \frac{A_{12}}{\left(1 + \frac{A_{12} x_1}{A_{21} x_2}\right)^2}$$

$$\ln \gamma_2 = \frac{A_{21}}{\left(1 + \frac{A_{21} x_2}{A_{12} x_1}\right)^2}$$
(2-65)

where $A_{12} = 2q_1a_{12}$ and $A_{21} = 2q_2a_{12}$ are empirical constants. Prausnitz suggest that it is not necessary to know the values of q_1 and q_2 since A_{12} and A_{21} are obtained empirically, and that it is not possible to find a value for a_{12} unless an assumption of q_1 and q_2 are made.

b) The Wilson Model (Wilson, 1964)

A more superior model to Van Laar's model is that model developed by Wilson. This model is based on the dependence of interactions between molecules on local concentrations, expressed as volume fractions Walas (1985, cited by Soni, 2003). The detail of the derivation of the Wilson equation is given by Prausnitz *et al.* (1986).

This model has two adjustable parameters ($\lambda_{12}-\lambda_{11}$) and ($\lambda_{21}-\lambda_{22}$). The temperature dependence of these adjustable parameters cannot be neglected for accurate computations, however they are fairly temperature insensitive over a modest temperature range (Prausnitz *et al.*, 1986), thus it can be used for isobaric systems if the temperature range is not broad.

The Wilson model can be applied to multi-component systems with parameters evaluated from the constituent binary systems. However, it cannot be applied to the prediction of liquid immiscibility or extrema in the activity coefficients (Prausnitz *et al.*, 1986)

The Gibbs Excess model for Wilson is as follows:

$$\frac{G^E}{RT} = -x_1 \ln(x_1 + x_2 \Lambda_{12}) - x_2 \ln(x_2 + x_1 \Lambda_{21})$$
(2-66)

The activity coefficients for the Wilson Model (Equation 2-63) are obtained by assessing Equation 2-58 together with Equation 2-62.

$$\begin{aligned}\ln \gamma_1 &= -\ln(x_1 + x_2\Lambda_{12}) + x_2 \left(\frac{\Lambda_{12}}{x_1 + x_2\Lambda_{12}} - \frac{\Lambda_{21}}{x_2 + x_1\Lambda_{21}} \right) \\ \ln \gamma_2 &= -\ln(x_2 + x_1\Lambda_{21}) + x_1 \left(\frac{\Lambda_{12}}{x_1 + x_2\Lambda_{12}} - \frac{\Lambda_{21}}{x_2 + x_1\Lambda_{21}} \right)\end{aligned}\quad (2-67)$$

where,

$$\begin{aligned}\Lambda_{12} &= \frac{V_2}{V_1} \exp\left(-\frac{\lambda_{12} - \lambda_{11}}{RT}\right) \\ \Lambda_{21} &= \frac{V_1}{V_2} \exp\left(-\frac{\lambda_{21} - \lambda_{22}}{RT}\right)\end{aligned}\quad (2-68)$$

and the symbol, λ_{ij} , represents the energies of interaction between the molecules i and j . The volumes can be obtained by the use of the Rackett equation (Equation 2-21).

c) The Non-Random Two Liquid Model (NRTL) (Renon and Prausnitz, 1968)

The NRTL model has three adjustable parameters: $(g_{12}-g_{11})$, $(g_{21}-g_{22})$ and α_{12} which has the same value as α_{21} . The parameter α_{12} represents the non-randomness of the fluid, i.e. for a completely random mixture it would equal zero and is estimated to have a value from 0.1 - 0.47, depending on the nature of the chemicals present (Renon and Prausnitz, 1968). According to Walas (1985) the activity coefficients are relatively insensitive to values of α_{12} between 0.1 and 0.5. Walas (1985) recommended a value of 0.3 for non-aqueous mixtures and 0.4 for aqueous mixtures. It was suggested by Raal and Mühlbauer (1998) that the value of α_{12} be determined and not set at a fixed value.

The NRTL model can be used to predict multi-component system behaviour from binary parameters. It has the advantage over the Wilson model of being applicable to liquid-liquid equilibria, but the disadvantage of having three adjustable parameters.

The NRTL expansion equation is more suitable for excess enthalpy than excess Gibbs energy (Abrams and Prausnitz, 1975).

Gibbs excess and activity coefficient equations for the NRTL model are as follows:

$$\frac{G^E}{RT} = x_1 x_2 \left(\frac{\tau_{21} G_{21}}{x_1 + x_2 G_{21}} + \frac{\tau_{12} G_{12}}{x_2 + x_1 G_{12}} \right) \quad (2-69)$$

$$\begin{aligned} \ln \gamma_1 &= x_2^2 \left(\tau_{21} \left[\frac{G_{21}}{x_1 + x_2 G_{21}} \right]^2 + \left[\frac{\tau_{12} G_{12}}{(x_2 + x_1 G_{12})^2} \right] \right) \\ \ln \gamma_2 &= x_1^2 \left(\tau_{12} \left[\frac{G_{12}}{x_2 + x_1 G_{12}} \right]^2 + \left[\frac{\tau_{21} G_{21}}{(x_1 + x_2 G_{21})^2} \right] \right) \end{aligned} \quad (2-70)$$

where

$$G_{ij} = \exp(-\alpha_{ij} \tau_{ij}) \quad (2-71)$$

and

$$\tau_{ji} = \frac{g_{ji} - g_{ii}}{RT} \quad (2-72)$$

d) The UNIQUAC (Universal Quasi-chemical) Model (Abrams and Prausnitz, 1975)

The UNIQUAC model uses two adjustable parameters per binary and its extension to multi-component systems does not require higher parameters. It is applicable to mixtures whose molecules are significantly different in shape and size due to the inclusion of structural parameters obtained from pure component data (Abrams and Prausnitz, 1975). The UNIQUAC equation according to Abrams and Prausnitz (1975) offers good representation of both vapour-liquid and liquid-liquid equilibria, except where the data are highly precise and plentiful (Prausnitz *et al.*, 1986), for both binary and multi-component systems consisting of a variety of non-electrolyte components. These include polar and non-polar fluids such as hydrocarbons, ketones, esters, amines, alcohols, nitriles and water.

The UNIQUAC model can result in any one of the more popular Gibbs excess energy models (NRTL, Wilson and Van Laar) when well-defined simplifying assumptions are made.

The UNIQUAC equation for Gibbs excess energy consists of a *combinatorial* and *residual* part. The *combinatorial* describes the dominant entropic contribution and is determined by the composition and the size and shape of the molecules only (Prausnitz *et al.*, 1986). It only requires pure component data. The *residual* part is attributed mainly to intermolecular forces that are responsible for the enthalpy of mixing and depends on intermolecular forces. The two adjustable parameters appear only in the residual part.

The Gibbs Excess equation for the UNIQUAC model is written as

$$\frac{G^E}{RT} = \left(\frac{G^E}{RT} \right)_{\text{combinatorial}} + \left(\frac{G^E}{RT} \right)_{\text{residual}} \quad (2-73)$$

where

$$\left(\frac{G^E}{RT} \right)_{\text{combinatorial}} = x_1 \ln \frac{\Phi_1}{x_1} + x_2 \ln \frac{\Phi_2}{x_2} + \frac{z}{2} \left(q_1 x_1 \ln \frac{\theta_1}{\Phi_1} + q_2 x_2 \ln \frac{\theta_2}{\Phi_2} \right) \quad (2-74)$$

and

$$\left(\frac{G^E}{RT} \right)_{\text{residual}} = -q_1 x_1 \ln[\theta_1 + \theta_2 \tau_{21}] - q_2 x_2 \ln[\theta_2 + \theta_1 \tau_{12}] \quad (2-75)$$

The segment fraction, Φ_{ij} and area fraction, θ_{ij} are given by Equations 2-76 and 2-77, respectively, below.

$$\Phi_{ij} = \frac{x_i r_i}{x_i r_i + x_j r_j} \quad (2-76)$$

$$\theta_{ij} = \frac{x_i q_i}{x_i q_i + x_j q_j} \quad (2-77)$$

The adjustable parameters for each binary is given by

$$\tau_{ij} = \exp\left(-\frac{u_{ij} - u_{ii}}{RT}\right) \quad (2-78)$$

where, $u_{ij} - u_{ii}$, is the characteristic energy and according to Prausnitz *et al.* (1986), is often weakly dependent on temperature.

The parameters r and q are the pure component volume and area parameters respectively and can be found for a number of components in Dortmund Databank. The coordination number, z , in Equation 2-74 above is often set to 10.

The activity coefficients for the UNIQUAC equation can be calculated by the following equations

$$\ln \gamma_i = \ln \gamma_{i(\text{combinatorial})} + \ln \gamma_{i(\text{residual})} \quad (2-79)$$

where

$$\ln \gamma_{i(\text{combinatorial})} = \ln \frac{\Phi_i}{x_i} + \frac{z}{2} q_i \ln \frac{\theta_i}{\Phi_i} + \Phi_j \left(l_i - \frac{r_i}{r_j} l_j \right) \quad (2-80)$$

and

$$\ln \gamma_{i(\text{residual})} = -q_i \ln(\theta_i + \theta_j \tau_{ji}) + \theta_j q_i \left(\frac{\tau_{ji}}{\theta_i + \theta_j \tau_{ji}} - \frac{\tau_{ij}}{\theta_j + \theta_i \tau_{ji}} \right) \quad (2-81)$$

and

$$l_i = \frac{z}{2} (r_i - q_i) - (r_i - 1) \quad (2-82)$$

The UNIQUAC equation can provide satisfactory descriptions of many mixtures although it cannot always represent high quality data with high accuracy due to only two adjustable binary parameters (Prausnitz *et al.* 1986).

2.2.2 Evaluating Limiting Activity Coefficients

The activity of coefficient at infinite dilution or limiting activity coefficient is defined as the activity coefficient of species i as x_i approaches zero and is symbolised by γ_i^∞ .

Limiting activity coefficients are vital for the design and operation of separation processes especially those concerned with separating high purity chemicals from solution. Limited activity coefficients can be obtained in two ways. Firstly, by measurement, using specialised equipment and methods such as the inert gas stripping technique used by Soni (2003). Secondly, they can be calculated from experimental P-x-y data and directly from fitted G^E models. Since the coefficients obtained from the G^E models are only as good as the model fit to the experimental data it is a less desired method.

The equations of Gatreux and Coates (1955, cited by Maher and Smith, 1979) relate γ_i^∞ to the partial derivative of pressure with respect to vapour composition. The equations are

$$\gamma_1^\infty = \epsilon_1^\infty \left(\frac{P_2^{sat}}{P_1^{sat}} \right) \left\{ 1 + \beta_2 \left(\frac{1}{P_2^{sat}} \right) \left(\frac{\partial P}{\partial x_1} \right)_{T, x=0} \right\} \quad (2-83)$$

where

$$\epsilon_1^\infty = \exp \left[\frac{(B_{11} - V_1)(P_2^{sat} - P_1^{sat}) + \delta_{12} P_2^{sat}}{RT} \right] \quad (2-84)$$

$$\beta_2 = 1 + P_2^{sat} \left(\frac{B_{22} - V_2}{RT} \right) \quad (2-85)$$

$$\delta_{12} = 2B_{12} - B_{11} - B_{22} \quad (2-86)$$

where B is the second virial equation and V is the liquid molar volume.

The accuracy of the limiting activity coefficient value depends upon the evaluation of the partial derivative in the equation above. Maher and Smith (1979) modified the method of Jonah and Ellis used to estimate the partial derivative. According to Maher and Smith (1979), P versus x_1 data can be converted to deviation pressure, P_D versus x_1 values where P_D is defined as follows

$$P_D = P - [P_2^{sat} + (P_1^{sat} - P_2^{sat})x_1] \quad (2-87)$$

Differentiating the above equation and taking the limits as x_1 approaches 0, the following equation is obtained

$$\left(\frac{P_D}{x_1 x_2} \right)_{x_1=0} = \left(\frac{\partial P}{\partial x} \right)_{x_1=0} - P_1^{sat} + P_2^{sat} \quad (2-88)$$

$\left(\frac{P_D}{x_1 x_2} \right)_{x_1=0}$ is determined by extrapolating a linear plot of $\left(\frac{P_D}{x_1 x_2} \right)$ versus x_1 to $x_1 = 0$. If the

slope is not linear then Maher and Smith (1979) suggest plotting $\left(\frac{x_1 x_2}{P_D} \right)$ versus x_1 . A similar procedure is used to determine γ_2^∞ .

2.3 The Gamma-Phi Approach

In general, the approach offered by this method is one of both vapour and liquid phase correction for the respective phase departures from ideality. For the vapour phase correction, an equation of state is used to calculate the fugacity coefficient and for the liquid phase correction, Gibbs excess energy models are used to define activity coefficients.

According to Van Ness and Abbott (1998) this method is suitable for low pressure measurements and a simple equation of state such as the virial equation of state is sufficient for calculations.

The Gamma-phi representation of VLE was given earlier

$$y_i \Phi_i P = x_i \gamma_i P_i^{sat} \quad (2-19)$$

where the definition of the fugacity coefficient was in given in Equation 2-20.

At low pressures this term (Φ_i) reduces to 1 as P approaches P_i^{sat} and ϕ_i approaches ϕ_i^{sat} . This reduces the equation to Modified Raoult's Law

$$x_i \gamma_i P_i^{sat} = y_i P \quad (2-89)$$

The modified Raoult's law equation accounts for the liquid phase non-ideality and assumes an ideal vapour phase.

In the case where the liquid is assumed to behave as an ideal solution and the vapour is described by the ideal gas law Equation 2-19 is reduced to Raoult's Law, the simplest expression describing VLE.

$$x_i P_i^{sat} = y_i P \quad (2-90)$$

The strategy employed in modelling the isobaric VLE data was labelled a Bubble Temperature Calculation. This logic flow outputs a temperature value for the system as well as vapour compositions when the isobaric system pressure and liquid compositions are inputted. The flow diagram is presented below in Figure 2-2.

The reduction can be performed by using the following equation for P_j^{sat}

$$P_j^{sat} = \frac{P}{\sum_i \left(\frac{x_i \gamma_i}{\Phi_i} \right) \left(\frac{P_i^{sat}}{P_j^{sat}} \right)} \quad (2-91)$$

The generalised form of the Antoine Equation is:

$$\ln P_i^{sat} = A_i - \frac{B_i}{T + C_i} \quad (2-92)$$

where the temperature can be evaluated by changing the subject of the formula of the above equation

$$T = \frac{B_j}{A_j - \ln P_j^{sat}} - C_j \quad (2-93)$$

Constants for the Antoine Equation are given in Table B2, Appendix B.

An alternative expression used for calculating the saturated pressure is as follows:

$$\ln \left(\frac{P_i^{sat}}{P_c} \right) = (1 - X)^{-1} [AX + BX^{1.5} + CX^3 + DX^6] \quad (2-94)$$

where

$$X = 1 - \frac{T}{T_c} \quad (2-95)$$

and constants A, B, C and D are specific to a chemical and can be found in Reid *et al.* (1998).

The activity coefficients are evaluated using the Gibbs excess models and the fugacity coefficients by using the equation of state.

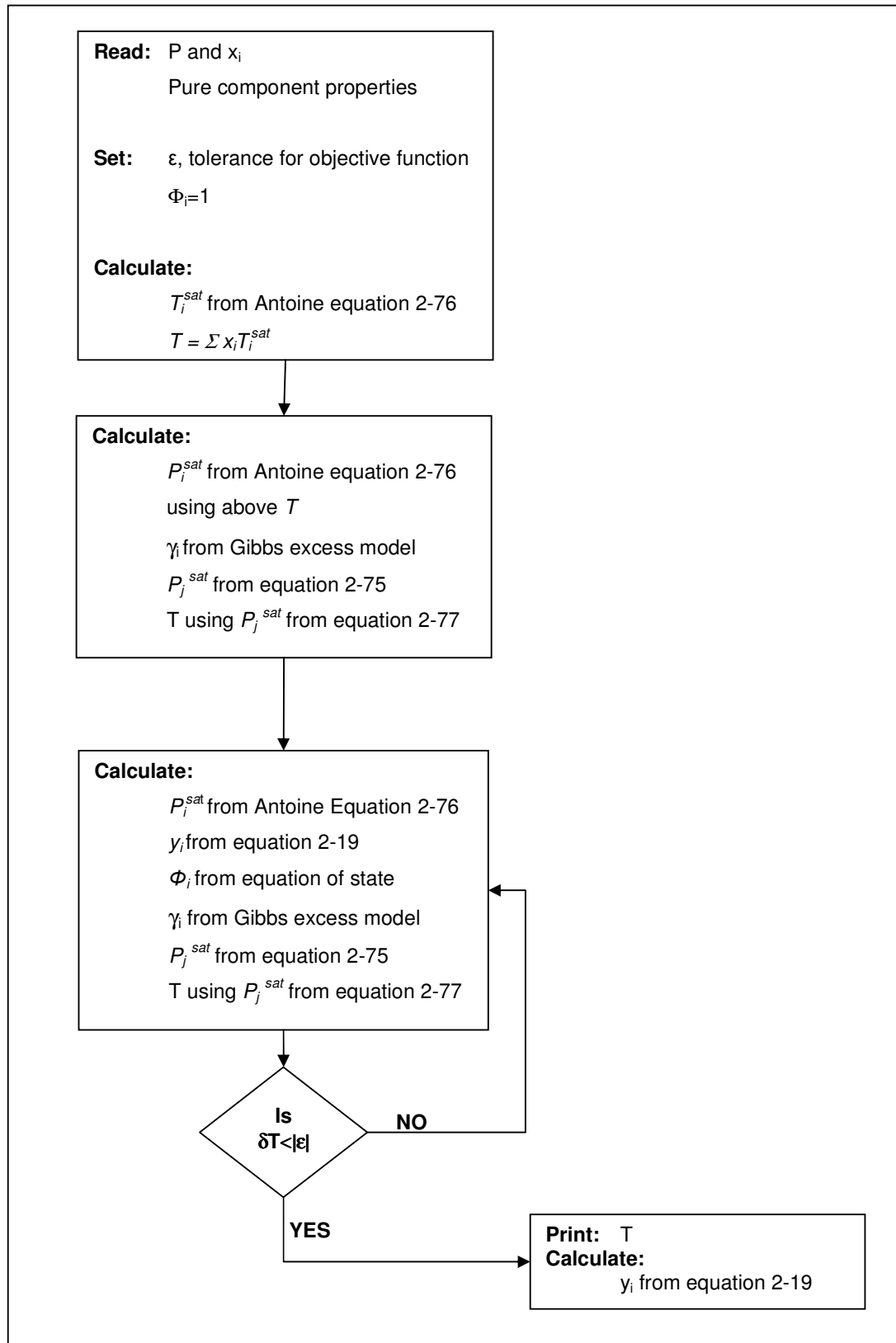


Figure 2-2: Algorithm for the bubble point temperature iteration for the combined method (Smith *et al.*, 2001).

The process, by which the model with the best representation of VLE data is determined, is named data reduction. In this particular case, isobaric VLE data was reduced and bubble point temperatures and vapour mole fractions were calculated (as shown using the gamma-phi method). In the case of isothermal data the procedure is similar but with T as an input. For the determination of the parameters in the activity coefficient models, it is sufficient to use data points of liquid mole fractions and temperature values at a specific pressure. Van Ness *et al.* (1978) stated that the sole reason for the measurement of the vapour mole fractions is for use in a thermodynamic consistency test.

Van Ness *et al.* (1978) defined the difference between calculated and experimental values as the residual $[\delta]$. Popular choices for the evaluated residuals are δT , δy_1 , $\delta \gamma_1$, $\delta \gamma_2$ and $\delta(G^E/RT)$.

A set of parameters that minimizes the sum of the squares of residuals is desired for data regression. Van Ness and Abbott (1982) define S as the objective function (where δY is the chosen residual).

$$S = \sum (\delta Y)^2 \quad (2-96)$$

For the case of the isobaric system in this study, the objective function of δT was chosen as suggested by Van Ness and Abbott (1982).

If two parameters residuals are minimized simultaneously, they must be normalized using normalizing factors, i.e. objective function (Equation 2-82) becomes

$$S = \sum \left(\frac{\delta P}{w_p} \right)^2 + \left(\frac{\delta y_1}{w_y} \right)^2 \quad (2-97)$$

Normalizing factor w_p = root mean square (RMS) value of δP resulting from a minimization of $\Sigma(\delta y_1)^2$ and w_y = RMS value of δy_1 from the minimization of $\Sigma(\delta P)^2$ (Van Ness & Abbott, 1982).

2.4 Equation of State Approach

The phi-phi method or equation of state approach uses an equation of state to represent vapour and liquid departures from ideality by use of the fugacity coefficient. It is suitable for systems at elevated pressures (Van Ness and Abbott, 1998). From equation 2-15 one can write

$$x_i \hat{\phi}_i^l = y_i \hat{\phi}_i^v \quad (2-98)$$

In order to simplify calculations the equilibrium variable K_i is introduced and is defined as follows

$$y_i = K_i x_i \quad (2-99)$$

Since $\sum_i y_i = 1$, then $\sum_i K_i x_i = 1$.

where K_i can be written as

$$K_i = \frac{y_i}{x_i} = \frac{\hat{\phi}_i^l}{\hat{\phi}_i^v} \quad (2-100)$$

Similarly to the gamma-phi approach, the phi-phi approach can be used in either bubble temperature (isobaric) or bubble pressure (isothermal) calculations. Since the phi-phi method was used to describe the isothermal systems in this study, the bubble pressure procedure will be illustrated (Figure 2-3).

Mühlbauer and Raal (1995) highlight some difficulties associated with the application of this method:

- a. Appropriate selection of an equation of state to describe the liquid and vapour non-idealities. Due to the vast number of equation of states available in literature, Mühlbauer and Raal (1995) suggest that the main criteria should be flexibility of EOS of state to fully describe the pressure, temperature and volume behaviour of both phases within the temperature and pressure range of the investigation.
- b. Appropriate selection of mixing rules that, although, are based on theoretical assumptions are empirical in nature and tend to be system specific.
- c. Location of appropriate roots for liquid and vapour molar density when higher than cubic equations of state are used.

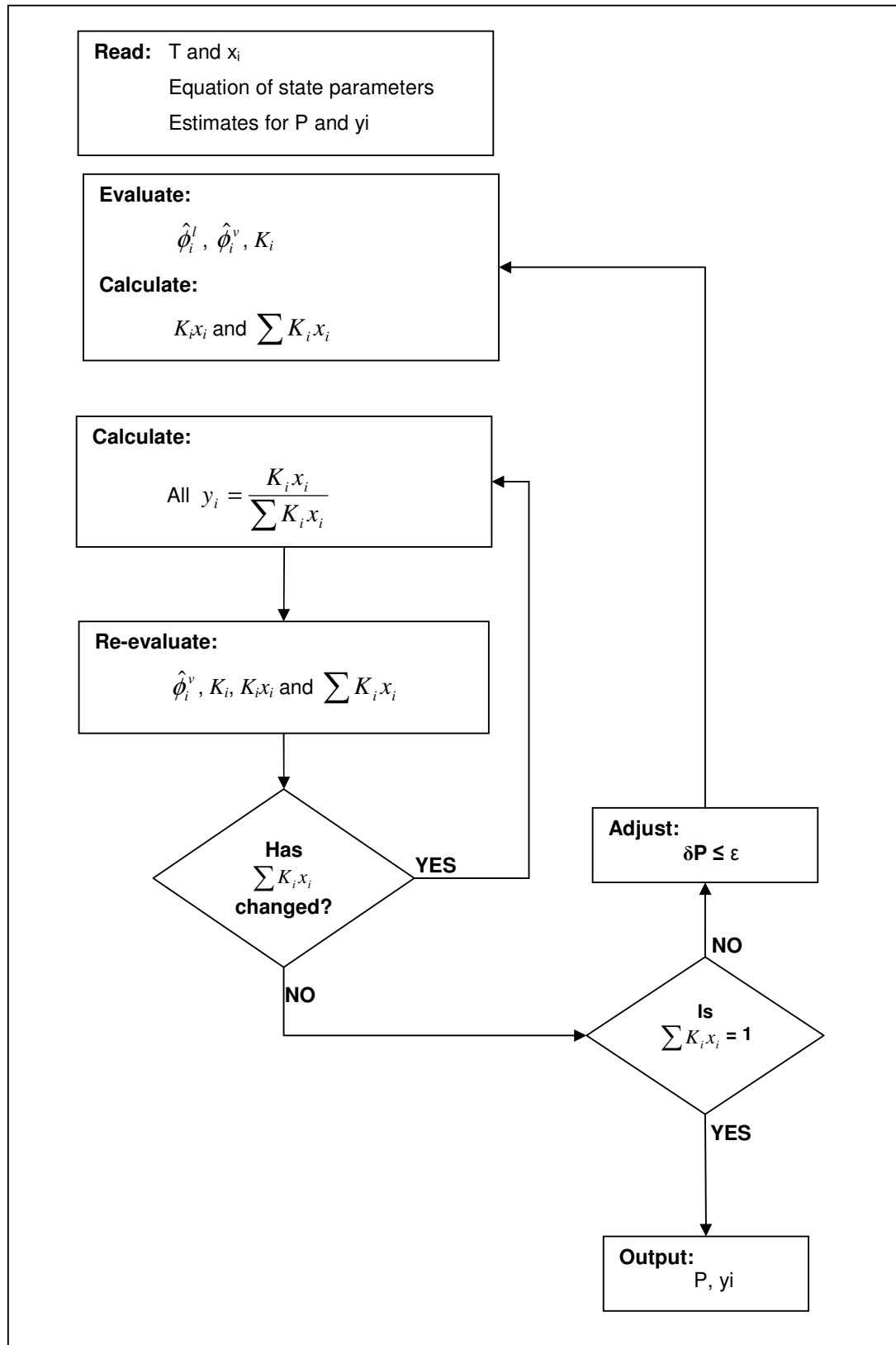


Figure 2-3: Algorithm for the bubble point pressure iteration for the direct method (Smith *et al.*, 2001).

2.5 Thermodynamic consistency tests for binary VLE

The Gibbs-Duhem equation relates excess properties to activity coefficients and forms the basis of the consistency tests. The Gibbs Duhem equation,

$$\sum x_i d \ln \gamma_i = \frac{V^E}{RT} dP - \frac{H^E}{RT^2} dT \quad (2-101)$$

VLE data are considered consistent if they satisfy the Gibbs-Duhem equation.

At constant temperature and pressure this equation becomes

$$\sum_i x_i d \ln \gamma_i = 0 \quad (2-102)$$

If the data is not thermodynamically consistent, it cannot be correct.

2.5.1 Area test

The area test was proposed by Herington (1947) and Redlich and Kister (1948) (Van Ness, 1995). The test is relatively simple and provides a necessary but not sufficient condition for the evaluation of thermodynamic consistency, as will be discussed later.

Equation 2-56 can be re-written for experimental data as

$$\left(\frac{G^E}{RT} \right)^{\text{exp}} = x_1 \ln \gamma_1^{\text{exp}} + x_2 \ln \gamma_2^{\text{exp}} \quad (2-103)$$

Differentiating the above equation and integrating over the entire composition range, and considering that

$$\left(\frac{G^E}{RT} \right)^{\text{exp}} = 0 \quad (2-104)$$

at $x_1 = 0$ and $x_1 = 1$.

One obtains the following expression:

$$\int_0^1 \left(\ln \frac{\gamma_1^{\text{exp}}}{\gamma_2^{\text{exp}}} + \varepsilon \right) dx_1 = 0 \quad (2-105)$$

The bracketed term is plotted against the mole fraction of component such that a graph creating an area both above and below the x_1 -axis exists. The area test requires that the area above the x_1 -axis be similar to area below x_1 -axis (net area = 0).

Van Ness (1995) imposed the criterion for using the test that stated that the difference of areas divided by the sum of the absolute areas should be less than or equal to 0.1 or 10%.

$$\frac{a_1 - a_2}{a_1 + a_2} \leq 10\% \quad (2-106)$$

This is a necessary but not sufficient condition because the most important and accurately measured variable pressure is ignored in the test due to the ratio of activity coefficients, given below. Van Ness (1995) also states that while the pressure can be ignored it does however enter into the calculation of the minor factor Φ_i .

$$\frac{\gamma_1}{\gamma_2} = \frac{y_1 \Phi_1 P / x_1 P_1^{\text{sat}}}{y_2 \Phi_2 P / x_2 P_2^{\text{sat}}} = \frac{y_1 \Phi_1 x_2 \left(\frac{P_2^{\text{sat}}}{P_1^{\text{sat}}} \right)}{y_2 \Phi_2 x_1 \left(\frac{P_1^{\text{sat}}}{P_2^{\text{sat}}} \right)} \quad (2-19a)$$

According to Van Ness (1995), the area test only checks the appropriateness of the vapour pressure ratio, $\left(\frac{P_2^{\text{sat}}}{P_1^{\text{sat}}} \right)$ to the x-y data of an isothermal system. Application of the area test to isobaric data is complex, as the excess enthalpy term, represented in Equation 2-91 as ε , in the Gibbs Duhem equation has to be taken into account. However, the data needed to evaluate it is often unavailable.

2.5.2 Point test

The point test is a more rigorous thermodynamic consistency test and was developed as an improvement to the area test, discussed above. This method uses any of the three measured variables of the four available variables (P, T, x, y) where the fourth variable is calculated from an appropriate correlation and compared to the experimental value.

The vapour phase composition is the greatest source of error and is therefore used to check the thermodynamic consistency by a process of data reduction. The residuals of measured and predicted vapour composition values from the data regression should scatter evenly about the x-axis for thermodynamic consistency. Further, the average absolute deviation can be calculated between the experimental and predicted vapour phase composition, and is suggested to be less than 0.01.

CHAPTER THREE

EQUIPMENT REVIEW

The development of vapour-liquid equilibria (VLE) equipment and methods has been documented as early as 1909. Over the years many experimenters have pioneered through various permutations of modifications and tests, in the quest of reliable equipment and methods suitable for the measurement of any type of VLE data set.

This chapter highlights the development of VLE equipment and methods including the features and challenges associated with operating them, all of which are applicable to the equipment used in this investigation.

3.1 High Pressure Vapour-Liquid Equilibria (HPVLE)

3.1.1 Classification of HPVLE Equipment

Raal and Mühlbauer (1998) provide a comprehensive review on the classification of HPVLE methods and equipment. Presented below is a summarised version.

There are two main means in which one can classify HPVLE methods. According to Deiters and Schneider (1986, cited by Raal and Mühlbauer, 1998) they can be classified according to primary variables observed; mainly synthetic and analytical methods. Raal and Mühlbauer (1998), however, classify HPVLE on the basis of whether liquid, vapour or both are circulated through the equilibrium cell; mainly dynamic (if circulation takes place) and static (if circulation does not take place).

A basic scheme of this classification, adapted from Raal and Mühlbauer (1998) is shown below.

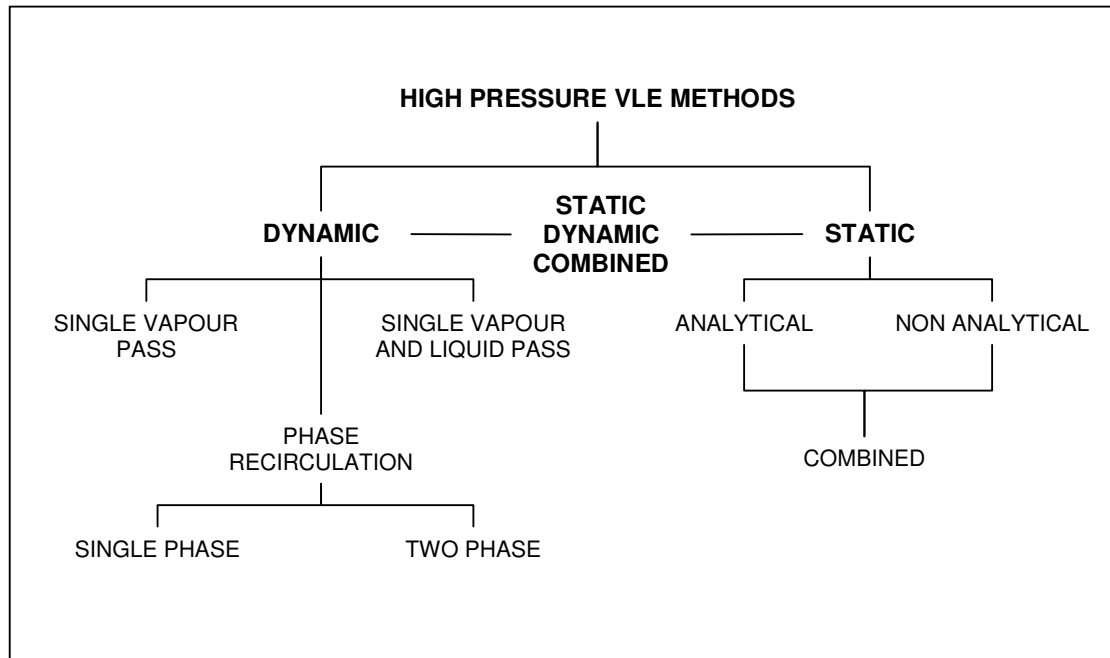


Figure 3-1: Classification of HPVLE (adapted from Raal and Mühlbauer, 1998).

In the case of the static method, subdivision depends on whether the phases are sampled (static analytical) or not (static non-analytical). In this method isothermal (P-x-y), isobaric (T-x-y) or isopleth (P-T) phase diagrams can be produced.

In the case of the dynamic method, which is analytical by nature, subdivision only depends on the circulation phase being either vapour, liquid or both. This is further divided into single pass (vapour or liquid and vapour) and phase recirculation (single phase or two phase). Dynamic methods produce isothermal or isobaric phase equilibrium data.

The equipment used in this investigation falls under dynamic re-circulating two phase type and the current chapter will thus focus on these aspects.

In the recirculation method, either single phase or both phases are continuously withdrawn from the equilibrium cell and re-circulated until equilibrium is established.

3.1.2 HPVLE Two Phase Recirculation Method

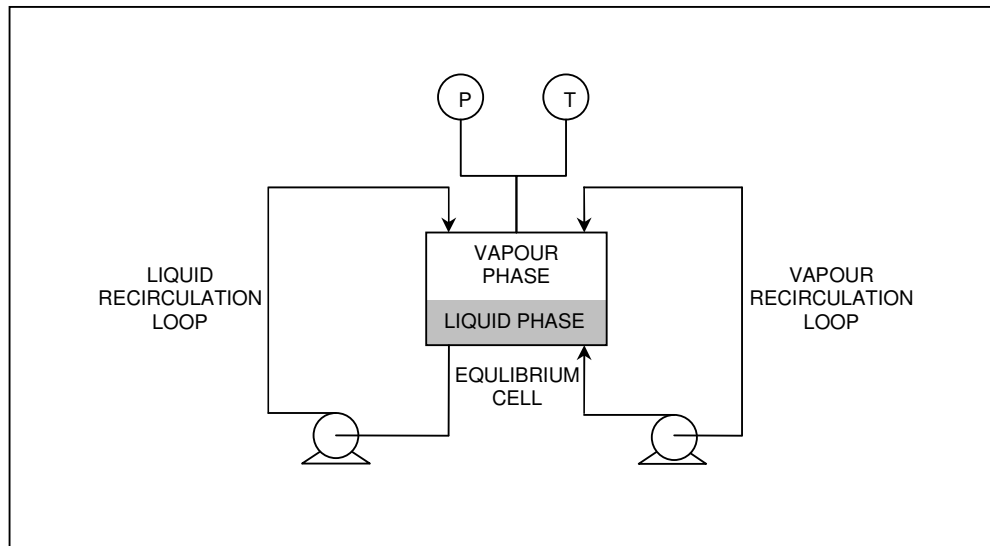


Figure 3-2: Schematic of common HPVLE two phase recirculating apparatus, adapted from Harris (2004).

The equilibrium cell used in this investigation consisted of the recirculation of both the liquid and vapour phases. It is therefore important that HPVLE with focus on circulation of both phases is discussed.

A general feature of this type of apparatus is an equilibrium cell thermostatted in an air, water or oil bath. The cell is charged with a mixture and allowed to attain equilibrium. The resulting phases (liquid and vapour) are allowed to circulate. Both phases are circulated counter-currently. The vapour bubbles through the liquid phase and the liquid (entering at the top of the equilibrium cell) falls to the bulk mixture. Sampling is possible and made simple by diverting a part of the liquid and vapour stream and isolating it. However, this can be overlooked due to the complexity of phase recirculation loops. Maintaining an adequate liquid level in the cell and avoiding pressure gradients within the cell are some of the problems associated with these methods.

Presented in Appendix A is a brief summary of developments of HPVLE highlighted in Raal and Mühlbauer (1998). The reader is referred to Naidoo (2004) for a more detailed summary from 1943 through to 2001. The main highlights include temperature and pressure limits, sampling provisions/devices, material of construction and equilibrium time.

3.1.3 Features of HPVLE Equipment

HPVLE equipment consists of the following features (Raal and Mühlbauer, 1998):

1. An equilibrium cell within which the phases of the mixture are at equilibrium.
2. An environment that controls the temperature of the cell. This can be in the form of an air, nitrogen, oil or water bath or, an aluminium or copper jacket.
3. A method for effective agitation of the contents of the equilibrium cell to facilitate the attainment of equilibrium. Static and dynamic methods employ different mechanisms to fulfil this important requirement. Static methods use an internal magnetic stirrer and in some cases rocking of the equilibrium cell have been reported. (Huang et. al., 1985 cited by Reddy, 2006). However in dynamic methods agitation of the equilibrium mixture is achieved by the circulation of one or more phases. The use of magnetic stirring in dynamic recirculation methods has also been reported in a few cases.
4. A method for accurately analyzing the vapour and liquid phases. This can occur by two means; either *in situ* or externally to the equilibrium cell. *In situ* analysis is used mainly in static methods and requires special sampling devices in the apparatus for analyzing liquid and/or vapour phases.

External analysis, mainly used in equipment employing dynamic methods, requires that the sample (liquid or vapour) be removed from the equilibrium cell and analysed using an analytical device, such as a gas chromatograph. In the case of two phase recirculation and, single liquid and vapour pass, sampling is more efficient as the circulating operation (through external loops) is conducive to easy sampling (Raal and Mühlbauer, 1998).

5. Temperature and pressure sensors are an integral feature of the equilibrium cell. The proper calibration of these devices allow for accurate measurement of the cell temperature and pressure. Common temperature sensors include the platinum resistance thermometer (Pt-100) and thermocouples. Pressure measurement devices include electronic pressure sensors (transducers, transmitters) and mechanical pressure gauges (Reddy, 2006).
6. A novel feature for the observation of phase separation, according to Reddy (2006), is being able to visually (sight glasses) or optically (camera) observe the phase behaviour in the equilibrium chamber.

3.1.4 Experimental Challenges in the Acquisition of HPVLE Data

Experimental challenges in the field of HPVLE have been reviewed in detail by, Raal and Mühlbauer (2006). Presented below is a summary of these challenges:

a) Establishing equilibrium

Equilibrium can be defined as a situation in which there are no internal macroscopic changes within a system and no changes in the properties of the materials with respect to time. Equilibrium is therefore greatly affected by fluctuations in experimental temperature, pressure and volume.

Since equilibrium requires this balance of all potentials that may cause change, the rate of approach to equilibrium is clearly proportional to the difference in potential between the actual state and the equilibrium state.

In general, agitation of reboiler contents results in greater contact between the phases thus reducing the time taken to reach equilibrium. However, it should be noted that this may cause “fluid friction” (Reddy, 2006), and possible thermal gradients are generated in the fluid, hindering the attainment of equilibrium. True equilibrium is therefore probably never established due to the continuous variations in the surrounding environment including difficulties in experimental pressure and temperature control (Reddy, 2006).

Thus equilibrium is assumed when the system temperature, pressure and phase composition remain stable, within a predefined tolerance, over a period of time.

According to Fredenslund (1973 cited by Raal and Mühlbauer, 1998), a change in pressure of less than 0.05% in 30 minutes is a good indication of equilibrium.

In the case of composition analysis, as an indication of equilibrium, repeated vapour and liquid samples should give reproducible results, within the limits of the analysis method.

b) Maintaining equilibrium conditions.

In order for vapour and liquid compositions to reflect equilibrium conditions; the equilibrium cell needs to be cleared of any thermal gradients. Even small temperature gradients can cause significant error in the measured data. Raal and Mühlbauer (1998) suggest the use of a bath heater to avoid hot spots, copper lining on the inside of the baths and the installation of several temperature sensors in the equilibrium cell and bath to monitor temperature homogeneity. This

will enable the experimenter to draw up temperature profiles. Bath and equilibrium cell temperature profiles have been reported in literature, however, for static cells only.

Temperature control can be achieved through the use of a thermostat (Reddy, 2006) in the form of an isothermal fluid bath. The temperature of the system is detected by a thermal sensor and relayed to a control unit, which will adjust the heating element current.

In a similar manner pressure control can be established as well. The control strategy typically allows for system variables (temperature and pressure) to be controlled within a tolerance, with reference to a set point or predetermined value. The greater the deviation between the system variables and the set point variables, the greater the difficulty in controlling the system and acquiring consistent equilibrium data (Reddy, 2006). Reddy attributes this to the proportional relationship between temperature and pressure.

Typical pressure control devices include electronic shut off valves (on-off) and control valves (regulation). Solenoid valves (electromagnetic) have also found widespread use in pressure control systems. Shut off valves are able to control the system pressure by opening to a low and high pressure source, to maintain a set point pressure, with the two limits. The control however is limited by the response time of the feedback system and the control unit and the pulsation of the valve. The opening of the valves can be fine tuned by pulse-width modulation (Reddy, 2006).

c) Measurement of system variables

Reddy (2006), suggests that even though there are sensors (temperature and pressure) available that are highly accurate, linear and robust their accuracy is limited by the resolution of the instrument display or multimeter readings (number of decimal points). Reddy (2006) also highlights, at the same time that aspects like the physical placement of the sensor, good signal conditioning and noise interferences would affect the accuracy of temperature and pressure measurements. The challenge therefore is not the sensor itself but also the possible factors mentioned above including the calibration of the variable sensor, which, if done incorrectly may hinder accuracy of measurements.

d) Sampling

Raal and Mühlbauer (1998) cover two main challenges with regard to sampling. The first challenge is the possible disturbance of equilibrium during sampling and the second, the withdrawal of the sample prior to analysis.

Sampling results in a change in volume of material in the equilibrium cell. The larger the volume withdrawn from the cell for sampling, the greater the disturbance to the equilibrium condition. Raal and Mühlbauer (1998) suggest that the way to avoid this situation is to let the volume required by the analytical device (e.g. gas chromatograph) dictate the volume of sample to be withdrawn. Another solution, employed by Mühlbauer (1990, cited by Raal and Mühlbauer, 1998) is the use of a larger equilibrium cell. If the same analytical device is used, that dictates the sample size withdrawn, then the percentage cell volume change of material for large equilibrium cells is significantly smaller than for small equilibrium cells. The problem with larger equilibrium cells though is that they require a lot more material.

The benefit of phase recirculation methods is that a portion of the liquid and vapour flow is diverted and isolated enabling the withdrawal of a sample. This does not affect the equilibrium cell volume with regard to the sampling method. Only the sample volume is affected which should be dictated by the analytical device. Other solutions covered by Raal and Mühlbauer (1998), include faster sampling methods to minimise time available for equilibrium changes and the use of in situ analysis of equilibrium cell contents.

The second challenge associated with sampling is that of overcoming experimental variables during sampling. In particular, sampling obtained at low or high pressures. Reddy (2006) states that in the case of HPVLE that the equilibrium conditions, with regard to temperature and pressure, of a sample are different from the operating conditions of the analytical device (e.g. a gas chromatograph). It is therefore necessary to ensure that the sample obtained, when analysed, is representative of the equilibrium conditions as far as possible. Another problem experienced in cases of volatile/non-volatile systems (Raal and Mühlbauer, 1998) or mixtures of components with a large difference in volatility, is that of preferential flashing of the more volatile component during sampling and partial condensation of the withdrawn non-volatile component. The solution here is the employment of homogenisation techniques on the withdrawn liquid sample, to prevent partial condensation. Raal and Mühlbauer (1998) highlight a few of the developments over the years, from literature.

e) Analysis

Two of the more common methods used to analyse phase samples from HPVLE experiments are gas chromatography (external analysis) and spectroscopy (*in-situ* analysis). The most common in recent years is gas chromatography. Since external analysis is particular to dynamic methods, only gas chromatography will be discussed.

The disadvantage of gas chromatography, as mentioned above is the operating conditions of the GC are different from the equilibrium condition of high temperature and pressure. Gas chromatography is characterised by the calibration of the detector (thermal conductivity or flame ionisation detectors) over the entire mole fraction range as the response factor ratios are not constant and vary with concentration (Raal and Mühlbauer, 1998). The problem arises in the calibration of high pressure gas or gas-liquid mixtures. This problem is solved with the use of a precision volumetric calibration device developed by Raal and described in Raal and Mühlbauer (1998).

3.2 Low Pressure Vapour-Liquid Equilibria (LPVLE)

3.2.1 Classification of low pressure vapour-liquid equilibria (LPVLE) equipment

The classification of LPVLE can be divided in a similar manner to the classification of HPVLE. Hala et al. (1967) classifies LPVLE into four major methods: distillation, circulation, static and dew and bubble point. Malanowski (1982) further classifies circulation methods, based on the number of phases to be recirculated.

A basic scheme of this classification is shown below.

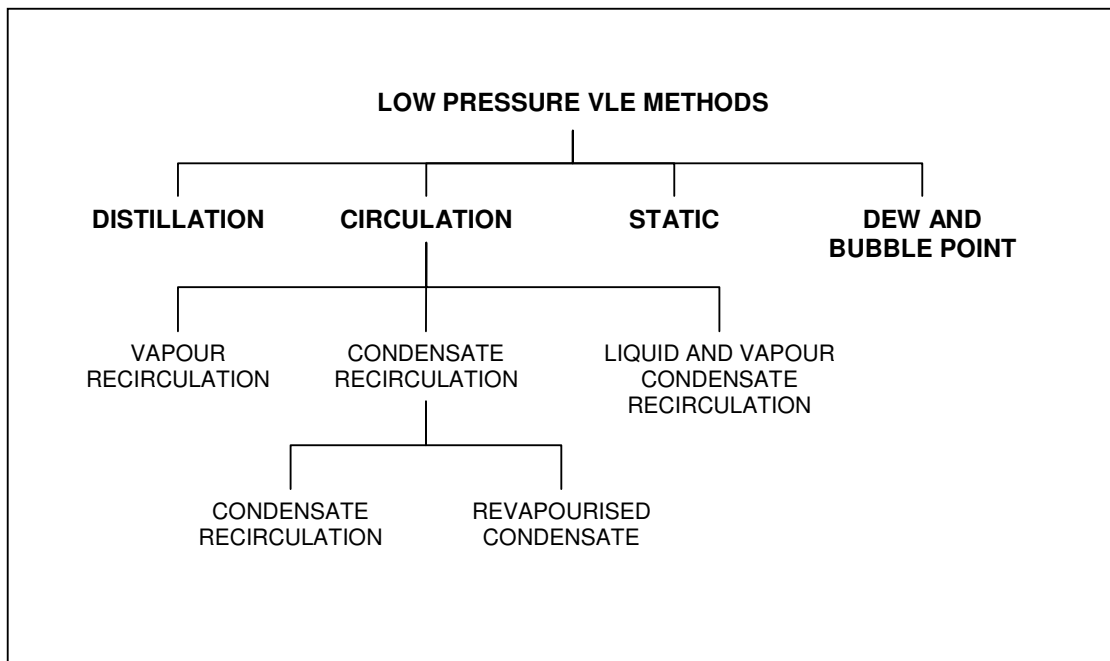


Figure 3-3: Classification of LPVLE equipment (adapted from Reddy, 2006).

Recirculation of liquid and vapour are of relevance to this project and will therefore form the focus of the sections to follow. In the recent years the recirculation method has become a popular method of choice, attributing to the fact that the method allows for reliable results of high accuracy to be obtained in a simple and rapid manner (Malanowski, 1982).

The defining principles common to all recirculation methods are highlighted in Malanowski (1982):

1. Isobaric and isothermal operation
2. Operation under steady state
3. Continuous separation of the vapour from the liquid phase

4. The vapour phase condenses into a receiver (except for methods with direct circulation of the vapour phase)
5. Measurement of thermodynamic parameters like temperature, pressure and composition.
6. Recirculation of condensate (or vapour phase) back to liquid.

Some of the design criteria particular to low pressure recirculating stills are summarised below from the extensive review by Malanowski (1982):

1. Simplistic design.
2. Smaller samples required for measurements.
3. Design must include accurate temperature and pressure measurement facilities.
4. Steady state should be achieved in a short time after start up or after any adjustment to equilibrium parameters like temperature, pressure or composition.
5. There should not be any partial condensation of vapour on the temperature sensor; neither should there be any overheating in the region of the sensor.
6. No presence of liquid drops should appear in the vapour stream leaving the equilibrium chamber after disengagement from the liquid phase.
7. The circulated vapour should be well mixed with the liquid phase to achieve uniform composition and to avoid secondary evaporation during mixing.
8. The composition and flow of the circulated streams should be steady.
9. The design should prevent the accumulation of material.
10. Sampling and introducing material into the still should be made possible without having to interrupt boiling.

3.2.4 LPVLE Recirculating Stills

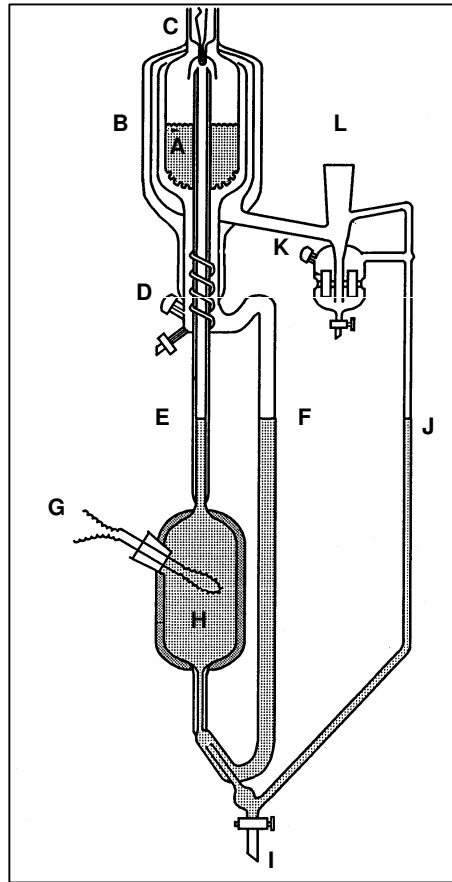


Figure 3-4: Low-pressure recirculating still of Raal and Mühlbauer (1998).

A-Packed equilibrium chamber; **B**-Vacuum jacket for the equilibrium chamber; **C**-Thermowell; **D**-Liquid Sample point; **E**-Vacuum jacketed Cottrell pump; **F**-Liquid return line; **G**-Heater cartridge; **H**-Boiling chamber; **I**-Drain valve; **J**-Vapour return line; **K**-Vapour sample point; **L**-Condenser attached

LPVLE recirculating stills form the basis of the equipment used in this study. It is therefore important that these types of stills and more particularly the development to present, is discussed. In Soni (2004), the development of the still is discussed in conjunction with the development of the ebulliometer as they are both closely linked. An ebulliometer is a device used to accurately measure the boiling temperature of a substance (Soni, 2004). Initially stills based on this principle were used for the measurement of boiling points.

Refer to Figure 3-4. Essentially in the modern day VLE still, a chemical mixture is boiled in the reboiler, **H** (boiling chamber) and transported to the equilibrium chamber (**A**). The liquid and vapour phases are allowed to equilibrate at which point they disengage. The liquid phase is returned to the reboiler via the liquid return line (**F**) and the vapour phase is transported to the

condenser (**L**). It is important to note that the phases are sampled (**D** and **K**) prior to their return to the reboiler.

Table A-2, Appendix A presents a chronological order of discoveries/developments of LPVLE equipment highlighted in Malanowski (1982).

3.2.2 Features of LPVLE Recirculating Equipment

Since the early 1900's, the LPVLE recirculation still has evolved through many innovative and defining modifications affording it the title of modern "state of the art" still. Many of these modifications have become more of features to the still, as highlighted by Reddy 2006. These features are summarised below. Refer to Figure 3-3.

1. The boiling chamber (**H**) is required to provide sufficient heat to initiate and sustain boiling of the mixture. This is achieved by the addition of two heaters; an external heater (around **H**) that compensates for heat losses to the surrounding environment, and an internal heater (**G**) situated in close contact with the fluid providing the bulk of the heating duty. The external heater prevents the formation of temperature gradients thus maximising energy efficiency of the equilibrium still.
2. The addition of stirrers in the sample traps (vapour condensate, **K**, and liquid, **D**) and boiling chamber (**H**) prevents concentration gradients and flashing of the more volatile component upon re-entry into the boiling chamber (from the return lines, **F** and **G**).
3. The Cottrell pump (**E**) provides transport of the liquid to the equilibrium chamber (**A**).
4. The equilibrium chamber (**A**), where contact and disengagement of the phases occur and equilibrium temperature can be monitored with the use of a temperature sensor.
5. Sample traps (**K** and **D**) are also an important feature of the recirculating still as they allow for efficient sampling of the phases for composition analysis.
6. The addition of computer aided control of pressure and temperature for isobaric and isothermal operation is a novel feature. (Joseph *et al.* 2001)

3.2.3 Challenges of LPVLE Recirculating Equipment

Some challenges faced by LPVLE equipment are similar to those of HPVLE equipment. In Raal and Ramjugernath (2005) these challenges or problems are highlighted and methods and techniques to overcome these are discussed. Though VLE circulating stills have become popular over recent years their problems can be major, if, according to Raal (2005) accurate data is required for extremely non-ideal systems.

These challenges taken from Raal (2005) include uncertainty in achieving equilibrium and condensation of the equilibrium vapour. With regard to system variables (temperature and pressure), there are problems associated with controlling these variables to achieve constant boiling and a steady state and measuring system variables (temperature, pressure and composition).

3.3 Development of LPVLE Still for Operation at High Pressures and High Temperatures

Reddy (2006) assessed that less than five pieces of equipment based on traditional LPVLE have been published from 1978 to 1999. One can therefore conclude from Reddy's observation that the extrapolation of LPVLE designs to handle high temperatures and pressures is not an easy task.

Reddy (2006) gives an extensive review on the development and design of LPVLE recirculation still for operation at both high pressure and high temperature.

The equipment used in this investigation (Reddy, 2006) was based on the design of Harris (Harris, 2004) that was also developed in the Thermodynamics Research Unit at the University of KwaZulu-Natal. The still addresses the flaws of Harris to produce a higher quality piece of equipment. The comparisons between Harris and Reddy are highlighted in Chapter four. The still of Harris will be discussed in this section and is illustrated in Figure 3-5 below.

The still of Harris (2004) is based on the successful VLE still of Raal (Raal and Mülhbauer, 1998). It was constructed out of stainless steel with an operating range of 300 to 700K and 1 kPa to 30MPa. The still of Harris (2004) weighed approximately 50 kg due to the stainless steel and the thick walls, resulting in a large thermal capacity. The apparatus is computer controlled and

can operate under isobaric and isothermal mode and, has provisions for sampling. The still also is able to attain equilibrium rapidly.

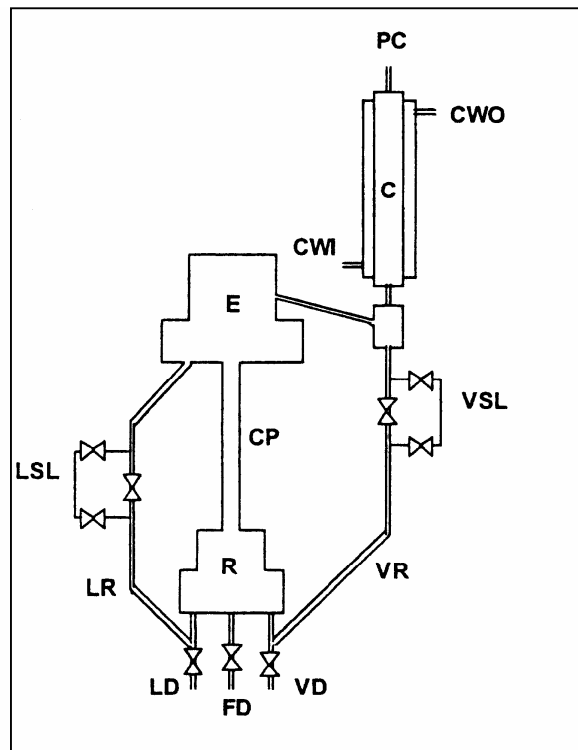


Figure 3-5: Schematic of apparatus of Harris (Harris, 2004)

R, reboiler; **E**, equilibrium chamber; **C**, condenser; **CP**, Cottrell pump; **LR**, liquid return; **VR**, vapour return; **LSL**, liquid sampling loop; **VSL**, vapour sampling loop; **PC**, pressure control point; **CWI**, cooling water in; **CWO**, cooling water out; **LD**, liquid drain; **VD**, vapour drain; **FD**, feed drain

The three main unit operations of the still of Harris are, as discussed in Harris (2004):

- Reboiler - where a chemical mixture is boiled and the superheated mixture is transported to the equilibrium chamber.
- Equilibrium chamber - where the liquid and vapour phases of the mixture are allowed to reach equilibrium.
- Condenser - condenses the vapour phase.

Two major problems that Harris experienced were temperature fluctuations and erroneous vapour phase compositions. In the case of temperature fluctuations the possible causes according to Harris (2004) are that volume of material in the reboiler may be insufficient, the cooled condensed vapour is disrupting reboiler operation and too much heat is being lost from the system. To remedy these problems Harris (2004) changed charge volumes and insulated the still, however all of these had little or no effect.

For the erroneous vapour phase compositions, interestingly experienced at high temperatures for systems of high relative volatility and also when the system was left for a long time to run, Harris (2004), suggested that volume in the reboiler may be insufficient. Harris (2004) also suggested that the reboiler charge is boiling material into the vapour return line, the insulation is retaining too much heat and the superheat from the Cottrell tube is being transferred into the equilibrium chamber thus heating the chamber to above the equilibrium temperature and causing the liquid to flash. The solutions however, had little or no effect.

3.3.1 Difference between HPVLE equipment and LPVLE equipment modified for high temperatures and pressures

Harris (2004) highlights the major differences between traditional HPVLE recirculation equipment and LPVLE recirculation equipment modified for high pressures and high temperatures. These are tabulated in the table below. Refer to Figures 3-2 and 3-4.

Table 3-3: Differences between traditional HPVLE recirculation equipment and LPVLE recirculation equipment modified for high pressures and high temperatures.

HPVLE	LPVLE (modified)
<p>a. Pumps are required to circulate vapour and liquid phases. This poses one of the challenges associated with designing HPVLE equipment, as pumps can cause disturb equilibrium pressure.</p>	<p>a. The Cottrell tube transports the liquid to the equilibrium chamber. Due to the static head, the liquid phase and the vapour condensate are returned to the reboiler.</p>
<p>b. Degassing of liquids is required to remove dissolved gases prior to experimentation. If this is not done the dissolved gases can affect equilibrium pressure.</p>	<p>b. Degassing of liquid occurs while the still is in operation. The gases do not condense as the condenser temperature is above 283.15 K and they are evacuated through the vacuum pump.</p>
<p>c. Operating temperature is restricted by the thermostating fluid (air, water or oil).</p>	<p>c. There is no thermostating fluid however the temperature restrictions occur because of the material of construction and range of heaters.</p>
<p>d. HPVLE equipment are excellent for measurements of supercritical fluids. The vapour phase containing non-condensable material is circulated by the pumps.</p>	<p>d. Supercritical fluids cannot be measured by this equipment as the fluid will not condense and thus not be recirculated.</p>

CHAPTER FOUR

EXPERIMENTAL EQUIPMENT

The equipment used in this project is the novel VLE apparatus of Reddy (2006). This equipment was designed and constructed at the Thermodynamics Research Unit in the School of Chemical engineering, as part of Reddy's PhD project.

The equipment is a complete re-working of the design of Harris (2004) and addresses the irregularities in the equipment operation and in the acquisition of experimental data of Harris (2004). The apparatus of Harris (2004) is discussed in Reddy (2006) with particular focus on design and shortcomings. Since the still of Reddy is based on that of Harris, this section will highlight some of the major structural differences of equipment between Reddy and Harris, and focus on the operational benefits of the still design of Reddy (2006).

The apparatus of Harris was designed for a temperature range of 300 to 700 K and a pressure range of 1kPa to 30 MPa. The apparatus of Reddy can operate in a much narrower range with temperatures up to 600 K and pressures up to 750 kPa. Both apparatus can operate under isothermal and isobaric conditions, have significantly quick equilibration time and have provisions for sampling of the phases.

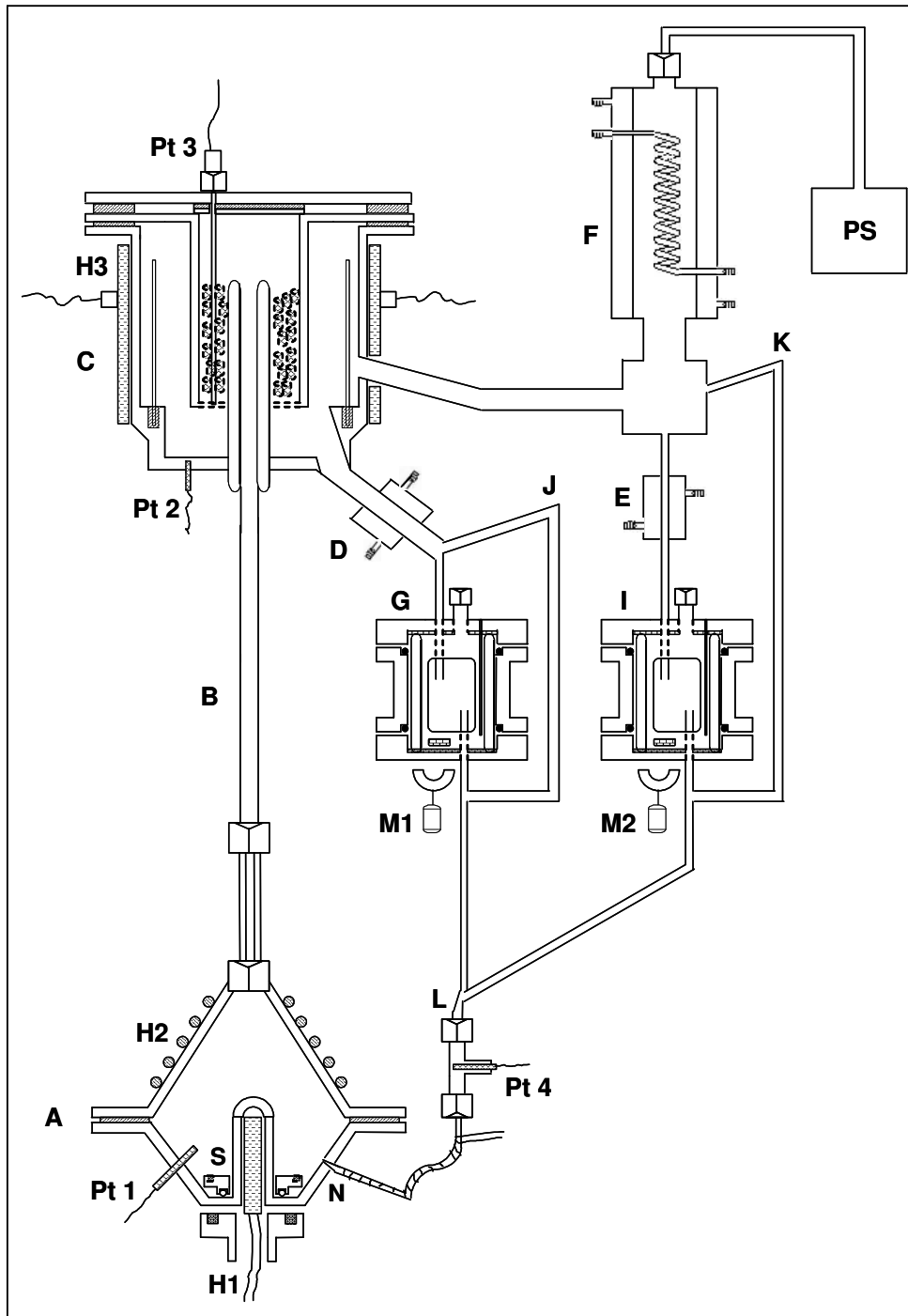


Figure 4-1: Schematic of VLE apparatus (Reddy, 2006)

A, reboiler; B, Cottrell tube; C, equilibrium chamber; D, liquid cooler; E, vapour condensate cooler; F, condenser; G, liquid sample trap; H1, H2, H3; heaters; I, vapour condensate sample trap; J, liquid trap pressure equalizer tube; K, vapour condensate sample trap equalizer tube; L, return line union; N, capillary; M1, M2, motor-shaft mounted magnets; PS, pressure stabilization system; Pt1, Pt2, Pt3, Pt4, platinum temperature resistors; S, reboiler stirrer.

4.1 Description of experimental apparatus

Due to the complexity of the equipment used in this project the author deems it necessary to discuss it in sufficient detail. The following will be discussed:

- a) Reboiler
- b) Cottrell tube
- c) Equilibrium Chamber
- d) Sample traps
- e) Pressure control system

The schematic of VLE apparatus used in this investigation is given in Figure 4-1 and the general layout in Figure 4-2 below.

The description follows from Reddy (2006). Refer to Figure 4-1.

a) Reboiler (**B**)

The reboiler consists of two main parts: the lower and upper flange sections. The lower flange is made up of the heater cartridge insert, inlet for the drain/fill valve and the return line, incorporation of the temperature sensor, stirrer and associated drive system.

The surface of the heater cartridge cavity is roughened to facilitate the creation of nucleation sites. This aids in steady boiling by disrupting the surface energy of the molecules.

The drain/fill valve (not shown in the figure) reduces the addition of unnecessary features on the reboiler and its position minimizes the effect of dead volume or any stagnant concentration spaces in the operation of the apparatus. The valve used has a temperature rating of 588 K, which allows high temperature experiments to be carried out.

Return lines are positioned on the side of the reboiler with a capillary section (**N**) that minimizes backflow and smoothes the return flow of the mixed streams into the reboiler. This avoids turbulence which contributes to uneven boiling.

One of the main features of the reboiler and also that of the still is the mechanical stirrer (**S**). Reddy had incorporated a 316 SS machined stirrer that spins on an open race of 316 SS 3 mm balls. The stirrer is situated around the heater cartridge cavity (**H1**) and uses impellers to agitate

the liquid in the reboiler. The importance of stirring is that it ensures the dissipation of concentration gradients which minimizes the occurrence of flashing and superheating.

Two of the stills main sources of heat input are located in the reboiler, the internal heater cartridge (**H1**) and the external heater (**H2**). The external heater is a 900 W supernozzle heater, custom made for the apparatus and coiled around the upper flange of the reboiler, which is insulated with refractory cement to limit heat loss. The lower flange is insulated with graphite and glass wool tape for this purpose as well.

b) Cottrell tube (**B**)

The Cottrell tube is transparent which is achieved by the use of a Pyrex borosilicate glass insert. The glass insert is annealed to reduce vulnerability to shock or strain induced breakages. The insert is located between the boiling chamber (**A**) and equilibrium chamber (**C**) and graphite was used as a seal for the glass to metal couplings.

The advantages of the Cottrell tube being transparent is that it is more convenient to observe the boiling and flow characteristics of the contents, and also it is possible to determine the ideal volume of material to charge the still as opposed to the design of Harris (2004). Being able to observe the flow characteristics is an important indicator of the proper operation of the still.

To prevent breakage of the glass due to shock and misalignment, Reddy attached a flexible SS hose tube between the equilibrium chamber and glass insert. The flexible hosing has a pressure rating up to 750 kPa.

c) Equilibrium Chamber (**C**)

The equilibrium chamber(**C**) is also constructed from stainless steel and is made of three flanged sections sealed with graphite and held together by eight 6 mm bolts. The top flange contains the main Pt-100 sensor, from which the equilibrium temperature is recorded. The middle flange houses the packed section and the outermost flange is the main body.

The packing used in the equilibrium chamber is 3 mm rolled 316 SS wire mesh cylinders filled to a level just below the top of the discharge point of the Cottrell tube, similar to the still of Joseph *et al.* (2001). The base of the packed section has a uniform distribution of radially symmetric exit or drain holes for the exit of phases through the perforations. To ensure that the

most reliable temperature is measured, the sensor is placed near the bottom of the packed section, as suggested by Raal and Mühlbauer (1998).

The main body is designed to allow for rapid disengagement of the phases and to minimize dead volume. Unlike the still of Raal and Mühlbauer (1998), the equilibrium chamber has an external band heater. This ensures that there is no temperature gradient between the interior of the chamber and the environment. It also aids in the attainment of an internal thermal equilibrium in the main body of the chamber. The inclusion of the external heater (**H3**) is important for cases where insulation material is insufficient and when operating at high temperatures.

d) Sample traps (**G** and **I**)

The sample traps for the liquid (**G**) and vapour condensate (**I**) were both of magnetically stirred over-flow type. Reddy designed the sample traps to allow for operation at elevated pressures and at the same time retain some transparency.

This resulted in a trap that consisted of two outer flanged sections and a middle supporting frame for a sight glass section. The top flange consists of the inlet for the cooled streams and the sample nut fitting for the sample septum. The bottom flange is made up of the drain valve for draining material from the sample trap and an exit tube that is welded into the base of the trap. The amount of liquid that remains in a dynamic state in the sample trap is determined by the height of the exit tube or overflow tube. Reddy states that this was a crucial design factor as hold-up in any part of the equilibrium still, can slow down the approach to equilibrium especially for measurements in the dilute regions.

Pressure equalization tubes (**J** and **K**) were included across the traps ensuring that there is minimal hold-up of phases exiting the sample traps. Sealing of the sample trap was achieved with the aid of sealing gaskets (Teflon discs), Viton o-rings and fire-polishing the edges of the glass insert for a smooth finish.

An added cooling system is incorporated in the equilibrium still, which includes liquid (**D**) and vapour condensate (**E**) cooling jackets around the return lines. This cooling system is to be used for measurements at high temperatures and was not necessary for this project as the highest temperature recorded was 105°C. It should be noted however, that measurements performed at high temperatures may compromise the septa and sealing materials in the sample traps.

e) Pressure Control system

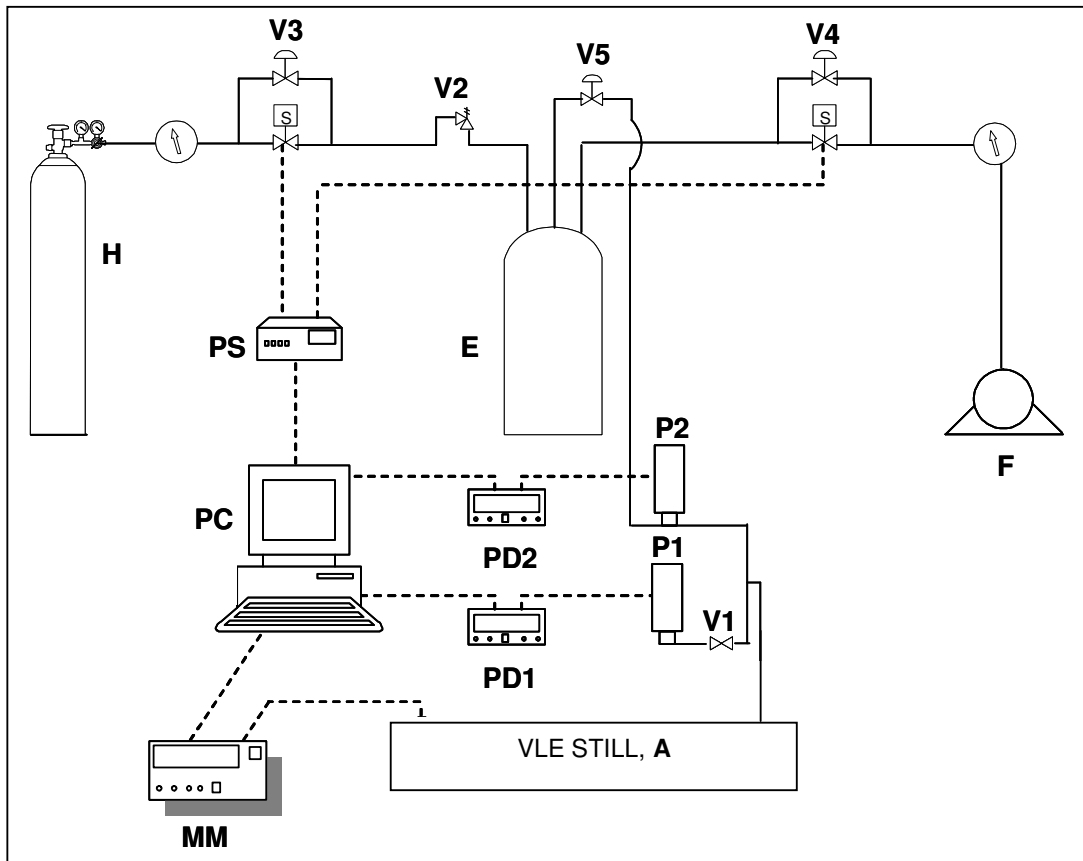


Figure 4-2: Schematic to illustrate pressure control system

A, VLE still; E, ballast tank; F, vacuum pump; H, gas cylinder; MM, multimeter; P1, pressure transmitter (Wika); P2, pressure transducer (Sensotec); PC, personal computer; PD1, PD2, pressure displays; PS, power supply unit; S1, S2, Solenoid Valves; V1, shut-off valve; V2, safety relief valve; V3, V4, V5, control valves;electronic lines; ————— pneumatic lines.

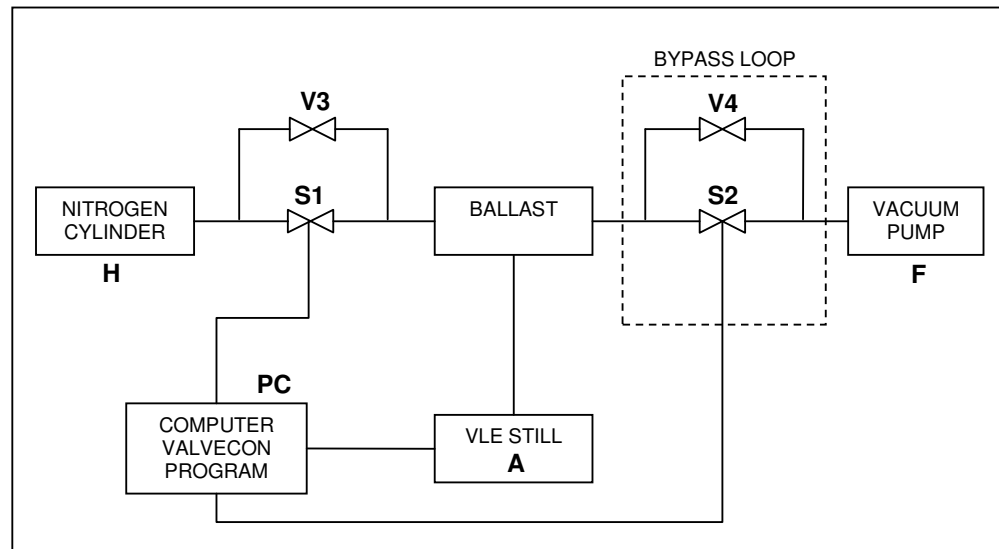


Figure 4-3: Schematic to illustrate pressure control

Pressure is controlled by the use of a VALVECON program and solenoid valves with a rating of 105 psia allowing for operations at low and elevated pressures. Refer to Figure 4-2 for schematic of pressure control system.

A Microsoft Visual basic software interface program, VALVECON, communicates with a personal computer via the RS232 port and logs system temperature and pressure data that is displayed on an Agilent multimeter (MM) and DPM pressure displays (PD1 and PD2) respectively.

The data logging interface allows for system variables, from the respective sensors, to be monitored in real time. This in turn permits the execution of the VALVECON program to control the temperature and pressure from the feed back system within a predefined tolerance. The hardware for the control of the system pressure is in the form of a pulse width modulation control strategy of two 12 VDC Clippard “on-off” solenoid valves which are normally set in the closed position and when actuated, opened.

The solenoid valves (S1 and S2) are connected to a power supply (PS) to activate the valves to control pressure and to high (compressed nitrogen high pressure cylinder, H) and low (vacuum pump, F) sources on either side of the ballast flask (E). The valves are suitable for fine pressure control as they allow for a relatively small flow. However, in cases where the system pressure has to be changed in a short space of time, either for pressurization or evacuation, bypass loops in conjunction with larger needle valves (V3 and V4) have been incorporated across each solenoid valve for this purpose.

When the set point pressure is entered into the VALVECON program interface, the appropriate solenoid valve is activated to control and correct the system pressure. If the pressure in the system is higher than the set pressure, this would mean that the system pressure needs to be lowered to reach the desired pressure. To effect this change the solenoid valve connected to the low pressure side (**S2**) is activated to open. Similarly for a system pressure greater than the set pressure, the solenoid valve connected to the nitrogen cylinder is activated to open (**S1**).

Another input that is required by the VALVECON control program is the “dead-band” value. Reddy describes the dead-band value as the allowed tolerance for the system pressure before the solenoid valves are activated (to open or close) to control the pressure. The dead-band input is normally entered as 0.1 in units of pressure.

To assist with the inevitable fluctuation in pressure, the VALVECON program can control, by adjusting the sampling rate through the control option, the amount of logged pressure points that are used to give an average pressure value. The VALVECON program then responds to this value which is the system pressure and executes the necessary control strategy. The system pressure can be controlled to ± 0.001 bar, of the set point pressure.

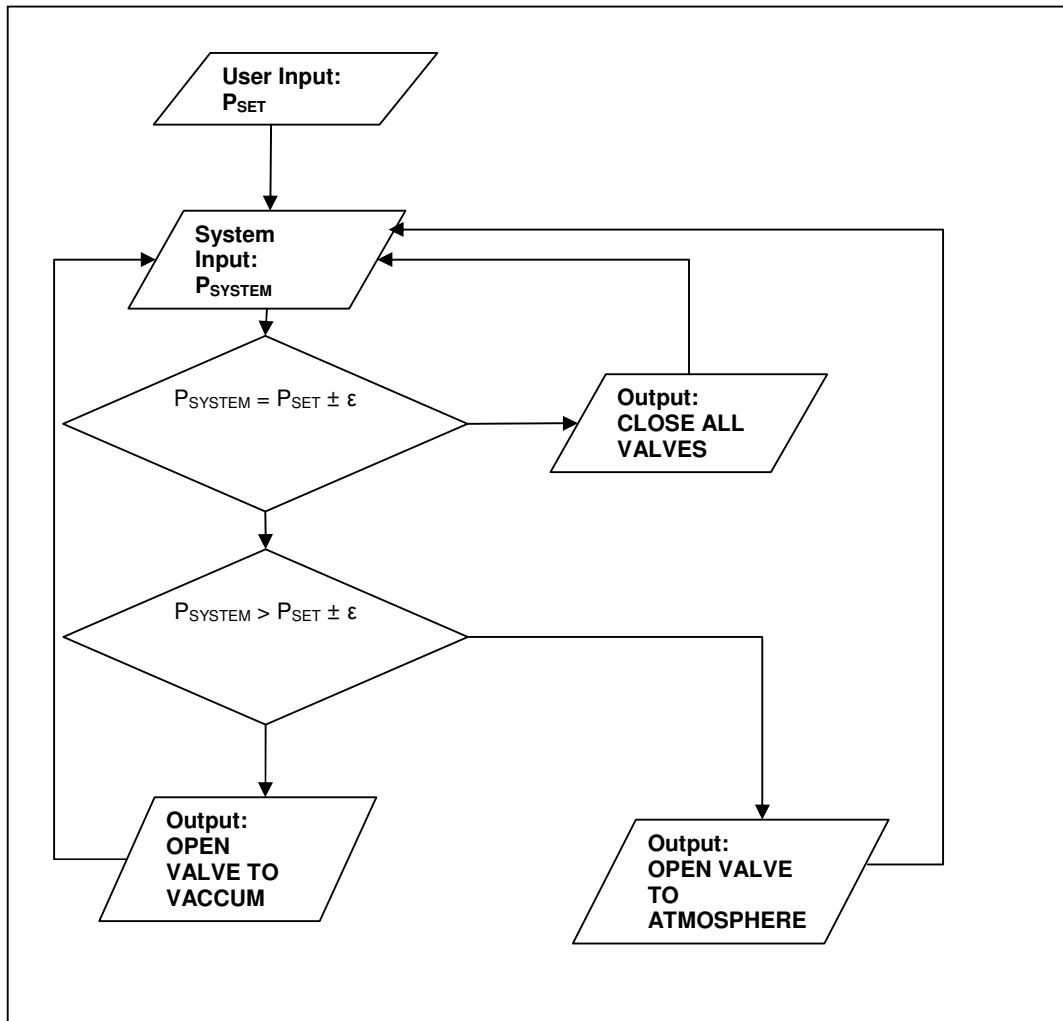


Figure 4-4: Isobaric control flow sheet (Harris, 2004).

Isothermal control is also possible with the VALVECON program but was not implemented in this project. The reader is referred to Reddy (2006) for a detailed explanation. Isothermal control is comparatively more difficult than isobaric control as is described in Harris (2004), where increasing instability of the temperature control was observed at elevated temperatures. The procedure for isothermal operation will be discussed in Chapter five.

4.2 Features of experimental apparatus

Some of the shortcomings of Harris were discussed in Chapter three. In the current equipment design, Reddy attempted to remedy these shortcomings. Presented below are brief summaries of the features of the equipment of Reddy some of which that were developed due to investigations performed on Harris (2004). Refer to Figure 4-1.

a) Thinner walls and new operating pressure limit

Harris recommended that the walls of the apparatus be thinner. Both the apparatus of Reddy and Harris were constructed from 316 SS. The large thermal capacity of the large bulk of stainless steel adversely affects the attainment of and internal thermal equilibrium. This directly produces a poor thermal response to the change in heat input of the VLE apparatus and makes operating the equipment a time consuming procedure (Reddy, 2006). As a result of this, Reddy thought it would be more suitable to reduce the thickness of the walls and to also consider a more realistic and reasonable pressure range.

b) Flanges and gasket

Harris recommended the use of screw type design for the reboiler (**A**) and equilibrium chamber (**C**). However, after investigating the sealing properties and resilience of graphite based gaskets, Reddy felt that the optimal choice would be the use of flanges and gaskets. This would also facilitate in the disassembly and re-assembly of equipment.

c) Mechanical agitation

The design of Harris did not include any type of mechanical agitation to the reboiler contents or vapour and liquid phases, and was most likely responsible for the erroneous data obtained by Harris as discussed in Chapter three. The lack of mixing of phases would have led to flashing, temperature fluctuation and erroneous vapour phase compositions.

With the now thinner 316 SS walls it was possible to achieve a magnetic flux through the walls; allowing the incorporation of a magnetically coupled stirrer. The stirring mechanism is based on a stainless steel ball bearing on ceramic bush around the heater cartridge in the reboiler (**S**).

d) Transparent sections

One of the greatest advantages of the glass still is that it is possible to monitor the fluid flow characteristics in the Cottrell tube, the flow into the liquid trap and the condensation rate in the vapour sample trap. This was one of the limitations of the equipment of Harris. There was uncertainty with the volume of material to be charged into the still to allow for good circulation. The efficiency and continuity of the vapour liquid mixture transported up the Cottrell tube with change in temperature and the general fluid flow characteristic of the system could also not be observed. Also with the uncertainty of material volume to be charged in to the still, the problem of back flow into the lines and even into the sample traps occurs. As a result of the above findings, Reddy incorporated transparent sections to aid in the above at the cost of reducing the operating pressure limit of the apparatus. The transparent sections are located in very strategic points to assist the experimentalist. They can be found in the Cottrell tube (**B**) and the liquid and vapour condensate sample traps (**G** and **I**).

e) Sample traps

Sample traps should be made to allow for the observation of the nature of the flow of the phases with regard to drop count and back flow into traps. They should also allow mechanical agitation and appropriate sampling provisions (Reddy, 2006). The design of Harris did not allow for the above provisions. In the design of Reddy, an overflow weir type design was incorporated in the sample traps (**G** and **I**). This ensures that a small amount of material remains in the sample trap and is constantly mixed to remove any concentration gradients. For operation at elevated pressures, a stainless steel flanged body with a glass housing insert was used. Pressure equalization was also incorporated across the sample traps to ensure that fluid pressure build up does not occur in the traps. The traps were sealed with Teflon discs and Viton o-rings and Teflon stirrer bars were used to mix the material in each trap.

f) Temperature Sensors (**Pt1**, **Pt2**, **Pt3**, **Pt4**)

The addition of temperature sensors in key sections of the apparatus ensures that the temperature profile of the operational areas can be effectively monitored. All the temperature sensors (three) used in this equipment are Pt-100 sensors. The fourth Pt-100 sensor (**Pt4**) is located on the return line to the reboiler and was not required for this investigation. The temperature sensor in the reboiler (**Pt1**) allows for one to monitor the temperature of the reboiler contents as a function of energy input from the internal and external heaters from the variable-voltage transformers (Reddy, 2006). This will also help prevent the experimenter from overheating the mixture during operation of the still.

A temperature sensor is located in the equilibrium chamber (**Pt2**) in addition to the sensor in the packed section (**Pt3**). An external heater is required for the pre-heating of the main body, this is imperative as it ensures that no excessive heating of the equilibrium chamber takes place.

g) Return Lines

The vapour and liquid return lines were combined into a single line (**L**) a fair distance away from the reboiler (Reddy, 2006). This necessitated premixing of the phases to occur. The equipment also allows for the return lines to be heated when working at fairly high temperatures. The heating of the return lines do not occur in the vicinity of the sample traps as back flow may occur due to excessive heating.

Cooling of the liquid and condensate lines is also possible (**D** and **E**). This is done by incorporating a jacket around them for the flow of coolant. The reason for this inclusion is to ensure that measurements at extremely high temperature do not damage the seals on the trap, mainly Teflon and Viton, both of which have a temperature rating of about 200 °C.

h) Pressure stabilization

The equipment has a 50 L ballast flask and was noted by Reddy, to be highly effective for smoothing or dampening pressure fluctuations. The ballast is connected to a high pressure gas cylinder (nitrogen) for operation above atmosphere and to a vacuum pump for operation below atmosphere. As a safety measure pressure release valves were also included on the ballast to prevent over-pressurisation of the apparatus.

4.3 Modifications to VLE still

Three main modifications were made to the VLE apparatus as a solution to the specific and continuous problems experienced. The problems together with the solution are highlighted in this section.

1. Pressure fluctuations. It was observed that every time the equilibrium band heater was turned and the voltage altered, the pressure display would immediately fluctuate. It was not certain whether the problem was specific to the pressure display or the pressure sensor, however seeing as how the solenoid valves are activated in response to the pressure reading this directly affected the pressure control and pressure in the still.

A possible reason for the fluctuations was that the coating on the equilibrium band heater was being worn off over time thus causing interference with the pressure transducer when switched on. The resistance of the band heater was recorded over several days. Theoretically if the coating was wearing off the resistance should decrease!

To shield the pressure transducer from the interference a plastic fitting was placed between the pressure transducer and the still. This solved the problem of the pressure fluctuations. However, it should be noted that this is a temporary solution.

2. Refer to Figure 4-5. Very slight pressure fluctuations still occurred in the still, but only after operating the still for a long time. The possible reason was due to the placement of the pressure transducers (C), Diagram I, which were placed along the line below the condenser (B). This causes some material which may not have condensed to escape and condense near the transducer leading to erroneous pressure readings. This was solved by changing the position of the transducers, Diagram II, to above the condenser as is shown by the front view schematic of the still. The line and the transducer were fitted at a slight angle to allow any material that may condense at the point to drain back to the condenser or to be evacuated by the pump. This solved the problem and is recommended for dynamic VLE stills.

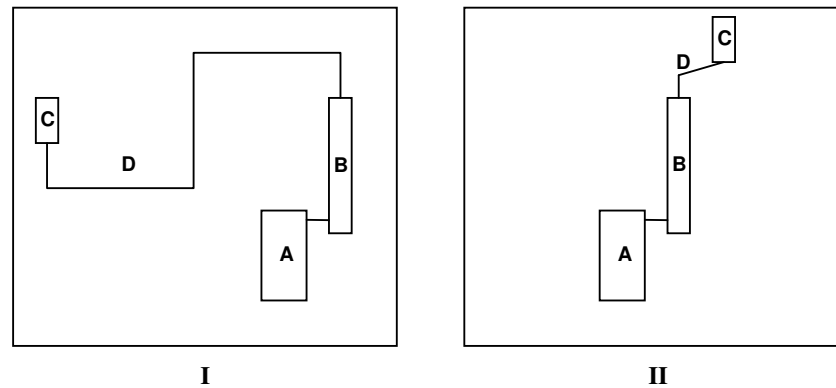


Figure 4-5: Schematic of position of transducers.

A - VLE Still, B - Condenser, C - Pressure transducers, D - line between condenser and pressure transducers.

3. The third modification made to the VLE still is not a major modification but makes a significant difference during operation and sampling.

The sample points for both the liquid and vapour condensate traps are in the form of a septum coupled with a stainless steel fitting. The opening on the fitting for the vapour condensate trap is significantly larger than that of the liquid thus exposing more of the septum. The problem arises when the still is operated under high pressure, as multiple samples are taken the strength of the septum is compromised. This causes the septum to protrude and the contact between the septum and the valve on the trap is broken resulting in leaks and difficulty in maintaining a set pressure.

The solution was to machine a new fitting that exposes less of the septum thus keeping it firmly in place after multiple samples and preventing leaks during operation at high pressures.

CHAPTER FIVE

EXPERIMENTAL PROCEDURE

In any research based work the operating procedure and calibrations play a vital role. Thus the experimental data is only as accurate as the calibrations of the instruments, upon which it is based. Leaks in equipment and contamination of equipment contribute towards erroneous data. Also, the proper operation of the equipment is imperative in the pursuit of reliable data. In light of the importance of the above mentioned aspects associated with the acquisition of VLE data; this section will discuss the following aspects with regard to the operation of the VLE recirculating still of Reddy (2006) which was used in this investigation:

- Leak testing
- Calibrations of temperature and pressure sensors and gas chromatograph detector
- Start up and shut down procedures
- Operation of the still to attain equilibrium for both isobaric and isothermal mode
- Cleaning of the VLE still

5.1 Leak test

The presence of leaks is one of the most common and time consuming problems experienced with VLE equipment. Leaks in equipment affect temperature and pressure measurements and also in the case of control programs, lead to difficulty in maintaining a purely isothermal or isobaric state. This in turn, affects the attainment of equilibrium. Loss of material can also be experienced leading to incorrect equilibrium phase compositions.

Leak testing is therefore carried out thoroughly and regularly. Leak testing is performed both under high pressure and vacuum. The system is either pressurized or evacuated, at which point the still is isolated from the ballast to ensure that the leaks are detected quickly. The decrease or increase in pressure is noted over time in order to establish if a leak is present.

For pressurized leak testing the apparatus is pressurized to about 150 kPa and a surfactant based liquid is applied to the various fittings and seals. If a leak is detected the surfactant begins to bubble in areas where it was applied.

5.2 Sensor and detector calibration

5.2.1 Pressure calibration

There are two pressure sensors located on the VLE apparatus. A low pressure range, Sensotec pressure transducer (0 - 1.5 bar) and high pressure range, WIKA transmitter (0 - 10 bar). The sensors were connected to the still and their readings were compared to a standard pressure sensor also connected to the still. Pressures were chosen across the experimental range and a plot of P_{ACTUAL} (from the standard sensor) vs. $P_{READING}$ (from the two sensors) was obtained as the calibration curve. Pressures were chosen using the pressure control program described in Chapter four. Uncertainty in pressure measurements due to resolution on the pressure display is ± 0.001 bar. The accuracy of the Sensotec pressure transducer and the WIKA pressure transmitter was 0.05% as stated by Reddy (2006).

5.2.2 Temperature calibration

The equilibrium still has three Pt-100 sensors located in the boiling chamber, at the base of the equilibrium chamber and at the top of the equilibrium chamber. The equilibrium Pt-100 was custom made by Wika Instruments and was also calibrated by them, however as with the pressure sensors, the sensor had to be calibrated. Calibration was done in-situ and was achieved by boiling a chemical, with a boiling temperature within the experimental operating temperatures and pressures, at various pressures. A plot of resistance (from the multi-meter connected to the Pt-100) vs. temperature (from the Antoine equation of the chemical at the known pressure) is obtained as the calibration graph. The accuracy of the WIKA Pt-100, as stated by Reddy (2006) is ± 0.005 K.

5.2.3 Gas chromatograph detector calibration

Gas chromatography was chosen as the analytical method for determining the phase compositions. Apart from being readily available, it is also one of the most popular analytical methods due to sample sizes required, detection limits, reproducibility and simple operating procedure (Reddy, 2006).

The procedure for calibration of the detector, as suggested by Raal and Mülhbauer (1998), is described below:

- a. Samples of each binary system are gravimetrically prepared such that the ratios of the mole fractions range from 0.1 to 1.2 (approximately).
- b. The samples are analysed by chromatography until the results are repeatable within a tolerance. The peak areas of each chemical are noted.
- c. Plots of A_1/A_2 versus x_1/x_2 and A_2/A_1 versus x_2/x_1 are obtained.
- d. If the detector response is linear, the data sets can be reduced to straight lines passing through the origin. The inverse of the slope of A_1/A_2 versus x_1/x_2 should be approximately equal to the slope of A_2/A_1 versus x_2/x_1 and vice versa.

The GC used in this investigation is the SHIMADZU GC17A installed with a 30m capillary column. The detector used was a FID (Flame ionisation detector). The column, detector and injector temperature settings of the gas chromatograph for each of the three systems investigated are tabulated in Chapter six, Table 6-1 and the results are given in Figures 6-3 to 6-8.

5.3 Start up procedure

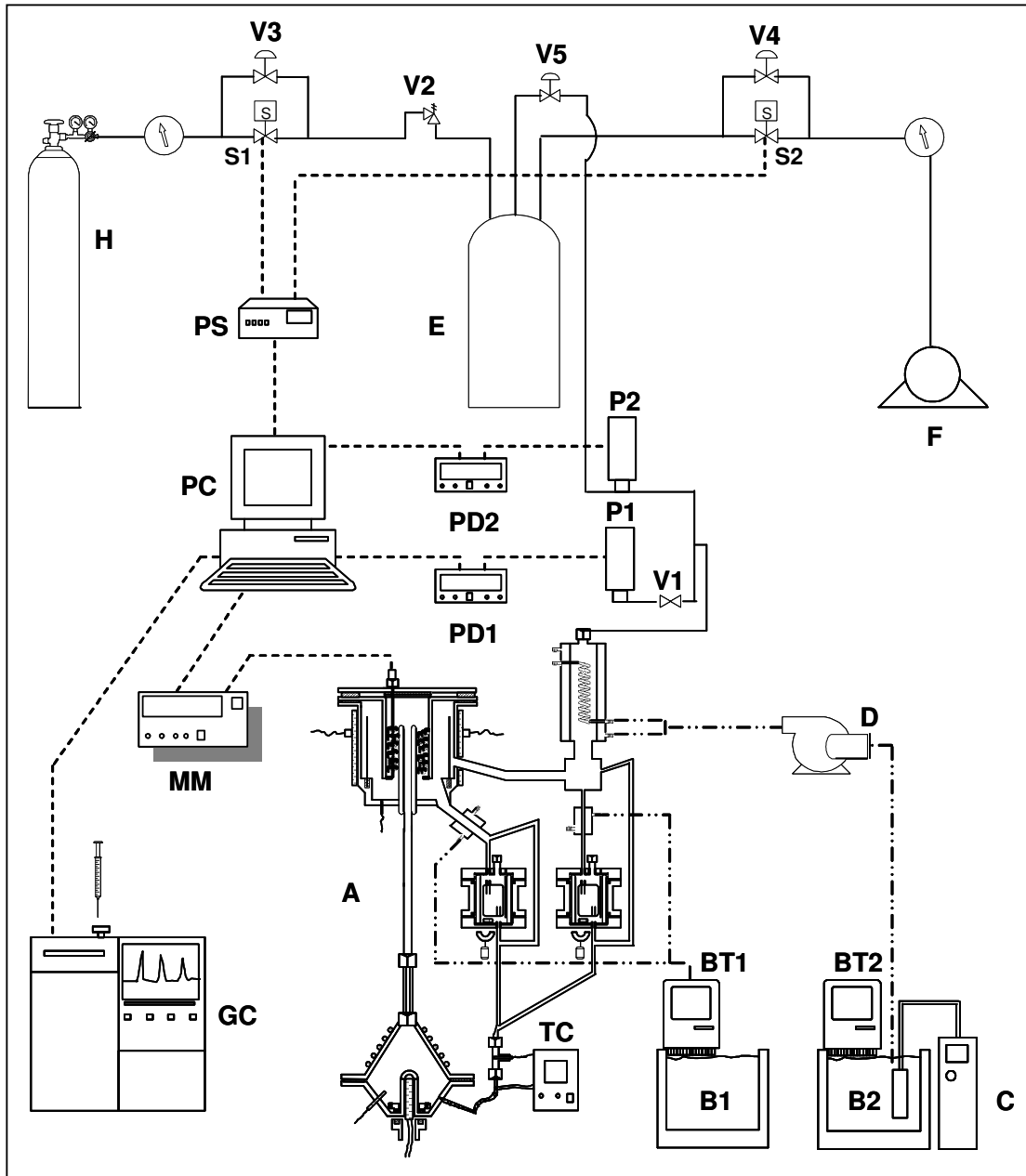


Figure 5-1: Auxiliary equipment and layout of experimental apparatus (Reddy, 2006): A, VLE still; B1,B2, waterbaths; BT1, BT2, thermostats/circulator pumps; C, refrigeration apparatus; D, coolant fluid pump; E, ballast tank; F, vacuum pump; GC, gas chromatograph; H, gas cylinder; MM, multimeter; P1, pressure transmitter (Wika); P2, pressure transducer (Sensotec); PC, personal computer; PD1, PD2, pressure displays; PS, power supply unit; S1, S2, Solenoid Valves TC, temperature controller; V1, shut-off valve; V2, safety relief valve; V3,V4,V5, control valves;electronic lines;water lines; pneumatic lines.

1. The still is charged by firstly creating a vacuum in the still. This is done to create a pressure gradient, which allows the chemical to be “drawn” into the still.

The pump (**F**) is switched on and the outlet is attached to the ballast flask (**H**). The by pass valve (**V4**) on the solenoid valve (**S2**) is open so that the pressure drops in minimum time. The pressure has to be low enough that suction is created. About 0.93 bar is sufficient. It is important that the vacuum used be higher than the vapour pressure of the chemical used to avoid flashing of the chemical when it introduced into the still (Reddy, 2006). The liquid is slowly introduced through the drain valve located at the base of the boiling chamber until the level was just above the glass insert in the Cottrell tube. The chamber volume is approximately 170 ml but extra liquid (200ml) is added to account for the vapour and liquid sample traps. This volume is variable with regard to the temperature and pressure range, the thermophysical properties of the chemical components and the circulation rate as controlled by the heat input into the still (Reddy, 2006). The level of the liquid is very important as too little liquid will cause flashing in the boiling chamber and too much will cause back flow in sample traps.

2. Once the still is charged and the liquid level is correct the computer (**PC**) is switched on. The power supply for the stirrers, located in the boiling chamber and the sample traps, were also turned on. A suitable current input determined an optimal stirring rate for the still contents (Reddy, 2006). The VALVECON program is opened but control does not begin until some boiling is observed. This is done to avoid strain on the solenoid valves. The bypass valve (**V4**) to the pump is closed and then, the nitrogen tank (**H**) and the bypass valve (**V3**) between the nitrogen tank and the ballast are open to increase the pressure (if working at high pressure) in the still. If operating at low pressure the nitrogen tank (**H**) is opened and once the required pressure is reached the bypass valve (**V4**) between the pump (**F**) and the ballast flask is closed.
3. The coldfinger or refrigeration apparatus (**C**), stirrers and heaters are turned on once system pressure approaches the required pressure. All the heaters (internal cartridge, external and equilibrium band heater) are set at 20V. Its is left at 20V until some boiling is observed at which time the control program is started with the operating set pressure and the dead band at 0.1, as inputs.

5.4 Procedure for the measurement of isobaric VLE (attaining equilibrium)

The procedure for isobaric experimentation is discussed below:

1. The still was sealed (all valves were closed), the vacuum pump is switched on or the nitrogen tank opened depending on whether the system is to be operated at low or high pressure respectively. Once the pressure value displayed on the pressure transducer had stabilised, the heaters are turned on. The coolant oil pump was switched on and the bath refrigerating device (cold finger) turned on, so that cool water could pass through the condenser.
2. The system was left to stabilise for approximately 15 – 20 minutes for low pressure and about 30-40 minutes for high pressures. All heaters are then increased to 40V, and the boiling and temperature observed. Thereafter, only the internal heater voltage was varied to increase and decrease power inputs to the system every 20 minutes. The values were noted at 5 minute intervals and a plot of temperature vs. voltage was created in order to assess the range over which the plateau occurred for the particular point under investigation. The plateau region is described by Kneisl et al. (1989), as the region where the boiling temperature remains unchanged when power input is increased slightly. Kneisl found that the boiling temperature was a function of power input and that by operating outside of this region, erroneous boiling points would result. It was thus ensured that the plateau region was indeed stable in temperature with changing power input.
3. Once the plateau region was found, the system was allowed to settle for a further 15 - 30 minutes to equilibrate, before samples were taken from the VLE still. Liquid and vapour samples were taken with a micro-litre syringe to eliminate the risk of contamination and degradation of the sample. This minimal volume extraction (0.5-1 μ l depending on the system sensitivity) also ensured that equilibrium was not disturbed. The samples were immediately injected into the GC for analysis. On average 3 samples of each of the phases were taken until acceptable reproducibility could be found (deviations of less than 0.05 %).
4. Once a point (liquid and vapour condensate) was obtained, a small amount of mixture is drained from the still and replaced with a pure sample of the second component. At this point it is important to note that the mixture can only be drained if the system pressure

is above atmosphere, creating a pressure gradient. Sample can only be drawn into the still if the system pressure is below atmosphere.

5. Step 2 - 4 is repeated until half the composition range is covered and half the phase diagram is generated.
6. The still is then evacuated and dried, and steps 1 to 5 are repeated, this time with component two as the initial charge and component one being added to obtain successive points.

5.5 Shut down Procedure

1. The heaters are turned off. The coldfinger and stirrers remain on to allow all the vapours to condense.
2. The control program is turned off as well.
3. Once boiling has stopped and the system has cooled significantly, about ± 50 °C, the pressure of the system is brought to atmospheric. If the system was initially at a high pressure then the pump (F) is switched on and the bypass valve (V4) opened. If the pressure was initially at a low pressure then the bypass valve (V3) between the nitrogen tank (H) and the ballast is opened to allow the pressure to increase to atmospheric.
4. Once the desired pressure is reached, all the valves are closed. The nitrogen tank is closed as well and the pump switched off.
5. The computer is then shut down.

5.6 Procedure for measurement of isothermal VLE

1. The procedure is similar to that of the isobaric procedure however the pressure is adjusted to maintain a constant temperature.
2. The start up procedure is the same.
3. The plateau region for various pressure set-points are found until the desired temperature is obtained for each change in composition as discussed above.
4. Steps 4 to 6 from the isobaric procedure are then followed.

5.7 Cleaning the still

Reddy (2006) suggested cleaning the still by means of evacuation. This was done by firstly draining the still and then evacuating it to about 0.1 kPa, by attaching the vacuum (F) pump to the suction point at the top of the condenser. The pump is left for several hours and the still (A) is heated slightly by turning on the internal heater cartridge and equilibrium band heater, to allow trace amounts of material to evacuate the still.

Other means of cleaning the still include, running a low boiling solvent like pentane, for several hours, through the still for effective removal of contaminants (Reddy, 2006). The common solvent used is acetone, however, according to Reddy (2006) it is incompatible with some of the sealant used in the still. Reddy (2006) also suggested running the more volatile of the components of the binary system to be investigated through the VLE still, as opposed to the use of pentane. This method isn't the most cost effective, especially if chemicals are expensive. Once this is done, the still is drained and evacuated as described above. The still is considered sufficiently clean when a sample of the chemical is run through the GC and no extra peaks, which would constitute contamination, are found.

CHAPTER SIX

EXPERIMENTAL RESULTS

The VLE measurements made with the apparatus of Reddy, discussed in Chapter four are presented in this section, including the calibrations of equipment sensors and the gas-chromatograph detector. The procedure used to calibrate the Pt-100 situated at the top of the equilibrium chamber; the pressure sensors and gas chromatograph detector were discussed in Chapter five. The results are presented below and can be summarised as follows:

- a) Calibrations
- b) Vapour pressures
- c) Results of systems investigated

VLE data was obtained for the system of 1-hexene with n-hexane at 55 C. This system was previously measured by Kirss et al. (1975) and was used as a test system to establish the accuracy of the equipment and the experimental procedure. VLE data for the systems of 1-hexene with n-hexane, 2-methyl-2-pentene with n-hexane and n-methyl-2-pyrrolidone with 1-hexene have not been measured or reported in the open literature.

6.1 Calibrations

6.1.1 Temperature calibration

The chemicals used for the temperature calibration were ethyl-acetate and 1-propanol. Ethyl acetate was used for temperatures from 45 to 70°C, and 1-propanol was used for temperatures between 90 and 105°C. The data set for 1-propanol followed the same trend as ethyl acetate, resulting in a linear representation and an R^2 value of 1.

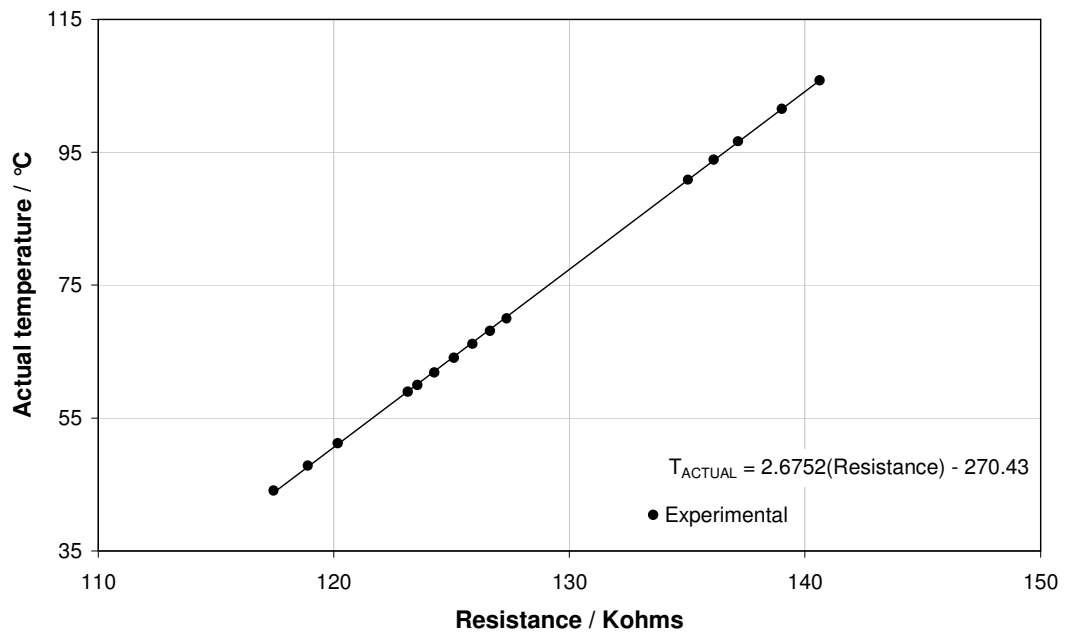


Figure 6-1: Plot of actual temperature versus resistance of Pt-100 sensor.

6.1.2 Pressure calibration

The pressure calibration was performed using a WIKA standard pressure transducer with a pressure range of 0 - 1 bar. The pressure measurement is estimated to be accurate to within ± 0.001 bar.

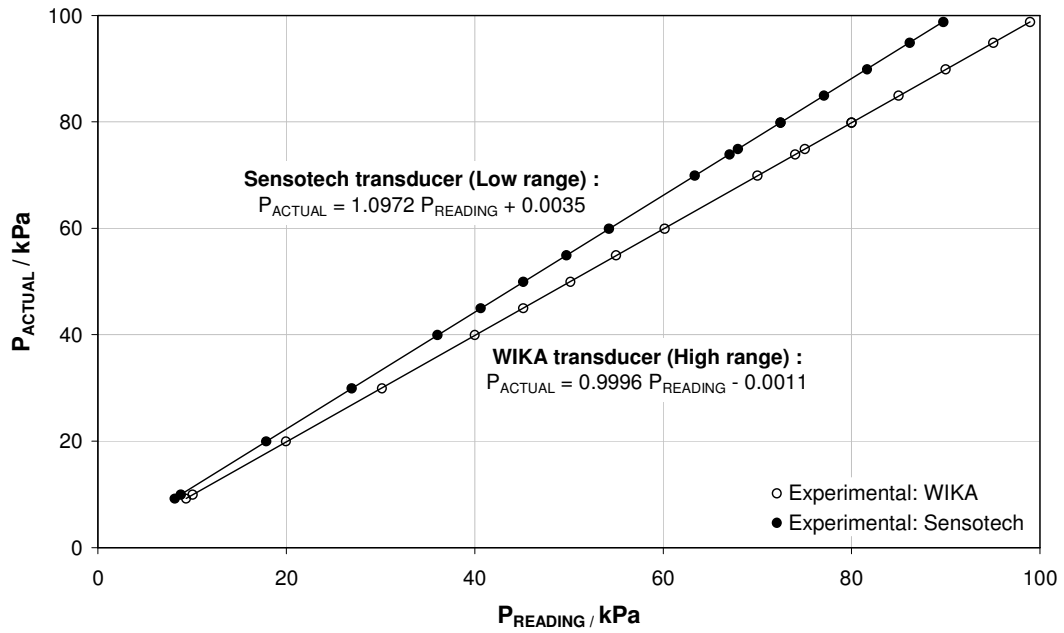


Figure 6-2: Plot of actual pressure versus pressure readings from transducers.

6.1.3 Gas Chromatograph calibrations

Gas chromatograph detector calibration was performed on the SHIMADZU GC17A. The GC operating conditions for each system investigated are presented below in Table 6-1. The detector responses are presented in Figures 6-3 to 6-8.

Table 6-1: Operating conditions of GC used during calibration and analysis of experimental VLE samples

SYSTEM	COLUMN	DETECTOR	INJECTOR
	T / °C	T / °C	T / °C
1-hexene + n-hexane	35	250	300
2-methyl-2-pentene + n-hexane	35	250	300
n-methyl-2-pyrrolidone + 1-Hexene	150	250	300

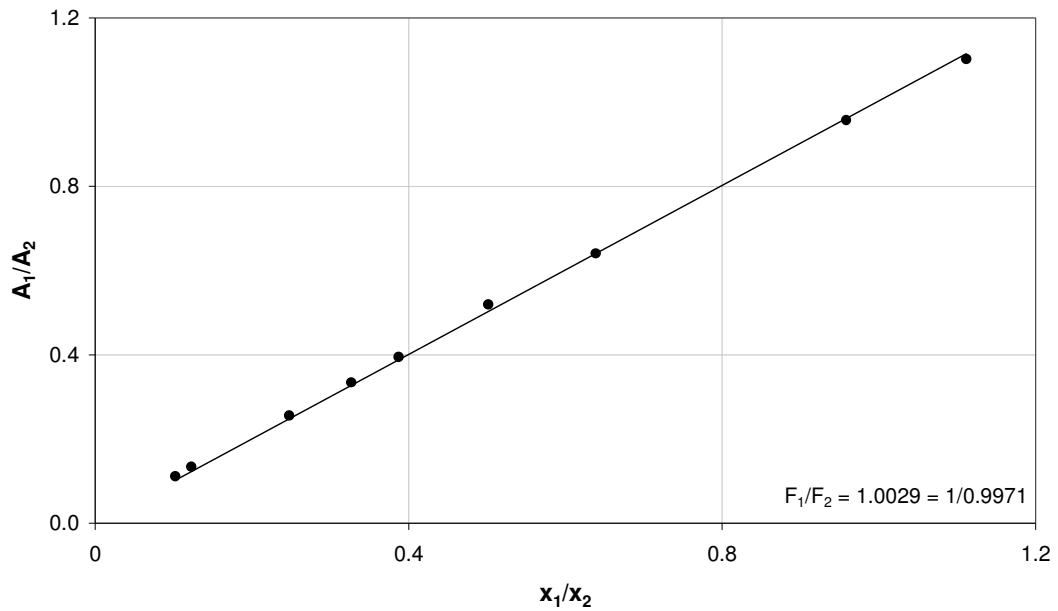


Figure 6-3: Calibration of GC detector response for 1-hexene (1) with n-hexane (2)

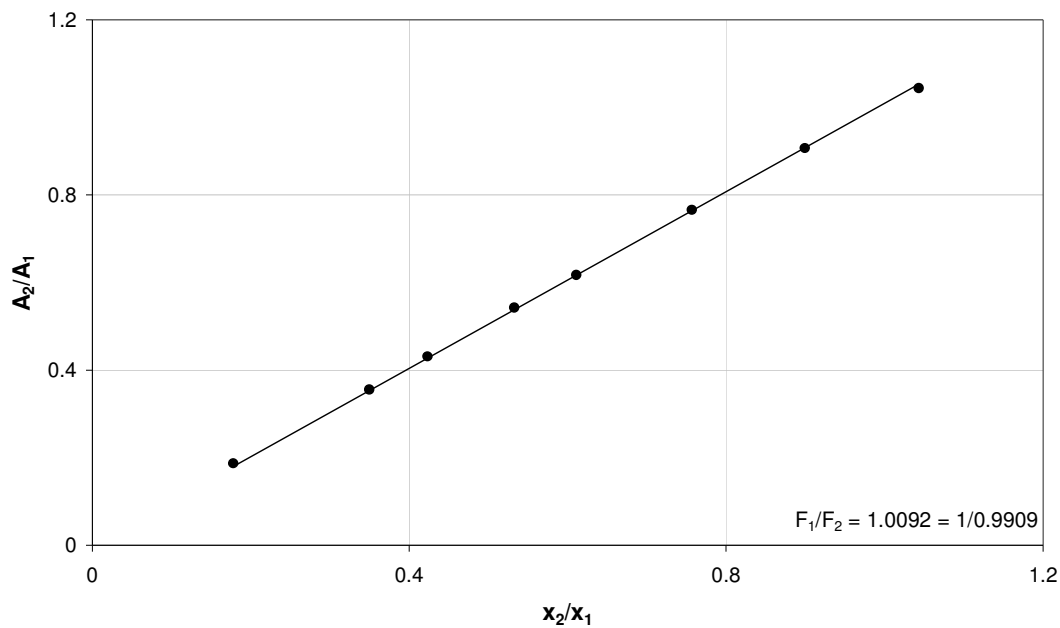


Figure 6-4: Calibration of GC detector response for 1-hexene (1) with n-hexane (2)

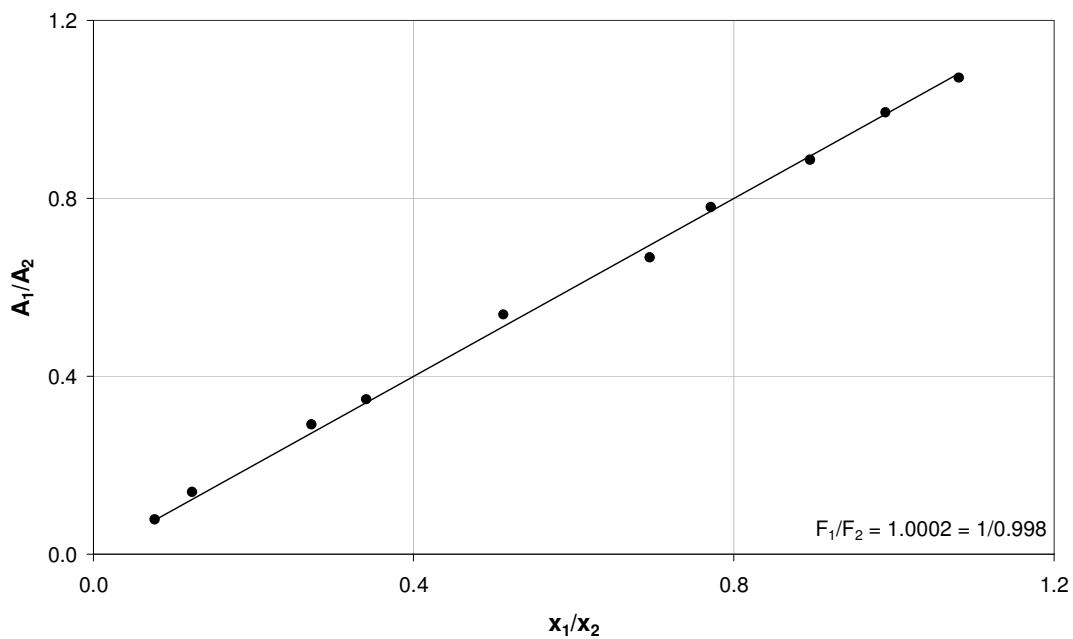


Figure 6-5: Calibration of GC detector response for 2-methyl-2-pentene (1) with n-hexane (2)

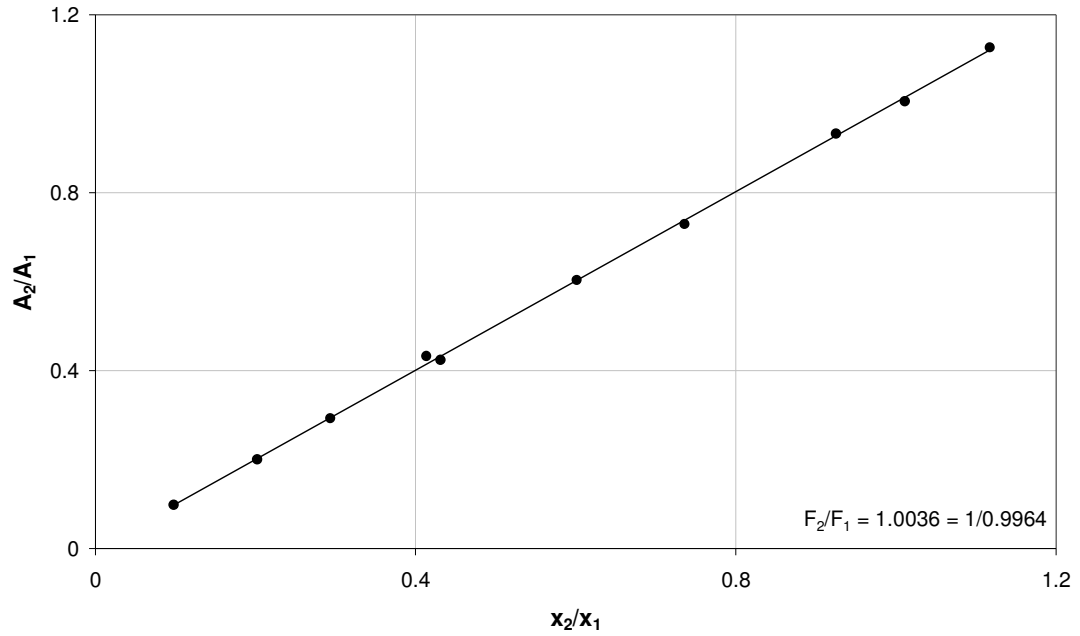


Figure 6-6: Calibration of GC detector response for 2-methyl-2-pentene (1) with n-hexane (2)

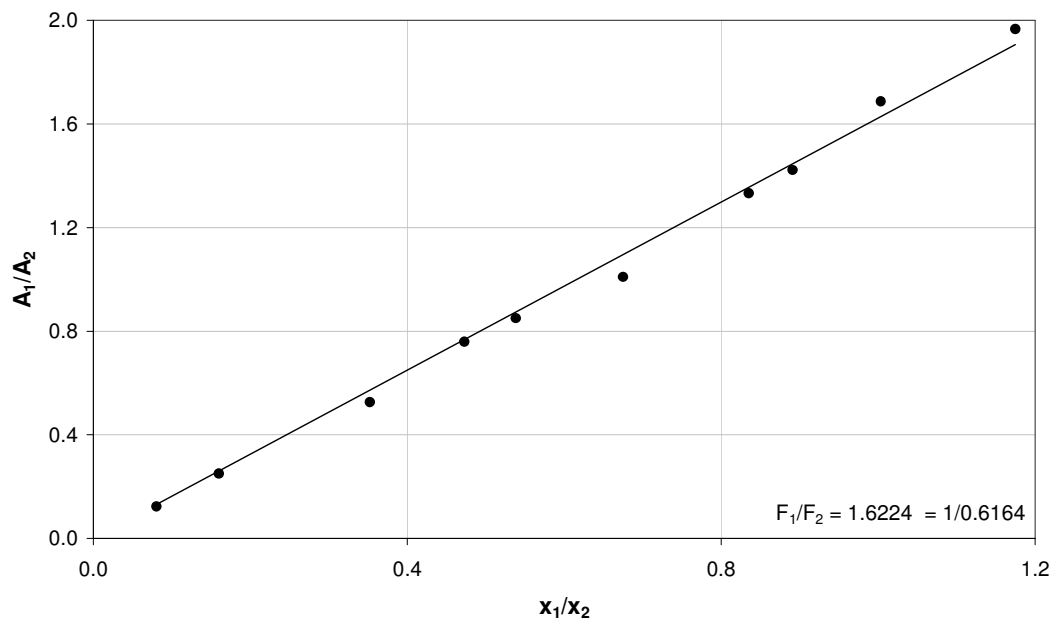


Figure 6-7: Calibration of GC detector response for n-methyl-2-pyrrolidone (1) + 1-hexene (2)

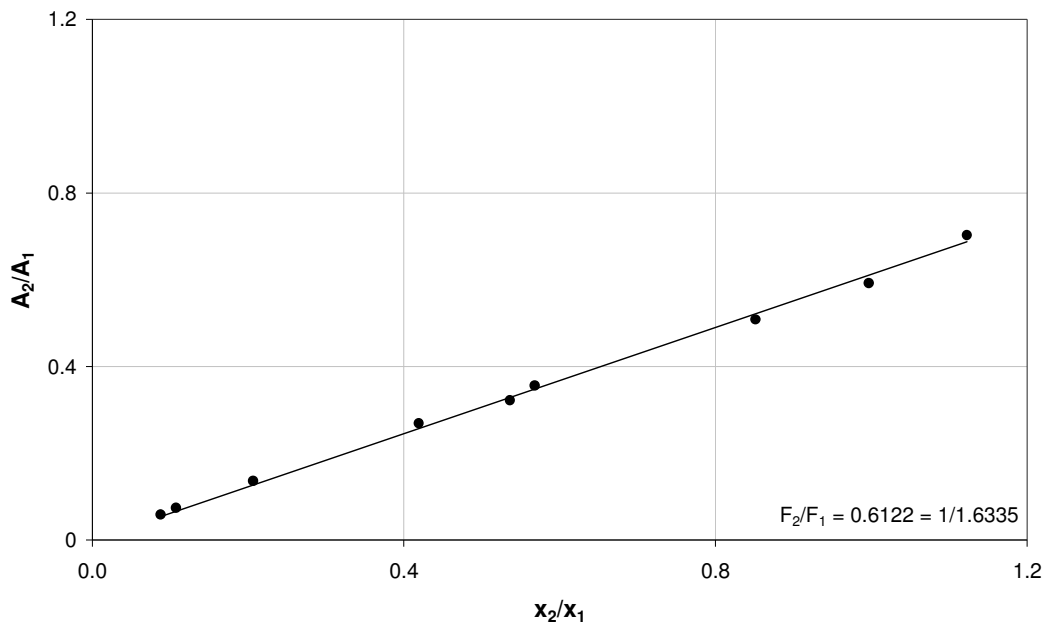


Figure 6-8: Calibration of GC detector response for n-methyl-2-pyrrolidone (1) + 1-hexene (2)

6.2 Vapour Pressures

Vapour pressure curves (pressure versus temperature) were established for all the chemicals used in the binary systems investigated. This was done to ensure proper operation of the equipment and to test the reliability of the calibrations. All resultant data points were compared to the respective literature data. Presented below in Figures 6-9 to 6-12, are the resultant vapour pressure curves for 1-hexene, n-hexane, 2-methyl-2-pentene and n-methyl-2-pyrrolidone respectively. The P-T data for each chemical is also presented in Tables 6-2 to 6-5 including the calculated temperatures obtained from the Antoine equation and the absolute difference between calculated and experimental temperature.

Table 6-2: P-T data for 1-hexene

P_{EXP} (kPa)	T_{EXP} (°C)	T_{CAL} (°C)	$ \Delta T $
74.860	54.270	54.633	0.363
76.659	54.983	55.339	0.356
94.852	61.613	61.827	0.214
139.834	74.399	74.458	0.059
164.824	80.153	80.149	0.004
199.810	87.118	87.092	0.026
249.790	95.304	95.550	0.247
316.763	104.687	105.067	0.380

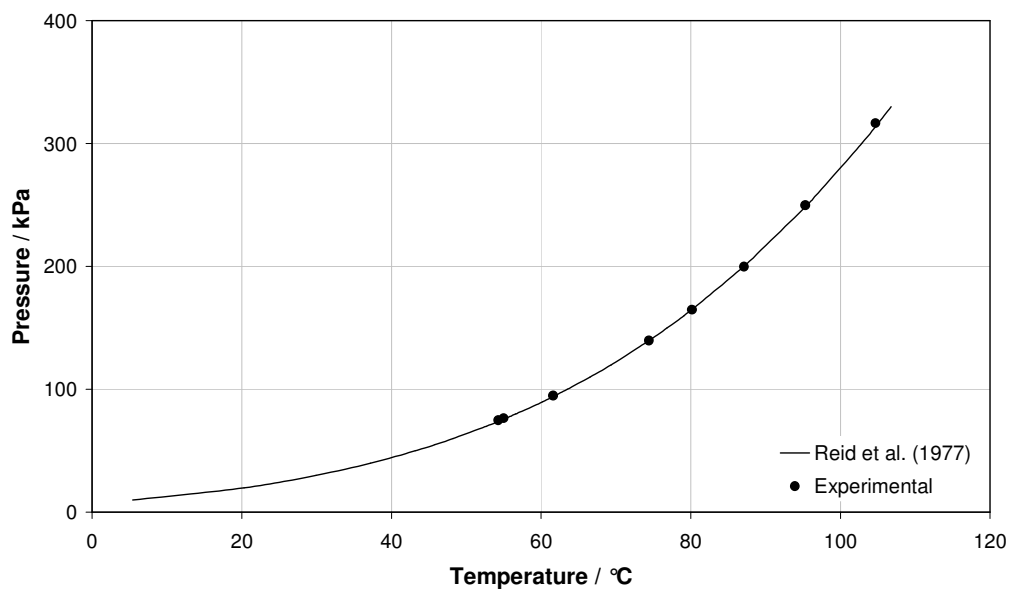
**Figure 6-9: Vapour pressure curve for 1-hexene**

Table 6-3: P-T data for n-hexane

P_{EXP} (kPa)	T_{EXP} (°C)	T_{CAL} (°C)	$ \Delta T $
59.866	52.644	52.865	0.221
64.464	54.974	54.990	0.016
79.858	61.184	61.327	0.143
119.842	74.195	74.164	0.031
140.734	80.002	79.570	0.432
159.826	84.128	83.991	0.136
219.502	95.707	95.598	0.108
279.778	105.061	105.082	0.021
62.065	53.777	53.897	0.119

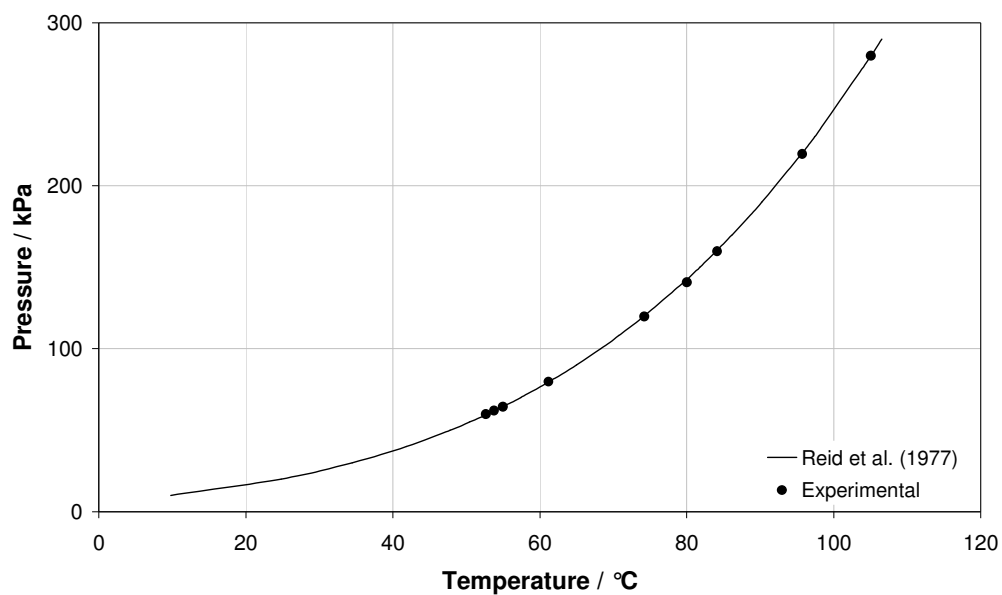
**Figure 6-10: Vapour pressure curve for n-hexane**

Table 6-4: P-T data for 2-methyl-2-pentene

P_{EXP} (kPa)	T_{EXP} (°C)	T_{CAL} (°C)	$ \Delta T $
29.878	33.325	33.355	0.030
44.872	43.695	43.755	0.059
54.868	49.123	49.212	0.089
67.163	55.022	54.927	0.095
84.856	62.421	61.840	0.581
94.852	65.490	65.253	0.236
119.842	73.082	72.692	0.390
149.230	80.509	80.022	0.487
148.830	80.443	79.930	0.512
159.826	82.944	82.389	0.554
189.814	88.958	88.488	0.470
219.802	94.218	93.885	0.334
249.790	99.115	98.744	0.371
292.773	104.993	104.986	0.007

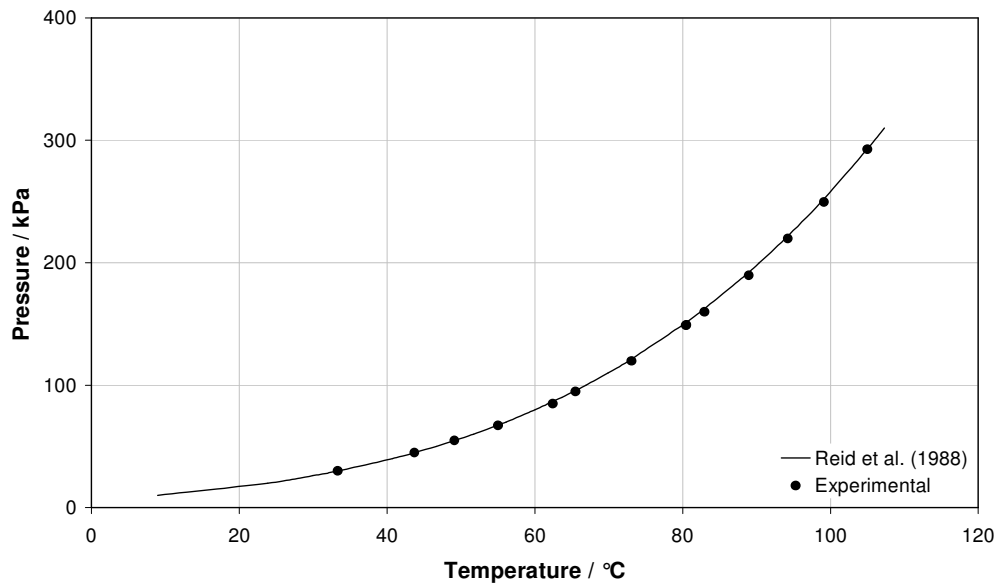
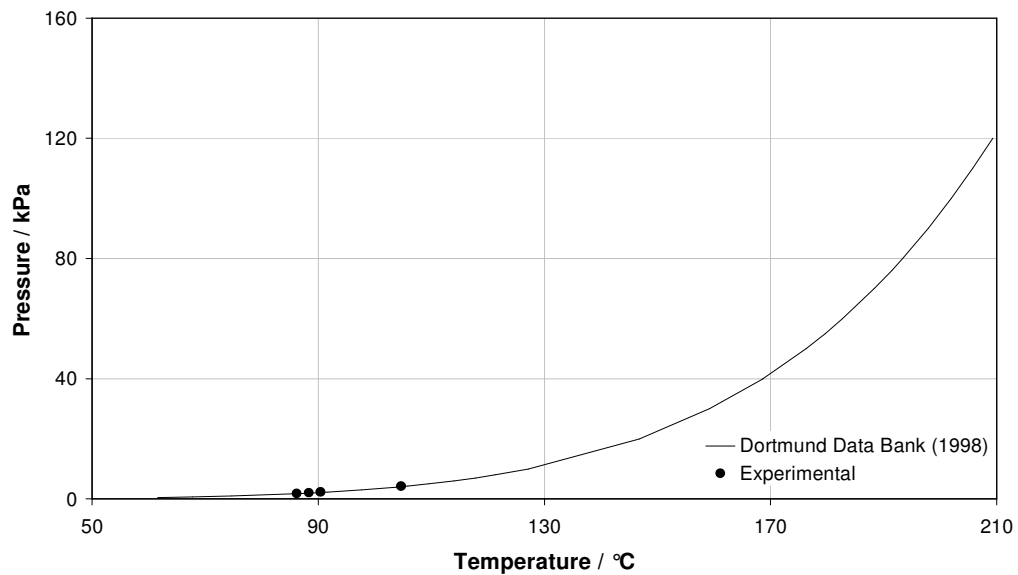
**Figure 6-11: Vapour pressure curve for 2-methyl-2-pentene**

Table 6-5: P-T data for n-methyl-2-pyrrolidone

P_{EXP} (kPa)	T_{EXP} (°C)	T_{CAL} (°C)	$ \Delta T $
1.889	86.157	87.590	1.434
2.089	88.317	89.722	1.405
2.289	90.388	91.685	1.297
4.288	104.632	105.862	1.230

**Figure 6-12: Vapour pressure curve for n-methyl-2-pyrrolidone**

6.2 VLE measurements for 1-hexene (1) + n-hexane (2) systems

Isothermal VLE data were obtained for this system at 55°C, 80°C and 105°C. The data are listed in Table 6-6 below and are presented in Figures 6-13 to 6-18. The 1-hexene (1) + n-hexane (2) system at 55°C is presented with the data set measured by Kirss et al. (1975) for comparison. The systems measured at 80°C and 105°C have not been previously reported in the open literature. Best fit lines are drawn through experimental data points to illustrate the trend.

Table 6-6: Isothermal data for the 1-hexene (1) + n-hexane (2) systems

T = 55°C			T = 80°C			T = 105°C		
P _{EXP} (kPa)	x ₁	y ₁	P _{EXP} (kPa)	x ₁	y ₁	P _{EXP} (kPa)	x ₁	y ₁
64.46	0.000	0.000	140.73	0.000	0.000	316.76	1.000	1.000
65.06	0.039	0.047	142.13	0.062	0.070	311.17	0.856	0.861
65.36	0.068	0.080	144.13	0.146	0.156	308.47	0.801	0.809
65.96	0.100	0.117	146.13	0.228	0.246	305.37	0.740	0.746
67.16	0.184	0.208	148.43	0.315	0.334	300.27	0.591	0.603
67.91	0.231	0.261	149.73	0.365	0.381	296.27	0.506	0.513
68.26	0.263	0.298	150.83	0.406	0.426	291.37	0.344	0.359
69.36	0.343	0.381	152.33	0.468	0.493	285.88	0.261	0.274
70.26	0.421	0.452	155.03	0.585	0.613	282.28	0.192	0.205
71.46	0.523	0.559	156.33	0.638	0.663	280.38	0.128	0.139
72.26	0.591	0.627	157.73	0.693	0.718	278.48	0.078	0.085
72.86	0.642	0.667	158.83	0.746	0.760	279.78	0.000	0.000
73.96	0.728	0.759	162.33	0.896	0.905			
74.56	0.778	0.803	164.82	1.000	1.000			
75.96	0.903	0.918						
75.06	0.826	0.845						
76.66	1.000	1.000						

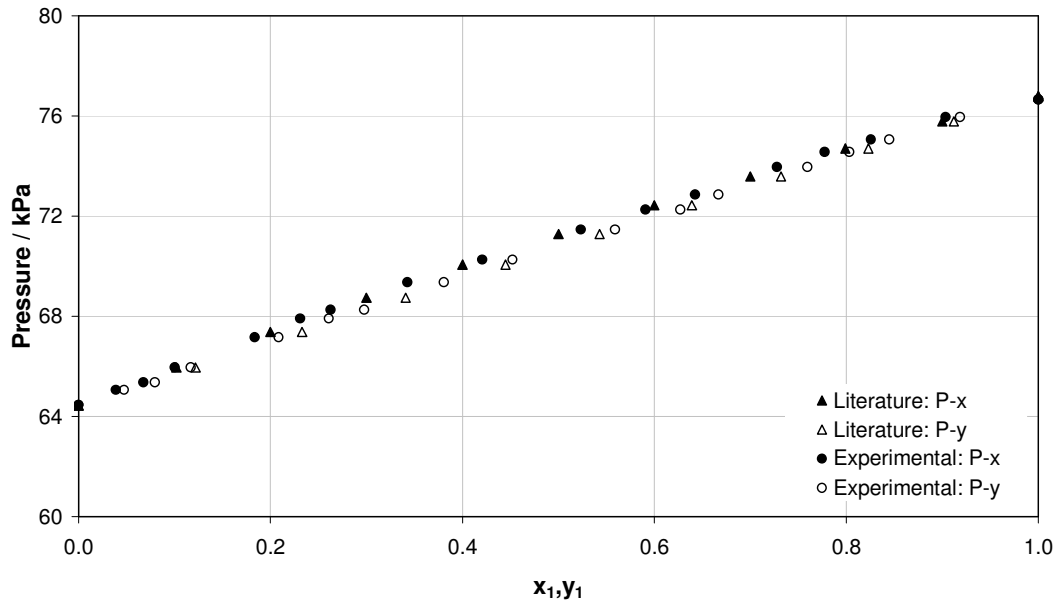


Figure 6-13: P-x-y diagram for the system of 1-hexene (1) + n-hexane (2) at 55°C

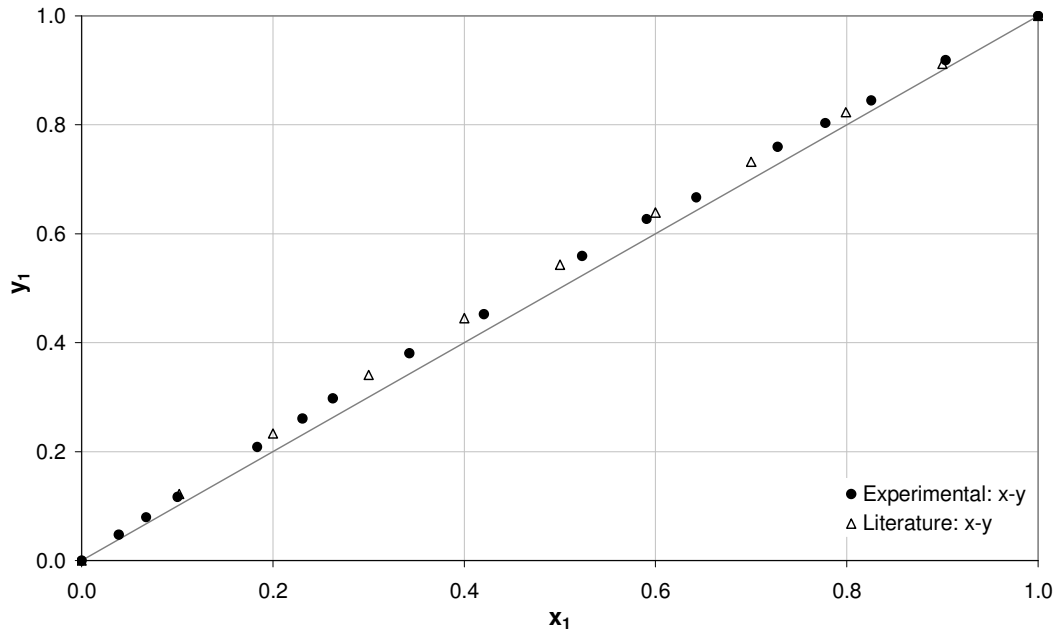


Figure 6-14: x-y diagram for system of 1-hexene (1) + n-Hexane (2) system at 55°C

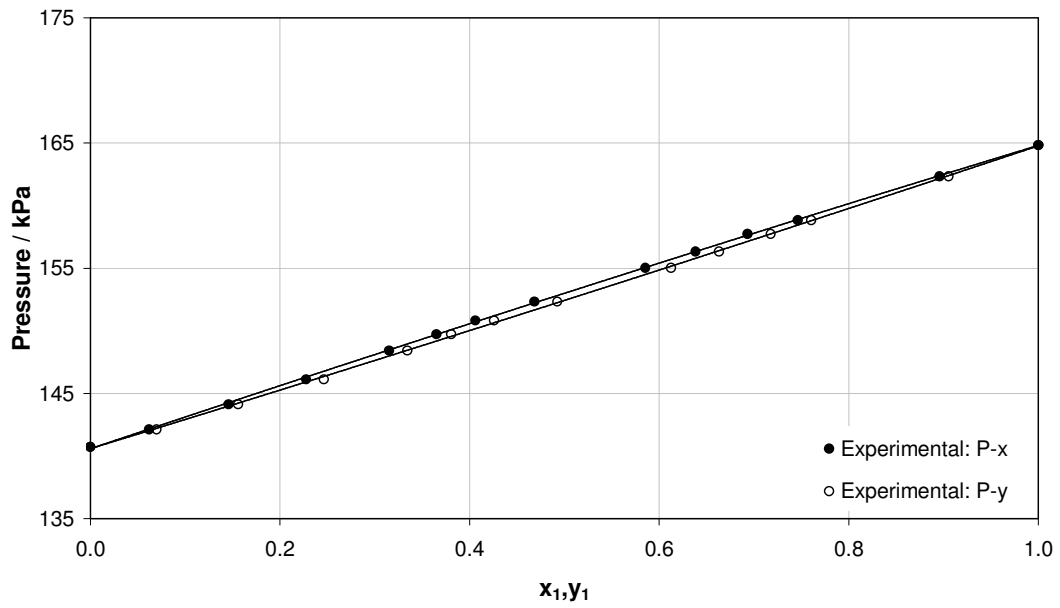


Figure 6-15: P-x-y diagram for the system of 1-hexene (1) + n-hexane (2) at 80°C

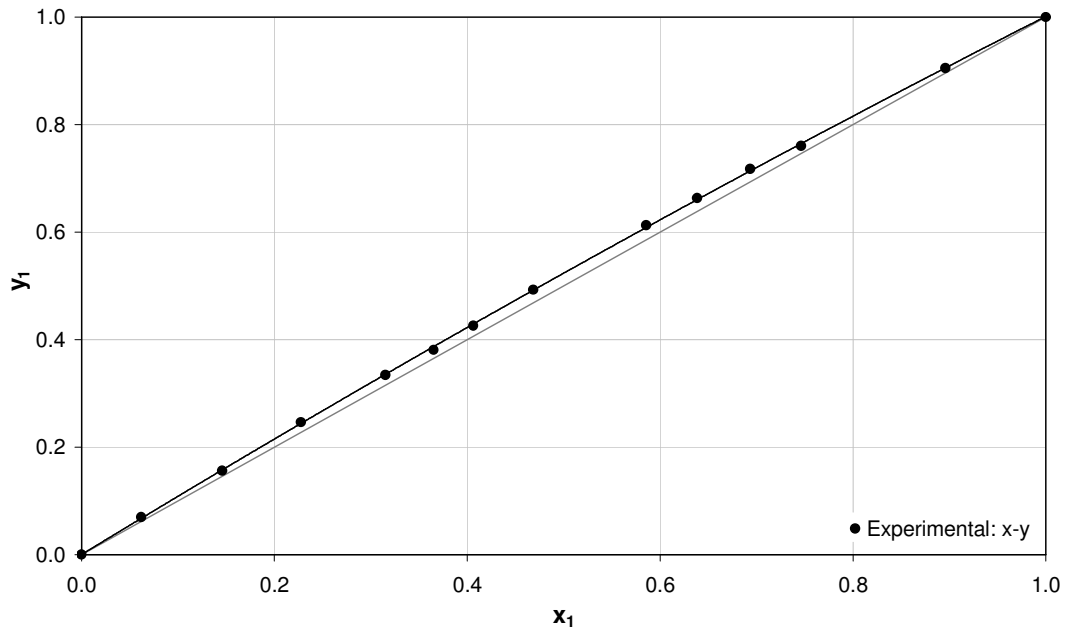


Figure 6-16: x-y diagram for system of 1-hexene (1) + n-Hexane (2) system at 80°C

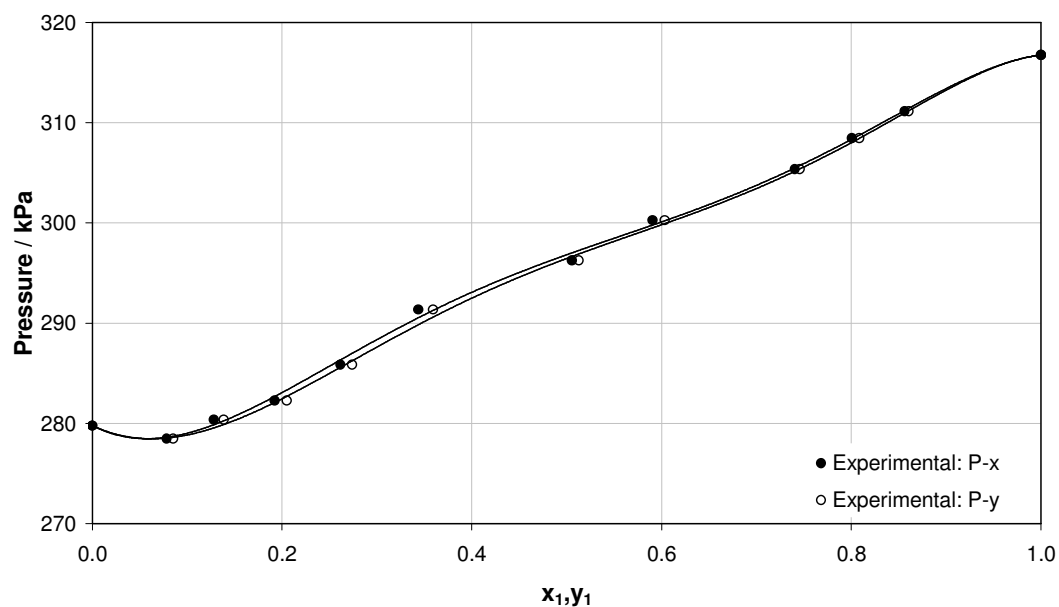


Figure 6-17: P-x-y diagram for the system of 1-hexene (1) + n-hexane (2) at 105°C

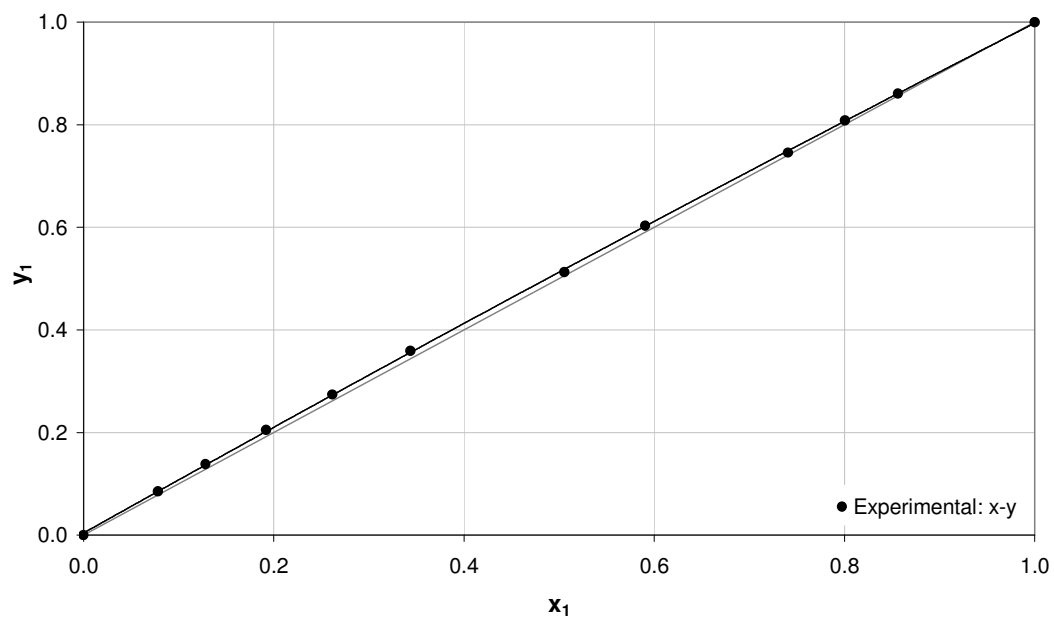


Figure 6-18: x-y diagram for the system of 1-hexene (1) + n-hexane (2) at 105°C

6.3 VLE measurements for 2-methyl-2-pentene (1) + n-hexane (2) systems

Isothermal VLE data were obtained for this system at 55°C, 80°C and 105°C all of which have not been previously measured. The data are listed in Table 6-7 below and are presented in Figures 6-19 to 6-24. Best fit lines are drawn through experimental data points to illustrate the trend.

Table 6-7: Isothermal data for 2-methyl-2-pentene (1) + n-hexane (2) systems

T = 55°C			T = 80°C			T = 105°C		
P _{EXP} (kPa)	x ₁	y ₁	P _{EXP} (kPa)	x ₁	y ₁	P _{EXP} (kPa)	x ₁	y ₁
64.46	0.000	0.000	140.73	0.000	0.000	279.78	0.000	0.000
64.76	0.069	0.074	141.13	0.070	0.073	279.78	0.072	0.073
65.06	0.146	0.152	141.33	0.147	0.152	282.78	0.146	0.161
65.36	0.220	0.228	141.93	0.224	0.233	287.08	0.221	0.236
65.76	0.297	0.318	142.63	0.317	0.317	287.18	0.297	0.307
65.96	0.364	0.383	143.33	0.372	0.382	287.28	0.373	0.384
66.16	0.547	0.553	144.83	0.547	0.557	287.28	0.549	0.555
66.26	0.612	0.620	145.03	0.616	0.622	287.28	0.616	0.623
66.46	0.698	0.704	145.33	0.700	0.706	287.37	0.700	0.706
66.56	0.774	0.779	145.73	0.776	0.781	287.37	0.776	0.780
66.66	0.841	0.843	146.13	0.842	0.845	287.47	0.841	0.845
66.86	0.909	0.911	147.83	0.909	0.911	287.77	0.912	0.912
67.16	1.000	1.000	149.23	1.000	1.000	292.77	1.000	1.000

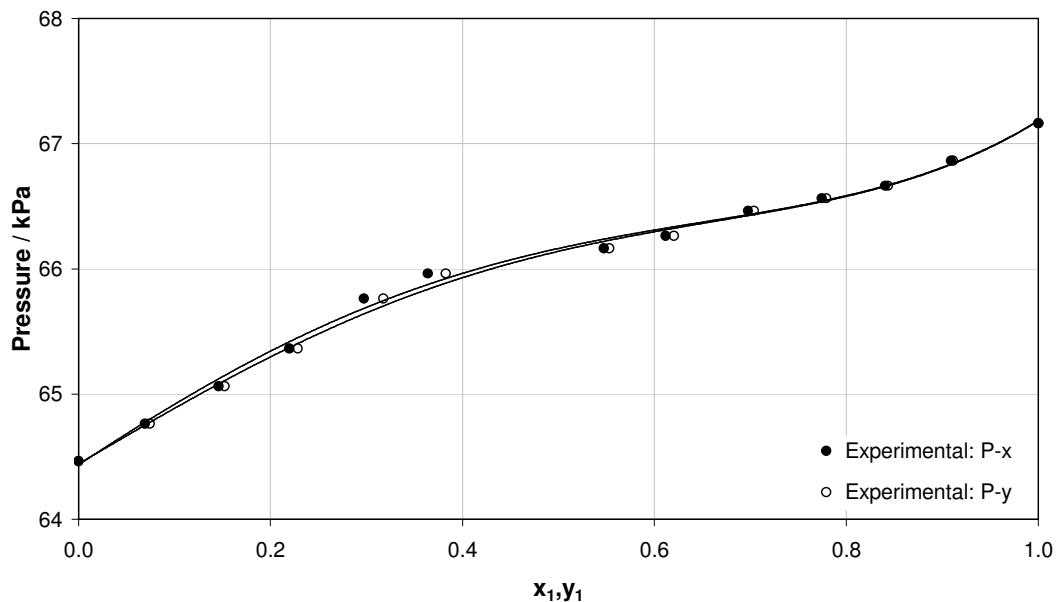


Figure 6-19: P- x-y diagram for the system 2-methyl-2-pentene (1) + n-hexane (2) at 55°C

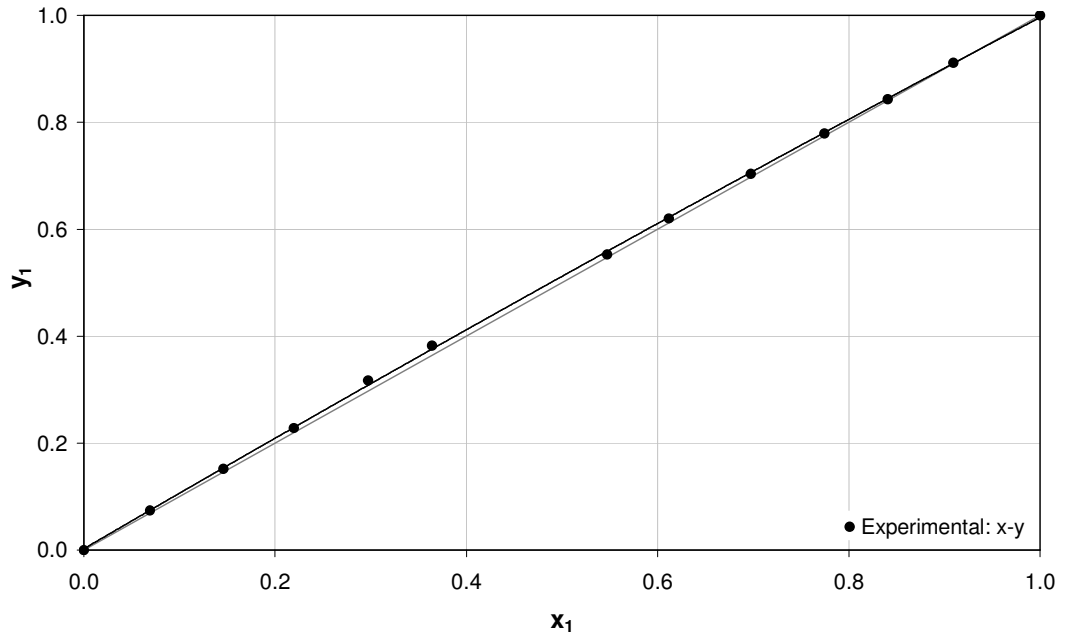


Figure 6-20: x-y diagram for the system 2-methyl-2-pentene (1) + n-hexane (2) at 55°C

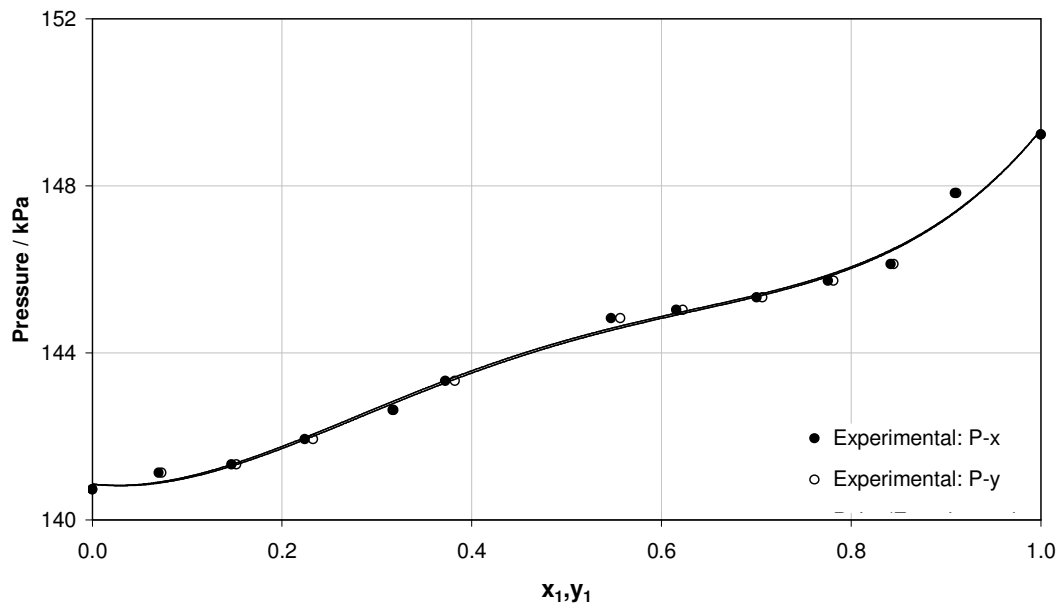


Figure 6-21: P- x-y diagram for the system 2-methyl-2-pentene (1) + n-hexane (2) at 80°C

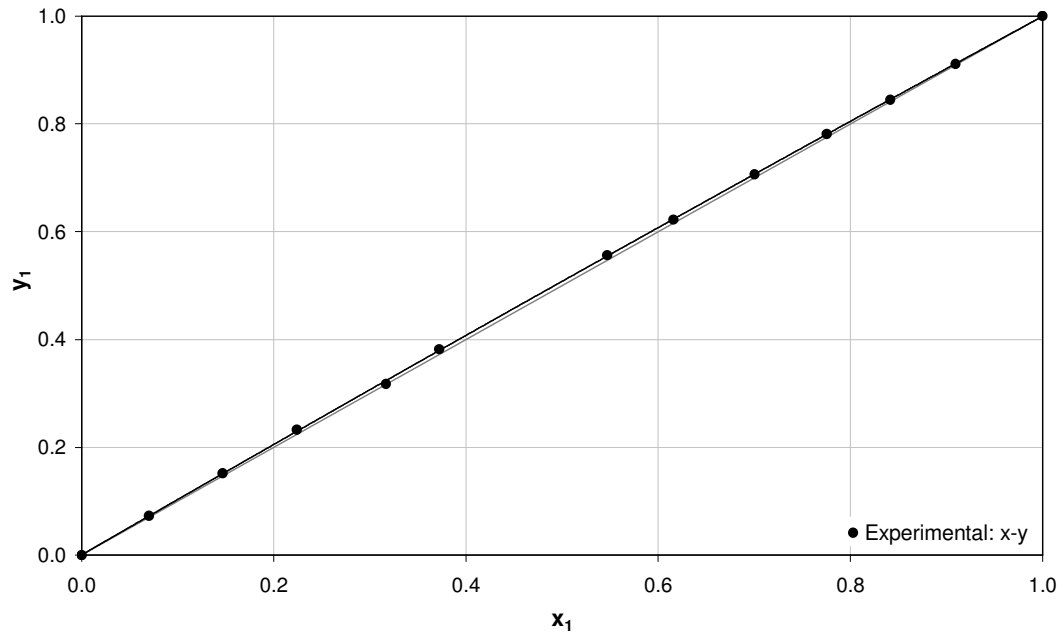


Figure 6-22: x-y diagram for the system 2-methyl-2-pentene (1) + n-hexane (2) at 80°C

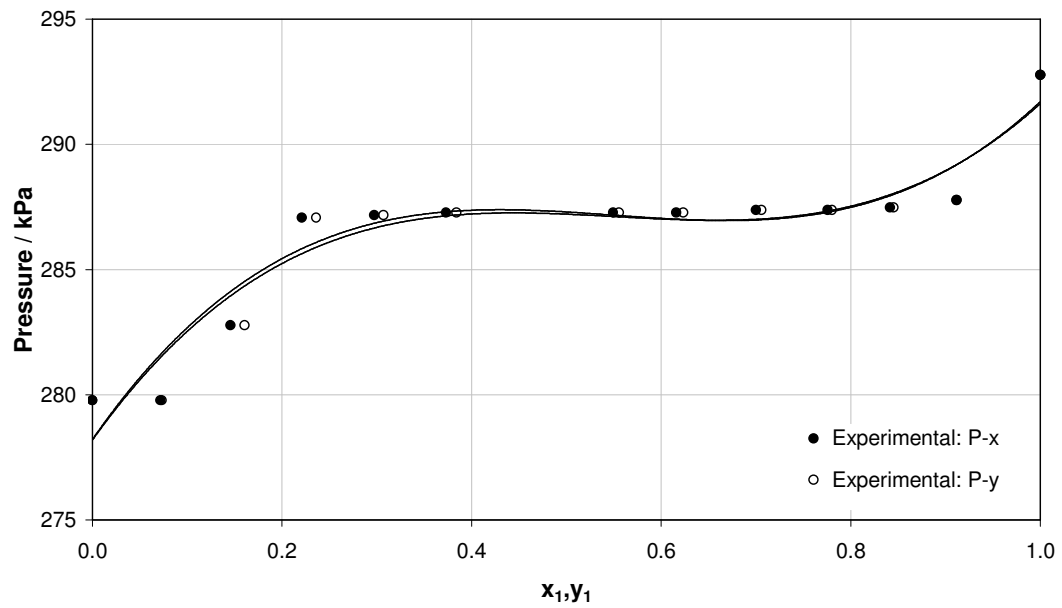


Figure 6-23: P- x-y diagram for the system 2-methyl-2-pentene (1) + n-hexane (2) at 105°C

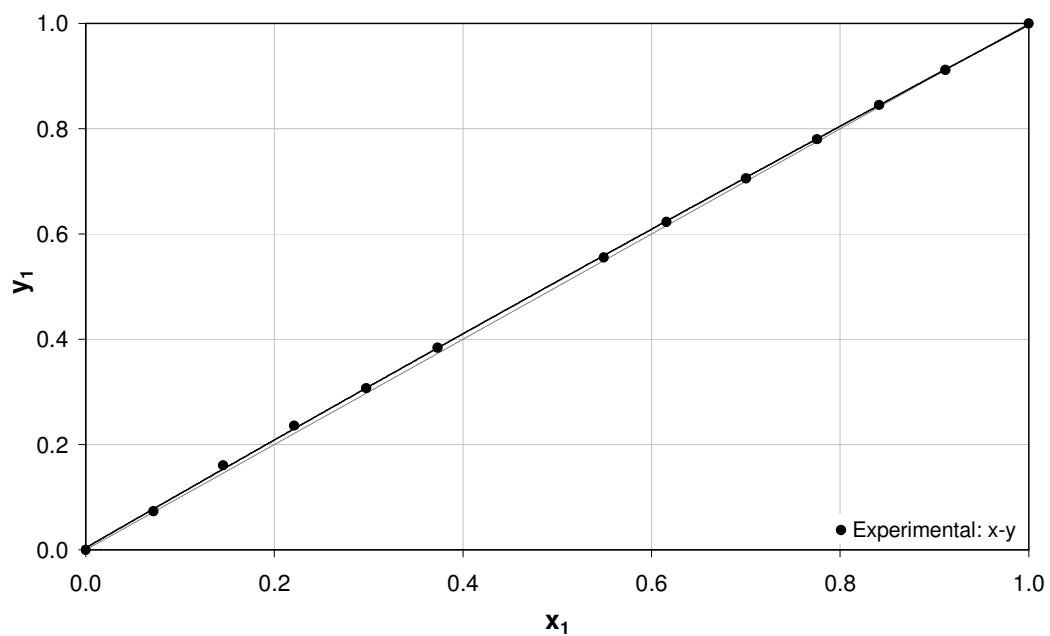


Figure 6-24: x-y diagram for the system 2-methyl-2-pentene (1) + n-hexane (2) at 105°C

6.4 VLE measurements for n-methyl-2-pyrrolidone (1) + 1-hexene (2) systems

Previously unmeasured isobaric VLE data were obtained for this system at 45 kPa, 80 kPa and 100 kPa. The data are listed in Table 6-8 below and are presented in Figures 6-25 to 6-30.

Table 6-8: Isobaric data for the systems of n-methyl-2-pyrrolidone (1) + 1-hexene (2)

P = 45 kPa			P = 80 kPa			P = 100 kPa		
T _{EXP} (°C)	x ₁	y ₁	T _{EXP} (°C)	x ₁	y ₁	T _{EXP} (°C)	x ₁	y ₁
40.24	0.000	0.000	63.44	0.000	0.000	63.44	0.000	0.000
43.32	0.212	0.003	60.63	0.210	0.005	67.91	0.210	0.005
43.72	0.270	0.003	61.14	0.257	0.005	68.47	0.249	0.005
44.11	0.310	0.003	61.69	0.298	0.005	69.09	0.296	0.006
44.69	0.428	0.003	62.50	0.361	0.005	69.86	0.332	0.006
47.72	0.655	0.004	67.68	0.557	0.008	79.59	0.408	0.012
52.69	0.707	0.007	97.19	0.883	0.057	107.72	0.886	0.089
93.19	0.944	0.069	112.60	0.919	0.115	201.93	1.000	1.000
172.55	1.000	1.000	193.29	1.000	1.000			

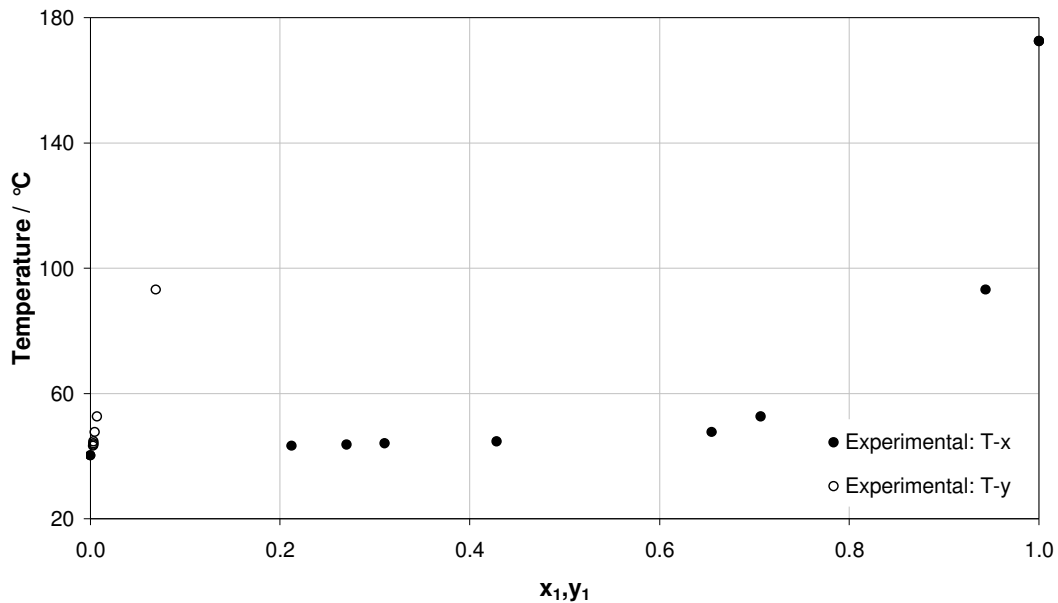


Figure 6-25: T- x-y diagram for the system n-methyl-2-pyrrolidone (1) + 1-hexene (2) at 45 kPa

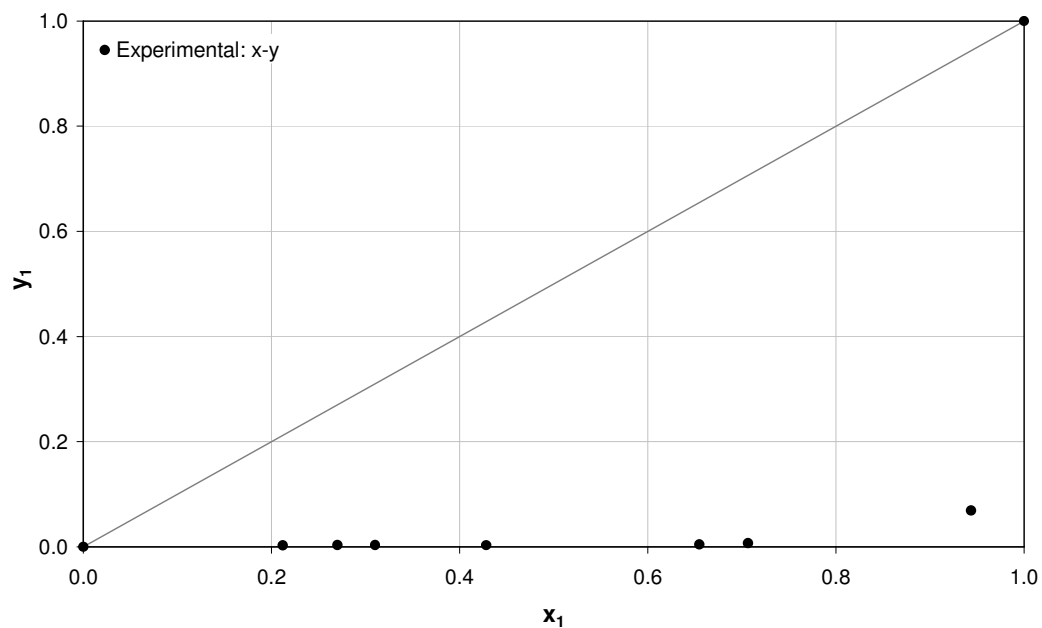


Figure 6-26: x-y diagram for the system n-methyl-2-pyrrolidone (1) + 1-hexene (2) at 45 kPa

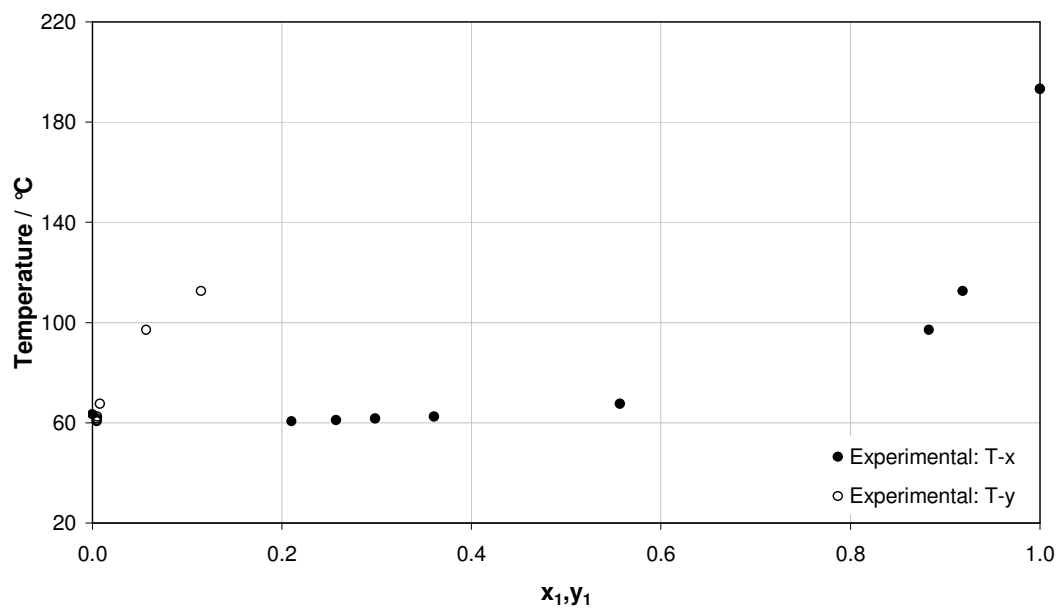


Figure 6-27: T- x-y diagram for the system n-methyl-2-pyrrolidone (1) + 1-hexene (2) at 80 kPa

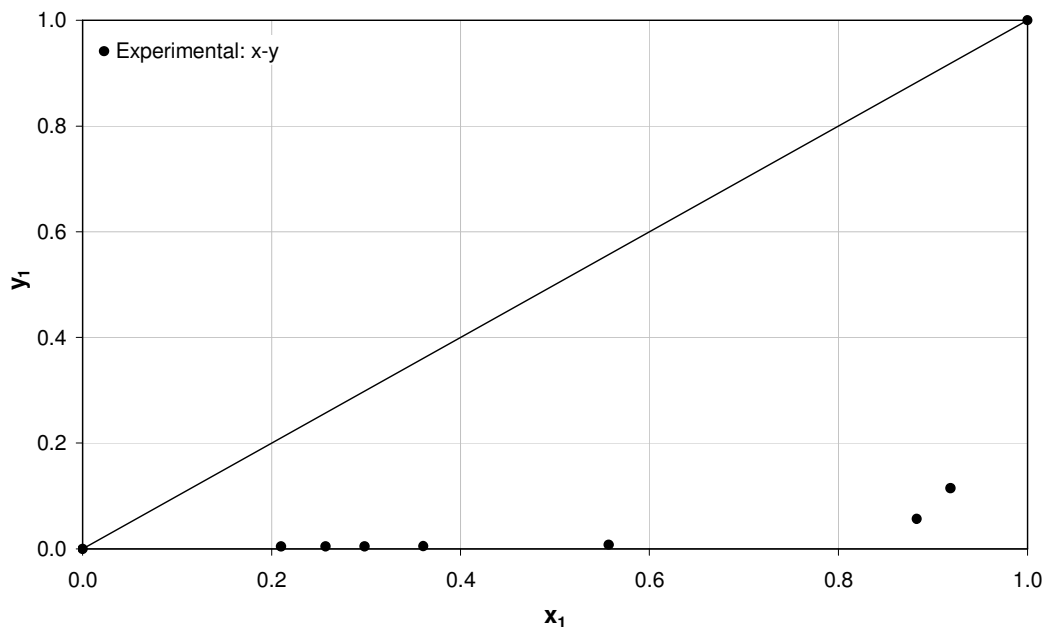


Figure 6-28: x-y diagram for the system n-methyl-2-pyrrolidone (1) + 1-hexene (2) at 80 kPa

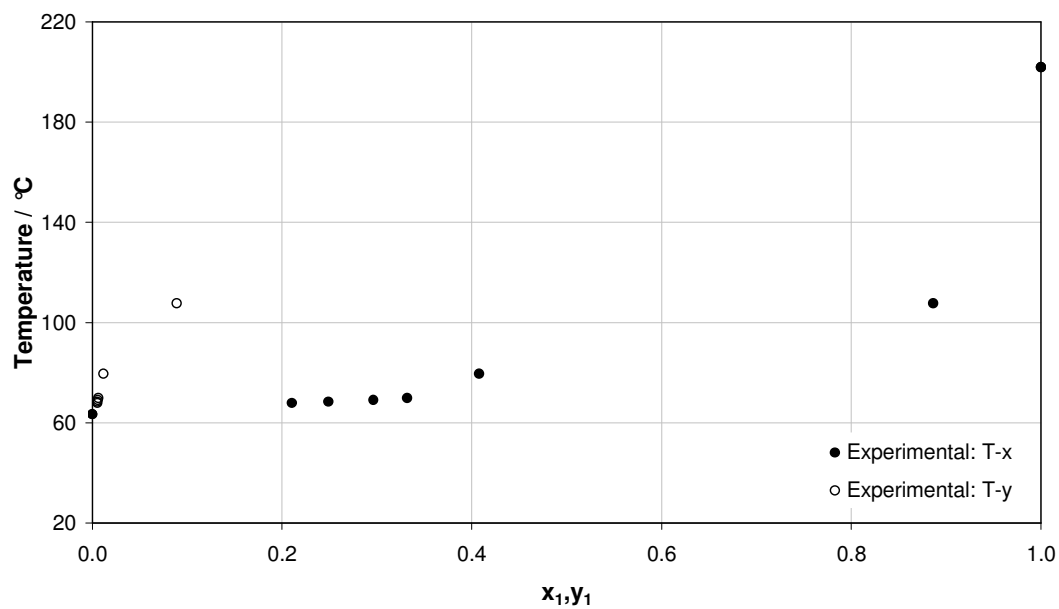


Figure 6-29: T- x-y diagram for the system n-methyl-2-pyrrolidone (1) + 1-hexene (2) at 100 kPa

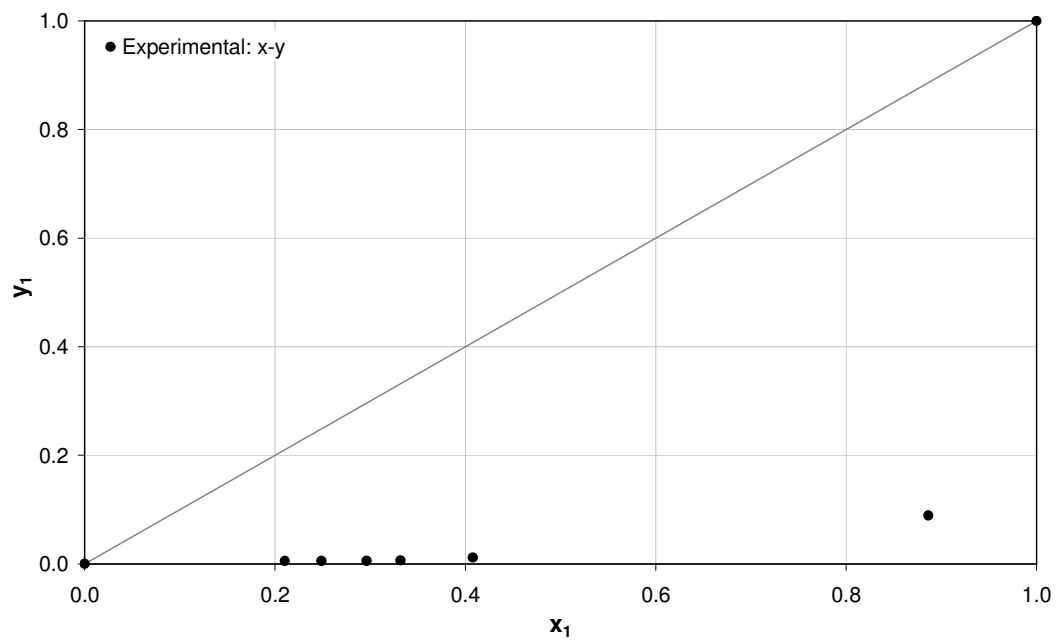


Figure 6-30: x-y diagram for the system n-methyl-2-pyrrolidone (1) + 1-hexene (2) at 100 kPa

CHAPTER SEVEN

DISCUSSION

This chapter discusses the experimental results presented in Chapter six and the analysis thereof. The experimental results that formed the aim of this investigation were:

- Isothermal data for the system of 1-hexene + n-hexane at 55 °C , 80 °C and 105 °C
- Isothermal data for the system of 2-methyl-2-pentene + n-hexane at 55 °C , 80 °C and 105 °C
- Isobaric data for the system of n-methyl-2-pyrrolidone + 1-hexene at 45 kPa, 80 kPa and 100 kPa

The analysis of the data is done to evaluate the quality of the data in the form of data reduction and consistency tests.

7.1 Chemicals used in this investigation

It is extremely important that chemicals used in VLE experiments be of high quality and purity to allow for reliable results. The chemicals used in this investigation and their measured GC purities are presented in Table 7-1. The refractive indices of the chemicals available in literature are presented together with the measured values. The chemicals did not require further purification.

Table 7-1: Purities of chemicals used in this study

CHEMICAL	SUPPLIER	MINIMUM ASSAY MASS%*	GC PEAK AREA %	REFRACTIVE INDEX	
				Measured**	Literature**
1-hexene	Merck	≥ 96	100	1.386	1.3751 ^a , 1.3852 ^b , 1.3851 ^c
n-hexane	Unilab	96	99.9	1.372	1.3837 ^a , 1.3724 ^c
2-methyl-2-pentene	Fluka	≥ 98	99.4	1.398	1.400 ^d
n-methyl-2-pyrrolidone	Merck	≥ 99.5	100	1.468	1.470 ^d

^a Weast (1985), ^b Wisniak (1996), ^c Hanson (1967), ^d Fluka (2006/2007)

* As stated by supplier, ** Data at 25 °C

Vapour pressure data were obtained for the above chemicals within the operating pressures and temperatures of the particular system being investigated. The results were compared with those calculated using the Antoine equation for all chemicals of the binary systems investigated. The average absolute deviations (AAD) between experimental and calculated temperatures, in the absolute Kelvin scale, are presented in Table 7-2. The formula for AAD is given in Equation 7-1 below, where variable X is either temperature, pressure or composition values.

$$\text{AAD \%} = \frac{\sum \text{abs}\left(\frac{X_{\text{EXP}} - X_{\text{CAL}}}{X_{\text{CAL}}}\right)}{N} \times 100 \quad (7-1)$$

The term N refers to the number of data points.

Table 7-2: AAD percentage between experimental and calculated temperature

CHEMICAL	AAD (T) %
1-hexene	0.059
n-hexane	0.040
2-methyl-2-pentene	0.086
n-methyl-2-pyrrolidone	0.339

The root mean square deviation for each chemical is as follows: 1-hexene – 0.25 °C, n-hexane – 0.18 °C, 2-methyl-2-pentene – 0.36 °C and n-methyl-2-pyrrolidone – 1.34 °C.

Antoine constants using the experimental vapour pressure data points were regressed for using Microsoft Excel with the Solver add-on. These values are tabulated below in Table 7-3 together with the literature Antoine constants for comparison. The experimental constants were based on the number of experimental data points obtained for each chemical.

Table 7-3: Comparison of experimental and literature Antoine constants

CHEMICAL	ANTOINE CONSTANTS		
	EXPERIMENTAL	LITERATURE	
1-hexene	A	11.7029	15.8089
	B	2653.18	2654.81
	C	-45.6	-47.3
n-hexane	A	3.9874	4.00139
	B	1168.870	1170.875
	C	224.887	224.317
2-methyl-2-pentene	A	9.2782	9.3221
	B	2724.59	2725.89
	C	-46.65	-47.64
n-methyl-2-pyrrolidone	A	5.76344	7.54826
	B	1985.44	1979.68
	C	225.615	222.162

7.2 VLE Systems Investigated

VLE measurements were performed on the recirculating still designed for operation at high pressures and temperatures. The description of the apparatus was provided in Chapter four and the experimental procedure in Chapter five. The systems investigated are presented below.

In the subsequent sections AAD percentage for experimental variables are presented. The value presented for AAD percentage for temperature, following from Equation 7-1 above, is the deviation between experimental reading and set value (*System Temperature*). The value presented for AAD percentage for composition is the average deviation between the mole fraction of component 1 and the average of the mole fractions of component 1. This is due to the fact that multiple samples are taken for one data point to ensure reproducibility.

Also presented below are the relative volatilities for the systems investigated. The relative volatility for a binary system can be represented as the ratio of K values of two species (Seader *et al.*, 1998):

$$\alpha_{ij} = \frac{K_i}{K_j} = \frac{y_i/x_i}{y_j/x_j} \quad (7-2)$$

Where K is known as the K value and is widely used in multi-component distillation calculations and, x_i and y_i are the liquid and vapour mole fraction respectively.

The relative volatility is a convenient way of deducing the ease or difficulty of separating two components by distillation (Seader *et al.*, 1998).

7.2.1 1-Hexene (1) + n-Hexane (2) System

The above system was investigated by Kirss *et al.* (1975) at 55 °C and was used as a test system to establish the correct functioning of the equipment and reliability of the equilibrium analysis i.e. temperature, pressure and composition. It can be seen from Figures 6-13 and 6-14 that the experimental data fits the literature trend quite well in both the P-x-y and x-y figures. It was thus confirmed that the experimental procedure and calibrations were accurate to produce reliable data. The systems of 1-hexene and n-hexane at 80 °C and 105 °C have not been previously measured.

The AAD percentage for temperature and composition variable obtained during experimental work are presented in Table 7-4. The pressure was controlled to within ± 0.001 bar of the set pressure. The temperature was maintained to within $\pm 0.1\%$ and repeated composition values were considered precise when they were within $\pm 0.1\%$ of an average. There is a distinct trend in the deviations obtained for the temperature variable as the system temperature increases. This is in agreement with the difficulty experienced in obtaining equilibrium during the 105 °C measurements relative to the other isothermal systems.

Table 7-4: AAD percentage of temperature and composition data for the systems of 1-hexene (1) + n-hexane (2)

System Temperature	AAD %	AAD %
	Temperature	Composition
55 °C	0.0009	0.26
80 °C	0.0031	0.22
105 °C	0.0286	0.26

This system displayed ideal behaviour due to their close boiling points. This is also presented in Table 7-5 as the relative volatilities approach one and is illustrated in the x-y diagrams, Figures 6-14, 6-16, 6-18 as the data lie close to the $x = y$ line. In the publication of Lei *et al.* (2007), 1-hexene with n-hexane was investigated at 50 °C and the system displayed a similar trend to the x-y figures presented here, where the x-y data lies close to the $x = y$ line. It is therefore clear

that in order to separate a system of this nature simple distillation will not be economical. Main forms of separation considered for this type of system include extraction with high pressure CO₂, adsorption, liquid-liquid extraction, membrane/extraction hybrid and extractive distillation (Lei *et al.*, 2007). Extractive distillation is simplest and is adequate enough to handle a large feedstock. However it requires the addition of a third component, an entrainer, which alters the relative volatility of one of the components thus allowing separation.

The study of this system is of particular interest to hydrocarbon processing as it represents the problem experienced with many close boiling systems. Lei *et al.* (2006) compare this system with the separation of olefins and paraffins which is difficult and expensive to separate by traditional distillation. In their investigation, olefins and paraffins are represented by 1-hexene and n-hexane respectively due to the consistent separation mechanism and 1-hexene is considered a high value-added product in industry. Their investigation of ionic liquids and liquid solvents as entrainers alters the relative volatilities of paraffins to olefins. A common entrainer used is the polar solvent n-methyl-2-pyrrolidone and will be discussed in Section 7.2.3.

Table 7-5: Relative volatilities of 1-hexene (1) + n-hexane (2) systems

T = 55°C			T = 80°C			T = 105°C		
P _{EXP} / kPa	x ₁	α ₁₂	P _{EXP} / kPa	x ₁	α ₁₂	P _{EXP} / kPa	x ₁	α ₁₂
64.46	0		140.73	0		316.76	1	
65.06	0.039	1.215	142.13	0.062	1.139	311.17	0.856	1.042
65.36	0.068	1.192	144.13	0.146	1.081	308.47	0.801	1.052
65.96	0.100	1.193	146.13	0.228	1.105	305.37	0.74	1.032
67.16	0.184	1.165	148.43	0.315	1.091	300.27	0.591	1.051
67.91	0.231	1.176	149.73	0.365	1.071	296.27	0.506	1.028
68.26	0.263	1.190	150.83	0.406	1.086	291.37	0.344	1.068
69.36	0.343	1.179	152.33	0.468	1.105	285.88	0.261	1.069
70.26	0.421	1.134	155.03	0.585	1.124	282.28	0.192	1.085
71.46	0.523	1.156	156.33	0.638	1.116	280.38	0.128	1.100
72.26	0.591	1.163	157.73	0.693	1.128	278.48	0.078	1.098
72.86	0.642	1.117	158.83	0.746	1.078	279.78	0	
73.96	0.728	1.177	162.33	0.896	1.106			
74.56	0.778	1.163	164.82	1				
75.96	0.903	1.203						
75.06	0.826	1.148						
76.66	1							

7.2.2 2-Methyl-2-pentene (1) + n-Hexane (2) System

This system was investigated at 55 °C, 80 °C and 105 °C. Similar to the system of 1-hexene + n-hexane, this system displays ideal behaviour as can be seen from the relative volatilities in Table 7-7 and Figures 6-20, 6-22 and 6-24. The P-x-y figures (Figures 6-19, 6-21 and 6-23) displays an ‘S’ shape which is more pronounced at the higher temperatures. The pressure was controlled to within ± 0.001 bar of the set pressure. The temperature was maintained to within $\pm 0.1\%$ and repeated compositions values were considered precise when they were within $\pm 0.1\%$ of an average. These values are presented in Table 7-6 below. There is a definite increase in the AAD percentage of both temperature and composition measurements as the temperature of the systems increases. Although these values are quiet small and still within the defined tolerances, it is important to note that stability of equilibrium, like for the system of 1-hexene and n-hexane, is affected at higher temperatures and pressures. These deviations can therefore explain the prominent “S” shaped curves as the temperature increases.

The boiling temperature difference between 2-methyl-2-pentene and n-hexane is 1.4 °C, similar to the system of 1-hexene with n-hexane presented above, and will also be difficult to separate.

Table 7-6: AAD percentage of temperature and composition data for the systems of 2-methyl-2-pentene (1) + n-hexane (2)

System Temperature	AAD %	AAD %
	Temperature	Composition
55 °C	0.0182	0.14
80 °C	0.0125	0.13
105 °C	0.0500	0.19

The data presented for the isothermal systems of 2-methyl-2-pentene (1) + n-hexane (2) have not been previously measured.

2-methyl-2-pentene and n-hexane form part of a mixture of chemicals present in the exit streams of petrochemical processes. The binary interactions of the constituents of such streams are valuable in the design and selection of the type of separation process.

In the publication of Wentik *et al.* (2007) a model is developed to describe the VLE of the ternary system 1-hexene with n-hexane and 2-methyl-1-pentene which is used to represent a Fischer-Tropsch stream. Wentik *et al.* (2007) found that such a mixture behaves ideally in the absence of a solvent. Although the 2-methyl-1-pentene is different in structure to 2-methyl-2-

pentene the results obtained in this investigation are in agreement with that described in Wentik *et al.* (2007); mainly the ideality of the system with relative volatilities close to one.

As highlighted above for ideal systems; separation is achieved by addition of a polar solvent and in the case of Wentik *et al.* (2007) the choice of distillation is reactive extractive distillation. Common to both the publications of Lei *et al.* (2006) and Wentik *et al.* (2007) is the difficulty in the choice of entrainer which must have a high selectivity and high capacity for a chemical in systems of relative volatilities close to unity. However, unlike the case of 1-hexene and n-hexane the separation considered in Wentik *et al.* (2007) is reactive extractive distillation since in extractive distillation the isomers respond in a similar manner to the solvent leaving the relative volatilities unchanged.

2-methyl-2-pentene is used in the synthesis of ether which is an important process in the oil industry due to its use as an octane enhancer in gasoline (Streicher *et al.*, 1995). This use for ether, highlighted in Streicher *et al.* (1995) was mainly due to environmental reasons as it reduces CO and unburned hydrocarbon emissions from engine exhaust gases. Essentially, ethers are obtained by the combination of an iso-olefin (2-methyl-2-pentene) with an alcohol.

Table 7-7: Relative volatilities of 2-methyl-2-pentene (1) + n-hexane (2) systems

T = 55°C			T = 80°C			T = 105°C		
P _{EXP} / kPa	x ₁	α ₁₂	P _{EXP} / kPa	x ₁	α ₁₂	P _{EXP} / kPa	x ₁	α ₁₂
64.46	0.000		140.73	0.000		279.78	0.000	
64.76	0.069	1.078	141.13	0.070	1.046	279.78	0.072	1.021
65.06	0.146	1.051	141.33	0.147	1.041	282.78	0.146	1.122
65.36	0.220	1.052	141.93	0.224	1.051	287.08	0.221	1.089
65.76	0.297	1.099	142.63	0.317	1.003	287.18	0.297	1.048
65.96	0.364	1.083	143.33	0.372	1.044	287.28	0.373	1.047
66.16	0.547	1.024	144.83	0.547	1.040	287.28	0.549	1.024
66.26	0.612	1.038	145.03	0.616	1.029	287.28	0.616	1.032
66.46	0.698	1.030	145.33	0.700	1.030	287.37	0.700	1.027
66.56	0.774	1.027	145.73	0.776	1.034	287.37	0.776	1.028
66.66	0.841	1.021	146.13	0.842	1.024	287.47	0.841	1.029
66.86	0.909	1.025	147.83	0.909	1.019	287.77	0.912	1.000
67.16	1.000		149.23	1.000		292.77	1.000	

7.2.3 n-Methyl-2-pyrrolidone (1) + 1-Hexene (2) System

This system was investigated at 45 kPa, 80 kPa and 100 kPa. The system is highly non-ideal as can be seen from the relative volatilities of 1-hexene (2) to n-methyl-2-pyrrolidone (1) in Table 7-9 and Figures 6-26, 6-28 and 6-30. The pressure was controlled to within ± 0.001 bar of the set pressure. The temperature was maintained to within $\pm 0.1\%$ of an average at each data point and repeated compositions values were considered precise if they were within $\pm 0.1\%$ of an average. The actual deviations are presented below in Table 7-8.

Table 7-8: AAD percentage of composition data for the systems of n-methyl-2-pyrrolidone (1) + 1-hexene (2)

System Pressure	AAD % Composition
40 kPa	0.23
80 kPa	0.51
100 kPa	0.43

Difficulty was experienced in the boiling of n-methyl-2-pyrrolidone to obtain a vapour pressure plot, Figure 6-12. Only four reliable points were established. A yellowish tint of n-methyl-2-pyrrolidone was also observed during operation. This did not affect the purity of the pure component or the system being investigated as the composition analysis of the n-methyl-2-pyrrolidone did not change. The possible causes could have been breakage of graphite packing from the boiling chamber into the chemical or contamination of apparatus from previous use. To confirm either of these possibilities two options were investigated. Firstly a small piece of graphite was placed in a conical flask of pure n-methyl-2-pyrrolidone and boiled at atmosphere with continuous stirring for several hours. This had no effect on the colour or purity of n-methyl-2-pyrrolidone. Secondly, several samples of n-methyl-2-pyrrolidone were analysed from the still over the course of a few days. This was done after cleaning and rinsing the still with acetone. Although, the colour did change slightly it had no effect on the purity of n-methyl-2-pyrrolidone. A similar observation was made by Kniesl *et al.* (1989) during the boiling of the chemical tetramethylurea where repeated boiling showed identical results of the recycled material. Tetramethylurea has a similar boiling point and dipole moment to n-methyl-2-pyrrolidone.

The AAD percentage between the measured and literature value (Antoine equation) obtained for temperature is 0.339 (Table 7-2) which is significantly higher than the deviations obtained for the other chemicals.

One of the possible reasons for this phenomenon is described in the publication of Kniesl *et al.* (1989) who address the lack of understanding with regard to high boiling polar compounds for use in ebulliometry and offers a correlation to establish whether a compound is suitable for ebulliometric study.

The correlation is given by

$$\log_{10} \left(\frac{dT}{dP} \right)_{\min} = -6.22 + 0.61\mu + 0.75\chi \quad (7-2)$$

where T is the temperature in Kelvin, P is power input in Watts and μ is the dipole moment in Debye. The term χ is the degree and type of molecular association within the fluid, with values of 0, 1 and 2 for hydrocarbons, compounds with hydrogen bonding and compounds capable of hydrogen bonding respectively. For a more detailed breakdown of these compounds the reader is referred to Kniesl *et al.* (1989).

Kniesl *et al.* (1989) found that the slope, $\left(\frac{dT}{dP} \right)$ of the curve of temperature versus power input, which is the response of the ebullimeter to a fluid, depends on purity of chemical as well as fluid property in particular. These fluid properties include the dipole moment and molecular association of the compound. Their investigation involved fourteen chemicals including the high boiling n-methyl-2-pyrrolidone which according to them is unsuitable for ebullimeter operation due to the high observed value for $\left(\frac{dT}{dP} \right)$ of $959 \mu\text{KW}^{-1}$. Although the results of the system of n-methyl-2-pyrrolidone (1) with 1-hexene (2) are consistent, the above findings of Kniesl *et al.* (1989) describe the reason for the difficulty in operation experienced during the vapour pressure experiments for n-methyl-2-pyrrolidone. Kniesl *et al.* (1989) state that values larger than $300 \mu\text{KW}^{-1}$ lead to reduced accuracy in operation or even impossibility of operation. Great difficulty was experienced in acquiring reliable data at higher pressure systems i.e. at 100 kPa. A high degree of flashing occurred in the reboiler due to the large relative volatilities. The difference in normal boiling points of n-methyl-2-pyrrolidone and 1-hexene is $133 \text{ }^\circ\text{C}$, and as described in Rogalski and Malanowski (1980) in their investigation of n-methyl-2-pyrrolidone and cyclohexane, having a boiling difference of 120 K, the determination of VLE parameters of such systems is “difficult” and “unreliable” regardless of the type of apparatus.

This is consistent with the work of Wisniewska *et al.* (1995), who in their development of a VLE apparatus to function at pressures up to 3 MPa found that for systems with a high difference in boiling points, the stability of the operation of the still worsened.

The purpose of this system, like other binary VLE data, assists in the determination of VLE data of multi-component systems. In particular, close boiling or azeotropic systems that are separated using extractive distillation with the addition of an entrainer, n-methyl-2-pyrrolidone. n-Methyl-2-pyrrolidone is the polar solvent of choice for use in extractive distillation as an entrainer. An entrainer, as mentioned earlier, is used to change the relative volatilities of close boiling or azeotropic systems, similar to 1-hexene with n-hexane. Fischer and Gmehling (1996) highlight the many attributes of NMP, but some worth noting include its selective affinity towards unsaturated hydrocarbons and in terms of physical and chemical properties, its high polarity, low volatility and thermal and chemical stability.

The mechanism that this type of separation is based on is highlighted in Lei *et al.* (2006). For some time ionic liquids were preferred for use as an entrainer and the mechanism employed in extractive distillation is based on the different mobility of the electron cloud for C-C and C=C bonds. This gives different interactions between solvent and the component to be separated. The mobility of the C=C bond is much larger than C-C bond lending itself to be easily polarised by polar solvent. n-Hexane is therefore obtained as the overhead product (light component), and 1-hexene (heavy component) and the solvent obtained as the bottoms product. It is therefore necessary to ascertain how 1-hexene and n-methyl-2-pyrrolidone (polar solvent) behave in order to separate them.

It should be noted that the choice and use of solvents has over the recent years been given great consideration due their adverse effects on the environment. According to Allen and Shonnard (2002) in 1991 the production of 25 of the most common solvents was more than 26 million tons per year. In 1994, 5 of the top 10 chemicals released or disposed of were solvents as recorded by the toxic release inventory (TRI). This estimated to approximately 687 million pounds which is 27 percent of the total quantity of TRI chemicals released or disposed in that year. The numbers are overwhelming and it is therefore imperative that these systems are investigated and where possible, alternatives are found.

Table 7-9: Relative volatilities of n-methyl-2-pyrrolidone (1) + 1-hexene (2) systems

P = 45 kPa			P = 80 kPa			P = 100 kPa		
T _{EXP} / °C	x ₁	α ₂₁	T _{EXP} / °C	x ₁	α ₂₁	T _{EXP} / °C	x ₁	α ₂₁
40.24	0.000		63.44	0.000		63.44	0.000	
43.32	0.212	96.915	60.63	0.210	58.430	67.91	0.210	48.839
43.72	0.270	112.221	61.14	0.257	72.633	68.47	0.249	63.610
44.11	0.310	136.054	61.69	0.298	91.115	69.09	0.296	72.181
44.69	0.428	228.842	62.50	0.361	109.239	69.86	0.332	77.579
47.72	0.655	419.880	67.68	0.557	154.799	79.59	0.408	58.207
52.69	0.707	342.570	97.19	0.883	124.999	107.72	0.886	79.866
93.19	0.944	226.722	112.60	0.919	87.054	201.93	1.000	
172.55	1.000		193.29	1.000				

7.3 Data Reduction

The data reduction for the measured systems was performed employing three programs:

- The isothermal data were reduced by use of the Orbey and Sandler (1996) programs.
- The isobaric data were reduced by use of Microsoft Excel work sheets and Aspen simulation program

The isothermal data regression is summarised in the Table 7-10 below.

Table 7-10: Summary of isothermal data regression

EQUATION OF STATE		METHOD	GIBBS EXCESS		
TYPE	NAME		ENERGY MODELS	MIXING RULE	PROGRAM
Cubic	PRSV	Direct	NRTL Wilson Van Laar	Wong Sandler Mixing Rules	Orbey and Sandler (1996)

The regression process initially requires pure component kappa values for the PRSV equation of state which were calculated using a specific program. The user inputs experimental vapour pressure data and an optimum *kappa* (κ) value is calculated. The κ values were calculated for n-methyl-2-pyrrolidone using the KOPT program by Orbey and Sandler (1996) and can be found in Table B1, Appendix B.

The isothermal systems (1-hexene + n-hexane and 2-methyl-2-pentene + n-hexane) were regressed using the phi-phi approach (Equation of state approach) using the PRSV equation of state and Wong-Sandler mixing rules. Due to the complexity of the calculations, a computer program (Orbey and Sandler, 1996) was used to obtain reliable results.

Significant errors occurred in the calculation of the saturated pressures by the program and as a result had to be omitted during the modelling of the systems. The experimental saturated vapour pressures were included after the system was modelled for graphical representation.

The program prompts the user to select an option to either predict VLE data for a system or to fit model parameters for the VLE data entered by the user. Critical properties of components including the κ value in the PRSV equation of state are required by the user. These values for the chemicals used in the binary systems investigated are presented in Table B1, Appendix B.

The critical properties required include the critical temperature, pressure and eccentric factor. The user inputs the number of experimental data points to be reduced and then each experimental data point i.e. vapour and liquid mole fractions of component one and pressure in bar. The program allows the user to choose between several Gibbs excess energy models and then provide an initial estimate for model parameters. In the case of the NRTL, Van Laar and Wilson excess models these parameters are $g_{ij} - g_{ji}$, A_{ij} and Λ_{ij} respectively. The NRTL α parameter is also estimated by the user which is then regressed for by the program. Appropriate NRTL α parameter values were discussed in Chapter two.

The program outputs the calculated vapour phase mole fraction and pressure, as well as the absolute average deviation of vapour phase composition (AAD-y) and pressure (AAD-P) between calculated and experimental values. The equation for the value of AAD is given by Equation 7-1, where X is the pressure or vapour composition variable.

Infinite dilution activity coefficients described in Chapter two were calculated for the isothermal systems using the method highlighted in Maher and Smith (1979) and presented for the systems of 1-hexene with n-hexane and 2-methyl-2-pentene with n-hexane.

The isobaric data regression is summarised in Table 7-11.

Table 7-11: Summary of isobaric data regression

EQUATION OF STATE		METHOD	GIBBS EXCESS ENERGY MODELS	MIXING RULE	PROGRAM
TYPE	NAME				
Virial	Pitzer	Indirect	NRTL	Prausnitz Mixing Rules	Microsoft Excel
			Wilson		
			Van Laar		
Cubic	Redlich-Kwong	Indirect	UNIQUAC	Van der Waals Mixing Rule*	Aspen Simulation Program

* The mixing rule used is given by Equations 7-3 and 7-4. It is a form of the Van der Waals mixing rule

The isobaric data (n-methyl-2-pyrrolidone + 1-hexene) were regressed with the Gamma-Phi approach. The Gamma-Phi approach accounts for the liquid and vapour phase departure from ideality in terms of the activity and fugacity coefficients respectively.

The liquid phase non-ideality was accounted for using Gibbs Excess energy models, in particular NRTL, Wilson and Van Laar for the modelling performed in Microsoft Excel. The pressure range of the systems investigated is within the scope of the Gibbs excess models used. The vapour phase non-ideality was accounted for by the virial equation of state (two term) using the Pitzer correlation with Prausnitz mixing rules.

For the modelling performed using the Aspen simulation program, the property method, UNIQUAC defined by Aspen was chosen to model the data. This property method uses the UNIQUAC Gibbs excess equation to describe the non-ideality of the liquid phase and the Redlich-Kwong equation of state to describe the vapour phase non-ideality.

This particular property method was chosen based on the applicability of the UNIQUAC equation. Mainly, it's ability to describe highly non-ideal solutions consisting of any combination of polar or non-polar compounds.

The Redlich-Kwong EOS can calculate vapour phase thermodynamic properties at low pressures (maximum of 10 bar) where the vapour phase non-ideality is small (Aspen Help Files) and is not recommended for calculating liquid phase properties.

The Redlich-Kwong EOS given in Chapter two uses the following mixing rules as given by Aspen:

$$\sqrt{a} = \sum_i x_i \sqrt{a_i} \quad (7-3)$$

$$b = \sum_i x_i b_i \quad (7-4)$$

where the parameters a and b were defined in Chapter two.

The Aspen simulation program uses four main databanks for vapour-liquid applications consisting of parameter values as well as temperature, pressure and composition limits of data. The databank was developed by using binary VLE data from the Dortmund databank. Each databank is used along with a specific property method. In the case of UNIQU-RK, chosen here, the databank used is VLE_RK, as defined by Aspen. This databank consists of 3600 component pairs.

In the case of the system of NMP with 1-hexene, which is currently unavailable in literature, it can be assumed that initial guess for the parameter values used are obtained from a chemically similar mixture from the chosen databank.

The simulation is done by choosing an appropriate method which was *Data Regression*. A base *property method* is chosen (UNIQU-RK). The components (n-methyl-2-pyrrolidone and 1-hexene) are chosen from the built-in database and simulation specifications are inputted into the necessary forms. The T-x-y data set is also inputted and from the specified list of binary components the order of components (i.e. component 1 and component 2) is defined. On this form the system pressure is also inputted. The data regression can then be run and the results are tabulated including estimated/regressed values as well as experimental values (values inputted by the user). The program also allows the user to choose the option of performing consistency tests.

7.3.1 1-Hexene (1) + n-Hexane (2) System

The model parameters, as well as the average deviation between calculated and experimental vapour composition and pressures are presented in Table 7-15. The best fit models were chosen on the basis of the average absolute deviation of predicted pressure from experimental pressure (δP). The best fit models are presented below (Table 7-12) together with their corresponding δP values.

Table 7-12: Best fit models for the system of 1-hexene (1) + n-hexane (2)

1-hexene (1) + n-hexane (2) systems at	Model	Average δP (kPa)
55 °C	Wilson	0.0733
80 °C	NRTL	0.3394
105 °C	NRTL	1.2255

The absolute average deviation between vapour compositions is also presented in Table 7-14 which were used in the thermodynamic consistency point test. The models in Figures 7-2, 7-4 and 7-6 (x-y plots) fit the experimental data well. It can be seen from the P-x-y plots (Figures 7-1, 7-3 and 7-5) and the pressure deviations (Table 7-15) that the Van Laar model does not give satisfactory results for any of the systems. The pressure values are overestimated in the case of the 80 °C and 105 °C systems. This is most likely due to the experimental pressure values that were obtained with greater error in the higher temperature regions. Although the pressure of the system was controlled to within ± 0.001 bar of the set pressure, the relationship between temperature and pressure is proportional. Table 7-4, above presents the average percentage error of temperature and composition (vapour and liquid mole fraction). It can be seen that for systems at higher temperatures the average percentage error in the temperature stability increases thus affecting pressure.

The NRTL alpha parameter is inputted as an initial guess and the program regresses for it. In the table presented below (Table 7-15) the NRTL α parameter values are equivalent to the initial guess.

The liquid molar volumes (V , $\text{cm}^3 \text{mol}^{-1}$) and second virial coefficients (B , $\text{cm}^3 \text{mol}^{-1}$) of n-hexane used in the data reduction are presented below together with those values in Gierycz *et al.* (1985) in order of increasing temperature (T , °C). The values are not at the same temperature as those investigated but a definite trend is observed confirming the accuracy of the experimental values.

Table 7-13: Liquid molar volumes (V , $\text{cm}^3 \text{mol}^{-1}$) and second virial coefficients (B , $\text{cm}^3 \text{mol}^{-1}$) of n-hexane at different temperatures (T , $^\circ\text{C}$).

	Experimental	Gierycz <i>et al.</i> (1985)	Gierycz <i>et al.</i> (1985)	Experimental	Experimental
T	55	60	70	80	105
V	136.03	138.2	140.4	141.87	148.73
B	-1479.16	-1380	-1280	-1225.94	-1032.17

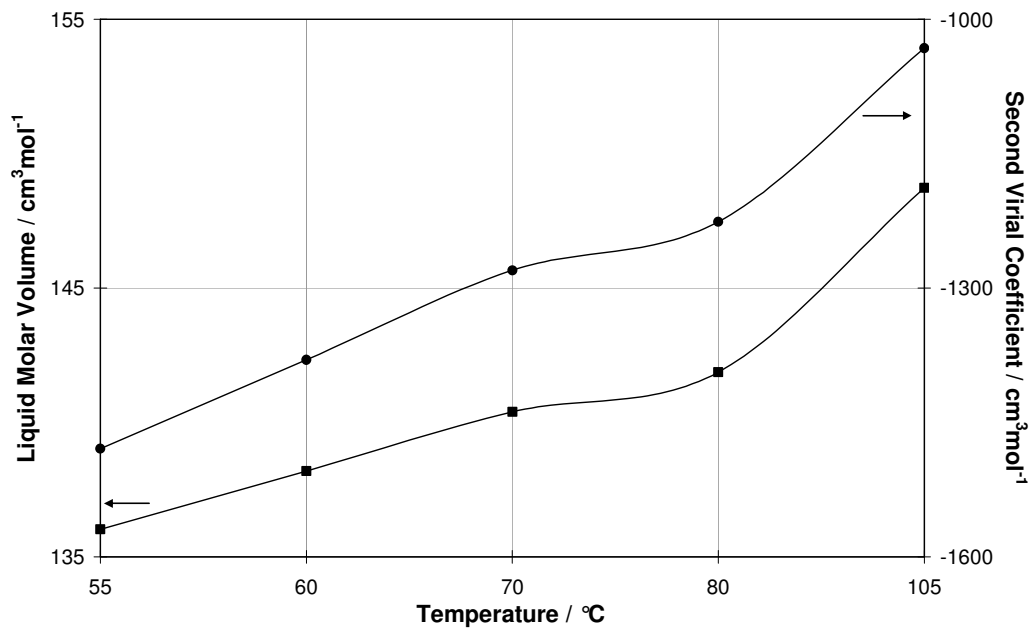


Figure 7-1: Plot of liquid molar volume and second virial coefficients against temperature

Infinite activity coefficients (γ_i^∞), as described in Chapter two, are essential in the design of distillation columns. The infinite activity coefficients are presented in Table 7-14 and the method was described in Chapter two. The plots used in the evaluation of the limiting activity coefficients can be found in Figures C-1 to C-3, Appendix C.

Table 7-14: Infinite activity coefficients for the systems of 1-hexene (1) + n-hexane (2)

Temperature / $^\circ\text{C}$	γ_1^∞	γ_2^∞
55	1.046	0.972
80	0.988	0.98
105	0.584	1.171

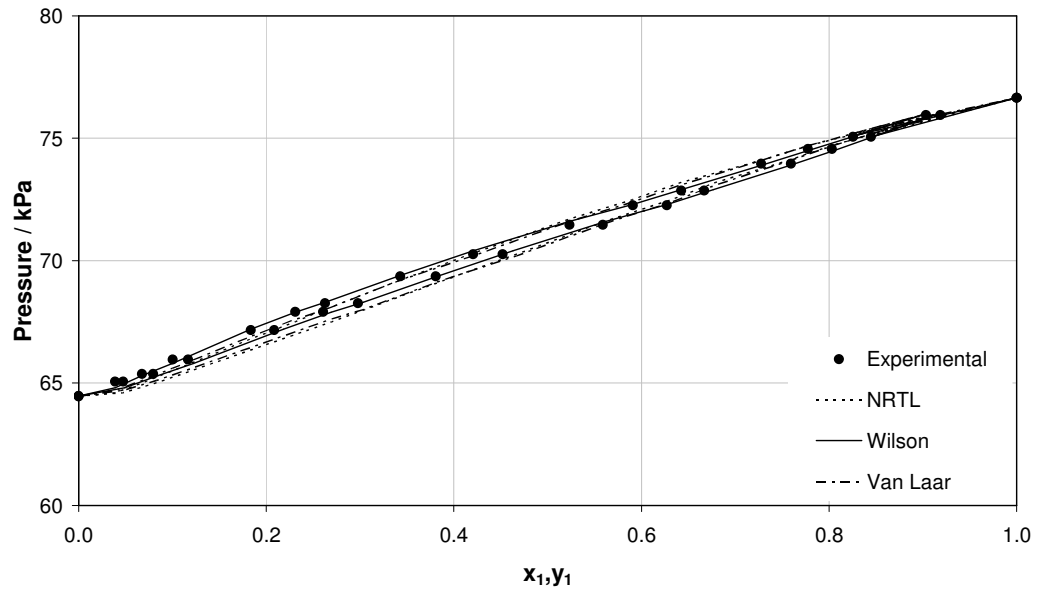


Figure 7-2: NRTL, Wilson and Van Laar model fits to P-x-y diagram of 1-hexene (1) + n-hexane (2) at 55°C

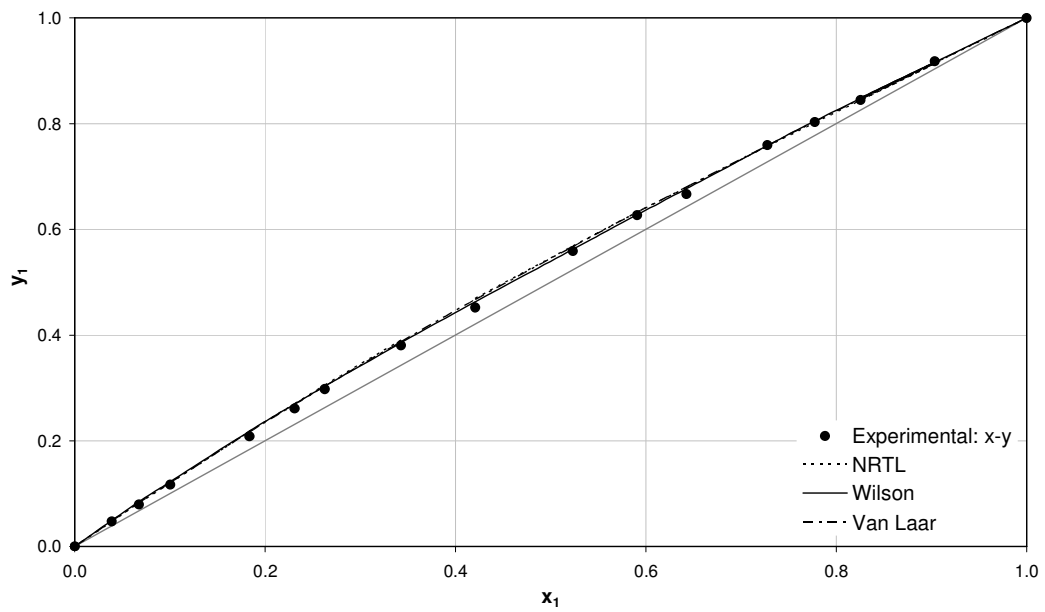


Figure 7-3: NRTL, Wilson and Van Laar model fits to x-y diagram of 1-hexene (1) + n-hexane (2) at 55°C

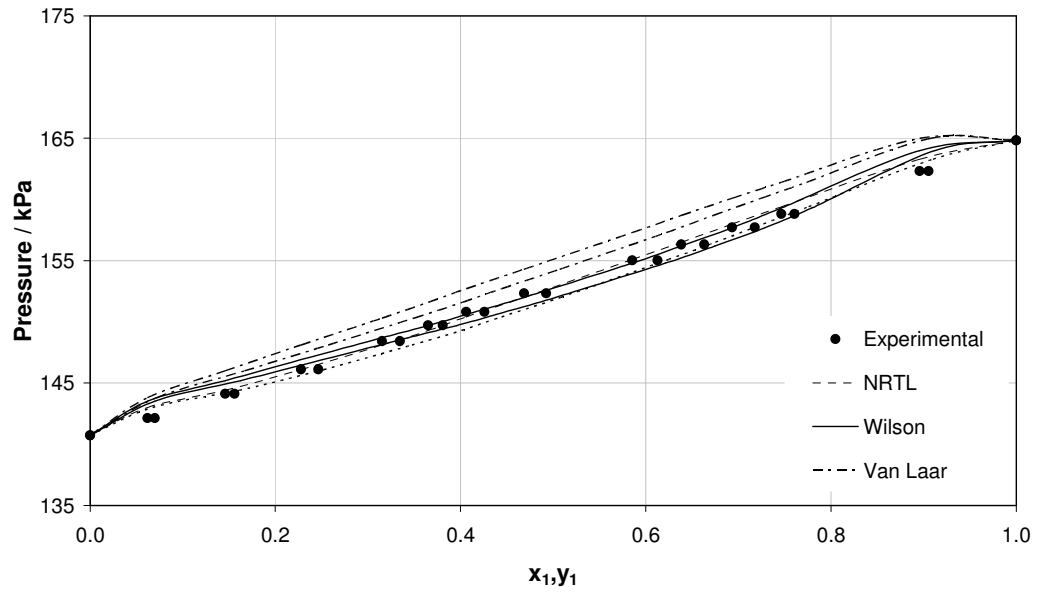


Figure 7-4: NRTL, Wilson and Van Laar model fits to P-x-y diagram of 1-hexene (1) + n-hexane (2) at 80°C

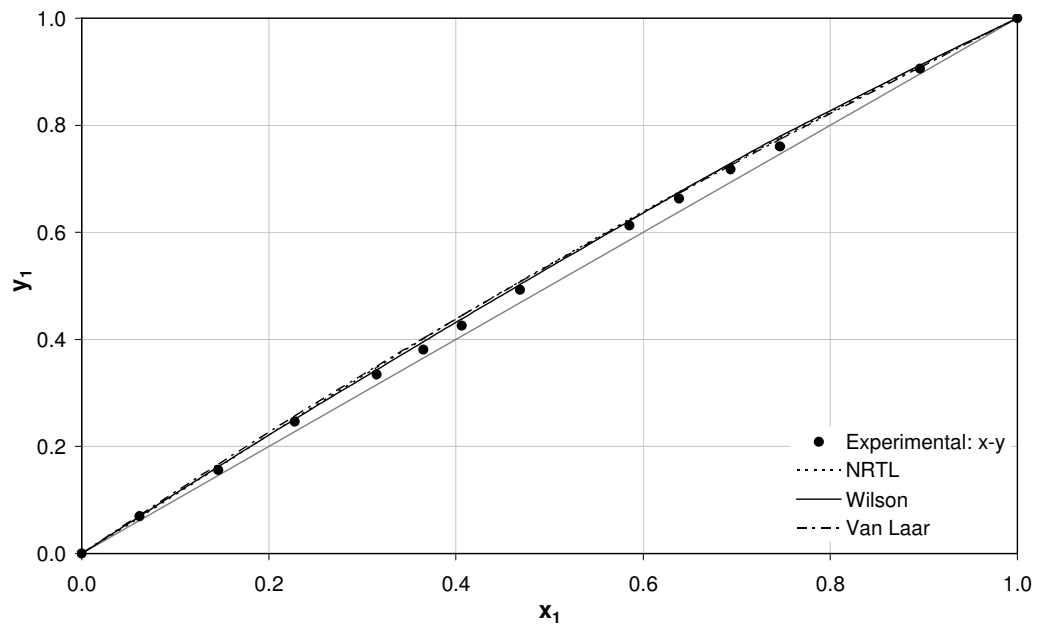


Figure 7-5: NRTL, Wilson and Van Laar model fits to x-y diagram of 1-hexene (1) + n-hexane (2) at 80°C

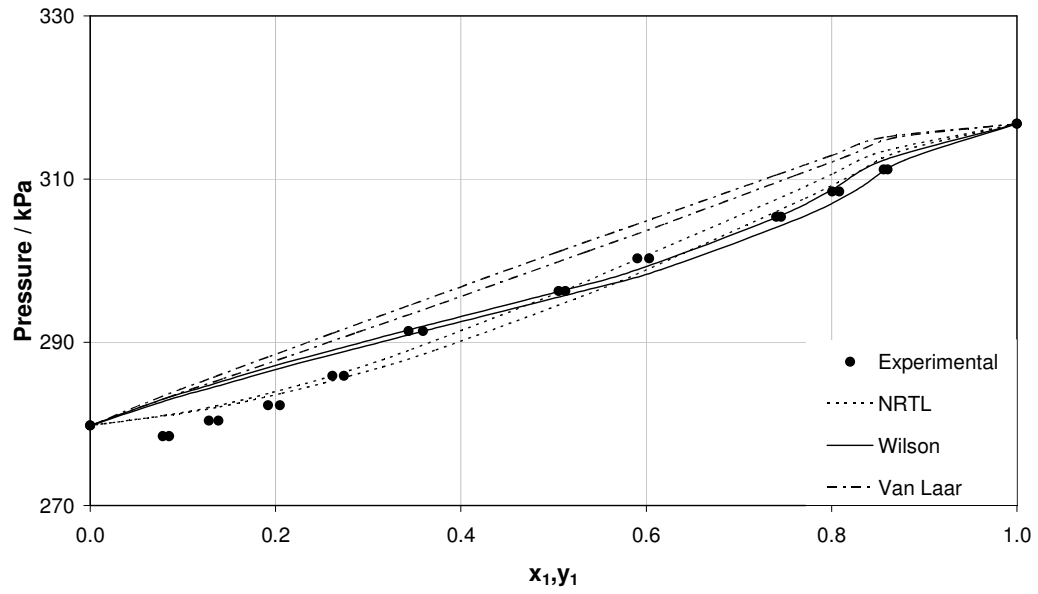


Figure 7-6: NRTL, Wilson and Van Laar model fits to P-x-y diagram of 1-hexene (1) + n-hexane (2) at 105°C

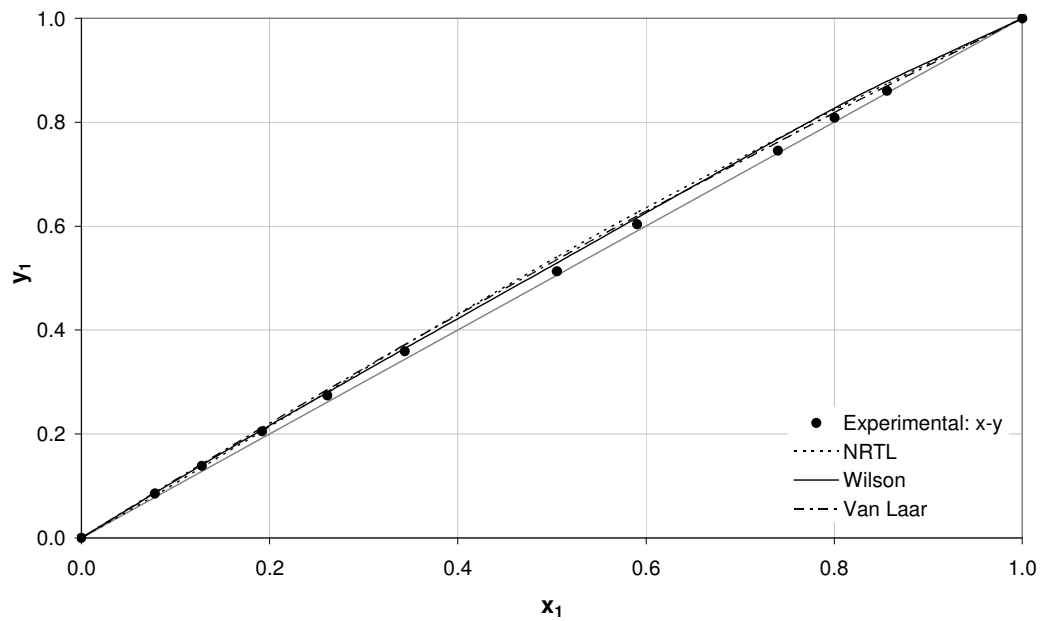


Figure 7-7: NRTL, Wilson and Van Laar model fits to x-y diagram of 1-hexene (1) + n-hexane (2) at 105°C

Table 7-15: Excess Gibbs energy parameters regressed for the system of 1-hexene (1) with n-hexane (2)

MODEL	1-Hexene (1) + n-Hexane (2) System		
	55 °C	80 °C	105 °C
NRTL			
$g_{12} - g_{21}$ (cal/mol)	-267.3609	-428.0856	-485.6784
$g_{22} - g_{12}$ (cal/mol)	43.3465	101.1122	90.1752
α	0.15	0.15	0.15
K_{12}	0.1506	0.1490	0.1504
Average δP (kPa)	0.2192	0.3394	1.2255
Average δy_1	0.0055	0.0096	0.0109
Van Laar			
A_{12}	0.0091	0.01	3.7950
A_{21}	0.1686	0.5	0.0893
K_{12}	0.02	0.001	0.1459
Average δP (kPa)	0.1783	1.8107	3.9064
Average δy_1	0.0049	0.0096	0.0096
Wilson			
Λ_{12}	3.4212	3.2469	0.01
Λ_{21}	0.1103	0.1144	0.01
K_{12}	0.1682	0.0972	0.001
Average δP (kPa)	0.0733	0.4709	1.6329
Average δy_1	0.0044	0.0081	0.0088

The parameters for the respective models are temperature dependent and are presented below for the system of 1-hexene with n-hexane in Figures 7-8, 7-9 and 7-10.

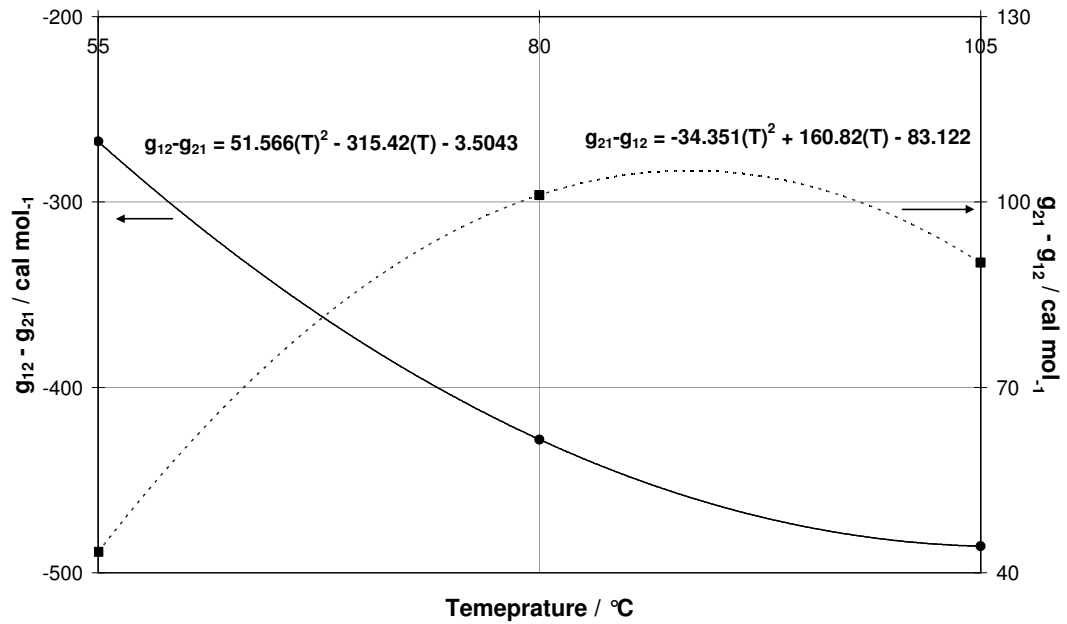


Figure 7-8: Temperature dependency of NRTL parameters for 1-hexene with n-hexane

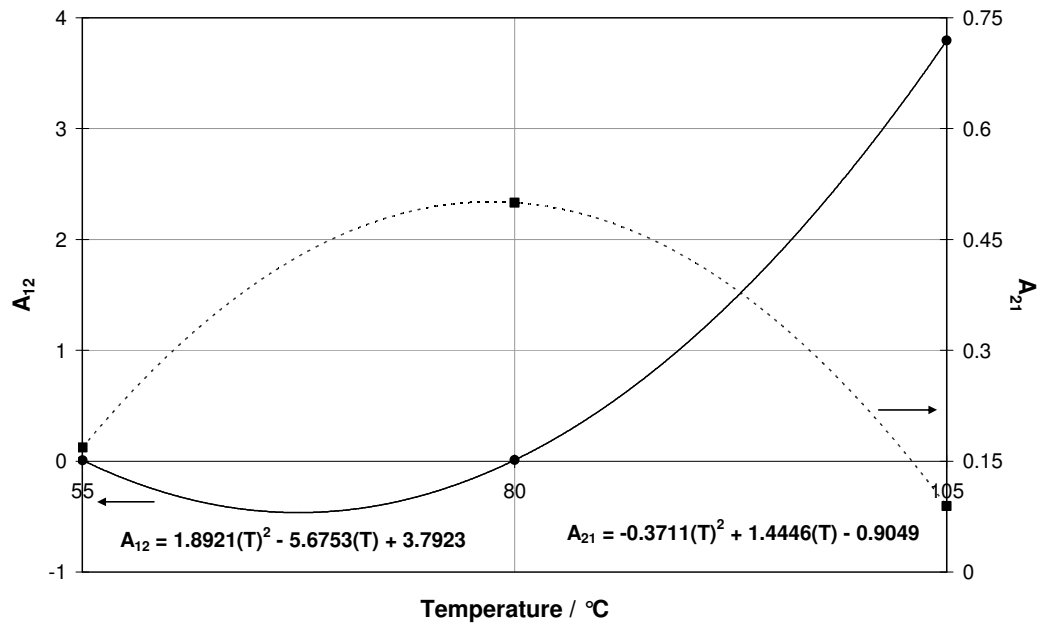


Figure 7-9: Temperature dependency of Van Laar parameters for 1-hexene with n-hexane

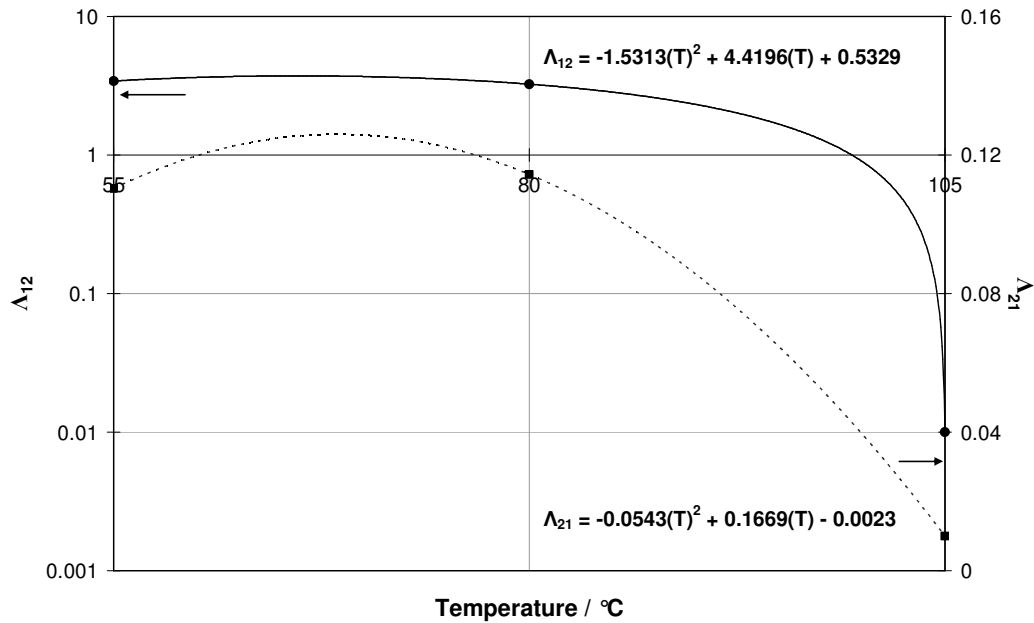


Figure 7-10: Temperature dependency of Wilson parameters for 1-hexene with n-hexane

7.3.2 2-Methyl-2-pentene (1) + n-Hexane (2) System

The model parameters as well the average deviation between calculated and experimental vapour composition and pressures are presented in Table 7-18. The best fit models were chosen on the basis of the average absolute deviation of predicted pressure from experimental pressure (δP). The best fit models are presented below (Table 7-16) together with their corresponding δP values.

Table 7-16: Best fit models for the system of 2-methyl-2-pentene (1) + n-hexane (2)

2-methyl-2-pentene (1) + n-hexane (2) systems at	Model	Average δP (kPa)
55 °C	Wilson	0.0679
80 °C	NRTL	0.3589
105 °C	Wilson	0.517

The absolute average deviation between vapour compositions is also presented in Table 7-17. The models in Figures 7-12, 7-14 and 7-16 (x-y plots) fit the experimental data well. It can be seen from the P-x-y plots (Figures 7-11, 7-13 and 7-15) and the pressure deviations (Table 7-18) that the Van Laar model does not give satisfactory results for any of the systems. The NRTL

alpha parameter is inputted as an initial guess and the program regresses for it. In Table 7-18, below the NRTL α parameter values are equivalent to the initial guess.

Infinite activity coefficients (γ_i^∞), as described in Chapter two, are essential in the design of distillation columns. The infinite activity coefficients are presented in Table 7-17 and the method was described in Chapter two. The plots used in the evaluation of the limiting activity coefficients can be found in Figures C-4 to C-8, Appendix C.

Table 7-17: Infinite dilution activity coefficients for the systems of 2-methyl-2-pentene (1) + n-hexane (2)

Temperature / °C	γ_1^∞	γ_2^∞
55	1.017	0.854
80	0.946	0.98
105	0.900	1.012

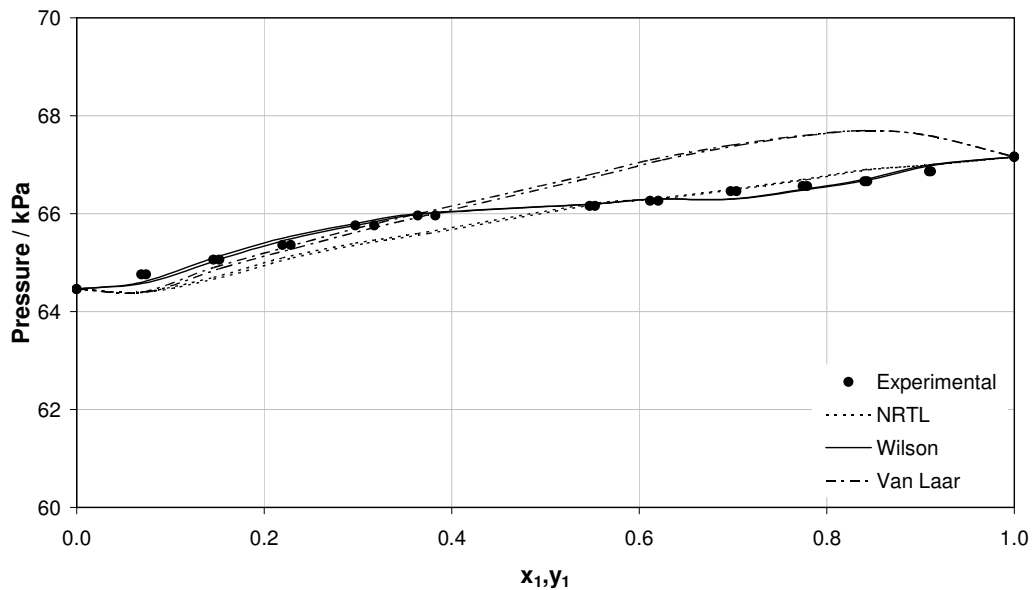


Figure 7-11: NRTL, Wilson and Van Laar model fits to P-x-y diagram of 2-methyl-2-pentene (1) + n-hexane (2) at 55°C

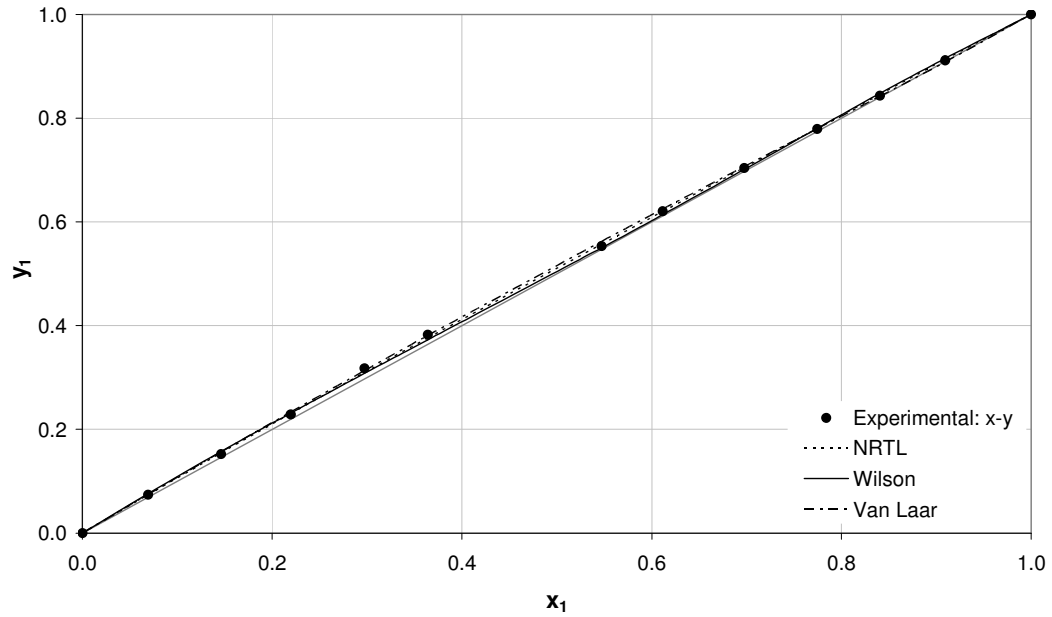


Figure 7-12: NRTL, Wilson and Van Laar model fits to x-y diagram of 2-methyl-2-pentene (1) + n-hexane (2) at 55°C

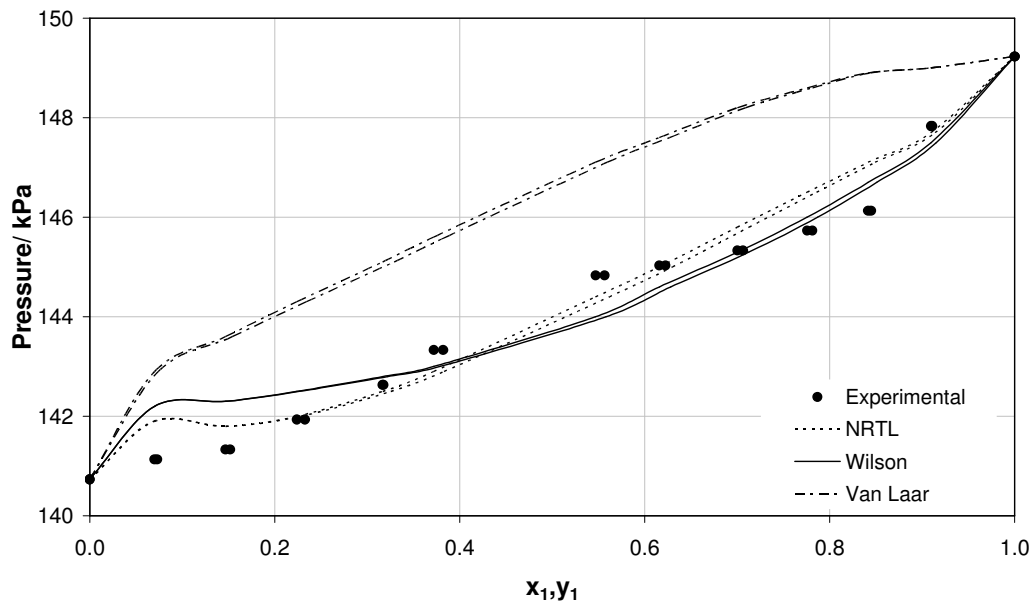


Figure 7-13: NRTL, Wilson and Van Laar model fits to P-x-y diagram of 2-methyl-2-pentene (1) + n-hexane (2) at 80°C

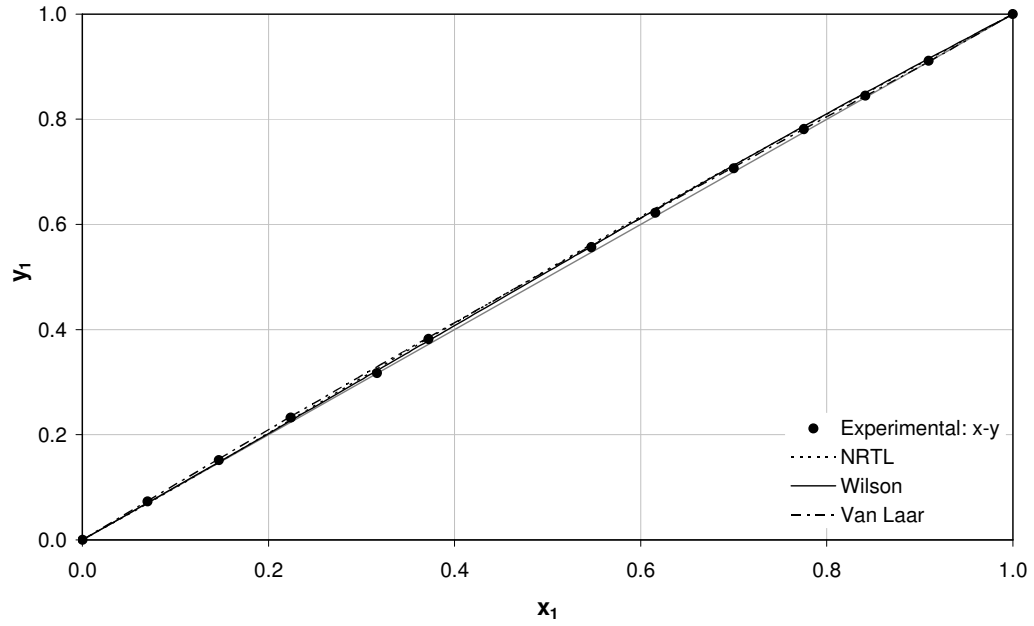


Figure 7-14: NRTL, Wilson and Van Laar model fits to x-y diagram of 2-methyl-2-pentene (1) + n-hexane (2) at 80°C

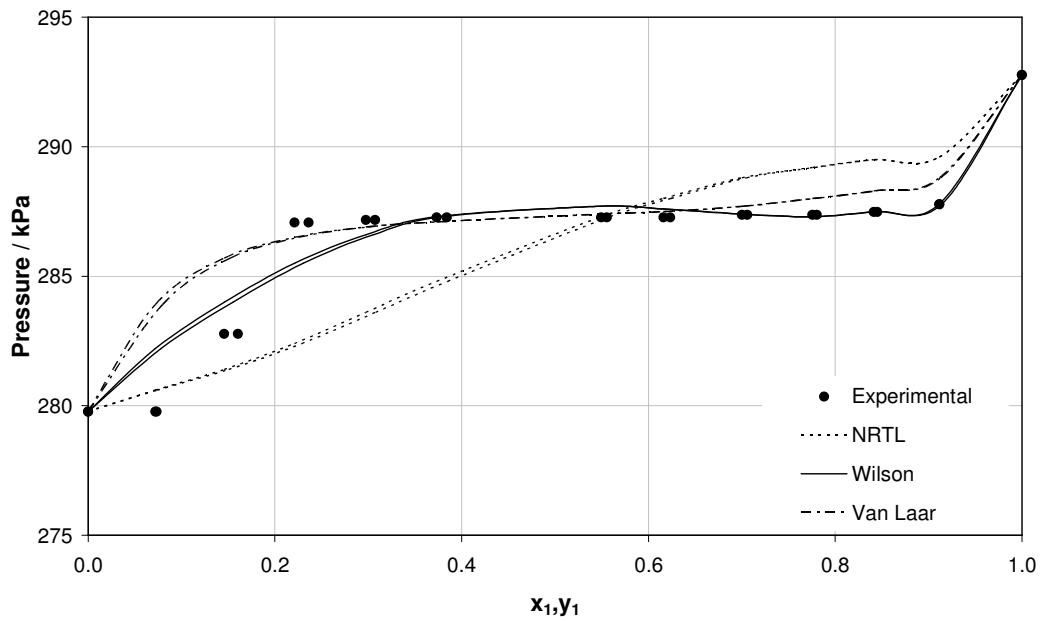


Figure 7-15: NRTL, Wilson and Van Laar model fits to P-x-y diagram of 2-methyl-2-pentene (1) + n-hexane (2) at 105°C

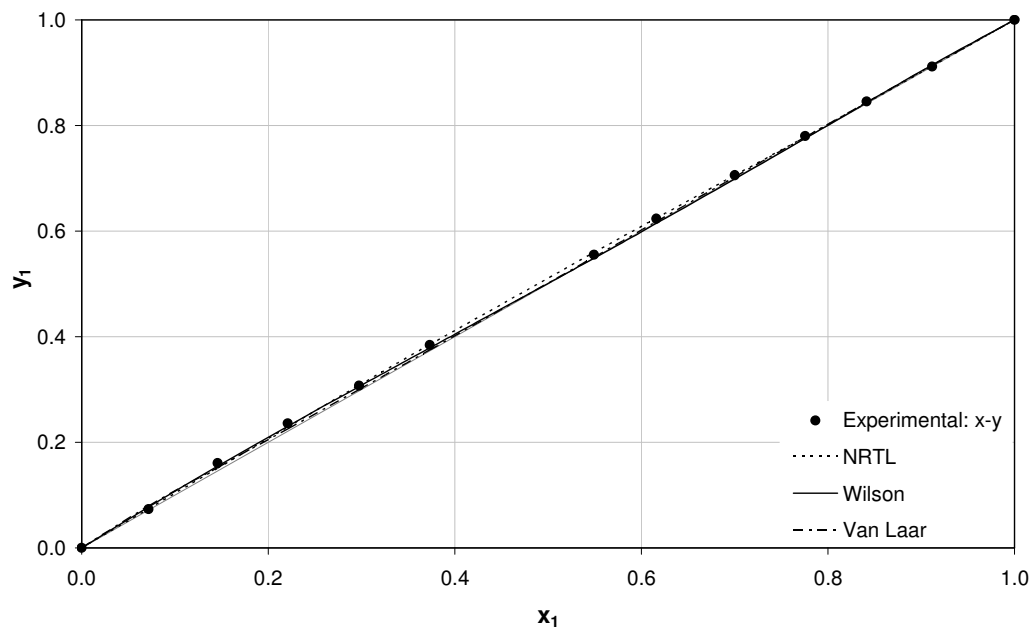


Figure 7-16: NRTL, Wilson and Van Laar model fits to x-y diagram of 2-methyl-2-pentene (1) + n-hexane (2) at 105°C

Table 7-18: Excess Gibbs energy parameters regressed for the system of 2-methyl-2-pentene (1) + n-hexane (2)

MODEL	2-Methyl-2-pentene (1) + n-Hexane (2) System		
	55 °C	80 °C	105 °C
NRTL			
$g_{12} - g_{21}$ (cal/mol)	301.3262	-533.3525	-495.9643
$g_{22} - g_{12}$ (cal/mol)	-521.6797	212.8964	205.2633
α	0.15	0.15	0.15
K_{12}	0.1502	0.1512	0.1504
Average δP (kPa)	0.1805	0.3589	1.5984
Average δy_1	0.0023	0.0042	0.0022
Van Laar			
A_{12}	0.0504	0.0313	0.4290
A_{21}	0.19	0.19	0.0672
K_{12}	0.0004	0.0004	-0.0198
Average δP (kPa)	0.4548	1.9727	0.8631
Average δy_1	0.0028	0.0025	0.0048
Wilson			
Λ_{12}	3.42	1.99	2.9161
Λ_{21}	0.1452	0.4	0.25
K_{12}	0.1774	0.0101	0.1515
Average δP (kPa)	0.0679	0.4279	0.517
Average δy_1	0.0039	0.0038	0.0043

The parameters for the respective models are temperature dependent and are presented below for the system of 1-hexene with n-hexane in Figures 7-17, 7-18 and 7-19.

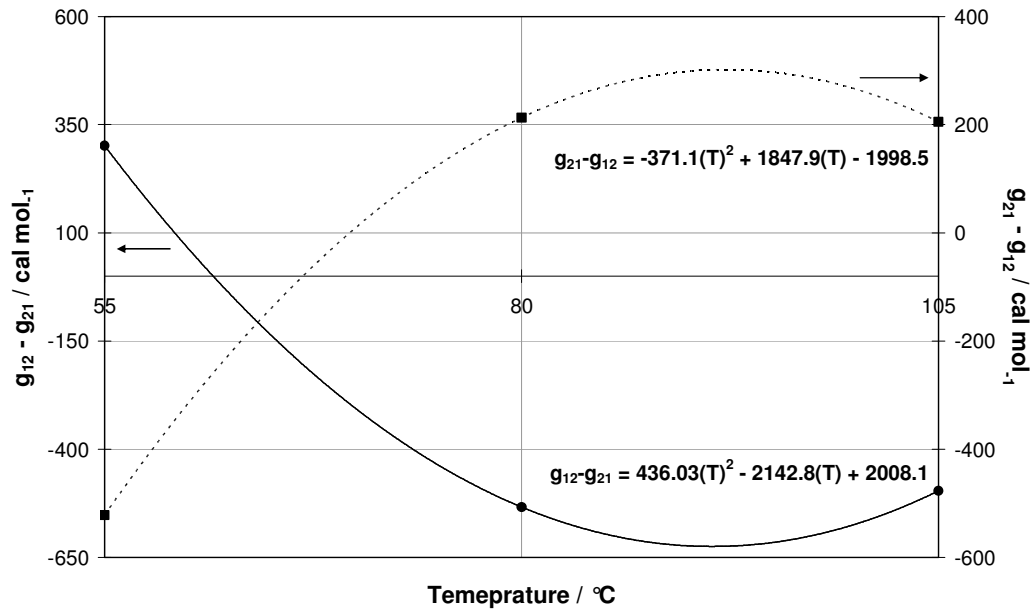


Figure 7-17: Temperature dependency of NRTL parameters for 2-methyl-2-pentene with n-hexane

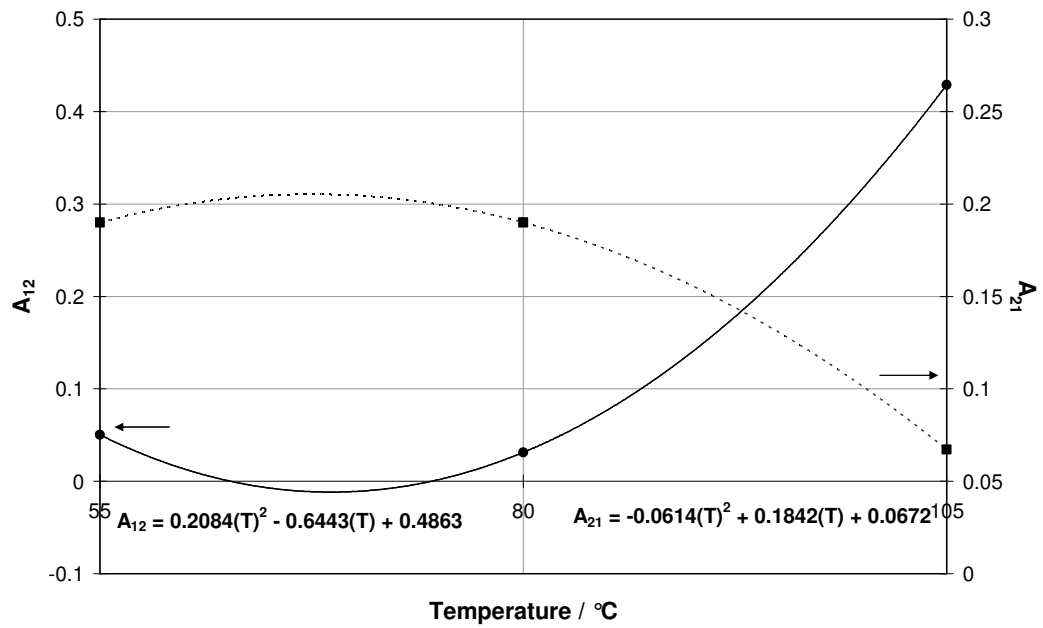


Figure 7-18: Temperature dependency of Van Laar parameters for 2-methyl-2-pentene with n-hexane

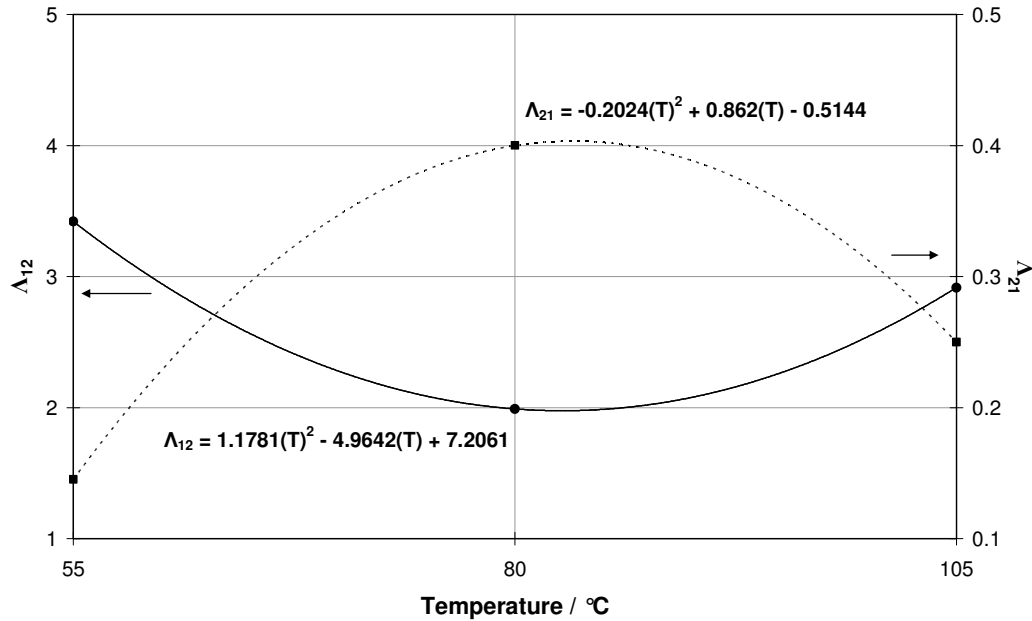


Figure 7-19: Temperature dependency of Wilson parameters for 2-methyl-2-pentene with n-hexane

7.3.3 n-Methyl-2-pyrrolidone (1) + 1-Hexene (2) System

The model parameters as well the average deviation between calculated and experimental vapour composition and pressures are presented in Table 7-20. The best fit models were chosen on the basis of the average absolute deviation of predicted temperature from experimental temperature since the objective function in the data regression is based on temperature residuals (δT). The best fit models are presented below (Table 7-19) together with their corresponding δT values.

Table 7-19: Best fit models for the system of n-methyl-2-pyrrolidone (1) + 1-hexene (2)

n-methyl-2-pyrrolidone (1) + 1-hexene (2) systems at	Model	Average δT (K)
45 kPa	Van Laar	0.3352
80 kPa	Wilson	1.2193
100 kPa	Wilson	1.6559

All models fit the experimental x-y data (Figures 7-22, 7-23, &-26, 7-27, 7-30 and 7-21) well with greater deviations around $x_1 > 0.8$. This is also illustrated by the low δy_1 values. The Van Laar model, predicts the experimental liquid phase data very well for the all the n-methyl-2-

pyrrolidone with 1-hexene systems. However, in the case of the vapour phase data the Van Laar model over estimates the data. It is important to note that the UNIQUAC model predicts the experimental data well, although the model line shown in the figures below are best fit and should not be mistaken for an unsuccessful model.

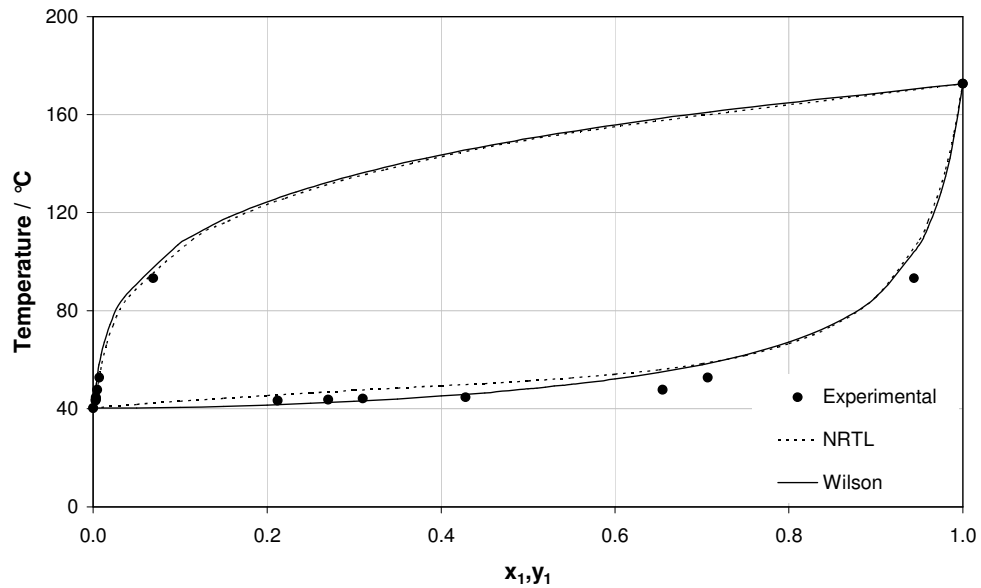


Figure 7-20: NRTL and Wilson model fits to T-x-y diagram of n-methyl-2-pyrrolidone (1) + 1-hexene (2) at 45 kPa

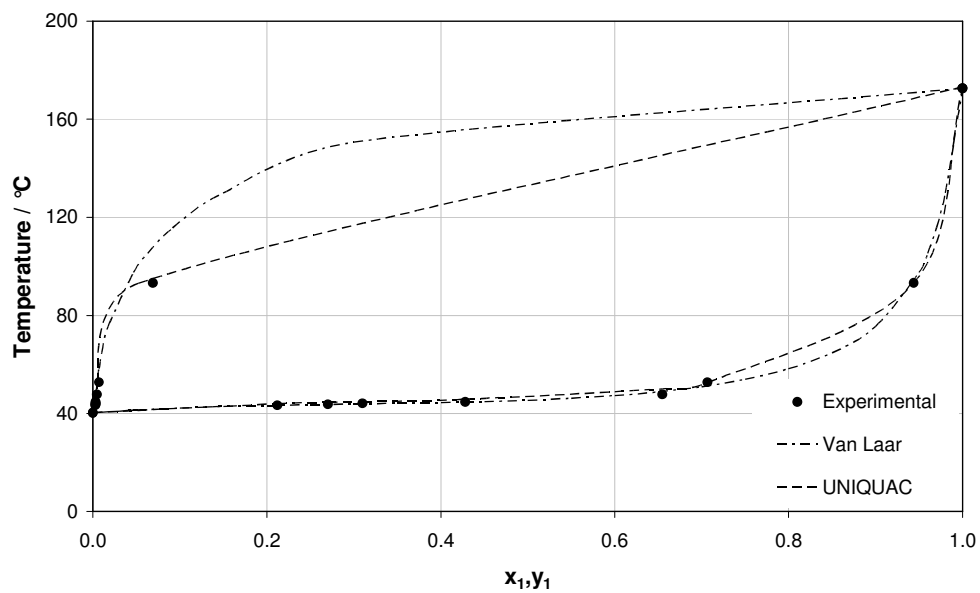


Figure 7-21: Van Laar and UNIQUAC model fits to T-x-y diagram of n-methyl-2-pyrrolidone (1) + 1-hexene (2) at 45 kPa

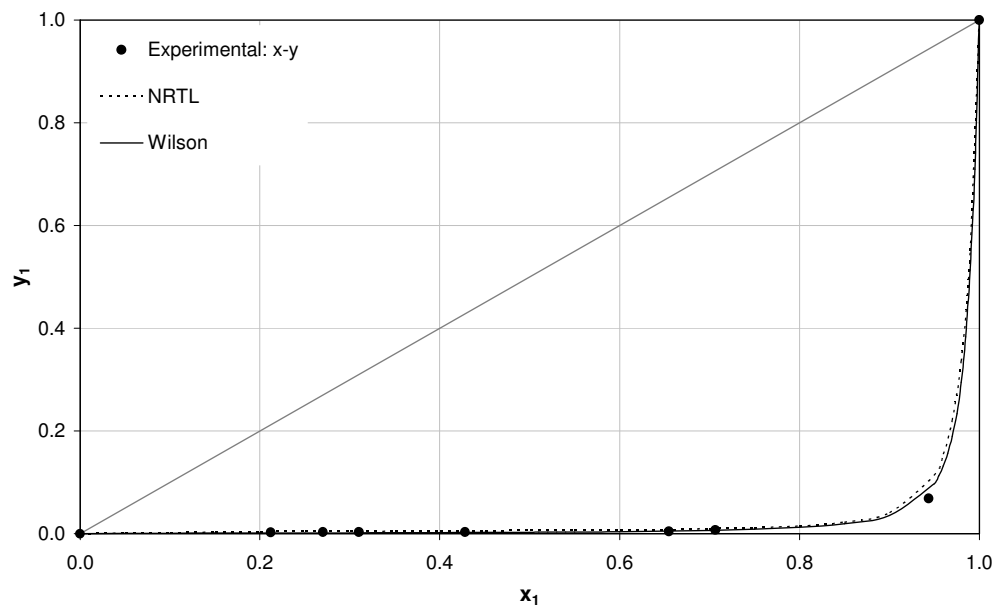


Figure 7-22: NRTL and Wilson model fits to x-y diagram of n-methyl-2-pyrrolidone (1) + 1-hexene (2) at 45 kPa

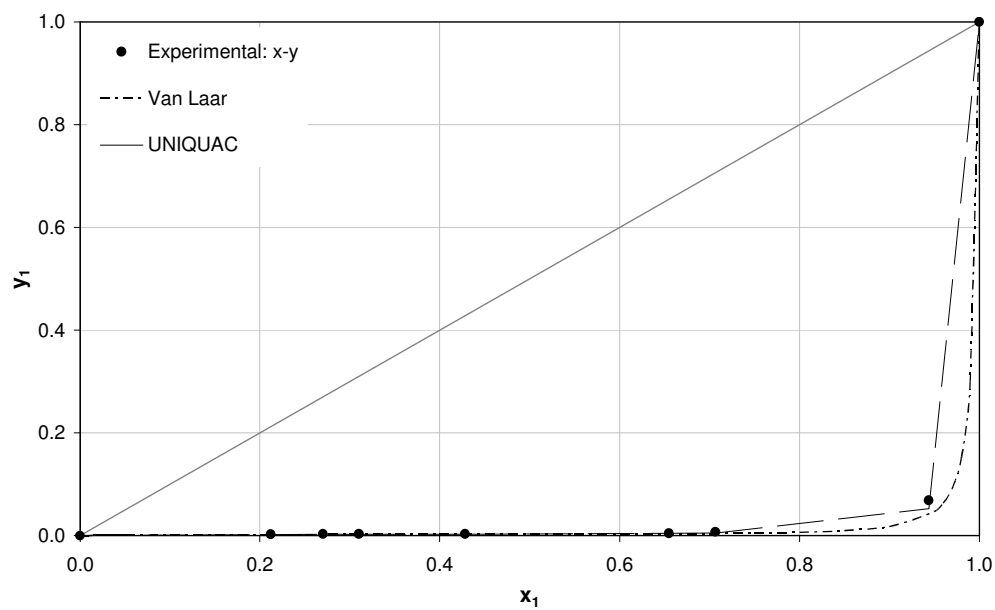


Figure 7-23: Van Laar and UNIQUAC model fits to x-y diagram of n-methyl-2-pyrrolidone (1) + 1-hexene (2) at 45 kPa

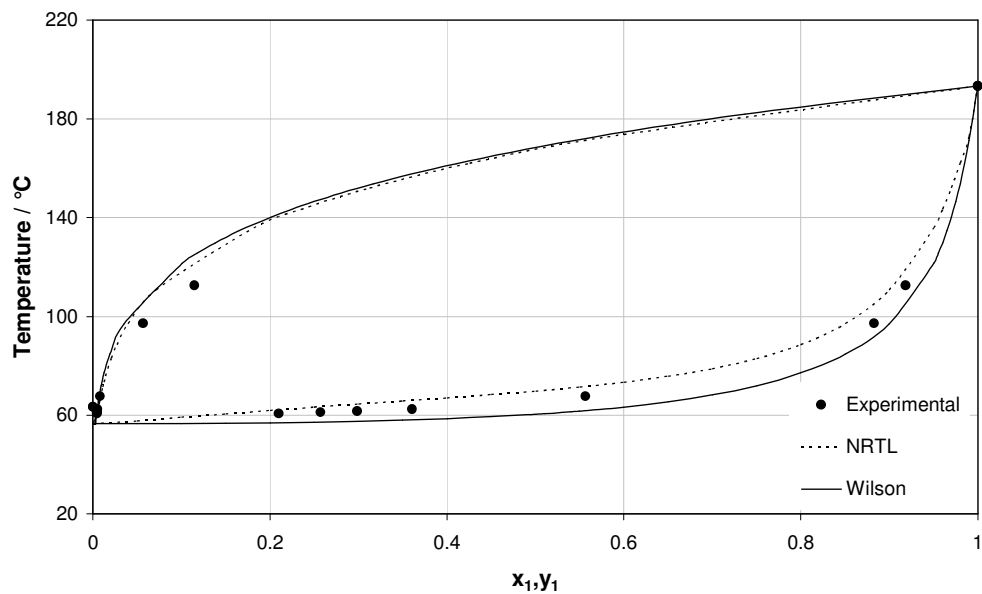


Figure 7-24: NRTL and Wilson model fits to T-x-y diagram of n-methyl-2-pyrrolidone (1) + 1-hexene (2) at 80 kPa

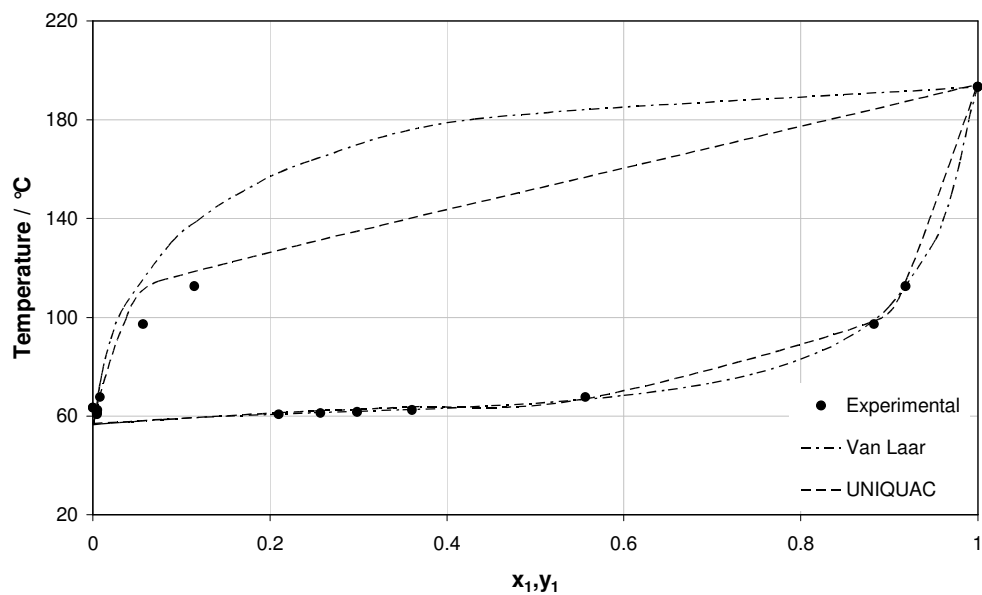


Figure 7-25: Van Laar and UNIQUAC model fits to T-x-y diagram of n-methyl-2-pyrrolidone (1) + 1-hexene (2) at 80 kPa

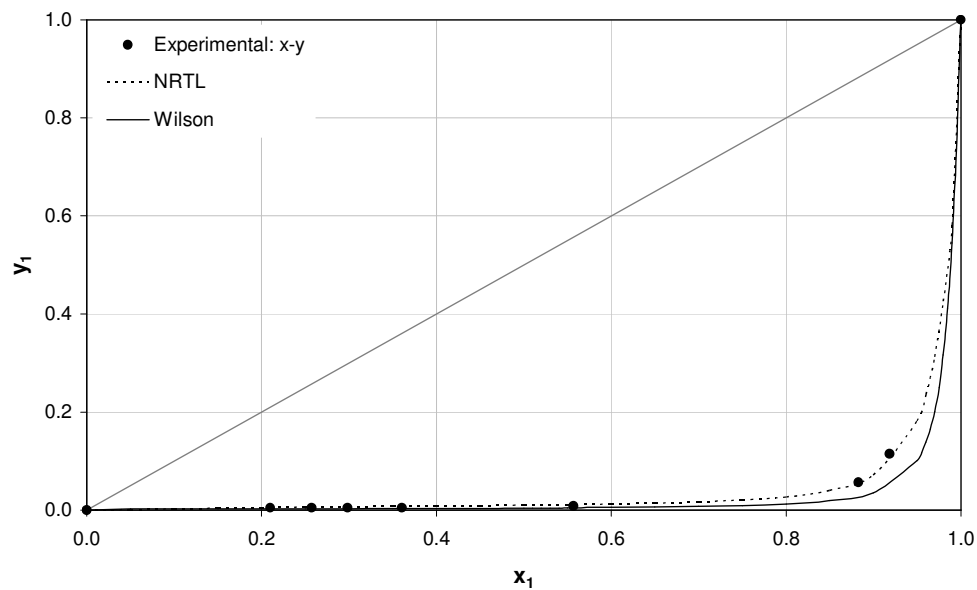


Figure 7-26: NRTL and Wilson model fits to x-y diagram of n-methyl-2-pyrrolidone (1) + 1-hexene (2) at 80 kPa

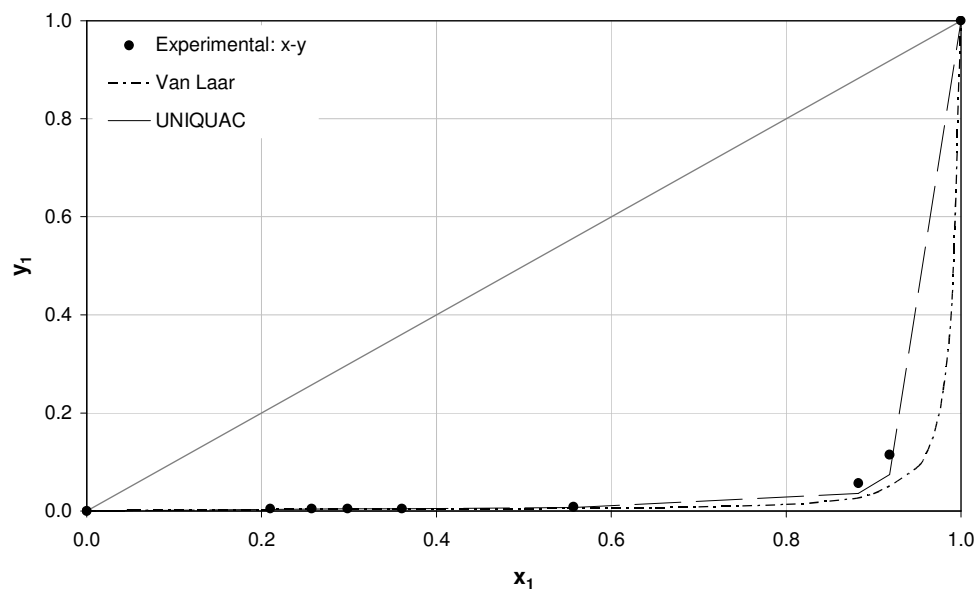


Figure 7-27: Van Laar and UNIQUAC model fits to x-y diagram of n-methyl-2-pyrrolidone (1) + 1-hexene (2) at 80 kPa

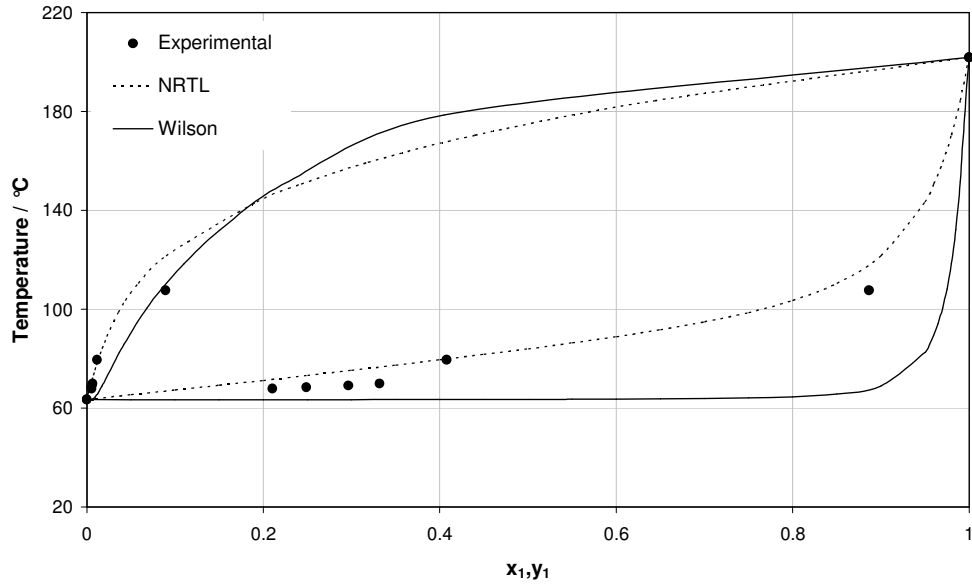


Figure 7-28: NRTL and Wilson model fits to T-x-y diagram of n-methyl-2-pyrrolidone (1) + 1-hexene (2) at 100 kPa

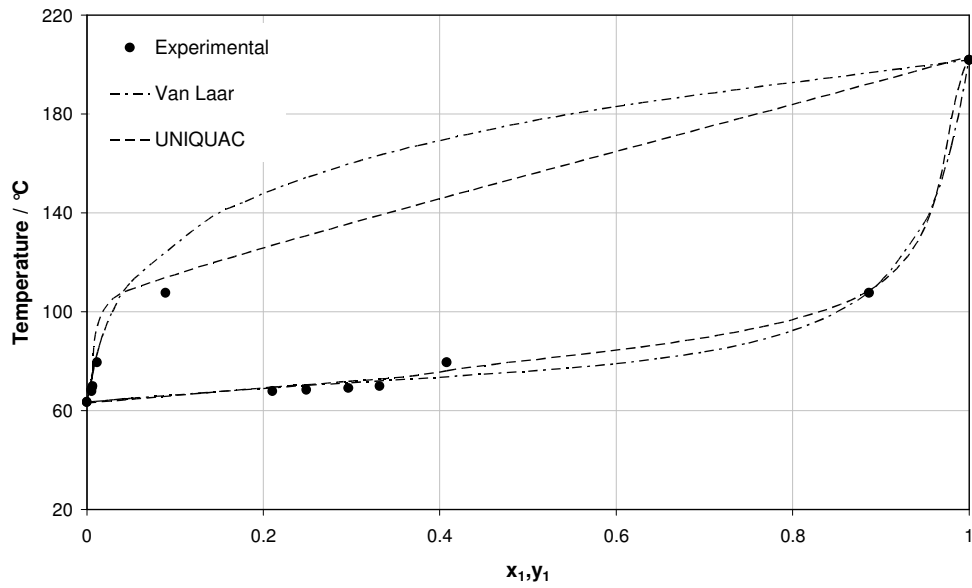


Figure 7-29: Van Laar and UNIQUAC model fits to T-x-y diagram of n-methyl-2-pyrrolidone (1) + 1-hexene (2) at 100 kPa

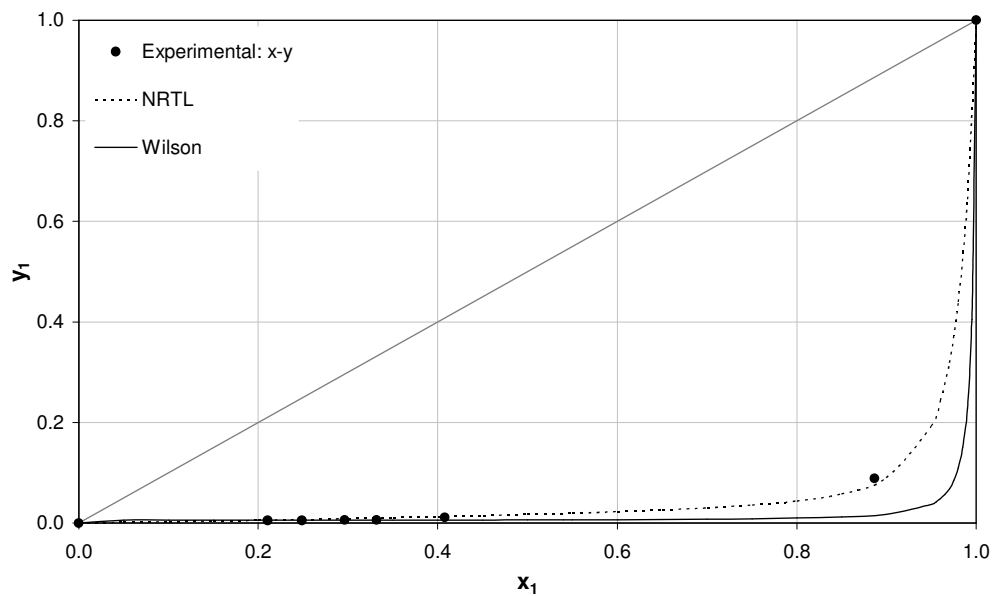


Figure 7-30: NRTL and Wilson model fits to x-y diagram of n-methyl-2-pyrrolidone (1) + 1-hexene (2) at 100 kPa

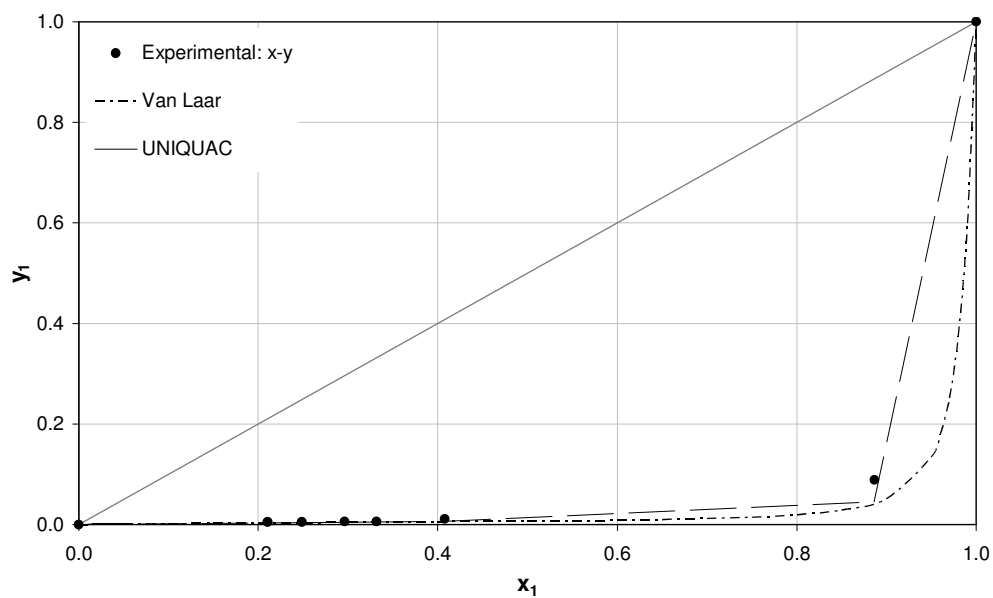


Figure 7-31: Van Laar and UNIQUAC model fits to x-y diagram of n-methyl-2-pyrrolidone (1) + 1-hexene (2) at 100 kPa

Table 7-20: Excess Gibbs energy parameters regressed for the system of n-methyl-2-pyrrolidone (1) + 1-hexene (2)

MODEL	n-Methyl-2-pyrrolidone(1) + 1-Hexene (2) System		
	45 kPa	80 kPa	100 kPa
NRTL^a			
$g_{12} - g_{21}$ (J/mol)	2447.783	2389.843	5194.789
$g_{22} - g_{12}$ (J/mol)	2556.108	1825.111	6171.581
α	0.1	0.1	0.4796
Average δT (K)	1.5423	2.0923	2.5029
Average δy_1	0.0029	0.0087	0.0068
Van Laar^a			
A_{12}	2.1507	1.7718	1.2913
A_{21}	1.3124	1.0958	1.2047
Average δT (K)	0.3352	1.2983	1.7037
Average δy_1	0.0026	0.0091	0.0073
Wilson^a			
$\lambda_{12} - \lambda_{11}$ (J/mol)	11712.58	5473.75	3088.48
$\lambda_{12} - \lambda_{22}$ (J/mol)	-224.65	36.94	1563.82
Average δT (K)	1.3215	1.2193	1.6559
Average δy_1	0.0022	0.0085	0.0066
UNIQUAC^b			
τ_{12}	0.21	14.48	-0.34
τ_{21}	-0.85	18.22	-0.0044
Average δT (K)	0.7212	1.7241	1.9163
Average δy_1	0.0023	0.0070	0.0067

^aModels regressed using the Microsoft Excel computer program.

^bModel regressed using Aspen simulation program.

7.4 Consistency Tests

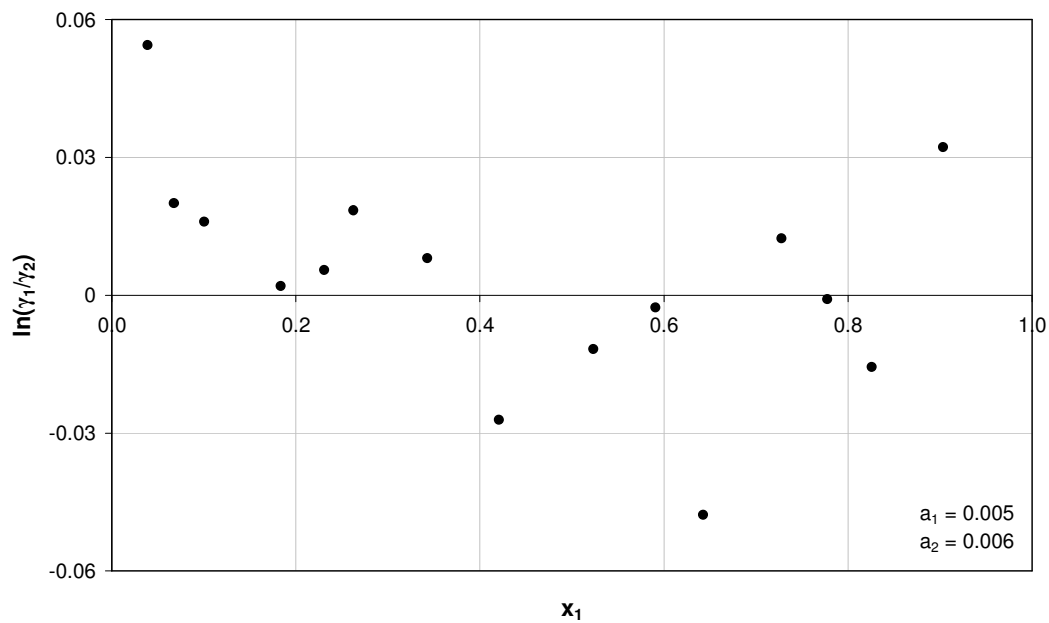
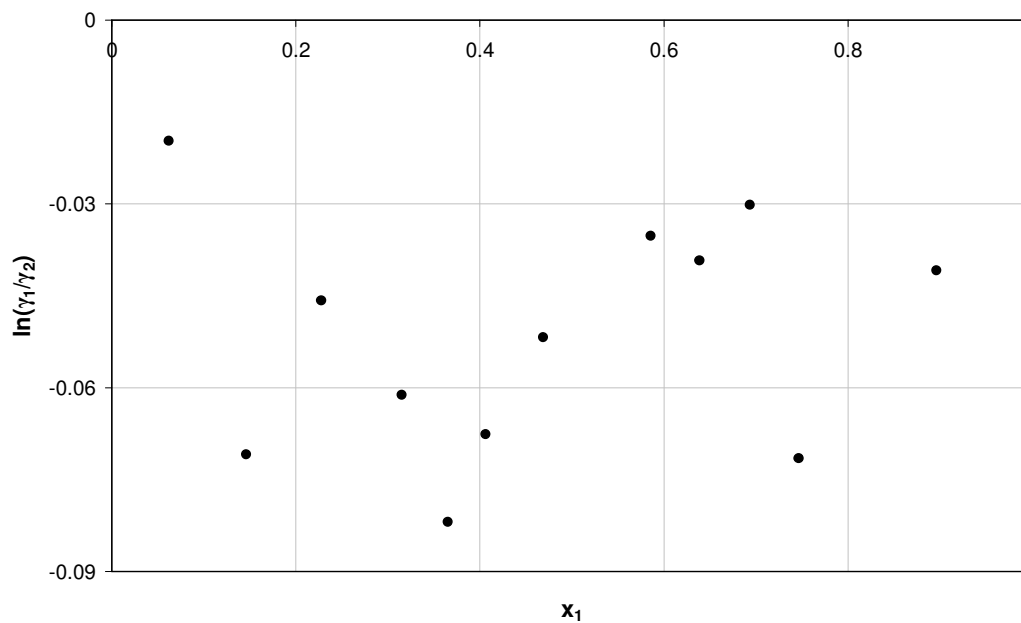
The Point test of Van Ness (Van Ness and Abbott, 1982) and the Area test of Redlich and Kister (1948) were used in this study. The procedures for these tests are described in Chapter two. The direct test (van Ness, 1995) could not be used due to the requirement that the data being reduced use an objective function based on the Gibbs excess energy residual. The results of the Area test and Point test are presented in this section.

7.4.1 Area Test

The area test was described in Chapter two and the results are presented here. As described in Chapter two the area test is based on the plot of the logarithm of the ratio of experimental activity coefficients against the liquid mole fraction, $\ln\left(\frac{\gamma_1}{\gamma_2}\right)$ versus x_1 . The defining value of this test is based on the net area relative to the total area which, according to Van Ness (1995) should be less than 0.1 or 10% (Equation 2-92). In order to approximate this value, a best fit trend line was fitted through the data points of the systems. The graphs were broken into two areas, a_1 (area below the graph) and a_2 (area above the graph) which were evaluated using numerical integration.

The thermodynamic consistency of the 1-hexene (1) + n-hexane (2) system at 80 °C and 105 °C, as well as 2-methyl-2-pentene (1) + n-hexane (2) at 80 °C could not be undertaken. This was due to the data not crossing the x-axis hence areas required for the test could not be calculated. This, however, does not validate the inconsistency of the data. It can be seen in Section 7.4.2 that all the experimental data pass the more rigorous consistency point test.

Tables 7-14 to 7-16 present the values obtained in evaluating the consistency of the data. The systems of 1-hexene (1) + n-hexane (2) at 55 °C and 2-methyl-2-pentene (1) + n-hexane (2) at 105 °C pass the test. However, the other systems fail the test which according to Van Ness (1995) only suggests that the measured vapour pressures are not consistent with the P-x-y data set. The system of n-methyl-2-pyrrolidone (1) + 1-hexene (2) fail the area test and this can be attributed to the negation of the ε term in equation 2-91, Chapter two. The term in the case of isobaric data representing excess enthalpy, is often considered negligible, however as explained in Chapter two this should not be the case.

7.4.1.1 1-Hexene (1) + n-Hexane (2) System**Figure 7-31: Consistency area test for 1-hexene (1) + n-hexane (2) at 55 °C****Figure 7-32: Consistency area test for 1-hexene (1) + n-hexane (2) at 80 °C**

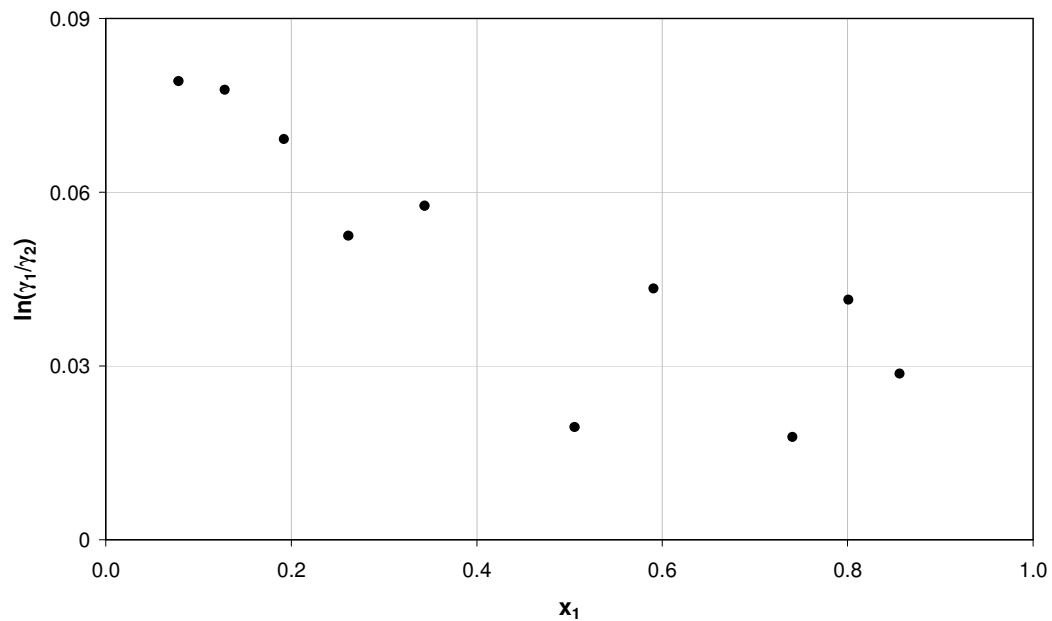


Figure 7-33: Consistency area test for 1-hexene (1) + n-hexane (2) at 105 °C

Table 7-21: Results of area test for 1-hexene (1) + n-hexane (2)

Temperature / °C	$\frac{a_1 - a_2}{a_1 + a_2}$
55	0.08
80	-
105	-

7.4.1.2 2-Methyl-2-pentene (1) + n-Hexane (2) System

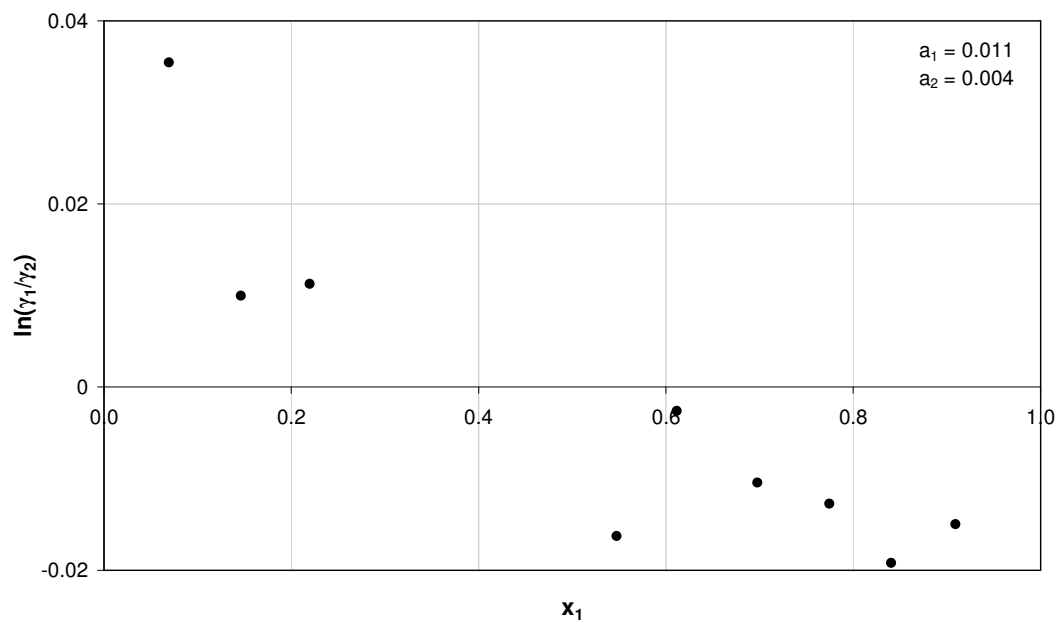


Figure 7-34: Consistency area test for 2-methyl-2-pentene (1) + n-hexane (2) at 55 °C

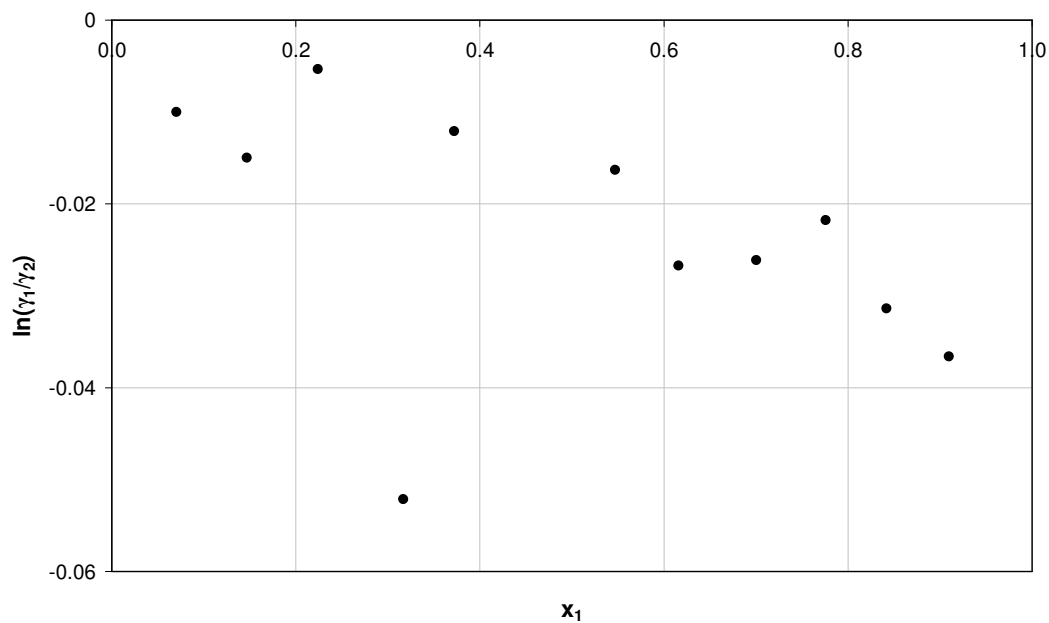


Figure 7-35: Consistency area test for 2-methyl-2-pentene (1) + n-hexane (2) at 80 °C

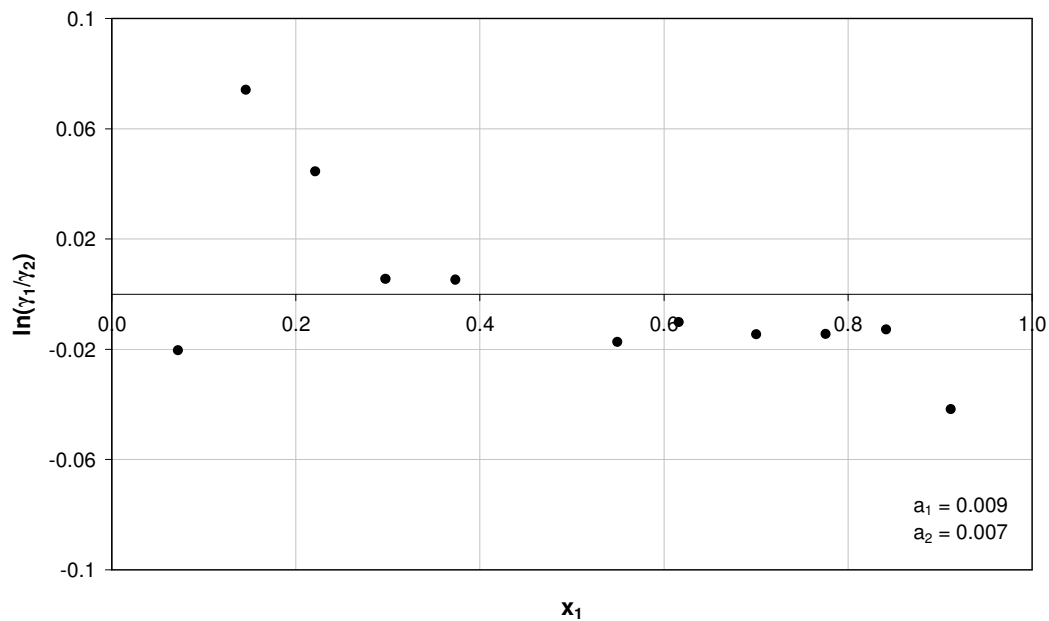
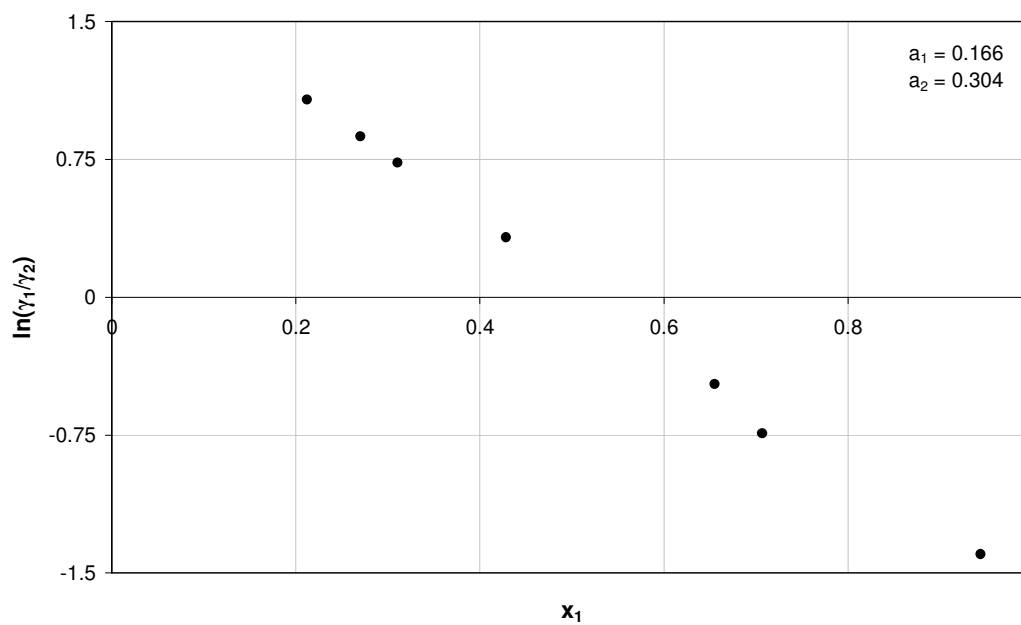
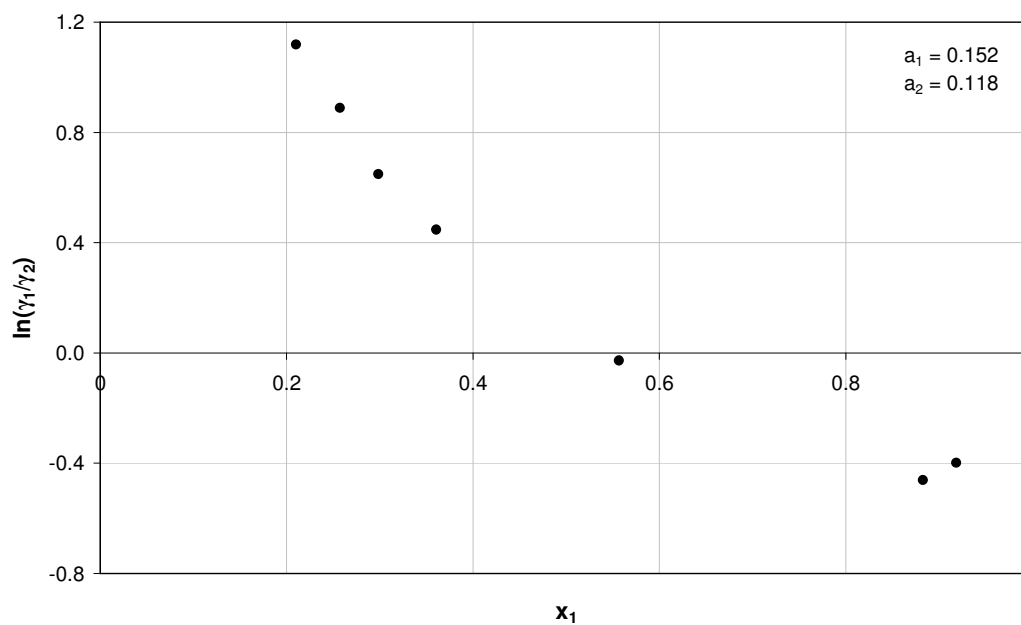


Figure 7-36: Consistency area test for 2-methyl-2-pentene (1) + n-hexane (2) at 105 °C

Table 7-22: Results of area test for 2-methyl-2-pentene (1) + n-hexane (2)

Temperature / °C	$\frac{a_1 - a_2}{a_1 + a_2}$
55	0.45
80	-
105	0.09

7.4.1.3 n-Methyl-2-pyrrolidone (1) + 1-Hexene (2) System**Figure 7-37: Consistency area test for n-methyl-2-pyrrolidone (1) + 1-hexene (2) at 45 kPa****Figure 7-38: Consistency area test for n-methyl-2-pyrrolidone (1) + 1-hexene (2) at 80 kPa**

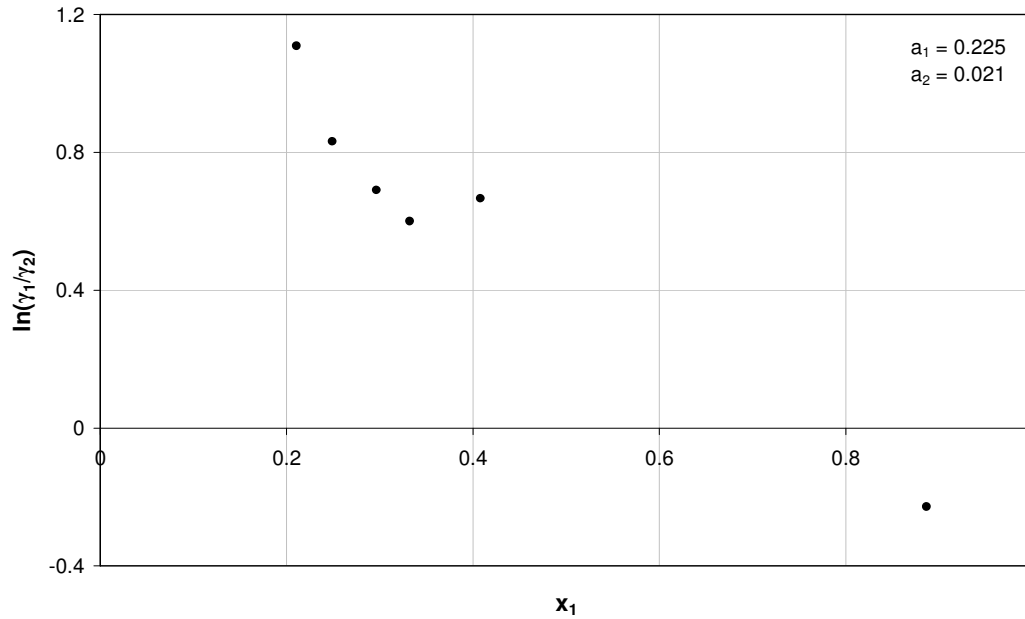


Figure 7-39: Consistency area test for n-methyl-2-pyrrolidone (1) + 1-hexene (2) at 100 kPa

Table 7-23: Results of area test for n-methyl-2-pyrrolidone (1) + 1-hexene (2)

Pressure / kPa	$\frac{a_1 - a_2}{a_1 + a_2}$
45	0.29
80	0.12
100	0.82

7.4.2 Point Test

The point test requires that the vapour composition residual scatters randomly across the liquid mole fraction range and is confirmed by Figures 7-28 to 7-36 for the systems investigated and Gibbs excess Energy models of NRTL, Wilson and Van Laar. For isothermal data the test requires that the data be reduced using the pressure residuals and in the case of isobaric data; temperature residuals are used. Furthermore, it was suggested that the absolute average deviation between experimental and calculated vapour compositions be less than 0.01. The calculated vapour compositions are obtained from data regression. The isothermal data was regressed using the direct method for VLE calculation with PRSV equation of state and Gibbs excess energy models. The isobaric data was regressed using the combined method with Pitzer type correlation for the equation of state and Gibbs excess energy models. As can be seen from

Tables 7-15, 7-18 and 7-20, absolute average deviation values of the vapour composition (δy) between experimental and calculated, using Gibbs excess energy models of NRTL, Wilson and Van Laar are all less than 0.01. This confirms the thermodynamic consistency of the data according to the Point test discussed in Chapter two. The figures below (Figure 7-40 to Figure 7-48) represent the best fit models for each system presented in Tables 7-12, 7-16 and 7-19. The results of the consistency point test for all systems investigated are presented in Appendix D.

Table 7-24: The best fit models and percentage bias

SYSTEM	CONDITION	MODEL	BIAS	PERCENTAGE
			-ve / +ve	
1-hexene with n-hexane	55 °C	Wilson	-	87
	80 °C	NRTL	-	92
	105 °C	NRTL	-	80
2-methyl-2-pentene with n-hexane	55 °C	Wilson	-	58
	80 °C	NRTL	-	73
	105 °C	Wilson	+	82
n-methyl-2-pyrrolidone with 1-hexene	45 kPa	Van Laar	+	100
	80 kPa	Wilson	+	100
	100 kPa	Wilson	+	100

7.4.2.1 1-Hexene (1) + n-Hexane (2) System

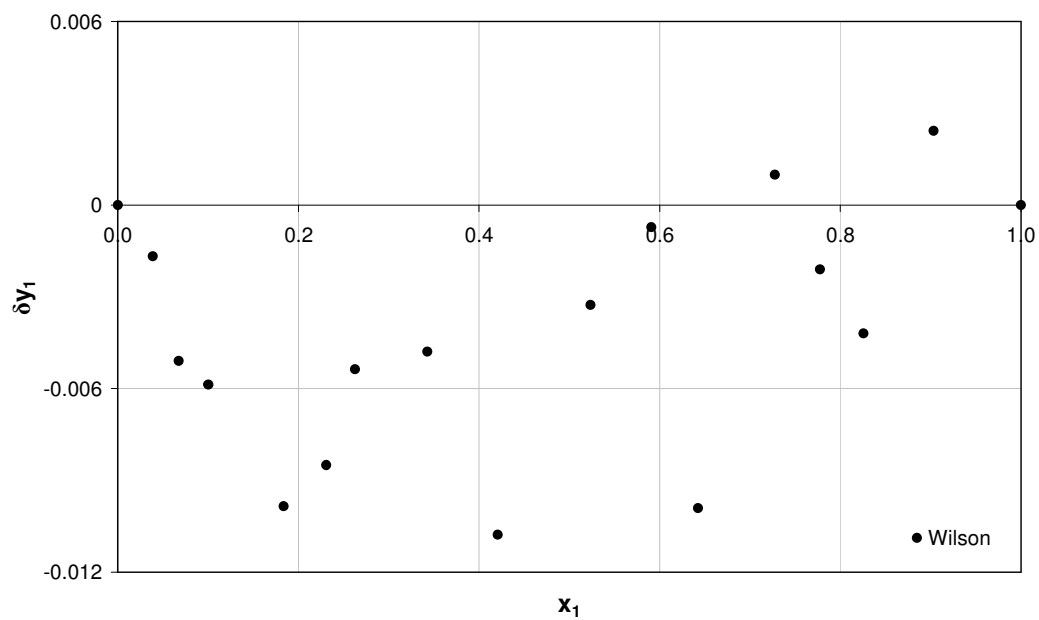


Figure 7-40: Consistency Point test for 1-hexene (1) + n-hexane (2) at 55 °C

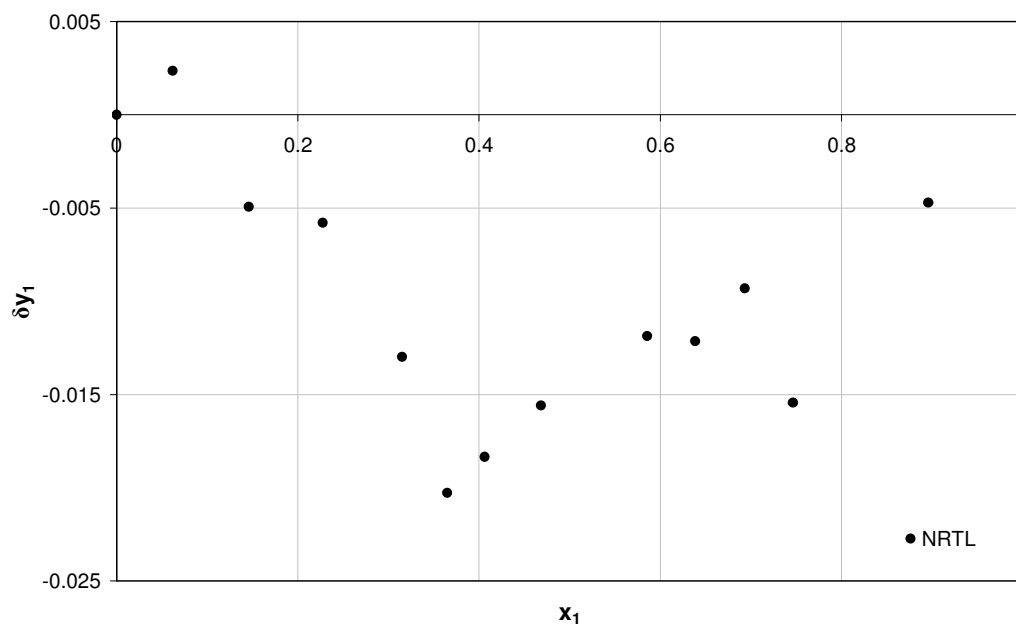


Figure 7-41: Consistency Point test for 1-hexene (1) + n-hexane (2) at 80 °C

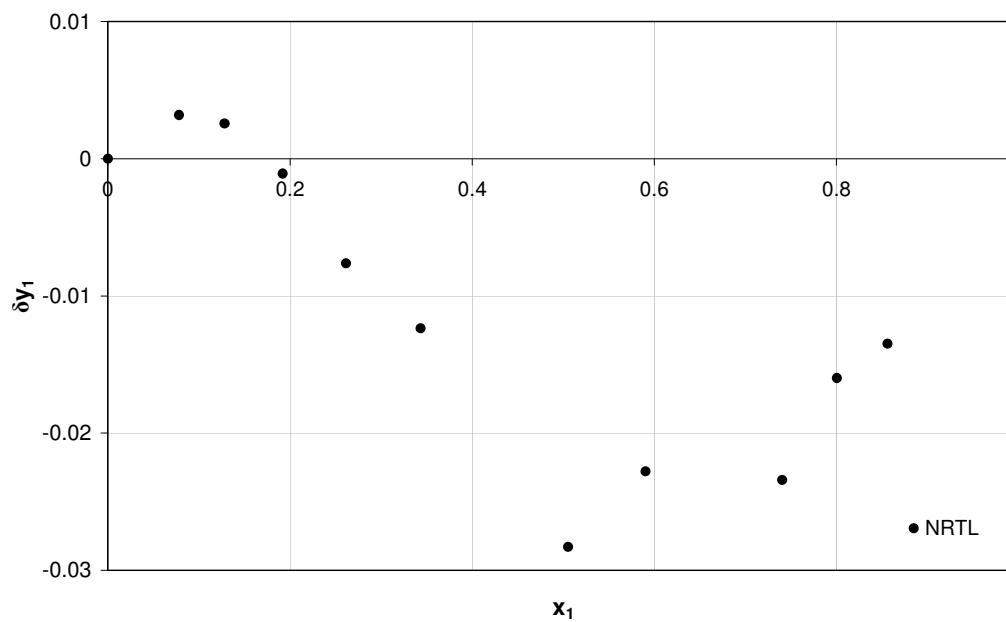


Figure 7-42: Consistency Point test for 1-hexene (1) + n-hexane (2) at 105 °C

7.4.2.2 2-methyl-2-pentene (1) + n-hexane (2) Systems

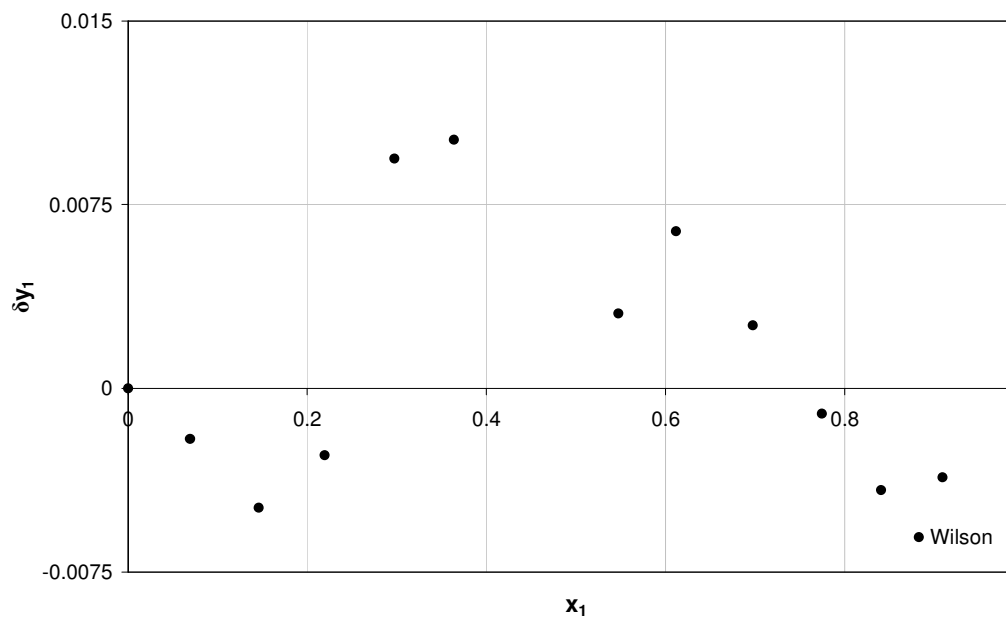


Figure 7-43: Consistency Point test for 2-methyl-2-pentene (1) + n-hexane (2) at 55 °C

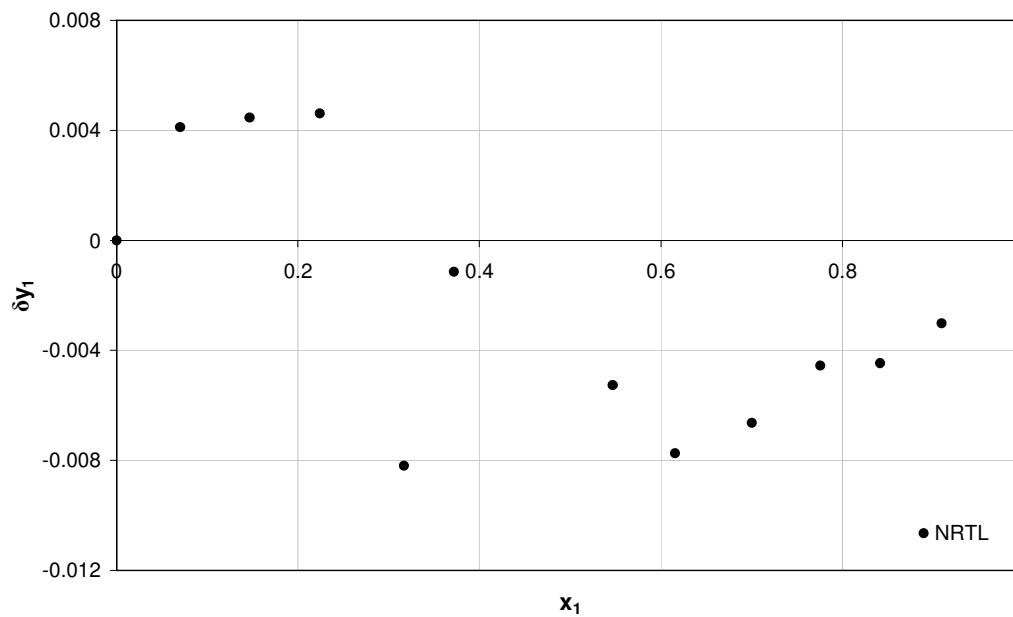


Figure 7-44: Consistency Point test for 2-methyl-2-pentene (1) + n-hexane (2) at 80 °C

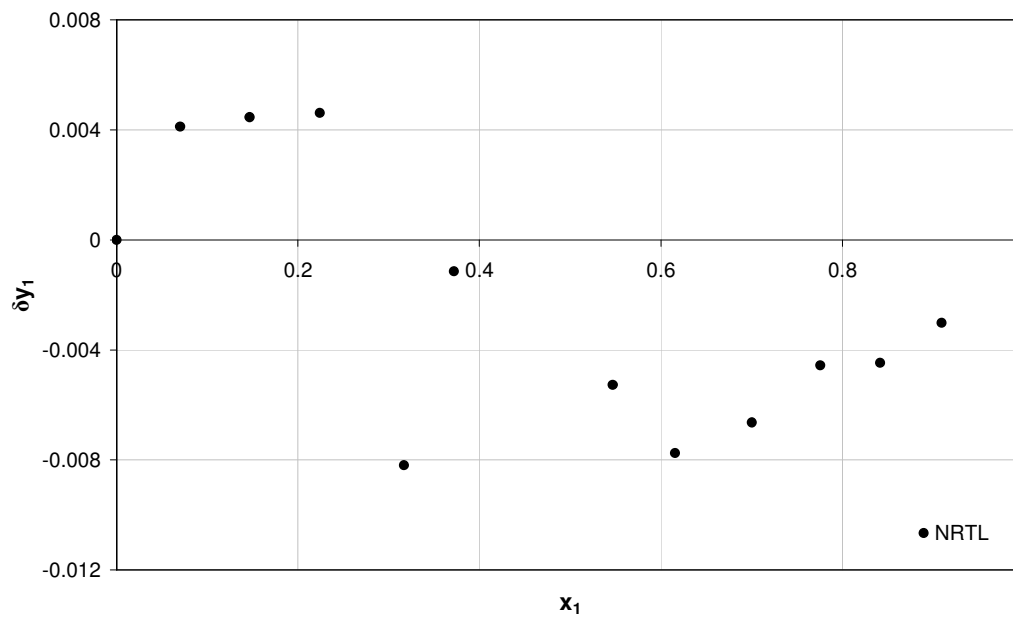
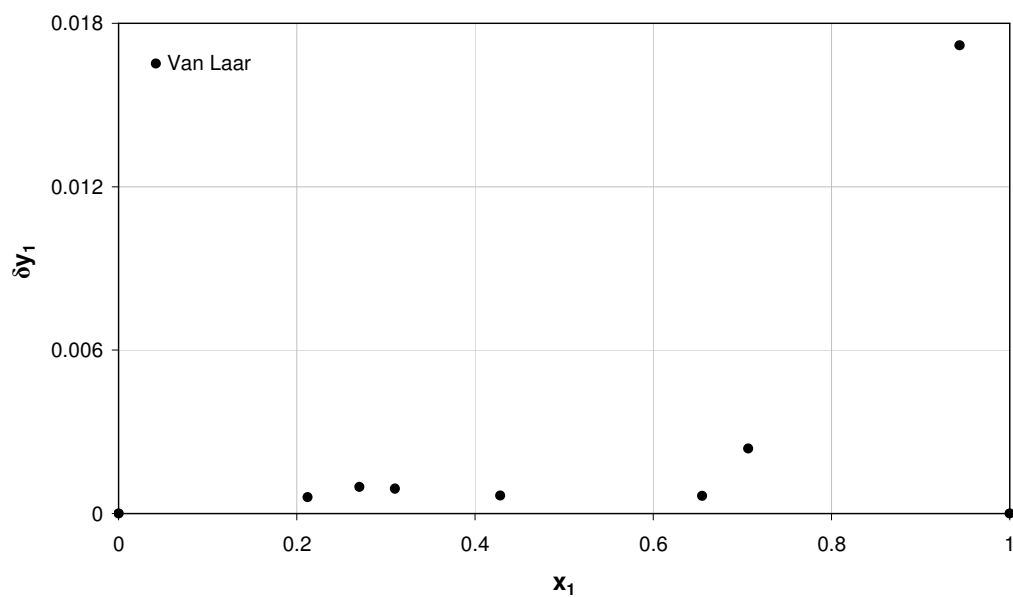
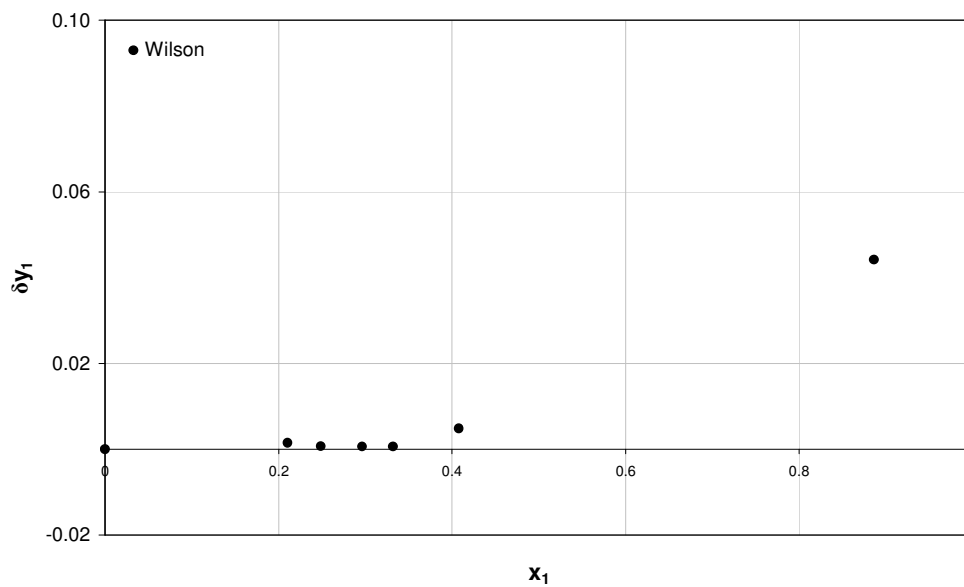


Figure 7-45: Consistency Point test for 2-methyl-2-pentene (1) + n-hexane (2) at 105 °C

7.4.2.3 n-Methyl-2-pyrrolidone (1) + 1-Hexene (2) System**Figure 7-46: Consistency Point test for n-methyl-2-pyrrolidone (1) + 1-hexene (2) at 45 kPa****Figure 7-47: Consistency Point test for n-methyl-2-pyrrolidone (1) + 1-hexene (2) at 80 kPa**

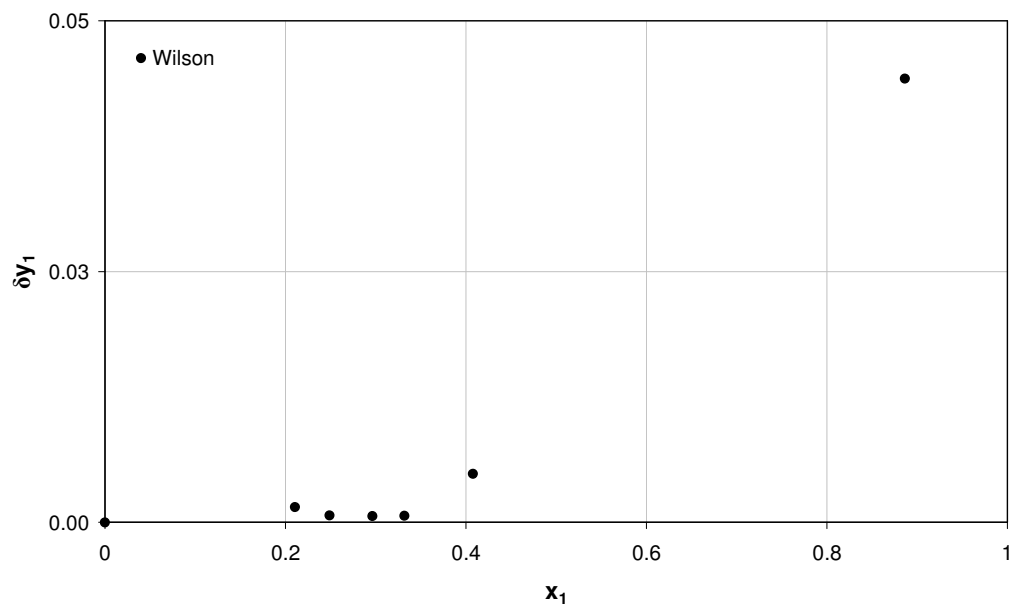


Figure 7-48: Consistency Point test for n-methyl-2-pyrrolidone (1) + 1-hexene (2) at 100 kPa

CHAPTER EIGHT

CONCLUSION

The objective of this study involved the investigation of VLE of binary systems of 1-hexene and n-hexane. The systems investigated were:

- a. 1-hexene with n-hexane at 55 °C, 80 °C and 105 °C,
- b. 2-methyl-2-pentene with n-hexane at 55 °C, 80 °C and 105 °C
- c. n-methyl-2-pyrrolidone with 1-hexene at 45 kPa, 80 kPa and 100 kPa

The conclusions arrived from the results and discussion presented in Chapters six and seven respectively are presented here.

The experimental values of the pure component vapour pressure data corresponded well with literature data hereby confirming the reliability and accuracy of the temperature and pressure calibrations. These calibrations were further warranted in the measurement of the highly ideal system of 1-hexene and n-hexane at 55°C. This system served as the test system and the resultant experimental vapour-liquid data agreed well with data available in literature (Kirss *et al.*, 1975). This also confirmed the accuracy in the operation of the still and the experimental method.

The VLE systems investigated and the treatment of the experimental VLE data were discussed in Chapter seven. A summary of the best fit models for each of these systems is presented below.

Table 8-1: Best fit models for all systems investigated

SYSTEM	CONDITION	MODEL
1-hexene (1) + n-hexane (2)	55 °C	Wilson
	80 °C	NRTL
	105 °C	NRTL
2-methyl-2-pentene (1) + n-hexane (2)	55 °C	Wilson
	80 °C	NRTL
	105 °C	Wilson
n-methyl-2-pyrrolidone (1) + 1-hexene (2)	45 kPa	Van Laar
	80 kPa	NRTL
	100 kPa	Wilson

All the systems were tested for consistency by the Point test and Area test. All the measured systems passed the more stringent Point test with average absolute deviations between experimental and calculated vapour compositions less than 0.01. However, for the Area test, only the 1-hexene (1) + n-hexane (2) system at 55 °C and 2-methyl-2-pentene (1) + n-hexane (2) at 105 °C passed the test.

The systems investigated are currently unavailable in literature except for the system of 1-hexene with n-hexane at 55°C.

CHAPTER NINE

RECOMMENDATIONS

1. It was suggested by Kniesl et al (1989) that fluid properties have an effect on the operation of the ebulliometer and the suitability of the chemical for measurement in an ebulliometer can be calculated. The correlation they propose should be implemented in future to screen chemicals prior to experiments.
2. A ballast of lower volume should be used. This will assist in shortening the time taken to fill and vent the ballast for operation at high and low pressures respectively. This will also save on the usage of nitrogen gas.
3. In terms of the systems investigated it is recommended that system of n-methyl-2-pyrrolidone with n-hexane be investigated preferably isothermal as well as n-methyl-2-pyrrolidone with 1-hexene. It will then be possible to ascertain the selectivity of n-methyl-2-pyrrolidone as an entrainer. The system of 2-methyl-2-pentene and 1-hexene should also be investigated at 55 °C, 80 °C and 105 °C.
4. For isobaric data reduction; regression implementing temperature dependency of parameters as suggested by Soni (2003) is advised. In an isobaric data set each point is said to have its own set of parameters, as the adjustable parameters of the activity coefficients models are temperature dependent (Soni, 2003). Soni (2003) highlights, that there is no theoretical basis to the equation that is suggested in his work, however it avoids making the assumption of temperature independence of these parameters during regression. An important point worth noting.
5. The use of the predictive model UNIFAC (not discussed in this investigation) is recommended to compare the experimental data for the systems investigated.

CHAPTER TEN

REFERENCES

- Abbot, M. M., 1986. Low-pressure phase equilibria: Measurement of VLE. *Fluid Phase Equilibria*, 29, 193-207.
- Abrams, D. S. and Prausnitz, J. M., 1975. Statistical thermodynamics of liquid mixtures: A new expression for the excess Gibbs energy of partly or completely miscible systems. *American Institute of Chemical Engineers Journal*, 21, 116-127.
- Allen, D. T. and Shonnard, D. R., 2002. *Green Engineering. Environmentally Conscious Design of Chemical Processes*. Upper Saddle River: Prentice-Hall.
- Aspen Simulation Program, 2008. *Help Files*
- Bertucco, A., Barolo, M. and Elvassore, N., 1997. Thermodynamic consistency of vapor-liquid equilibrium data at high pressure. *American Institute of Chemical Engineers Journal*, 43, 547-554.
- Dortmund Data Bank Software, Purchased 1998
- Fischer, K and Gmehling, J., 1996. Vapor-liquid equilibria, activity coefficients at infinite dilution and heats of mixing of N-methyl pyrrolidone-2 with C5 or C6 hydrocarbons and for hydrocarbon mixtures. *Fluid phase equilibria*, 119, 113-130.
- Fluka Catalogue, 2008/2007. Laboratory Chemicals and Analytical Reagents. *Sigma-Aldrich*
- Ghosh, P. and Taraphdar, T., 1998. Prediction of vapor –liquid equilibria of binary systems using PRSV equation of state and Wong-Sandler mixing rules. *Chemical Engineering Journal*, 70, 15-24.
- Gierycz, P, Rogalski, M and Malanowski, S., 1985. Vapour-liquid equilibria in binary systems formed by n-methylpyrrolidone with hydrocarbons and hydroxyl derivatives. *Fluid Phase Equilibria*, 22, 107-122.

- Griswold, J., Andres, D. and Klein, V. A. 1943. Determination of high pressure vapour liquid equilibrium. *Petroleum Refiner*, 22, 99-106.
- Hanson, D.O. and Van Winkle, M., 1967. Alteration of the relative volatility of n-hexane-1-hexene by oxygenated and chlorinated solvents. *Journal of Chemical Engineering Data*, 12 (3), 319-325.
- Harris, R., 2004. *Robust equipment for the measurement of vapor liquid equilibrium*. Thesis (PhD). University of Natal.
- Hayden, J. G. and O'Connell, J. P., 1975. A generalized method for predicting second virial coefficients. *Industrial and Engineering Chemistry: Process Design and Development*, 14, 209-215.
- Hernández-Garduza, O., García-Sánchez, F., Neau, E. and Rogalski, M., 2000. Equation of state associated with activity coefficient models to predict low and high pressure vapor-liquid equilibria. *Chemical Engineering Journal*, 79, 87-101.
- Kniesl, P., Zondlo, J.W., Whiting, W. B. and Bedell, M. 1989. The effect of fluid properties on ebulliometer operation. *Fluid Phase Equilibria*, 46, 85-94.
- Lei, Z, Wolfgang, A and Wasserscheid, P., 2006. Separation of 1-hexene and n-hexene with ionic liquids. *Fluid phase equilibria*, 241, 290-299.
- Lei, Z, Wolfgang, A and Wasserscheid, P., 2007. Selection of entrainers in the 1-hexene/n-hexane system with a limited solubility. *Fluid phase equilibria*, 260, 29-35.
- Maher, P. J. and Smith, B. D., 1979. Infinite dilution activity coefficient values from total pressure VLE data. Effect of equation of state used. *Industrial and Engineering Chemistry Fundamentals*, 18, 354-357.
- Malanowski, S., 1982. Experimental methods for vapour-liquid equilibria. Part I. Circulation methods. *Fluid Phase Equilibria*, 8, 197-219.
- Mühlbauer, A. L. and Raal, J. D., 1995. Computation and thermodynamic interpretation of high-pressure vapour-liquid equilibria-A Review. *Chemical Engineering Journal*, 60, 1-29.

- Naidoo, P., 2004. *High-pressure vapour-liquid equilibrium studies*. Thesis (PhD). University of KwaZulu-Natal.
- Narasigadu, C., 2006. *Phase equilibrium investigation of the water and acetonitrile solvent with heavy hydrocarbons*. Dissertation (MSc). University of KwaZulu-Natal.
- O'Connell, J. P. and Prausnitz, J. M., 1967. Empirical correlation of second Virial coefficients for vapour-liquid equilibrium calculations. *I and EC Process Design and Development*, 6, 245-250.
- Orbey, H. and Sandler, S. I., 1996. *Computer Program: Vapor-liquid equilibria with Wong-Sandler mixing rule*.
- Peng, D. Y. and Robinson, B. D., 1976. A new two-constant equation of state. *Industrial and Engineering Fundamentals*, 15, 59-64.
- Pitzer, S. K. and Curl, R. F., 1957. The volumetric and thermodynamic properties of fluids. III. Empirical equation for the second Virial coefficient. *Journal of American Chemical Society*, 79, 2369-2370.
- Pitzer, S. K., Lipmann, D. Z., Curl, R. F., Huggins, M. C and Petersen, D. E., 1955. The volumetric and thermodynamic properties of fluids. II. Compressibility factor, vapour pressure and entropy of vaporization. *Journal of American Chemical Society*, 77, 3433-3440.
- Prausnitz, J.M., Lichtenthaler, R. N. and de Azevedo, E. G., 1986. *Molecular Thermodynamics of Fluid-Phase Equilibria*. Englewoods, New Jersey: Prentice-Hall
- Raal, J. D. and Mühlbauer, A.L., 1998. *Phase Equilibria: Measurement and computation*. Washington: Taylor and Francis.
- Raal, J. D. and Ramjugernath, D., 2005. Vapour-liquid equilibrium at low pressure. In: R.D. Weir and TH. W. De Loos, eds. *Measurement of the thermodynamic properties of multiple phases*. Amsterdam: Elsevier. 71-87.
- Rackett, H. G., 1970. Equation of state for saturated liquids. *Journal of Chemical Engineering Data*, 15, 514-517.

- Reddy, P., 2006. *Development of a novel apparatus for Vapour-Liquid Equilibrium Measurements at Moderate Pressures*. Thesis (PhD). University of KwaZulu-Natal.
- Redlich, O. and Kwong, J. N. S. 1949. On the thermodynamics of solutions. V: An equation of state. Fugacities of gaseous solutions. *Chemical Reviews*, 44, 233-244.
- Reid, R. C., Prausnitz, J. M. and Sherwood, T. K., 1977. *The properties of gases and liquids*. Third ed. New York: McGraw-Hill.
- Reid, R. C., Prausnitz, J. M. and Poling, B. E., 1988. *The properties of gases and liquids*. Fourth ed. Singapore: McGraw-Hill.
- Renon, H. and Prausnitz, J. M., 1968. Local compositions in thermodynamic excess functions for liquid mixtures. *American Institute of Chemical Engineers Journal*, 14, 135-144.
- Rogalski, M. and Malanowski, S., 1980. Ebulliometers modified for the accurate determination of vapour-liquid equilibrium. *Fluid Phase Equilibria*, 5, 97-112.
- Seader, J. D. and Henley, E. J., 1998. *Separation Process Principles*. United States of America: John Wiley and Sons, Inc.
- Seader, J. D., Siirola, J. J. and Barnicki, S. D., 1998. Distillation. In: R. H. Perry and D. W. Green, eds. *Perry's Chemical Engineers' Handbook*. India: McGraw-Hill, 13-1 – 13-108.
- Soni, M., 2003. *Vapour-liquid equilibria and infinite dilution activity coefficient measurements of systems involving diketones*. Dissertation (MSc). University of KwaZulu-Natal.
- Streicher, C., Asselineau, L. and Forestière, A., 1995. Separation of alcohol/ether/hydrocarbon mixtures in industrial etherification processes for gasoline production. *Pure and Applied Chemistry*, 67, 985-992.
- Stryjek, R. and Vera, J. H., 1986. PRSV: An improved Peng-Robinson equation of state for pure compounds and mixtures. *The Canadian Journal of Chemical Engineering*, 64, 323-333.

- Tsonopoulos, C., 1974. An empirical correlation of second virial coefficients. *American Institute of Chemical Engineers Journal*, 20, 263-272.
- Van Ness, H. C., 1995. Thermodynamics in the treatment of (vapour + liquid) equilibria. *Journal of Chemical Thermodynamics*, 27, 113-134.
- Van Ness, H. C. and Abbott, M. M., 1982. *Classical Thermodynamics of Non Electrolyte Solutions: With Applications to Phase Equilibria*. New York: McGraw-Hill.
- Van Ness, H. C. and Abbott, M. M., 1998. Thermodynamics. In: R. H. Perry and D. W. Green, eds. *Perry's Chemical Engineers' Handbook*. India: McGraw-Hill, 4-1 – 4-36.
- Weast, R. C. ed., 1985. *Handbook of chemistry and physics*. 6th Edition. Boca Raton, Florida: CRC Press.
- Wentink, A. E., Kuipers, N. J. M., de Haan, A. B., Scholtz, J., Mulder, H., 2007. Olefin isomer separation by reactive extractive distillation: Modelling of vapour-liquid equilibria and conceptual design for 1-hexene purification. *Chemical Engineering and Processing*, 47, 800-809.
- Wisniak, J and Gabai, E. 1996. Isobaric Vapour-liquid equilibria in the systems methyl acetate+1-hexene and 1-hexene +2-propanol. *J. Chem. Eng Data*, 41, 143-146.
- Wisniewska, B., 1993. Development of a vapour-liquid equilibrium apparatus to work at pressures up to 3MPa. *Fluid Phase equilibria*, 86, 173-186.
- Wong, D. S. H. and Sandler, S. I., 1992. A theoretically correct mixing rule for cubic equations of state. *American Institute of Chemical Engineers Journal*, 38, 671-680.

APPENDIX A

SUMMARIES OF LPVLE AND HPVLE EQUIPMENT

Table A-1 presents a brief summary of the HPVLE equipment in chronological order. All the references found in the table below have been cited by Raal and Mühlbauer (1998) unless stated otherwise.

Table A-1: Chronological order of HPVLE equipment development

YEAR	DEVELOPMENT/MODIFICATION
1965	Muirbrook and Prausnitz (1965) apparatus was one of the earliest examples of recirculation HPVLE methods. It was used to measure the ternary nitrogen/oxygen/carbon dioxide system. The circulation of the phases provided the necessary agitation required to obtain equilibrium. This was achieved by the use of special vane pumps.
1983	The experimental apparatus of Kubota et. al. (1983) used a six-port valve which allowed a high-pressure pump to circulate the vapour or liquid phase. On this equipment steady state takes an average of 2 hours. Samples are trapped in the four-port valve, released into a low pressure line and circulated until homogenised to be analysed using gas chromatography.
1985	The striking feature of Yorizane et al. (1985) equipment was the unusual means of achieving agitation. The apparatus included two equilibrium cells, one of which was fixed and the other able to move up and down. The motion resulted in a pressure gradient causing the phases to flow in opposite directions (making close contact) in an attempt to balance the pressure.
1989	The equilibrium cell of Kim et al. (1989) was immersed in an oil bath and equipped with two transparent glass windows. Due to the high flow rates of both phases, it was possible to have equilibration times as little as 15 minutes.
1989	In recent years sampling of the circulating vapour or liquid phases was accomplished by incorporating a commercially available valve directly in the circulation lines. Shibata and Sandler (1989) designed a complex method of sampling, by trapping vapour and liquid samples in sample bombs and transferring them to a gas chromatograph for analysis.

Table A-2 presents a brief summary of the LPVLE equipment in chronological order. All the references found in the table below have been cited by Malanowski (1982) unless stated otherwise.

Table A-2: Chronological order of LPVLE equipment development

YEAR	DEVELOPMENT/MODIFICATION
1910	The thermal lift pump was introduced by Cottrell. It was used to deliver a stream of boiling liquid to a thermometer. (Cottrell ,1919)
1924	The still was modified by Swietoslwaski and Romer (1924) and was found by Leslie and Kuehner (1968) to be more accurate in the acquisition of boiling temperature in the pressure ranges of 5 -200 kPa.
1929	Swietoslowski (1929) introduced the idea of collecting liquid and vapour condensate samples during operation of the equipment for a flow apparatus.
1931	Lee (1931) proposed the first still with both a Cottrell pump and the ability for removal of liquid and vapour condensate samples “after temporary cessation of circulation by pressure increase.
1946	Gillespie (1946) introduced two major modifications. These were the separator between liquid and condensate streams and the means of withdrawing samples without having to disturb boiling.
1948	Coulson et. al. (1948) found the still of Gillespie (1946) to be superior to stills with vapour condensate circulation (Othmer, 1943) and and additional Cottrell pump (Scatchard et. al, 1938).
1950	Brown and Ewald (1950) redesigned the still of Gillespie (1946), at which stage was going through numerous modifications. They redesigned the boiler to achieve continuous nucleation and steady boiling. The sample traps were also modified to prevent possible contamination.
1952	Brown (1952) further modified the above still due to several operating problems. These included the evaporation of condensate from the vapour trap which led to erroneous vapour compositions, and the occurrence of flashing when the condensate is mixed with hot circulating fluid. This only occurs for systems of high relative volatility. The modifications that followed included redesigning the sample traps and the addition of a condenser to cool the circulating liquid. The results obtained were accurate but the downfalls were the 4 hour for steady state operation and large sample size of 200 cm ³ .

YEAR	DEVELOPMENT/MODIFICATION
1963	Dvořák and Boublik (1963) proposed an apparatus suitable for systems of very high relative volatility and emphasised the importance of stirring in the liquid and vapour condensate traps.
1964	Yerazunis et. al. (1964 cited by Raal and Muhlbauer, 1998) introduced a packed equilibrium chamber with 1/8 inch Fenske helices. The benefits of the packed chamber were clearly illustrated in the experimental data that were thermodynamically consistent. One of the major benefits of the packed section was the short time of 30-45 minutes required for equilibrium.
1980	Rogalski and Malanowski (1980) modified the Swietoslowski ebulliometer for determination of VLE, in the low pressure region of a wide temperature range (Reddy, 2006) and at low concentrations (Rogalski and Malanowski, 1980). The two new modifications can produce reliable data rapidly, and achieve equilibrium in a short time after changing thermodynamic parameters, according to Rogalski and Malanowski (1980). The compositions of the phases at equilibrium do not have to be known in order for measurements to be carried out.
1998	Raal (1998 cited by Raal and Mühlbauer, 1998) developed a robust and compact still at the University of Natal. One of the many features of the still, as compared to its predecessor Yerazunis et. al. (1964) is the use of open structured packing (wire mesh cylinders) in the equilibrium chamber, to produce a low pressure drop. An advantage is the accessibility of the packing (for cleaning etc.) by removal of the temperature sensor thermowell. The Cottrell tube is central to the equilibrium chamber, making the chamber angularly symmetric and thus preventing the formation of temperature or concentration gradients. The Cottrell tube discharges onto a temperature sensor which according to Raal and Mühlbauer (1998) should be placed well into the packing for a reliable temperature measurement. The upper portion of the still including the Cottrell tube is vacuum jacketed. This feature reduces heat loss and insulates the equilibrium area from superheat effects. Other features worth noting are the use of stirrers in the boiling chamber and, liquid and vapour condensate receivers and the addition of internal and external heaters in the boiling chamber.

APPENDIX B

CHEMICAL PROPERTIES AND CONSTANTS

Table B1: Chemical properties

	1-hexene	n-hexane	2-methyl-2-pentene	n-methyl-2-pyrrolidone
Chemical formula	C ₆ H ₁₂	C ₆ H ₁₄	C ₆ H ₁₂	C ₅ H ₉ NO
T_b / K	336.3	341.9	340.5	475.13
P_c / bar	31.7	30.1	32.8	44.6
T_c / K	504	507.5	518	721.7
V_c / cm³ mol⁻¹	350	370	351	310.8
ω	0.285	0.299	0.229	0.3577
κ	0.1595	0.051 ^a	0.0088	0.0158 ^b

^aStryjek and Vera (1986)

^bCalculated using Sandler program

Table B2: Antoine constants

	1-hexene ^a	n-hexane ^a	2-methyl-2-pentene ^b	n-methyl-2-pyrrolidone ^c
A	15.8089	4.00139	9.3221	7.54826
B	2654.81	1170.875	2725.89	1979.68
C	-47.3	224.317	-47.64	222.162
	P in mmHg	P in bar	P in bar	P in mmHg
	T in K	T in °C	T in K	T in °C

^aReid et al. (1977)

^bReid et al. (1988)

^cDortmund Data Bank (1998)

APPENDIX C

LIMITING ACTIVITY COEFFICIENTS

The limiting activity coefficients determined by the method highlighted in Maher and Smith (1979) described in Chapter two are presented below in Figures C-1 to C-8 for the systems of 1-hexene with n-hexane and 2-methyl-2-pentene with n-hexane.

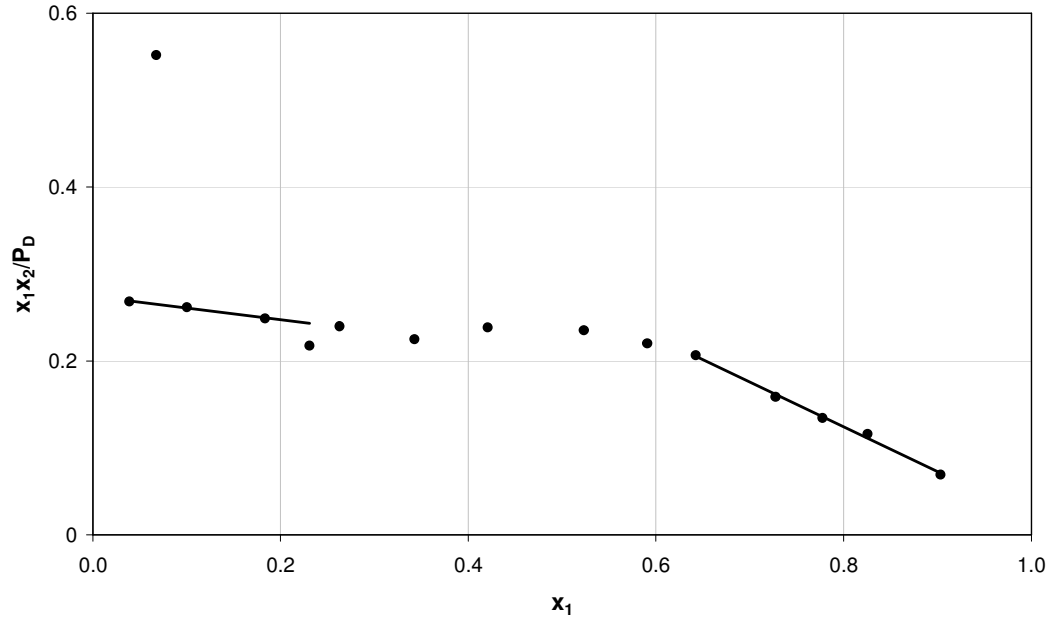


Figure C-1: Plot of $\left(\frac{x_1x_2}{P_D}\right)$ for 1-hexene (1) + n-hexane (2) system at 55 °C

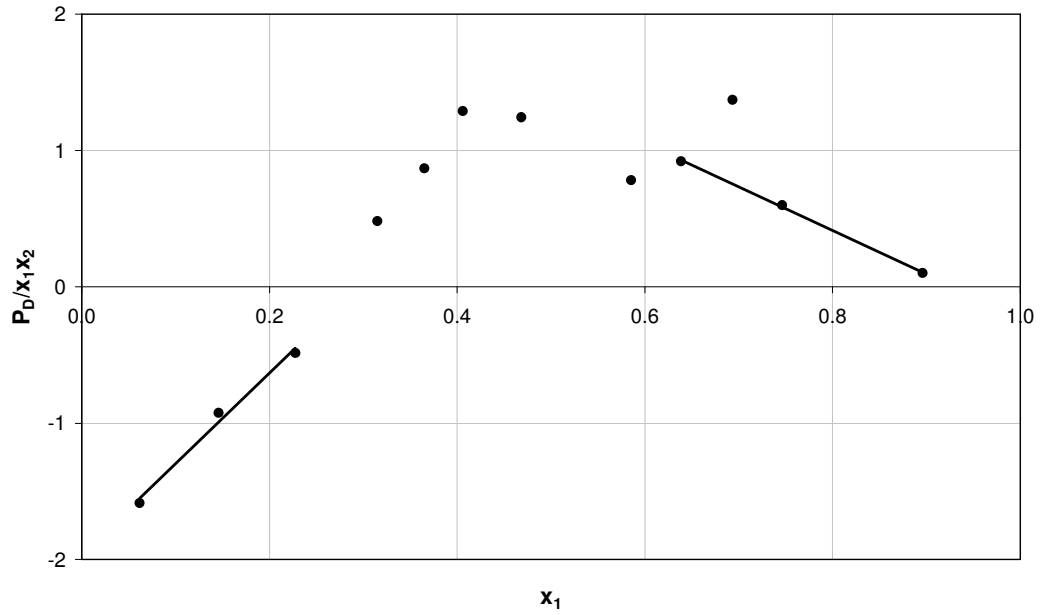


Figure C-2: Plot of $\left(\frac{P_D}{x_1 x_2}\right)$ for 1-hexene (1) + n-hexane (2) system at 80 °C

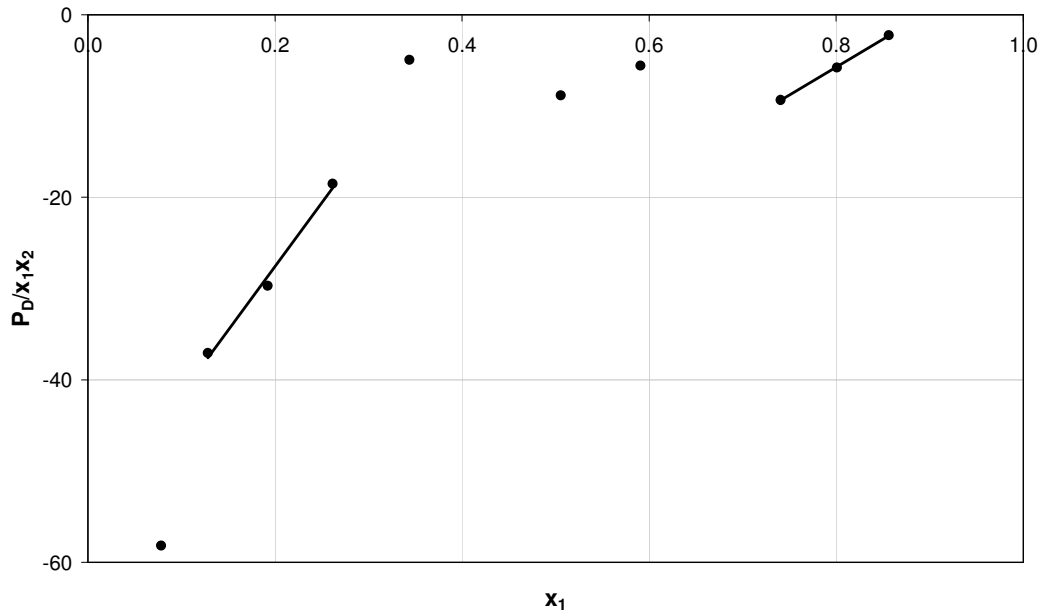


Figure C-3: Plot of $\left(\frac{P_D}{x_1 x_2}\right)$ for 1-hexene (1) + n-hexane (2) system at 105 °C

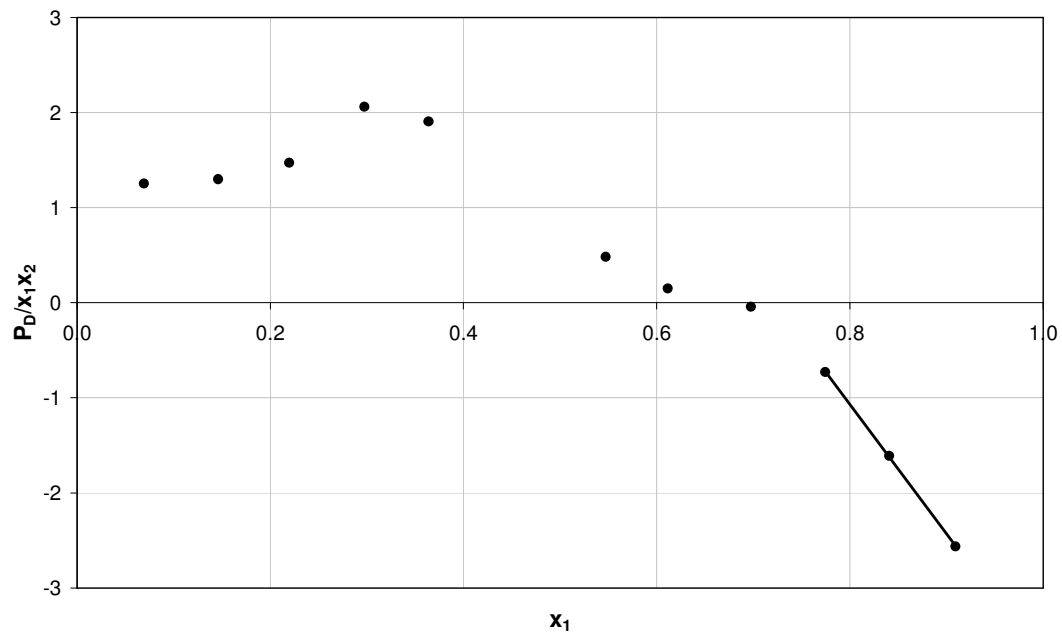


Figure C-4: Plot of $\left(\frac{P_D}{x_1 x_2}\right)$ for 2-methyl-2-pentene (1) + n-hexane (2) system at 55 °C

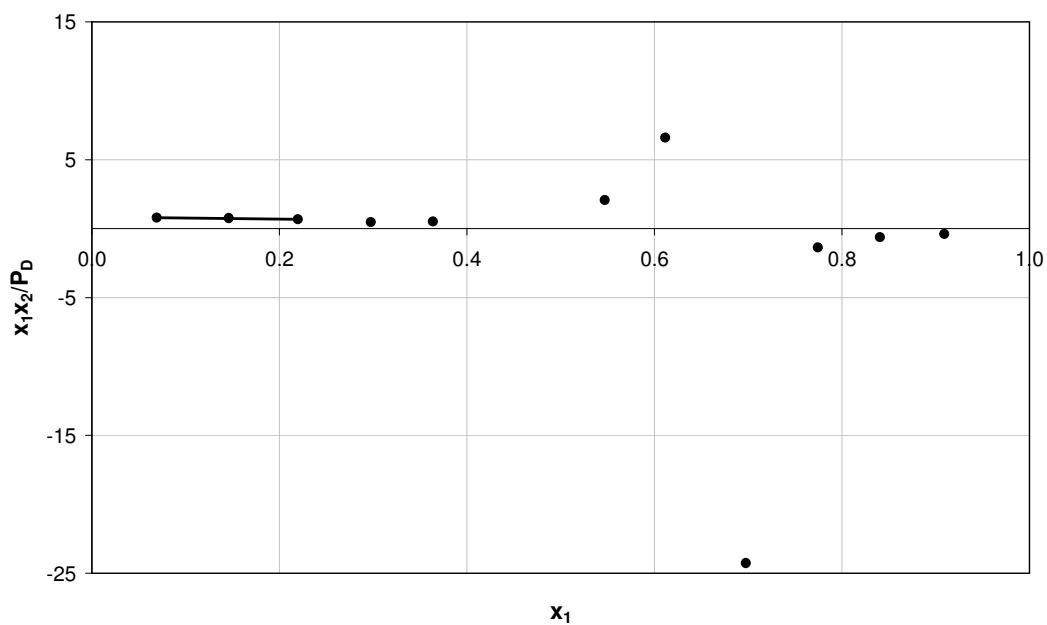


Figure C-5: Plot of $\left(\frac{x_1 x_2}{P_D}\right)$ for 2-methyl-2-pentene (1) + n-hexane (2) system at 55 °C

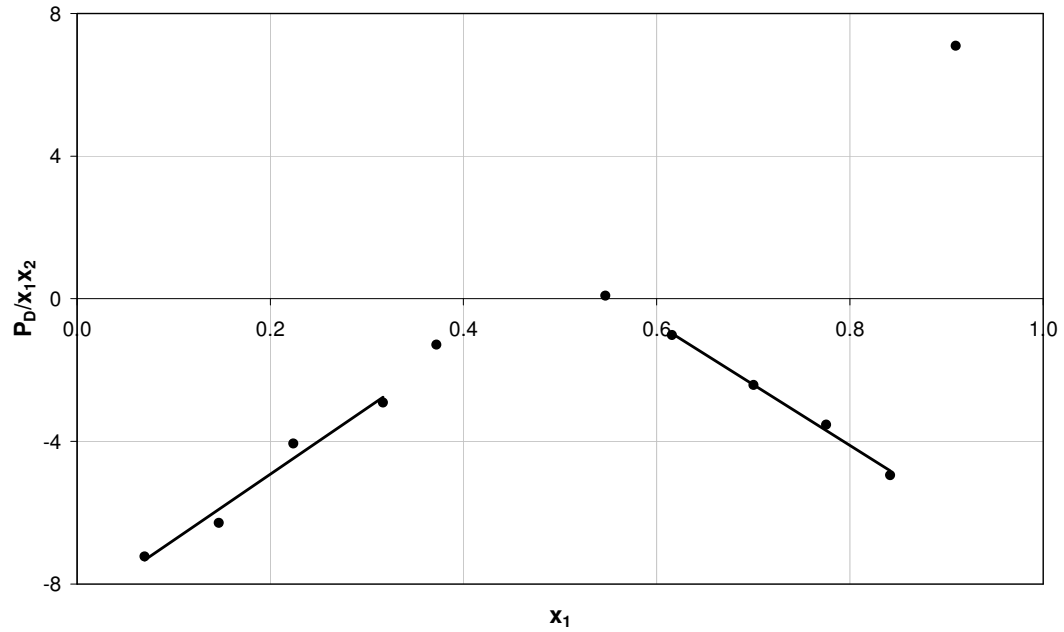


Figure C-6: Plot of $\left(\frac{P_D}{x_1x_2}\right)$ for 2-methyl-2-pentene (1) + n-hexane (2) system at 80 °C

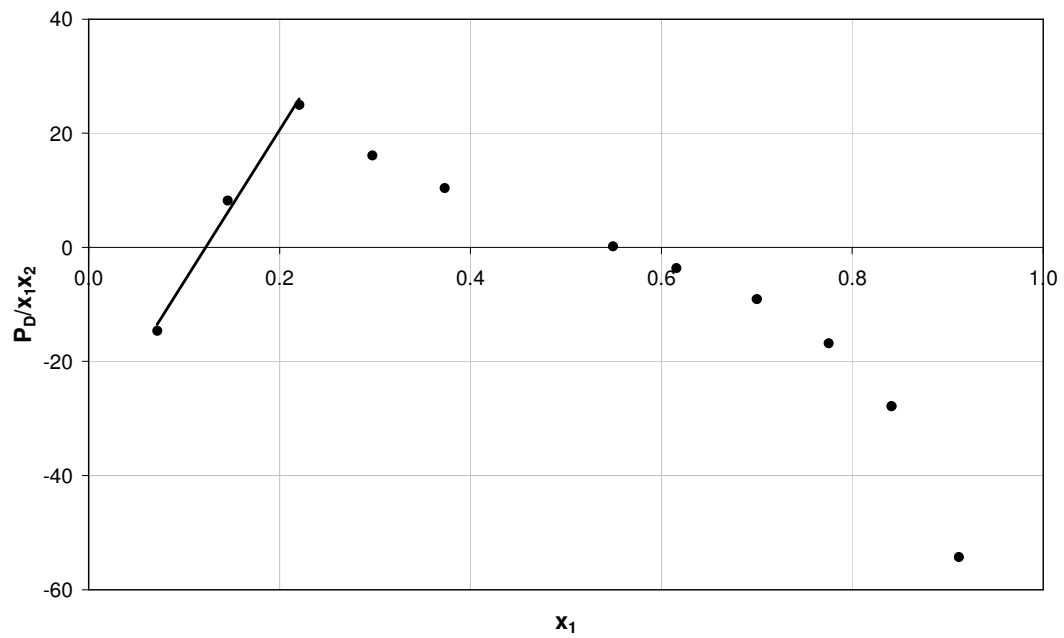


Figure C-7: Plot of $\left(\frac{P_D}{x_1x_2}\right)$ for 2-methyl-2-pentene (1) + n-hexane (2) system at 105 °C

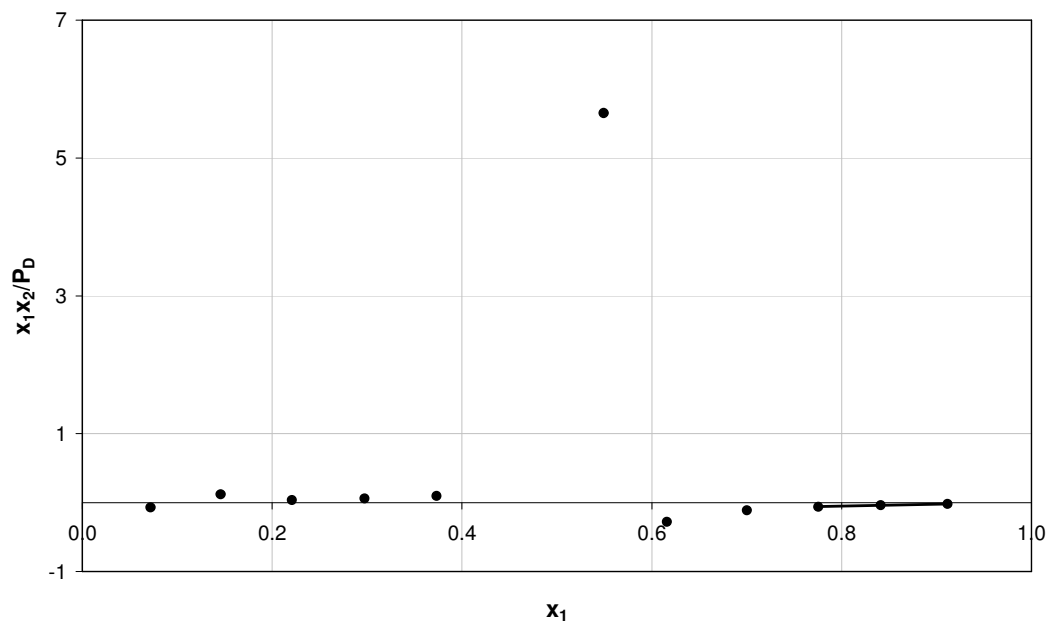


Figure C-8: Plot of $\left(\frac{x_1 x_2}{P_D}\right)$ for 2-methyl-2-pentene (1) + n-hexane (2) system at 105 °C

APPENDIX D

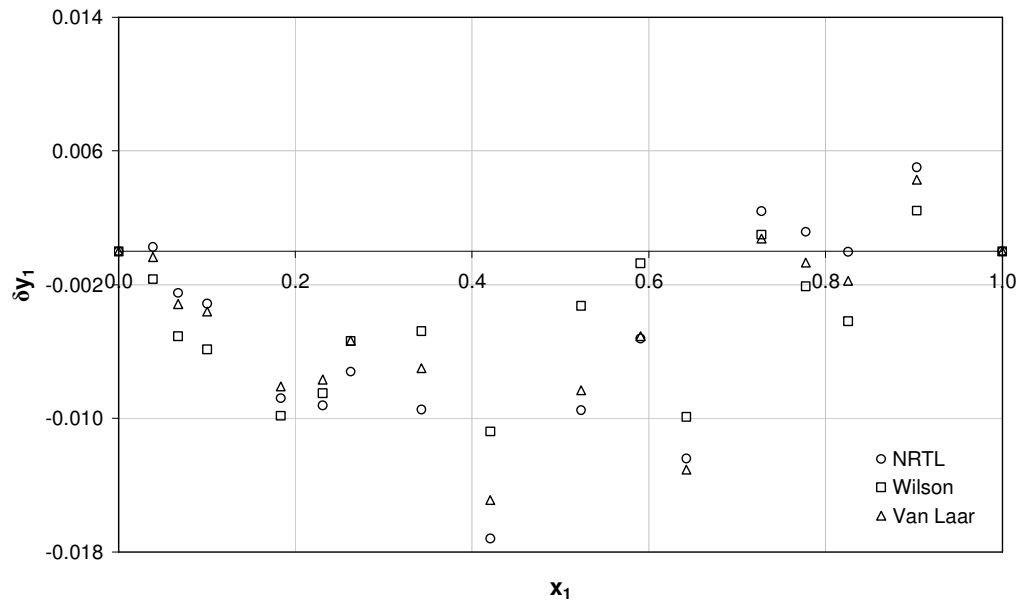
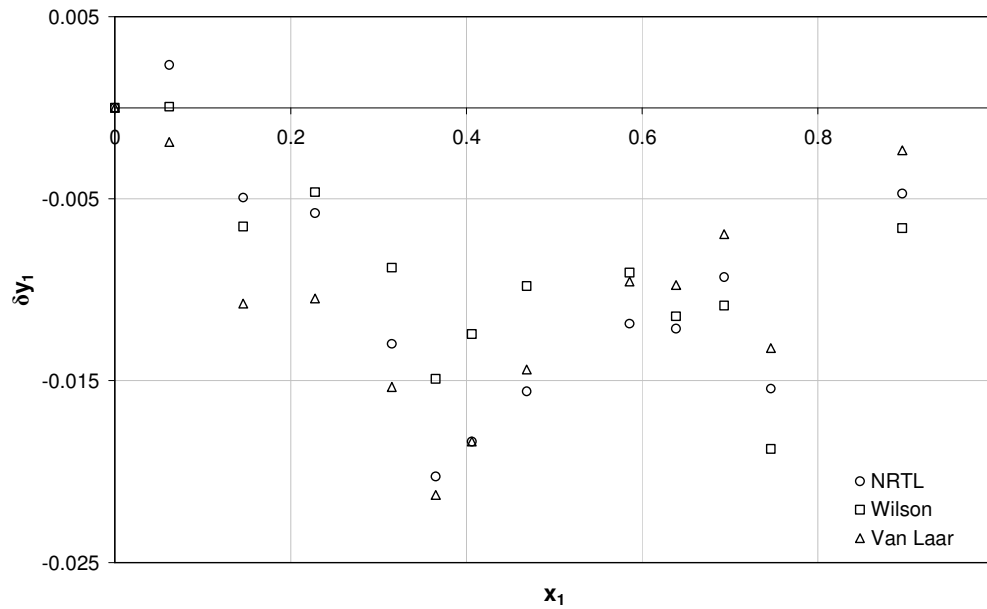
CONSISTENCY POINT TEST

The consistency point test was discussed in Chapter two and the best fit models were presented in Chapter seven. This section presents the results of all the systems investigated with all the Gibbs excess energy models.

The best fit models based on lowest δy values are presented below.

Table D-1: Best models for consistency point test

SYSTEM	CONDITION	MODEL	δy
1-hexene with n-hexane	55 °C	Wilson	0.0044
	80 °C	Wilson	0.0081
	105 °C	Wilson	0.0088
2-methyl-2-pentene with n-hexane	55 °C	NRTL	0.0023
	80 °C	Van Laar	0.0025
	105 °C	NRTL	0.0022
n-methyl-2-pyrrolidone with 1-hexene	45 kPa	Wilson	0.0022
	80 kPa	Wilson	0.0085
	100 kPa	Wilson	0.0066

D1. 1-Hexene (1) + n-Hexane (2) System**Figure D-1: Consistency Point test for 1-hexene (1) + n-hexane (2) at 55 °C****Figure D-2: Consistency Point test for 1-hexene (1) + n-hexane (2) at 80 °C**

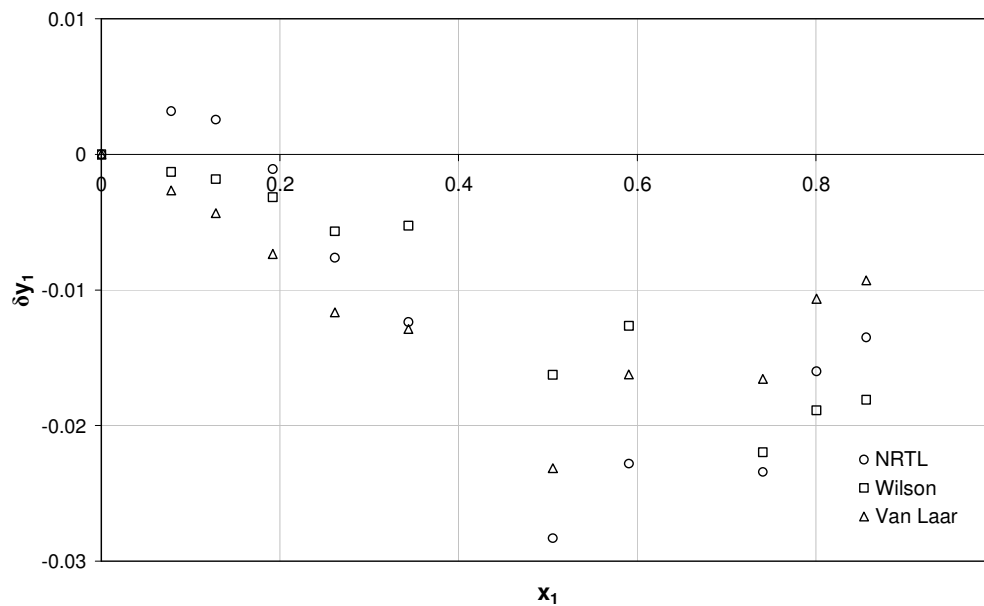
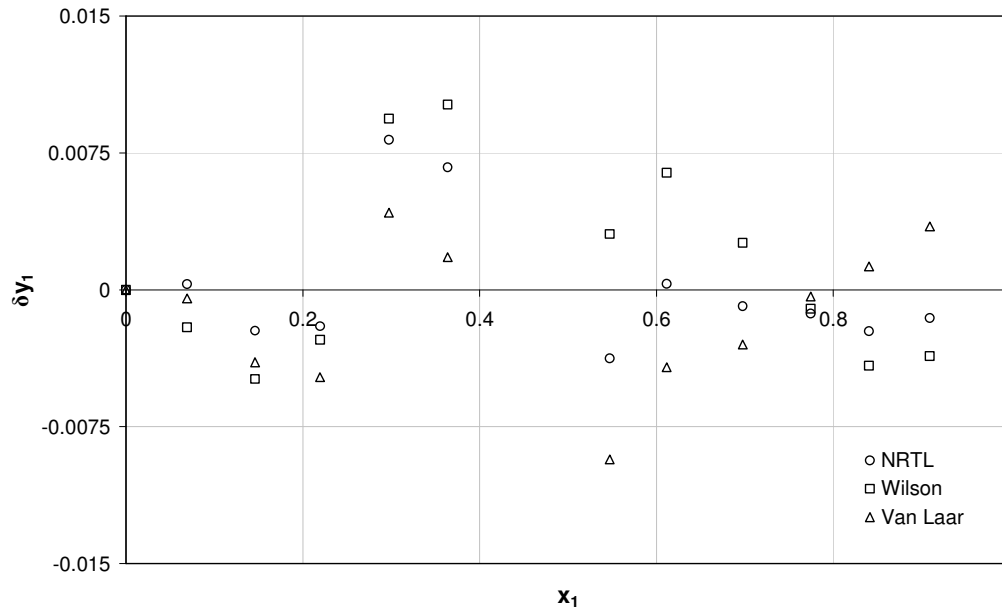
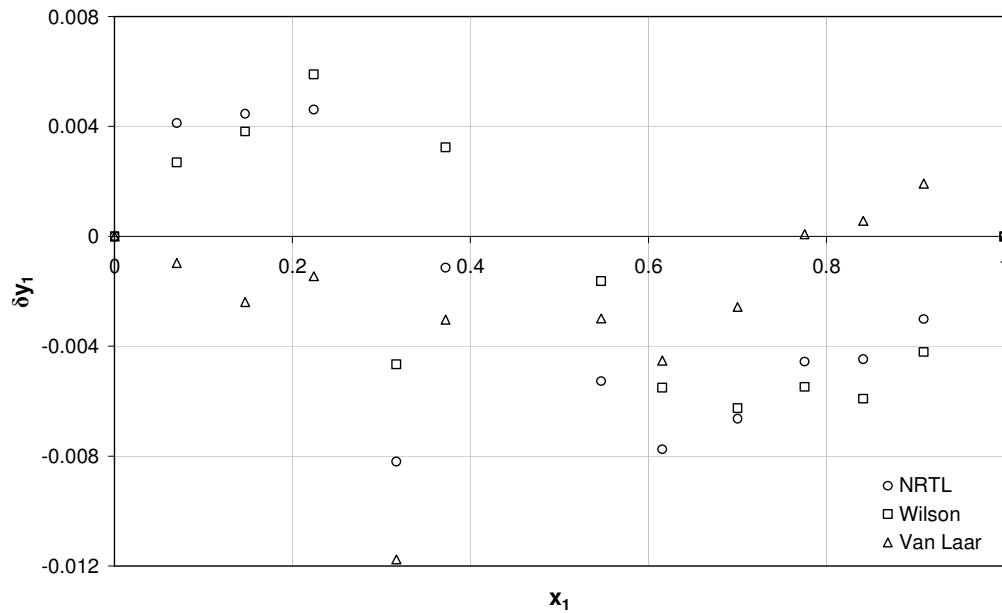


Figure D-3: Consistency Point test for 1-hexene (1) + n-hexane (2) at 105 °C

D2. 2-Methyl-2-pentene (1) + n-Hexane (2) System**Figure D-4: Consistency Point test for 2-methyl-2-pentene (1) + n-hexane (2) at 55 °C****Figure D-5: Consistency Point test for 2-methyl-2-pentene (1) + n-hexane (2) at 80 °C**

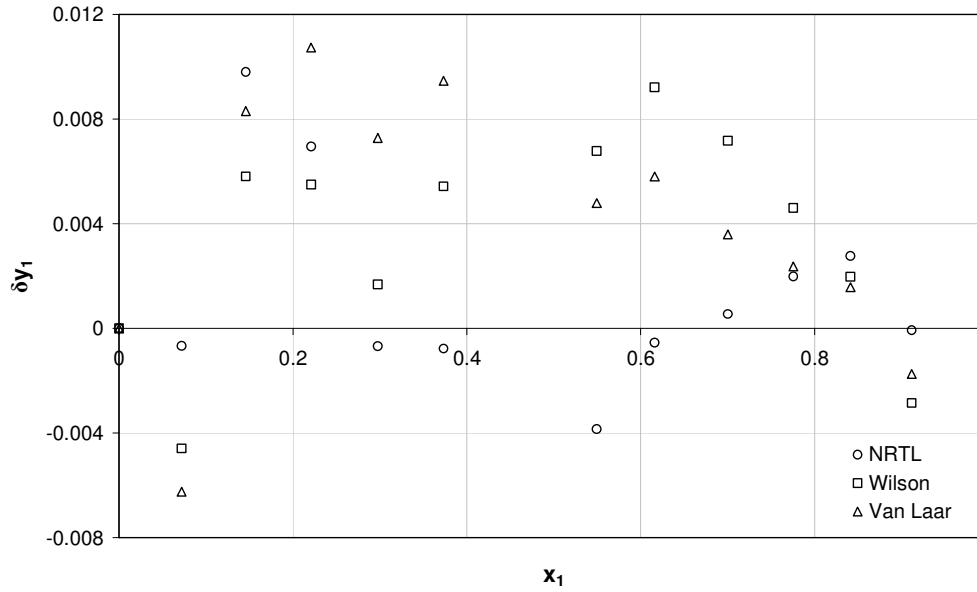


Figure D-6: Consistency Point test for 2-methyl-2-pentene (1) + n-hexane (2) at 105 °C

D3. n-Methyl-2-pyrrolidone (1) + n-Hexane (2) System

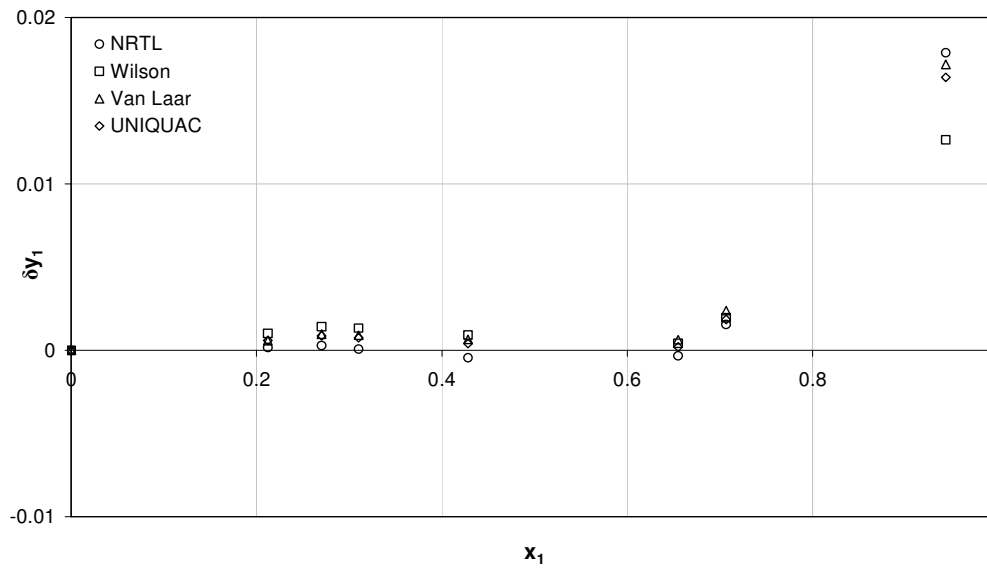


Figure D-7: Consistency Point test for n-methyl-2-pyrrolidone (1) + n-hexane (2) at 45 kPa

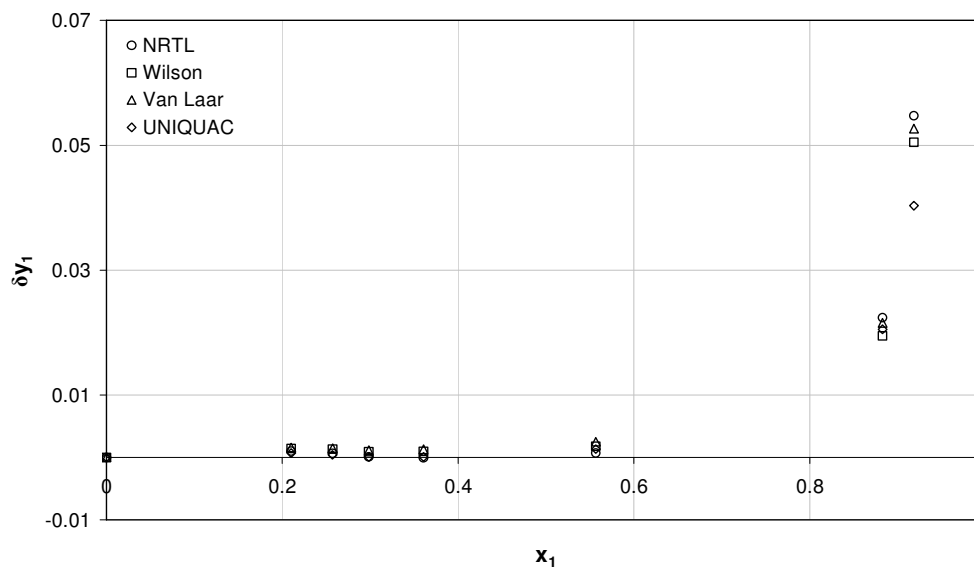


Figure D-8: Consistency Point test for n-methyl-2-pyrrolidone (1) + n-hexane (2) at 80 kPa

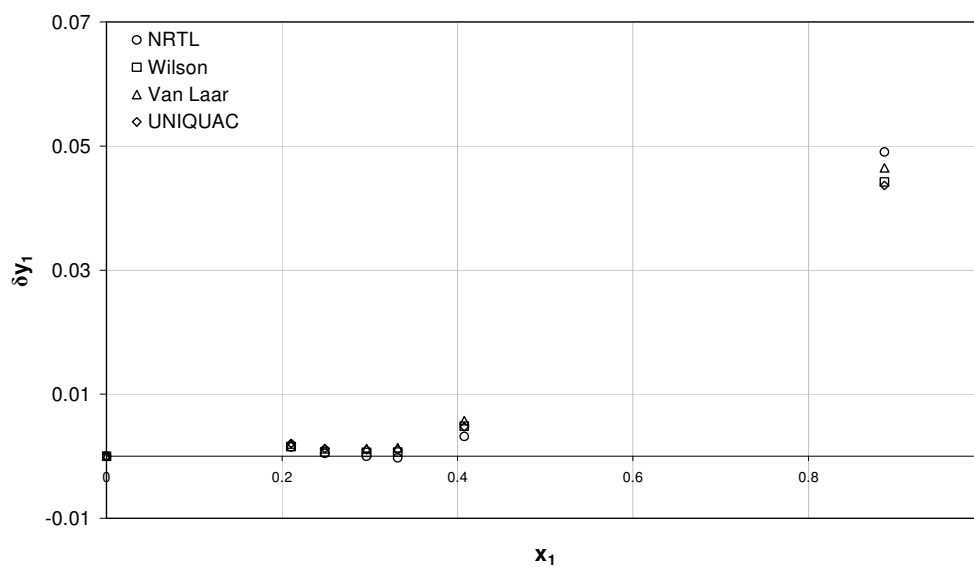


Figure D-9: Consistency Point test for n-methyl-2-pyrrolidone (1) + n-hexane (2) at 100 kPa